

Jochen Kühnl

**Regulation of the actin cytoskeleton  
by the protein SWAP-70**

2008

Biologie

**Regulation of the actin cytoskeleton  
by the protein SWAP-70**

Inaugural-Dissertation  
zur Erlangung des Doktorgrades der Naturwissenschaften  
im Fachbereich Biologie  
der Mathematisch-Naturwissenschaftlichen Fakultät  
der Westfälischen Wilhelms-Universität Münster

vorgelegt von  
Jochen Kühnl  
aus Hamburg  
-2007-

---

Dekan:	Prof. Dr. Norbert Sachser
Erster Gutachter:	Prof. Dr. Martin Bähler
Zweiter Gutachter:	Prof. Dr. Volker Gerke
Tag der mündlichen Prüfung:	01. April 2008
Tag der Promotion:	11. April 2008

## **Abstract**

The actin cytoskeleton is a major component of all eukaryotic cells and crucial for numerous cellular functions including cell motility, endocytosis and intracellular vesicle transport. Actin exists either in a monomeric globular form or can self-assemble into a filamentous form (F-actin). Signaling pathways including the family of small GTPases control the spatio-temporally coordinated assembly, cross-linking and disassembly of F-actin which allows directed cell migration. Cells utilize several F-actin binding proteins to facilitate the subsequent assembly of complex three-dimensional structures with different functionality. SWAP-70 is an actin associated protein which labels a special subset of actin filament arrays in motile cells (Hilpelä *et al.*, 2003). SWAP-70 deficient cells show severe defects in migration (Pearce *et al.*, 2006) and uptake of extracellular material via macropinocytosis (Oberbanscheidt *et al.*, 2007). However, the role of SWAP-70 in these processes is not understood. It is postulated, that SWAP-70 resides in an inactive cytosolic conformation and is activated by phosphoinositides at the plasma membrane where it associates with F-actin. For this reason, the effects of artificially membrane-targeted SWAP-70 were investigated in this study. It turned out that membrane targeted SWAP-70 induces an expression-level dependent disorganization of the actin cytoskeleton leading to filopodia- and microspike-formation and elongated cell morphology. Membrane targeted SWAP-70 affects the activity levels of small GTPases, resulting in upregulation of activated Ras and Cdc42 and downregulation of activated RhoA. Changes in Rac activity levels could not be observed. In order to identify the domains of SWAP-70 responsible for these effects, cells were transfected with various truncation constructs. This approach revealed a crucial function for the C-terminal part of the protein containing a predicted coiled-coil-region domain and the necessity of the actin binding C-terminal 60 residues. Different regulators of the actin cytoskeleton influence the distribution and localization of SWAP-70 (Oberbanscheidt *et al.*, in preparation). In this study, the influence of different small GTPases of the Ras superfamily was investigated. It could be shown that dominant active H- and R-Ras have a strong and unique influence on actin filament arrays and on SWAP-70 association with F-actin. Activated PI3 kinase was necessary for the association of SWAP-70 with actin filaments but not sufficient for the formation of the actin filament arrays. To elucidate further the function of SWAP-70, a bacterial two-hybrid-screen was performed to find interacting proteins of SWAP-70. An interesting candidate identified in the screen was the RasGEF RasGRP1. The interaction is mediated between the N-terminal part of SWAP-70 and the C-terminal part of RasGRP1. The interaction of SWAP-70 with RasGRP1 could be confirmed by pull-down assays and colocalisation studies. SWAP-70's actin binding property was necessary for filamentous colocalisation of cotransfected RasGRP1. It is hypothesized that SWAP-70 recruits RasGRP1 to cortical F-actin.

# **Table of Contents**

<b>Abstract</b> .....	<b>I</b>
<b>Table of Contents</b> .....	<b>II-VI</b>
<b>1. Introduction</b> .....	<b>1</b>
1.1 Cytoskeletal elements .....	1
1.2 The actin cytoskeleton .....	2
1.2.1 Properties of the actin molecule .....	2
1.2.2 Actin polarity and treadmilling mechanism .....	4
1.2.3 Capping and monomer binding proteins preserve a high level of G-actin.....	5
1.3 Generation of free barbed ends .....	6
1.3.1 Uncapping of actin filaments.....	6
1.3.2 Severing of actin filaments .....	7
1.4 The nucleation of new actin filaments .....	7
1.4.1 The Arp2/3 complex.....	8
1.4.2 Activation of the Arp2/3 complex .....	9
1.4.3 Formins.....	12
1.4.4 Spire.....	12
1.4.5 Cordon bleu .....	13
1.5 Actin cross-linking proteins.....	14
1.5.1 Actin bundling proteins .....	14
1.5.2 Talin and Vinculin connect the actin cytoskeleton to integrins.....	15
1.5.3 ERM-proteins: tethering cortical actin to the plasma membrane .....	15
1.6 The actin cytoskeleton in cell migration: Four steps to motility .....	16
1.6.1 Leading edge protrusion via synergistic effects of capping, severing and nucleation .....	16
1.6.2 Adhesion to the extracellular matrix .....	18
1.6.3 Ruffle formation .....	20
1.6.4 Stress fiber assembly and contractility .....	21

1.6.5	Detachment from the extracellular matrix,.....	22
1.7	Mechanisms of directed cell migration.....	23
1.7.1	Cells sense and respond to extracellular gradients.....	23
1.7.2	PH-domains as important links between gradient sensing and signaling.....	24
1.7.3	Small GTPases are regulators of the actin cytoskeleton.....	25
1.8	The protein SWAP-70.....	32
1.8.1	Structure and expression of SWAP-70.....	33
1.8.2	Physiological functions of SWAP-70.....	34
<b>2.</b>	<b>Aims of the present study .....</b>	<b>39</b>
<b>3.</b>	<b>Materials .....</b>	<b>40</b>
3.1	Equipment.....	40
3.2	Chemicals.....	41
3.3	Molecular biology.....	42
3.3.1	Prokaryotic cell lines.....	42
3.3.2	Media for prokaryotes.....	42
3.3.3	Antibiotics.....	44
3.3.4.	Additional reagents for the bacterial two-hybrid screen.....	45
3.3.5	Materials for molecular biology.....	45
3.3.6	Solutions for plasmid DNA preparations by alkaline extraction.....	45
3.3.7	Solutions for agarose gel electrophoresis:.....	46
3.3.8	Oligonucleotides.....	47
3.3.9	Plasmids.....	48
3.4.	Proteins.....	49
3.4.1	Proteins and enzymes for molecular biology.....	49
3.4.2	Antibodies.....	50
3.4.3	Phalloidins.....	50
3.5	Cell culture.....	51
3.5.1	Cell lines.....	51
3.5.2	Cell culture materials.....	51
3.5.3	Media for eukaryotic cells.....	51

3.5.4	Solutions and reagents for eukaryotic cell culture.....	53
3.6	Solutions and materials for immuno-histochemical methods.....	54
3.7	Proteinbiochemie .....	54
3.7.1	Proteins and materials for biochemical experiments.....	54
3.7.2	Solutions for biochemical methods .....	55
3.8	Software .....	58
<b>4.</b>	<b>Methods.....</b>	<b>59</b>
4.1	Molecular biology.....	59
4.2	Generation of SWAP-70 constructs.....	61
4.3	BacterioMatch <sup>®</sup> Two-Hybrid System.....	62
4.4	Cloning of palmitoylated SWAP-70 constructs.....	63
4.5	Cultivation and storage of bacteria .....	64
4.6	Biochemical Methods .....	64
4.6.1	GST-fusion protein expression and purification .....	64
4.6.2	Qualitative binding-assay (GST-pull down assay).....	66
4.6.3	Bradford protein assay.....	66
4.6.4	F-actin cosedimentation assays .....	66
4.6.5	SDS-polyacrylamide gel electrophoresis of proteins (SDS-PAGE) .....	67
4.6.6	Immunoblotting .....	67
4.6.7	Pyrene-actin polymerization assay .....	68
4.7	Cell culture.....	68
4.7.1	Cultivation of cells .....	68
4.7.2	Transfection of cells .....	69
4.8	Preparation of cells for microscopy .....	70
4.8.1	Seeding of cells.....	70
4.8.2	Pharmacological treatment of cells.....	70
4.8.3	Fixation and staining .....	70
4.9	Microscopy .....	71
4.9.1	Epifluorescence microscopy.....	71
4.9.2	Confocal laser-scanning microscopy.....	71
4.9.3	Life-cell microscopy.....	71

4.9.4	TIRF-microscopy .....	72
<b>5.</b>	<b>Results .....</b>	<b>73</b>
5.1	The C-terminal part of SWAP-70 binds to non-muscle F-actin .....	73
5.2	Artificial plasma membrane targeting of SWAP-70 results in alterations of the actin cytoskeleton and cell morphology. ....	74
5.2.1	Palmitoylated SWAP-70 localizes to the plasma membrane .....	74
5.2.2	PM-SWAP-70 induces morphological alterations .....	75
5.2.3	PM-SWAP-70 induces morphological changes in different cell lines .....	79
5.2.4	Palmitoylated SWAP-70 alters cell morphology independently of the extracellular matrix.....	80
5.2.5	Formation of vinculin containing focal adhesions is reduced in PM-SWAP-70 transfected NIH/3T3 cells. ....	81
5.2.6	Plasma-membrane localization of SWAP-70 is sufficient for F-actin binding .....	82
5.2.7	Dominant negative Rac does not rescue the phenotype induced by PM-GFP-SWAP-70 .....	83
5.3	Different domains of SWAP-70 induce distinctive changes in cell morphology. ....	84
5.3.1	PM-SWAP-70 (1-525) that lacks the actin binding domain of SWAP-70 induces dramatic morphological changes.....	85
5.3.2	PM-SWAP-(305-525) induces similar changes in cell morphology as PM-SWAP-70 (1-525).....	88
5.3.3	The palmitoylated C-terminal part of SWAP-70 (305-585) induces a phenotype similar to the palmitoylated full-length construct.....	91
5.3.4	The palmitoylated N-terminal part of SWAP-70 does not induce morphological changes .....	92
5.4	Artificially membrane targeted SWAP-70 affects the activation levels of RhoA, Ras and Cdc42 but not Rac .....	93
5.5	Ras regulates the subcellular localization of SWAP-70 .....	95
5.5.1	Dominant active Ras induces the association of SWAP-70 with F-actin arrays .....	95
5.5.2	Ras dependent activation of PI3 kinase is crucial for the localization of SWAP-70.....	100
5.5.3	A functional PH-domain is necessary for Ras-induced F-actin binding of SWAP-70.....	101



5.6	SWAP-70 interacts with RasGRP1.....	103
5.6.1	Bacterial-Two-Hybrid-screen.....	103
5.6.2	RasGRP1 interacts with SWAP-70 in the bacterial-two-hybrid system .....	105
5.6.3	Bacterially expressed GST-SWAP-70 binds to RasGRP1 .....	107
5.6.4	SWAP-70 interacts specifically with the C-terminal part of RasGRP1 .....	107
5.7	Colocalization studies of RasGRP1 with SWAP-70 .....	108
5.7.1	GFP-RasGRP1 partially colocalizes with endogenous SWAP-70 .....	108
5.7.2	Fluorophore tagged SWAP-70 and RasGRP1 colocalize in cotransfected B16F1 and NIH/3T3-cells. ....	109
5.7.3	SWAP-70 colocalizes with RasGRP1 but not with RasGRP2 .....	113
5.7.4	Colocalization of fluorophore tagged RasGRP1 and SWAP-70 depends on the actin binding properties of SWAP-70 .....	114
<b>6</b>	<b>Discussion.....</b>	<b>116</b>
6.1	SWAP-70 binds directly to nonmuscle actin .....	116
6.2	Activation of SWAP-70 .....	118
6.3	Targeting of SWAP-70 to the membrane by palmitoylation .....	118
6.4	Effects of overexpression of palmitoylated SWAP-70 on cellular morphology and the actin cytoskeleton.....	120
6.5	Regulation of small GTPases by palmitoylated SWAP-70 .....	122
6.6	The palmitoylated C-terminal region of PM-SWAP-70 induces actin reorganization .....	125
6.7	Deletion of the F-actin binding sequence results in a different phenotype.....	126
6.8	Effects of dominant active Ras on the actin cytoskeleton and localization of SWAP-70 .....	129
6.9	RasGRP1, an interactor of SWAP-70? .....	132
<b>7.</b>	<b>References .....</b>	<b>140</b>
<b>8.</b>	<b>Appendices .....</b>	<b>160</b>
8.1	Abbreviations.....	160
8.2	Supplemental Data .....	164
8.3	Lebenslauf.....	167
8.4	Danksagung .....	168

Für Henne, Walter und Stefan

## **1. Introduction**

Different cytoskeletal elements contribute to nearly every aspect of cellular function. The cellular cytoskeleton is no rigid scaffold. Its dynamic nature is based on transient and manifold regulated interactions of proteins. Elements of the cytoskeleton confer cellular shape, provide intracellular infrastructure, contribute to perception of extracellular signaling and are necessary for cell migration. Millions of immune cells migrate on patrol through our body every day. Hundreds of vesicles move along cytoskeletal tracks in each single cell. During development, billions of neuronal growth cones crawled towards their target location, forming the neuronal networks we think with.

### **1.1 Cytoskeletal elements**

Microtubules, intermediate filaments and actin-filaments are the three main cytoskeletal systems of vertebrate and many invertebrate cells. They all are polymers consisting of building blocks of monomeric proteins.

Microtubules are composed of alpha- and beta-tubulin, small globular GTPases which can self-associate to form hollow cylindrical structures that can be nucleated in the perinuclear region at the *microtubule organization center* (MTOC) and at the golgi-apparatus (Alberts *et al.*, 2004; Efimov *et al.*, 2007). From these MTOCs, microtubules extend to the cell periphery, representing e.g. tracks for motor proteins of the kinesin and dynein families (Mallik and Gross, 2004). Microtubules are also essential for nuclear division since they form the mitotic and meiotic spindles.

Intermediate filaments are formed by a heterogeneous group of proteins categorized into five different groups. Intermediate filament proteins share a conserved substructure that is necessary for their self-assembly into filaments of ~10 nm diameter. In contrast to microtubules and actin-filaments, which are assembled from highly conserved globular proteins with GTPase or ATPase activity, the building blocks of intermediate filaments are not known to have enzymatic activity (Chang and Goldman, 2004; Chou *et al.*, 2007).

Actin-filaments are formed by polymerization of the evolutionary highly conserved ATPase G-actin. Actin is among the most abundant cellular proteins and numerous cellular functions have been associated with monomeric actin (G-actin) and filamentous actin (F-actin). This work will mainly focus on the F-actin cytoskeleton.

Cells are surrounded by the plasma membrane which can not maintain a specialized form or withstand force by itself. The actin cytoskeleton is essential for the shape and plasticity of the membrane, forming a dense cortical meshwork which is tethered to the membrane. However, actin is not the only regulator of membrane plasticity. Proteins like IRSp53 and

MIM contain IM-domains which bind to phospholipids, thereby inducing or stabilizing a curvature of the membrane (Mattila *et al.*, 2007). Different additional protein domains have been identified which influence the shape of the cell membrane and therefore, act as a membrane scaffold.

### **1.2 The actin cytoskeleton**

This work focuses on a protein which binds to and influences the F-actin cytoskeleton. Hence, the organization and dynamics of the actin cytoskeleton will be explained in more detail.

#### **1.2.1 Properties of the actin molecule**

The actin cytoskeletons basic building block is monomeric actin with a molecular weight of 42 kDa. The structure of monomeric actin (G-actin) in complex with DNase I was solved by Kabsch and Holmes in 1990 (Fig. 1). The molecule has a globular structure and consists of four subdomains which are structurally separated by a cleft between subdomains 2 and 4 (Holmes *et al.*, 1990; Kabsch *et al.*, 1990). This cleft harbors a nucleotide binding site for ATP or ADP associated with a divalent cation ( $\text{Ca}^{2+}$  or  $\text{Mg}^{2+}$ ). There exist different actin isoforms in eukaryotes that mostly differ in their N-termini and are preferentially incorporated into different actin networks. Six different actin isoforms were found in vertebrates: four isoforms of  $\alpha$ -actin which are predominantly expressed in muscle cells and the less acidic  $\beta$ - and  $\gamma$ -actin which are primarily found in non-muscle cells. In plants, more than 100 different actin genes coding for at least 6 actin isoforms were found (McLean *et al.*, 1990).

Actin molecules can be posttranslationally modified by acetylation (Vandekerckhove and Weber, 1978; Rubenstein and Martin, 1983) and arginylation (Karakozova *et al.*, 2006). Recently, it has also been suggested that actin is phosphorylated by Akt (Vandermoere *et al.*, 2007). These modifications alter the biochemical properties of actin probably by influencing the association with actin binding proteins.

## Introduction

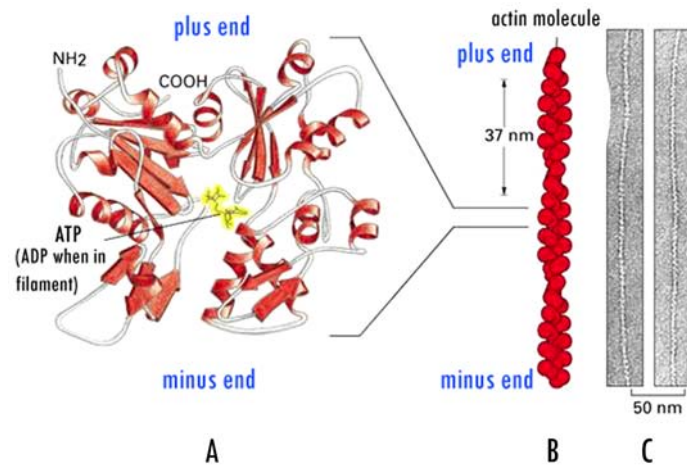


**Fig. 1. Monomeric actin polymerizes to form filamentous structures.** A: Ribbon model of an actin monomer B: Schematic drawing of an actin filament C: Electron-microscopy images of negatively stained actin filaments. (Source: Molecular Biology of the Cell, 2004)

As already mentioned, G-actin has a binding site for adenine-nucleotides (ATP or ADP) complexed with a bivalent cation. In the ATP-bound form, actin has a high affinity for other actin molecules which confers the ability to self-associate into two tightly intertwined right-handed helical filamentous polymers (F-actin; Figs. 1 and 2). Over thirty years ago it was discovered that actin has an intrinsic ATPase activity enabling it to hydrolyze bound ATP to ADP and free phosphate (Wegner, 1976). Shortly after addition of a new monomer to an existing filament, its bound ATP is hydrolyzed to ADP and the  $\gamma$ -phosphate then dissociates from the filament (Fig. 2). These events result in conformational changes of the filament which favor the dissociation of ADP-actin from the ends of the filament. *In vivo*, monomeric ADP-actin is not able to bind to F-actin. Therefore, its bound nucleotide ADP must be exchanged for ATP so that the actin monomer can incorporate into a filament.

## Introduction

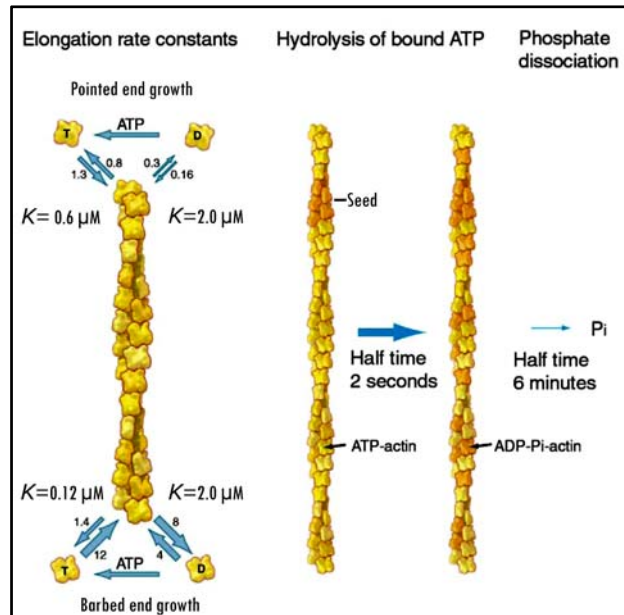


**Fig. 2. Actin filament elongation kinetics, ATP hydrolysis and phosphate dissociation.** The association rate constants (at arrows pointing towards the filament ends) have units of  $\mu\text{M}^{-1} \text{s}^{-1}$ . Dissociation rate constants (at arrows pointing away from the filaments) have units of  $\text{s}^{-1}$ .  $K$  is the dissociation rate equilibrium constant with units of  $\mu\text{M}$  and derives from the ratio of the dissociation rate constant to the association rate constant. Note that the equilibrium constants for ATP-actin differ at the two ends, giving rise to slow steady state treadmilling. While the hydrolysis of ATP bound to each subunit is fast, the dissociation of the  $\gamma$ -phosphate is very slow (altered after (Pollard and Borisy, 2003)).

### 1.2.2 Actin polarity and treadmilling mechanism

G-Actin interacts always in the same orientation with other G-actin molecules. Thus, the assembly into filaments leads to a polarized polymer with divergent characteristics at the two ends regarding the affinity for G-actin and binding of interaction partners. After the rate-limiting step of filament nucleation, ATP-bound actin can bind to both ends of the filament but with different affinities. The so-called barbed- or plus end has a roughly ten times higher association rate of monomeric actin than the pointed- or minus end (Goode and Eck, 2007). The rate of polymerization is directly proportional to the available G-actin concentration. At a concentration of  $30 \mu\text{M}$  G-actin, filaments grow by  $\sim 350$  added subunits per second. This rate roughly equals  $1 \mu\text{m}$  of polymer length per second (Goode and Eck, 2007).

The different properties of the filament ends also lead to a phenomenon known as “treadmilling mechanism” (Fig. 3) (Neuhaus *et al.*, 1983). The “critical concentration” of G-actin in which the association- and dissociation rates of monomers to the filament ends are equal, differ for the plus- and minus end. Therefore, polymerization at the plus- and depolymerization at the minus-end can occur at the equilibrium concentration of G-actin.

This leads to treadmilling, a steady state in which G-actin dissociates from the minus-end and reassociates with the plus end, resulting in a net flow of actin subunits through the filament (Revenu *et al.*, 2004; Small, 1995; Fujiwara *et al.*, 2002).

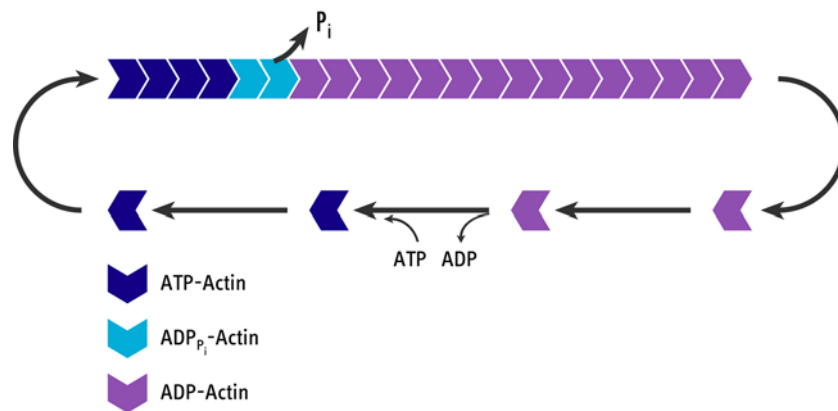


**Fig. 3. Schematic model of the treadmilling mechanism.** At the equilibrium of actin polymerization and depolymerization, actin monomers dissociate from the pointed end and associate with the barbed end due to different critical concentrations for actin polymerization of the two ends.

### 1.2.3. Capping and monomer binding proteins preserve a high level of G-actin

A prerequisite for actin based directed migration of cells is the ability to control the nucleation and the elongation of actin-filaments and to maintain a high concentration of G-actin. The ion concentration in the cytosol and the prevalent concentration of actin monomers ( $\sim 100\text{-}300\ \mu\text{M}$  in eukaryotic cells) would be sufficient for spontaneous polymerization of ATP-G-actin into filaments (Pantaloni *et al.*, 2001; Pollard *et al.*, 2000). Cells utilize different strategies to prevent this: (1) A variety of different *capping proteins* associate with existing barbed- and pointed ends to prevent further association of actin monomers and (2) the binding and sequestering of monomeric actin by G-actin binding proteins regulate the availability and the net concentration of G-actin.

#### **Capping**

Capping proteins like capZ, severin, gelsolin and villin and  $\beta 2$  (CP) bind to the barbed ends of actin filaments, restricting the number of free barbed ends with which G-actin can associate. Capping also leads to a spatially restricted net rise in G-actin concentration since monomers can still dissociate from the minus ends of existing filaments (Disanza *et al.*, 2005). Pointed ends of filaments are also a target for capping proteins such as e.g. tropomodulin that blocks (de-) polymerization (Fowler *et al.*, 2003; Weber *et al.*, 1994). A

lack of capping proteins leads to enhanced filament elongation and the formation of filopodia and microspikes.

### ***Actin monomer binding proteins***

Another strategy for maintaining a high G-actin concentration is to sequester G-actin monomers in a way that prevents their association with free barbed ends. Thymosin  $\beta$ 4 is one example of a sequestering protein. It binds actin monomers in their ATP-bound state and reduces the concentration of G-actin available for polymerization (Goldschmidt-Clermont *et al.*, 1992; Carlier *et al.*, 1993; Safer and Nachmias, 1994). The Profilins are another important family of G-actin binding proteins which influence actin dynamics. Profilins are small proteins with an approximate molecular mass of ~19 kDa (dos Remedios *et al.*, 2003). They are among the most highly expressed cytoplasmic proteins (20–100  $\mu$ M; Buss *et al.*, 1992) and are distributed throughout the cytoplasm. Probably the most important function of profilin is that it catalyzes the exchange of ADP for ATP in actin monomers (Sun *et al.*, 1995). Profilin is also reported to lower the critical concentration for actin polymerization at the barbed end. This is in keeping with reports that profilin-actin complexes are thought to be preferentially added to the barbed ends of actin filaments (Goode and Eck, 2007).

### **1.3 Generation of free barbed ends**

The elongation of actin filaments is coupled to the existence of free barbed ends. Three possibilities exist for the generation of free barbed ends. (1) The dissociation of capping proteins; (2) Severing of actin filaments; (3) *De novo* nucleation of new actin filaments from existing monomers. Cells utilize all three possibilities.

#### **1.3.1 Uncapping of actin filaments**

Uncapping of actin filaments creates free barbed ends for fast elongation. Extracellular signals induce a spatially controlled dissociation of capping proteins through phosphoinositide dependent mechanisms (Wear *et al.*, 2003). In platelets, numerous short actin filaments are capped by capZ. Activation of the platelet results in severing of these actin filaments by gelsolin. However, gelsolin stays bound at barbed ends after severing preventing further polymerization. A rise in phosphatidylinositol 4,5-P<sub>2</sub> levels provides the signal for gelsolin to dissociate, leading to fast elongation at the barbed ends and the formation of filopodia and lamellipodia (Barkalow *et al.*, 1996; Alberts *et al.*, 2004). However, it was recently reported that a rise in polyphosphoinositide levels is not sufficient for dissociation of capping proteins from F-actin in vertebrate cells (Kuhn and Pollard, 2007). Therefore, anti-capping activities by e.g. Ena/Vasp proteins (Bear *et al.*, 2002) and myotrophins (Bhattacharya *et al.*, 2006) probably contribute to uncapping.



### 1.3.2 Severing of actin filaments

Severing of actin filaments is a necessary step for the reorganization of F-actin assemblies. Severing of actin filaments provides new uncapped barbed ends at which elongation or (under G-actin limiting conditions) disassembly can occur. The protein-family of gelsolin has already been mentioned. Gelsolins are composed of six homologous domains which are connected by linker regions of various lengths. Gelsolin is regulated by calcium ions. At sub-micromolar concentrations of calcium, gelsolin is only partially activated and binds to actin, slowly severing and capping the filament. Upon a rise in calcium concentration to the micromolar range, gelsolin becomes fully active and severs actin filaments (Khaitlina and Hinssen, 2002; Sun *et al.*, 1995; McGough *et al.*, 2003). Capping of barbed ends by gelsolin is inhibited by PI(4,5)P<sub>2</sub> and probably inactivates it near the plasma membrane (Burtnick *et al.*, 2004).

Another important family of severing proteins are the Cofilins/ADFs (Actin Depolymerizing Factor) hereafter referred to as Cofilins. Cofilins are expressed in virtually all eukaryotic cells. They are relatively small (15–19 kDa) proteins that exist in multiple isoforms (dos Remedios *et al.*, 2003). Cofilins have emerged as major contributors to the actin dynamics at the plasma membrane during cell protrusion (Bamburg, 1999; Bamburg *et al.*, 1999; Pollard and Borisy, 2003; Ono, 2003). Cofilins bind monomeric and filamentous actin in the ADP-bound state. They were implicated in enhanced depolymerization rates at the pointed end as well as severing of existing filaments (Bamburg, 1999). Both activities are presumably due to a cooperative binding of cofilins to the side of F-actin causing a twist in the actin filament (5° per subunit) which leads to destabilization of actin-actin interactions and thus fragmentation of the filament (DesMarais *et al.*, 2005) and/or enhanced depolymerisation from the pointed end (Galkin *et al.*, 2001). The contributions of the severing activity to actin dynamics are still controversial, since cofilin activity has been either found to promote actin polymerization (Ghosh *et al.*, 2004) or to contribute to depolymerization of actin filaments (Hotulainen *et al.*, 2005).

### 1.4 The nucleation of new actin filaments

Severing and uncapping activities provide free barbed ends for actin filament elongation. The *de novo* formation of actin filaments is constrained by the energetically unfavoured assembly of three actin monomers. This nucleation event is catalyzed by nucleating proteins like the Arp2/3 (Actin Related Protein 2/3) complex, formins, spire proteins and a very recently found nucleator called *cordon bleu* (Cobl).

### 1.4.1 The Arp2/3 complex

The Arp2/3 complex is a large (~220 kDa), evolutionary conserved, assembly of seven protein subunits. It binds to preexisting “mother” filaments and catalyzes the *de novo* nucleation of new “daughter” filaments (Mullins *et al.*, 1998). The nucleated filaments grow at an angle of 70 degree in respect to the “mother” filaments, resulting in the formation of a mechanically rigid actin network with characteristic “Y-branches” (“dendritic” actin nucleation; Mullins *et al.*, 1998; Higgs and Pollard, 2001; Pollard *et al.*, 2000). The Arp2/3 complex is the main nucleator of the protrusive lamellipodial F-actin network, but it localizes also to regions of high actin turnover such as e.g. actin-comet-tails of vesicles and pathogens. Surprisingly for such a large complex, the assembly could be crystallized (Fig. 4). X-ray crystallography analysis suggested that the two actin-related proteins (Arp2 and Arp3) serve as nucleation site for addition of the first actin monomer in an activated Arp2/3 complex (Robinson *et al.*, 2001). Since actin filaments are coactivators of the Arp2/3 complex (Machesky and Gould, 1999; Pantaloni *et al.*, 2000), the reaction proceeds autocatalytically with newly formed actin filaments promoting the initiation of subsequent generations of filaments (Pollard and Borisy, 2003).

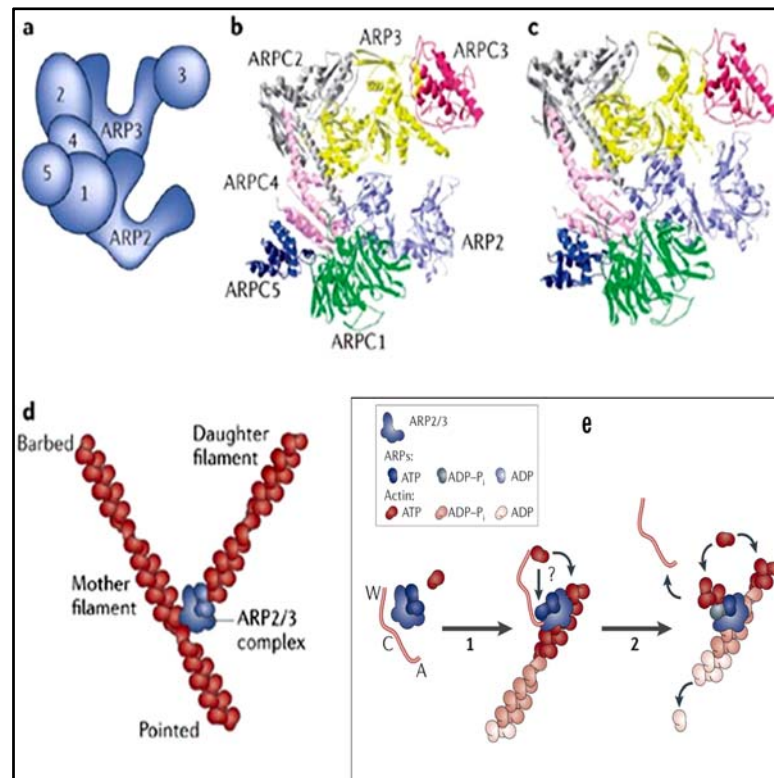


**Fig. 4. Organization and function of the Arp2/3 complex.** **a:** Schematic representation of the subunit organization in the inactive Arp2/3 complex. Arp2, Arp3 and Arp complex-1 (ARPC1) through ARPC5 are shown (labeled as 1-5). **b:** Ribbon diagram of the crystal structure of the inactive (open) conformation of the bovine Arp2/3 complex. The labeling of the different colored subunits is the same as in a. **c:** Ribbon diagram of the predicted active Arp2/3 conformation. Color coding as in b. Structure was modeled after that proposed by Robinson *et al.* (2001) **d:** Cartoon representation of the Arp2/3 complex binding to the side of the mother filament and the pointed end of the daughter filament. **e:** Model for the activation of the Arp2/3 complex. The inactive Arp2/3 complex binds to the WCA domain of WAVE. Binding results in a conformational change that primes the complex for activation. Binding of an Arp2/3-WCA-actin assembly to an existing actin filament initiates activation and the subsequent addition of a WCA bound actin monomer to the complex and possibly to the barbed end of the mother filaments (altered after (Goley and Welch, 2006).

## 1.4.2 Activation of the Arp2/3 complex

### 1.4.2.1 The Arp2/3 complex is activated by nucleation promoting factors

The Arp2/3 complex has a very low intrinsic F-actin nucleation activity (Pollard and Borisy, 2003). The complex is regulated by so called *Nucleation Promoting Factors* (NPFs) that can act as scaffold proteins for the assembly of a large molecular machine for *de novo* actin filament nucleation.

NPFs are divided in two subclasses. The best characterized members of the class I NPF proteins are the WASp (Wiscott-Aldrich Sndrome Protein) proteins and the WAVE

(WASP family Verprolin homologues) protein complex. Class one NPFs contain a VCA domain (Verprolin homology, Cofilin homology, and Acidic region domain). VCA-domains bind to G-actin and the Arp2/3 complex and this activated ternary complex interacts with an existing filament to initiate the growth of a “daughter” filament (Carrier *et al.*, 2003; Marchand *et al.*, 2001). An interesting attribute of WASP-proteins is their ability to integrate different signals. N-WASP was found to predominantly exist in an inactive form bound to WIP (WASP Interacting Protein; Anton *et al.*, 2002; Ho *et al.*, 2004). WIP has been reported to act as a chaperone for WASP and to protect WASP from degradation (de la Fuente *et al.*, 2007).

### **1.4.2.2 The Arp2/3 complex is mainly activated at the membrane**

Actin polymerization is proposed to happen at membrane surfaces mediated by membrane associated protein complexes. Regulators of F-actin dynamics often bind to lipids like phosphoinositides and phosphatidic acid. Actin filaments are thought to be semiflexible Brownian ratchets which push against the membrane through addition of monomers to the membrane directed barbed end of the filament. Nevertheless, for directed and continuous movement of vesicles, the actin filaments somehow have to be anchored to the membrane. The Arp2/3 activator N-WASP like many other actin associated proteins (e.g. cortactin, vinculin,  $\alpha$ -actinin, gelsolin) binds directly to phosphatidylinositol-4,5-bisphosphat (PtdIns(4,5)P<sub>2</sub>). This interaction leads to a structural rearrangement by which interaction sites for both actin and the Arp2/3 complex are exposed (Figs. 4 and 5). Simultaneous binding of the small GTPase Cdc42, probably in a complex with TOCA-1 (Transducer of Cdc42 dependent actin assembly; Ho *et al.*, 2004) is essential for this activation of WASP and N-WASP (Rohatgi *et al.*, 2000; Rohatgi *et al.*, 1999). Furthermore, WASP can be linked to activated tyrosine kinases via binding to SH3 domain containing adaptor proteins like WISH (WASP interacting SH3 protein; Fukuoka *et al.*, 2001), Nck and Grb2 (Rohatgi *et al.*, 2001; She *et al.*, 1997; Carrier *et al.*, 2000). The phosphorylation of two residues in the VCA domain of WASP and N-WASP might provide an additional regulatory mechanism (Cory *et al.*, 2003). Recently, the isolated WH2 domain of N-WASP has been shown to be a crucial link between growing actin filaments and membranes. It transiently attaches actin filaments to membranes and it is sufficient for continuous propulsive motility of lipid-coated glass beads by actin comet tails (Co *et al.*, 2007).

### **1.4.2.3 Arp2/3 can be activated by the WAVE complex**

The WASP related WAVE complex differs from WASP in that it is constitutively active *in vitro* and has to be regulated by a large complex of signaling and effector proteins (reviewed in (Stradal *et al.*, 2004; Stradal and Scita, 2006). Essential components of this complex include HSPC300, Abi1 and Nap1/Hem-1 (Gautreau *et al.*, 2004). WAVE activation is thought to depend on the small GTPase Rac and phosphatidylinositol 3,4,5-

## Introduction

trisphosphate [PtdIns(3,4,5)P<sub>3</sub>], that is produced locally and transiently by phosphatidylinositol 3-kinases (PI3K) at the leading edge of cells like neutrophils and *Dictyostelium discoideum* as they move in a chemotactic gradient (Oikawa *et al.*, 2004; Janmey and Lindberg, 2004). The activation mechanisms of WAVE are discussed controversially. WAVE-complexes have been shown to dissociate upon stimulation with Rac-GTP. Dissociation of the complex promotes actin polymerization *in vitro* (Eden *et al.*, 2002). The postulated inhibitory model was challenged by more recent *in vivo* and *in vitro* reconstitution assays that demonstrated that the integrity of the WAVE-Abi1-Nap1-Pir121/Sra1 complex positively regulates WAVE-dependent actin polymerization (Innocenti *et al.*, 2004; Steffen *et al.*, 2004). Dissociation of the complex by the addition of Rac-GTP was not observed in these experiments. Rac does not bind directly to WAVE, however, it is crucial for WAVE activation. Rac-WAVE interaction has been reported to depend on the insulin receptor substrate protein 53 (IRSp53) (Miki *et al.*, 2000). Recent studies showed that IRSp53 contributes to WAVE2 induced actin polymerization (Suetsugu *et al.*, 2006). This effect might be mediated by the Rac GEF TIAM which enhances binding of IRSp53 to the WAVE2 complex (Connolly *et al.*, 2005).

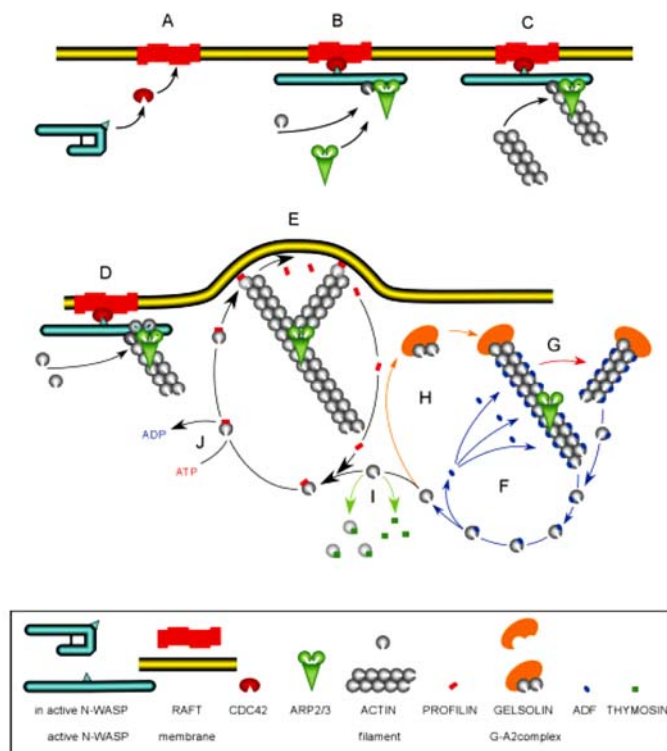


**Fig. 5. Model for N-WASP stimulated dendritic actin nucleation at the leading edge.** A: Targeting and activation of N-WASP and signaling molecules at the plasma membrane. B: Formation of a ternary branching complex consisting of Arp2/3, N-WASP and G-actin C,D: Association of the active complex with a barbed end of an existing actin filament. E: Elongation of the barbed end by addition of G-actin and profilin-actin. F,G,H: Regulation of actin dynamics through capping and severing proteins (gelsolin, ADF). I: Sequestering of monomeric ADP-actin by  $\beta$ 4-thymosin. J: Exchange of the nucleotide and re-entry in the polymerization cycle (Source: Carlier *et al* 2003).

Class II NPFs do not contain a monomeric actin binding VCA domain, but are instead equipped with a so called FAB (F-Actin Binding) domain. Metazoan cortactin and yeast Abp1p are members of the NPF class II family (reviewed by (Welch and Mullins, 2002). The class II NPF cortactin directly activates the Arp2/3 complex and stabilizes newly generated branching points, resulting in a more stable dendritic F-actin network (Weaver *et al.*, 2001).

### 1.4.3 Formins

Actin filament nucleation can also be initiated by proteins of the formin family. In contrast to the Arp2/3 complex which nucleates F-actin and from the minus end, formins nucleate filaments from the fast-growing ‘barbed’ end and they are able to catalyze the addition of G-actin to the barbed end while remaining associated to the growing filament end during elongation (Higashida *et al.*, 2004; Kovar and Pollard, 2004; Romero *et al.*, 2004). While the nucleation by the Arp2/3 complex gives rise to a dendritic network of actin filaments, formins promote the formation of unbranched actin filaments. Formins protect barbed ends from capping and promote the elongation of filaments by directing the addition of profilin-actin (Romero *et al.*, 2004; Kovar *et al.*, 2006). In this respect, formins can be seen as processive motor proteins which move by forming their own tracks. In the absence of profilin-actin, formins can act similar to capping proteins (Zigmond *et al.*, 2003), (Harris *et al.*, 2004). Members of the formin protein family interact directly with members of the Rho subfamily of small GTPases. Crystal structures of the regulatory N-terminal part of mDial and Rho have been solved by X-ray crystallography and provide evidence that binding of Rho-GTP to the N-terminal part of mDial displaces the C-terminal diaphaneous autoinhibitory domain leading to activation of the formin (Lammers *et al.*, 2005; Rose *et al.*, 2005).

### 1.4.4 Spire

A third mechanism for actin filament nucleation was discovered only recently with the protein Spire from *Drosophila melanogaster* (Quinlan *et al.*, 2005). Spire comprises multiple copies of a well-characterized actin binding domain, the WASp Homology 2 (WH2) motif (Wellington *et al.*, 1999). These evenly-spaced WH2 domains are thought to bring actin monomers into alignment to promote the formation of a single-stranded polymer (Fig. 6). In this way, Spire would act as a template for actin-nucleation. Spire stays bound to the pointed end of the growing filament, hence, the resulting unbranched filaments are resistant to pointed end disassembly (Quinlan *et al.*, 2005, (Baum and Kunda, 2005). Interestingly, other isoforms of Spire have been identified in *Drosophila*, which in

contrast to the originally identified Spire, do not nucleate actin filaments, but were reported to crosslink actin filaments with microtubules (Rosales-Nieves *et al.*, 2006).

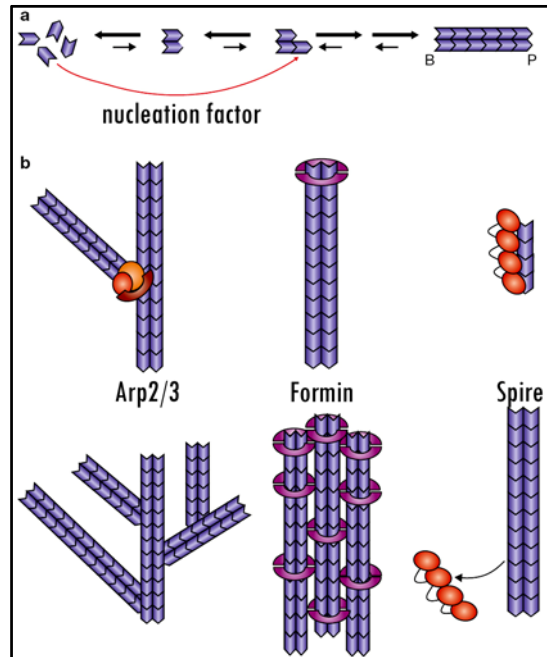


**Fig. 6. Comparison of the actin filaments derived from different nucleators.** **a:** Transition from actin monomers to a nucleus is an unfavoured event and catalyzed by nucleation factors. **b:** Nucleation by the Arp2/3 complex results in a branched dendritic actin array in which two filaments are oriented in a  $\sim 70^\circ$  angle. Formins processively elongate filaments from the barbed ends and thus result in unbranched filaments which are likely bundled by either formins or other bundling proteins. Spire proteins lead to the assembly of an actin nucleus which is elongated at its barbed end while Spire stays at the pointed end until it dissociates (Source: (Chhabra and Higgs, 2007)).

#### 1.4.5 Cordon bleu

While writing this work, the protein *cordon-bleu* (Cobl) has been reported to represent a new actin nucleator (Ahuja *et al.*, 2007). Cobl was identified in a yeast-two-hybrid assay as a syndapin I and Abp1p interacting protein and contains three highly similar WH2 domains, each able to bind and sequester an actin monomer. Ahuja and colleagues (2007) present a model, in which Cobl nucleates actin through interaction of each WH2 domain with one actin monomer, assembling a nucleating core of a linear actin dimer and a third actin monomer bound in cross-filament conformation. Thus, in contrast to the Arp2/3 complex which nucleates filaments by mimicking the conformation of an actin dimer and Spire which is thought to form a linear assembly of 4 monomers, Cobl forms a non-linear trimer which nucleates actin polymerization.

Taken together, actin filaments can be nucleated by different factors that give rise to different F-actin arrays.

## 1.5 Actin cross-linking proteins

### 1.5.1 Actin bundling proteins

Actin filaments in cells are organized into distinct arrays and structures such as lamellipodial networks, antiparallel bundles (stress fibers), parallel bundles (filopodia), peripheral concave or convex bundles as well as geodesic arrays (Small and Gimona, 1998; Heath and Holifield, 1993; Small *et al.*, 1998). Different sets of actin associated proteins control and stabilize the distinct properties of individual F-actin arrays. Single actin filaments can be bundled to form stiff unipolar structures or loosely crosslinked to form orthogonal networks or cortical meshworks underlying the plasma membrane. Among the multitude of more than 160 actin binding proteins identified, 13 proteins are F-actin crosslinking or –bundling proteins (dos Remedios *et al.*, 2003). These proteins determine the density of F-actin packing, the directionality of bundled actin filaments and they influence actin dynamics (Bartles, 2000). Actin cross-linking proteins, including  $\alpha$ -actinin, espin, fimbrin, and villin, are necessary for the formation of certain parallel actin bundles found in e.g. microvilli of the brush border epithelium, bristles from *Drosophila melanogaster* or stereocilia (Bartles, 2000; Bartles *et al.*, 1998; DeRosier and Tilney, 2000). Tight crosslinking of actin filaments is crucial for filopodial protrusion, since individual long actin filaments lack the stiffness to efficiently push the membrane forward. A major bundling factor for the formation of densely packed unipolar actin filaments in filopodial structures of cells is fascin. Apart from its actin bundling properties, fascin influences the cytoskeleton by binding to activated PKC (Hashimoto *et al.*, 2007). Downregulation of fascin inhibits filopodia formation (Vignjevic *et al.*, 2006) and carcinoma cell migration. Another protein family of bundling proteins are the espins which are the target of deafness mutations (Zheng *et al.*, 2000). Espins are present in the parallel actin bundles of hair cell stereocilia and epithelial brush border microvilli and appear to increase their steady-state length (Loomis *et al.*, 2003).

F-actin crosslinking proteins are also important for the viscoelastic properties of the cytoplasm (Xu *et al.*, 1998). The activities of the  $\alpha$ -actinins and filamins do not result in condensed actin bundles but rather in loose bundles or 3-dimensional orthogonal actin networks, respectively.  $\alpha$ -actinins which belong to the spectrin superfamily (reviewed in (Djinovic-Carugo *et al.*, 2002) are ubiquitously expressed proteins with a molecular weight of 93-103 kDa. Binding of  $\alpha$ -actinin to actin filaments leads to parallel or antiparallel actin bundles which can incorporate myosin II to form contractile F-actin bundles (Alberts, 2004). Binding of  $\alpha$ -actinin to F-actin results in filament crosslinking at low  $\alpha$ -actinin concentration and in filament bundling at higher  $\alpha$ -actinin concentration. In muscle cells,  $\alpha$ -actinin 2 and -3 crosslink actin filaments in the Z-disc and additionally connect F-actin with the huge sarcomeric protein titin upon activation by PtdIns(4,5)P<sub>2</sub> (Young and Gautel, 2000).



### 1.5.2 Talin and Vinculin connect the actin cytoskeleton to integrins

A major part of the actin cytoskeleton is closely associated with the plasma membrane and is linked directly or via adaptors to integral- as well as peripheral membrane proteins.

Integrins are the main transmembrane linkers between the actin cytoskeleton and the extracellular matrix (ECM) in which metazoan cells reside. Integrins are expressed in all metazoan cells, but are absent in prokaryotes, plants and fungi. Integrins are transmembrane linkers for the bidirectional transmission of mechanical force and biochemical signals across the plasma membrane. The transmembrane spanning integrins exhibit a large extracellular domain and a short cytoplasmic tail. They are heterodimeric proteins composed of two noncovalently associated transmembrane glycoprotein-subunits called  $\alpha$  and  $\beta$ . In vertebrates, 18 types of  $\alpha$ -subunits and 8 types of  $\beta$ -subunits have been described (Luo *et al.*, 2007). At least 24 known  $\alpha\beta$ -pairs with different properties concerning their substrates, affinities and signaling properties are formed through combination of different subunits. Many integrins recognize several ECM proteins. Conversely, individual matrix proteins, such as fibronectin, laminins, collagens, and vitronectin, bind to several integrins. Integrins can be regulated both by extracellular and by intracellular stimuli and thus serve as nexus for inside-out and outside-in signaling (Geiger *et al.*, 2001; Grashoff *et al.*, 2004). Integrins can be connected to actin filaments with the help of adaptor proteins such as talin and vinculin. Integrin clustering and linkage to the actin cytoskeleton results in adhesive structures like focal adhesions, focal complexes, fibrillar adhesions, immunological synapses and podosomes which are defined according to their molecular constituents, shape, size, subcellular localization and organization (Evans and Calderwood, 2007; Arnaout *et al.*, 2007)

### 1.5.3 ERM-proteins: tethering cortical actin to the plasma membrane

Other proteins implicated in membrane tethering of actin are the ERM-proteins (Ezrin, Radixin, Moesin). ERM proteins are generally found at sites where actin filaments are associated with the membrane e.g. ruffling membranes, filopodia and the cleavage furrow. At these sites, ERM proteins crosslink cortical actin with integral- and peripheral membrane proteins and are necessary for the generation of microvilli and cell-to-cell, as well as cell-to-substrate adhesions (Tsukita and Yonemura, 1997; Tsukita and Yonemura, 1999).

ERM-proteins are thought to reside in an inactive cytosolic state which is mediated by intramolecular interaction of the C-terminal with the N-terminal part of the proteins (Pearson *et al.*, 2000). A common motif in the highly conserved (85% identity) N-terminal half of these proteins was named FERM (band Four-point-one, Ezrin, Radixin, Moesin) domain. This domain was found in numerous actin associated proteins like the focal adhesion kinase (FAK) and myosin-X. The crystal structure of the Radixin FERM-domain shows that it consists of three subdomains which interact with one another to form a single

module. ERM proteins interact directly with adhesion molecules e.g. integrins (Hamada *et al.*, 2003) and they often exhibit binding sites for phosphatidylinositol (4,5) bisphosphate. Upon activation by phospholipids and perhaps additional phosphorylation in the C-terminal part, the intramolecular interaction is released and the protein is able to crosslink membrane proteins with F-actin. ERM proteins bind actin directly via their major actin binding site in the C-terminal 34 amino acids. Two more actin binding sites have been identified by Roy and colleagues in the Ezrin sequence (Roy *et al.*, 1997). ERM proteins attach to membranes by binding to specific integral membrane proteins such as the hyaluronan receptor CD44, CD43 and to peripheral membrane proteins such as ERM-binding phosphoprotein 50 (EBP50) to name a few (Tsukita *et al.*, 1994; Tsukita and Yonemura, 1999; Bretscher *et al.*, 2002). The interaction with integral membrane proteins is thought to be based on the interaction of the FERM domain with juxtamembrane polybasic amino acid clusters.

### **1.6 The actin cytoskeleton in cell migration: Four steps to motility**

Eukaryotic cells move by protruding a front and retracting a rear and the regulated actin polymerization and organization is fundamental for this (Small and Resch, 2005). Cell migration is thought to occur by a coordinated four-step cycle of (1) leading edge protrusion in the direction of migration, (2) adhesion to the substrate in the area of protrusion, (3) generation of tension on new adhesions to advance the cell body, and (4) de-adhesion of the trailing cell rear from the substrate and contraction (Lauffenburger and Horwitz, 1996; Gupton and Waterman-Storer, 2006). In the next chapters, some cellular structures necessary for this-four step cycle and some exemplary proteins contributing to them are introduced.

#### **1.6.1 Leading edge protrusion via synergistic effects of capping, severing and nucleation**

*To gain a true insight into the dynamics of the actin cytoskeleton it is important to reach beyond simply defining the inventory of molecules that control actin dynamics and to understand how these proteins act synergistically to modulate filament turnover (Carrier *et al.*, 2003).*

Leading edge protrusion depends on an Arp2/3 nucleated dense dendritic network of elongating actin filaments in which the polarized growth of the filaments exerts force against the plasma membrane. The force generated by the growth of a single F-actin molecule is  $\geq 1$  pN (Footer *et al.*, 2007). Some thousand growing barbed ends -approximately 100 polymerizing filaments per micrometer of the leading edge- are necessary to extend the front which is called the lamellipodium. The term lamellipodium was coined in 1970 in experiments with fibroblasts (Abercrombie *et al.*, 1970). The

## Introduction

lamellipodium is a thin leaflet of cytoplasm ~200 nm thick and 1-5 micrometres in width (Small and Resch, 2005; Prass *et al.*, 2006). The lamellipodial extension is thought to be driven by the treadmilling mechanism. However, the treadmilling mechanism can not be solely responsible for lamellipodium migration because the steady-state actin-turnover rate of  $0,27 \text{ s}^{-1}$  is two orders of magnitude too slow for it to be compatible with cell locomotion (Pollard, 1986; Michelot *et al.*, 2007). Thus, fast lamellipodial extension depends on synergistic activities of actin associated proteins that increase the rate of actin turnover in the treadmilling F-actin modul of the lamellipodium. The nucleation of new filaments via the main lamellipodial nucleator Arp2/3 goes hand in hand with severing and uncapping of existing filaments. Arp2/3 preferentially nucleates new daughter filaments from just recently polymerized F-actin. These processes lead to the generation of new barbed ends to which free ATP-actin monomers and profilin bound ATP-actin can be added, thereby elongating the filaments. The quite stable width of lamellipodia implies that actin filaments are depolymerized shortly after generation. Severing proteins like ADF/Cofilins not only contribute to the generation of free barbed ends but they also accelerate the depolymerization of older actin filaments, filling up the pool of actin monomers for new generation and elongation of actin filaments at the leading edge of lamellipodia and this activity is boosting the filament turnover. Recently, a large (~600 kDa) F-actin bound complex named CAP (Cyclase Associated Protein) has been identified which probably is involved in rapid, cofilin mediated actin turnover (Balcer *et al.*, 2003). CAP complexes exhibit a high affinity for ADP-actin compared to ATP-actin and are suggested to compete with cofilin for ADP-actin which results in an enhanced nucleotide exchange activity of actin by synergistic actions of profilin with CAP (Mattila *et al.*, 2004). CAP, monomeric ADP-actin and Profilin were reported to assemble into a ternary complex (Bertling *et al.*, 2007).

Most of the F-actin which is generated at the leading edge of lamellipodia is severed and depolymerized behind the lamellipodium and recycled to the cell front to feed lamellipodial protrusion at a rate faster than can be explained by simple diffusion (Zicha *et al.*, 2003). Some of the filaments generated at the leading edge do escape the severing activity and are incorporated into cellular F-actin based structures characterized by different F-actin binding proteins. Some of these structures are introduced in the next chapter.

Fluorescence speckle microscopy analysis revealed two different actin filament populations in the protruding region of migrating cells (Ponti *et al.*, 2004). The two populations differ in localization and kinetics: The first population, referred to as lamellipodial actin filaments, emerges at the very leading edge within an outer band of 1  $\mu\text{m}$ . These actin filament arrays exhibit rapid retrograde flow (300-500 nm/min) and then disappear 1-2  $\mu\text{m}$  behind in a narrow band of depolymerisation (Watanabe and Mitchison, 2002), Ponti *et al.*, 2004). The second population of speckles were observed with increasing frequency at some distance from the leading edge. Animated kinetic maps

showed a characteristic slower, myosin II dependent retrograde flow (100-250 nm/min) of F-actin in this region which was referred to as lamella. Later studies suggested, that persistent leading edge protrusion and rapid cell migration is dependent on the lamella network, but does not need the lamellipodial actin module (Gupton *et al.*, 2005). The junction between lamellipodium and the lamella is marked by substrate adhesions, that play an important role in cell migration.

### 1.6.2 Adhesion to the extracellular matrix

The actin cytoskeleton at the leading edge of the cell is connected to the extracellular matrix (ECM) through membrane spanning integrins which are the major linkages of the ECM to the actin cytoskeleton. A variety of >50 proteins are involved in the formation of adhesive structures (Zamir and Geiger, 2001). In cultured cells, focal contacts arise at the leading edge and provide early cell attachment. Recently, it has been reported that cells position conformationally activated beta1 integrins along the leading edge by actin driven sideways movements which probably probe for adhesion sites (Galbraith *et al.*, 2007). The formation of focal contacts is induced by the Rho GTPase family member Rac (Nobes and Hall, 1995; Rottner *et al.*, 1999). Focal contacts can mature into more stable focal adhesions that can in turn transform into fibrillary adhesions. The assembly of adhesion complexes is thought to be a hierarchical series of protein recruitments (Zaidel-Bar *et al.*, 2004). For example when cells spread on a rigid substrate, the initially formed complexes do contain paxillin, but not  $\alpha$ -actinin and zyxin which are recruited later (Laukaitis *et al.*, 2001; Zaidel-Bar *et al.*, 2003). One prerequisite for maturation of adhesion complexes is local tension (Galbraith *et al.*, 2002). Both, internal- and external forces transform small peripheral focal complexes into focal adhesions. Internal forces are dependent on Rho-signaling to Rho- associated kinase (ROCK) which activates myosin II dependent contractility of acto-myosin structures. Interestingly, when external mechanical force is applied, focal contacts mature independently of ROCK-signaling. This external force triggered maturation of focal contacts is dependent on active formin mDia1 (Riveline *et al.*, 2001). The different adhesive structures contain different integrin heterodimers and different adaptor assemblies for the link to the actin cytoskeleton (reviewed in (Berrier and Yamada, 2007). Characteristic of many focal-adhesion components is their multidomain architecture and thus their ability to interact with several distinct partner molecules. Among the proteins of integrin-adhesion plaques, Talin has received much interest as an essential adaptor protein between integrins and the actin cytoskeleton. Talin is recruited very early in the process of assembling adhesive structures (Delon and Brown, 2007) and binds directly to integrins via at least two binding sites of which one is a FERM domain. Talin's binding to integrins disrupts an intracellular salt bridge between the  $\alpha$ - and  $\beta$ -integrin subunits, leading to increased integrin affinity for the ECM (Vinogradova *et al.*,

## Introduction

2002). Talin binds in addition directly to F-actin via three actin-binding sites (Hemmings *et al.*, 1996). Furthermore, it is thought to recruit other adhesion proteins like vinculin, paxillin, tensin and  $\alpha$ -actinin which by themselves bind to F-actin and promote the formation of a stronger linkage to integrins (Fig. 7). Importantly, a focal adhesion structure is not a stable assembly, but rather turns over constantly as shown by fluorescence recovery after photobleaching. Integrin subunits were exchanged with a halftime of minutes, while proteins like paxillin and vinculin exchanged even more rapidly, with a recovery-halftime of 14 and 9 seconds, respectively (Ballestrem *et al.*, 2001). Correlational fluorescent speckle microscopy showed a correlated retrograde movement of various focal adhesion proteins with actin filaments, while integrins remained largely stationary. Therefore, vinculin, talin and actin filaments probably constitute a slippage connection between integrins and the actin cytoskeleton (Hu *et al.*, 2007). Focal adhesions are also signaling platforms. Important signaling proteins in the outside-in signaling of adhesion complexes are the integrin linked kinase (ILK), FAK and the Src family kinases (Src, Lck, fyn). ILK was originally identified through its association with the intracellular domains of  $\beta 1$  and  $\beta 3$  integrin subunits and its overexpression is sufficient to increase cell migration in a PI3 kinase and Rac-dependent manner (Qian *et al.*, 2005). A new family of actin binding proteins, named *parvins*, can be recruited by ILK and mediate association with F-actin (Legate *et al.*, 2006). The tyrosine kinase FAK associates with nascent focal adhesions. FAK binds strongly to integrin associated proteins like talin and paxillin (Chen *et al.* 1995, (Hildebrand *et al.*, 1995) and upon autophosphorylation or phosphorylation by Src confers signals to downstream effectors.

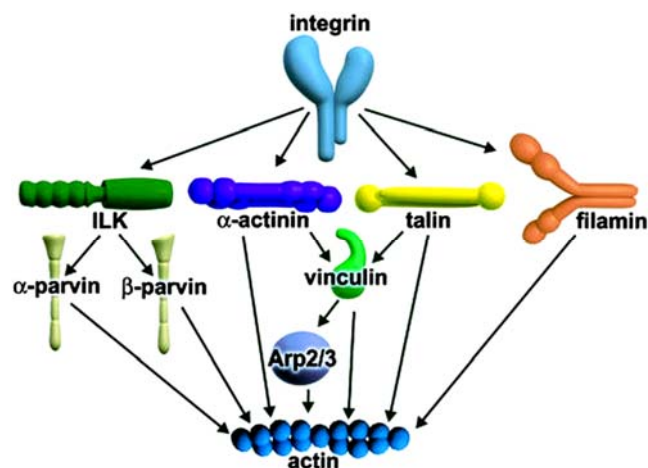


**Fig. 7. Overview of selected proteins connecting integrins with the actin cytoskeleton** (Source: Brakebusch and Fässler, 2003).

FAK activates Rac1- and Cdc42 GEFs of the Cool/  $\beta$ -PIX family (Zhao *et al.*, 2000), reviewed in (Brakebusch and Fässler, 2003). Integrin mediated adhesion is also coupled to F-actin polymerization and protrusion by direct binding of the Arp2/3 complex to Vinculin and the FERM domain of FAK (DeMali *et al.*, 2002; Serrels *et al.*, 2007).

### 1.6.3 Ruffle formation

One of the characteristic features of migrating cells is the formation of ruffles (Felder and Elson, 1990; Totsukawa *et al.*, 2004). Ruffles are defined as sheet-like membrane protrusions that do not attach to the substratum (Chhabra and Higgs, 2007). Different types of ruffles have been described. Peripheral ruffles are formed at the leading edge of motile cells (Fig. 8) from where they move centripetally and finally disappear between the cell lamella and the main cell body (Abercrombie, 1980).

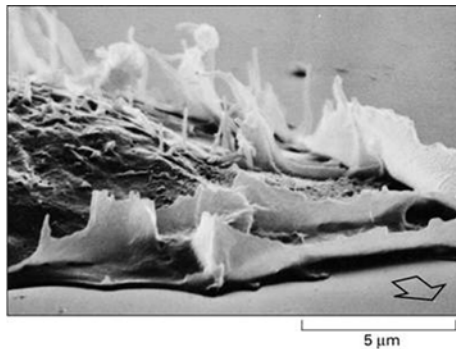


**Fig. 8. Ruffling fibroblast** Source: Alberts (2004).

Peripheral ruffles have been proposed to occur if the protruding front of the cell does not adhere properly to the ECM (Borm *et al.*, 2005). It has been reported that protrusion and adhesion-site formation occurs periodically at the leading edge (Giannone *et al.*, 2004). In a recent paper, the same authors provided

evidence that a myosin II based force pulls back a periodically regenerating F-actin module in the lamellipodium. In this model, ruffling would occur through this contractile force provided that the tip of the leading edge has not yet formed an adhesion site before the next cycle of pulling (Giannone *et al.*, 2007). Peripheral ruffling can be induced by the small GTPase Rac (Ridley *et al.*, 1992), but local RhoA activity is also necessary for formation of these structures (Kurokawa and Matsuda, 2005). Ruffles have been reported to contain actin cross-linking proteins like filamin and ezrin. Formins have also been found to localize to ruffles (Watanabe *et al.*, 1997).

A second type of ruffles coined “circular dorsal ruffles” or “waves” is assembled on the dorsal surface of cells. They can form circular structures and constrict, eventually forming macropinosomes. Circular ruffles contain  $\alpha$ -actinin-4 (Araki *et al.*, 2000) and the necessary dynamic F-actin remodeling depends on the large GTPase Dynamin 2 and the class II NPF cortactin (Krueger *et al.*, 2003). Circular dorsal ruffles are induced by receptor-tyrosine kinase-signaling, e.g. by platelet derived growth factor (PDGF) receptor- and epithelial growth factor (EGF) receptor signaling and are suggested to be an efficient mechanism to internalize sequestered growth factor receptors (Orth and McNiven, 2006). The small GTPases Rab5 and H-Ras are enriched in circular dorsal ruffles and three independent signals originating from PI3 kinase, Rab5 and Rac are simultaneously required for their formation (Lanzetti *et al.*, 2004). The plasma membrane of circular dorsal ruffles is probably enriched in PtdIns (3,4)P<sub>2</sub> since the PtdIns (3,4)P<sub>2</sub> binding Protein TAPP1 together with its binding partners of the syntrophin family localizes to circular dorsal ruffles (Hogan *et al.*, 2004).

#### 1.6.4 Stress fiber assembly and contractility

Stress fibers are contractile bundles of ~10-30 actin filaments and incorporated myosin II filaments. Stress fibers consist of anti-parallel actin filaments crosslinked by  $\alpha$ -actinin (Lazarides and Burridge, 1975). Other crosslinkers like filamin, espin and fascin have also been detected in stress fibers (reviewed in (Pellegrin and Mellor, 2007)). Binding of  $\alpha$ -actinin to F-actin is mutually exclusive with the binding of myosin II (Hotulainen and Lappalainen, 2006). In contrast to the sarcomeric structure of muscle cells, where each block of bundled actin filaments shows opposite polarity to its successive blocks, stress fibers of nonmuscle cells probably show a variety of other orientations (see Fig. 9). Stress fibers observed in fibroblasts have been divided in three different categories: Dorsal stress fibers, transverse arcs and ventral stress fibers (Small *et al.*, 1998; Heath and Holifield, 1993). These structures interact directly with one another to form a continuous and dynamic network (Hotulainen and Lappalainen, 2006).

Focal adhesions have emerged as points of dorsal stress fiber formation. In a recent elegant live-cell imaging analysis, Hotulainen and Lappalainen (2006) provided evidence that dorsal stress fibers arise from focal adhesions through the nucleation of actin filaments by mDia1/DRF, a member of the formin family. Stress fibers originate at the focal adhesions with a growth rate of ~ 0,2-0,4  $\mu\text{m}/\text{min}$  (Endlich *et al.*, 2007), Hotulainen and Lappalainen, 2006). Dorsal stress fibers can interact with transverse arcs or other focal adhesions. Since dorsal stress fibers are initially uniform actin structures, it is not easily explained how these structures can contract. Myosin II could not be detected in elongating dorsal stress fibers, but seems to be incorporated at later time points (Hotulainen and Lappalainen, 2006). Transverse arcs form by the assembly of small F-actin bundles of opposing orientation that are generated at the leading edge. These short F-actin bundles are crosslinked by  $\alpha$ -actinin and form longer bundles by annealing in an end-to-end manner with myosin II filaments. After their generation, arcs flow towards the cell center and form contractile arrays. Ventral stress fibers were reported to form through the interaction of growing dorsal stress fibers with arcs and a subsequent joining of the two dorsal stress fibers which results in a graded polarity of actin filaments and the ability to contract. Since both ends of the resulting ventral stress fiber originate from a focal adhesion, ventral stress fibers are spanned between these adhesions and able to exert force between these two anchoring points.

The contraction of stress fibers advances the cell body during cell migration. Stress fiber assembly and contraction is regulated through the Rho-GTPase pathway, which will be discussed later. Contraction is the result of myosin II interaction with actin. Myosin II is a hexamer composed of two myosin heavy chains and two pairs of essential and regulatory myosin light chains (MLC). Myosin II forms bipolar filaments that interact with F-actin and convert chemical energy derived from ATP-hydrolysis into mechanical force resulting in contraction of the stress fiber (Fig.9 B).

## Introduction

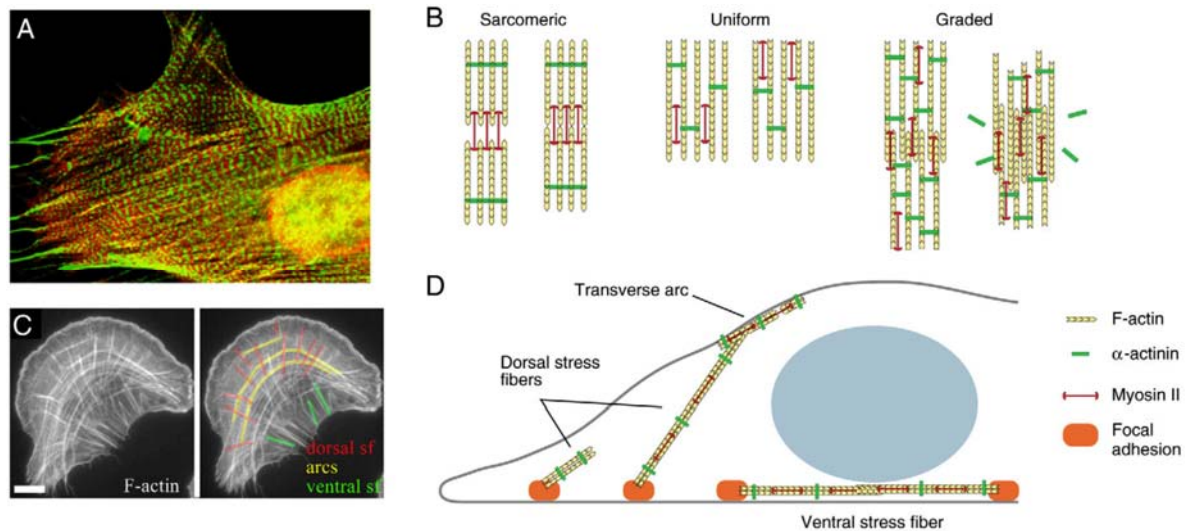


**Fig. 9. Structure and formation of stress fibers.** **A:** stress fibers in a gerbil fibroblast cell stained for  $\alpha$ -actinin (green) and non-muscle myosin (red) show a periodic pattern of these proteins. **B:** Models of stress fiber structure and contractility. Sarcomeric stress fibers consist of periodic arrangements of blocks of actin with alternating polarity and bands of interdigitating myosin bundles which are able to slide between the actin filaments resulting in contraction. Uniform stress fibers are thought to arise from focal adhesions. Myosin incorporation into these structures does not lead to contraction due to a lack of actin filaments with opposing polarity. Ventral stress fibers are thought to form from two stress fibers with uniform polarity joining at their pointed ends. This joining of overlapping filaments that are of opposite orientation could result in contraction via incorporation of myosin. **C:** U2OS osteosarcoma cells stained for F-actin. Three categories of actin stress fibers (dorsal, ventral, arcs) are visible and marked in the right hand picture in different colors. **D:** Schematic model for stress fiber formation. Dorsal stress fibers form at focal adhesions at the cell periphery and elongate up through the cell and eventually join with arcs at the surface. Ventral stress fibers derive from the joining of two dorsal stress fibers with an arc and subsequent drawing to the ventral side of the cell (Source: Pellegrin and Mellor, 2007; original model was adapted from Hotulainen and Lappalainen, 2006).

### 1.6.5 Detachment from the extracellular matrix,

Through a yet not completely understood mechanism, actomyosin based force reinforces the adhesion sites at the front of the cell and simultaneously contributes to the disassembly of adhesion sites at the rear of the cell. The separation of the cell from the ECM at the rear is the last step necessary for cell migration. The tyrosine phosphatase Shp2 was reported to influence adhesion site dynamics via regulation of FAK, thereby influencing the maturation of focal adhesions (von Wichert *et al.*, 2003). Phosphorylation of FAK at tyrosine 397 induces the disassembly of focal adhesions at the trailing edge of migrating cells (Hamadi *et al.*, 2005). A local rise in calcium concentration contributes to focal adhesion disassembly, probably again influencing FAK dynamics in focal adhesions (Giannone *et al.*, 2004). Calcium signaling also affects the activity of calpain family



proteases. Calpain-2- has been reported to mediate the proteolysis of talin 1 which is suggested to regulate adhesion turnover (Franco and Huttenlocher, 2005).

### 1.7 Mechanisms of directed cell migration

#### 1.7.1 Cells sense and respond to extracellular gradients

Directional cell movement depends on cellular polarization. Many cell types have the intrinsic ability to form pseudopodia and to move even in the absence of chemoattractants or nutrients (Sasaki *et al.*, 2007). Polarization in absence of chemoattractants is suggested to depend on a basal activation level of the signaling pathways necessary for polarization with stochastic fluctuations and feedback mechanisms leading to a steep gradient of intracellular signaling components. In *Dictyostelium discoideum* cells, pseudopodia are periodically formed even without stimulation (Wessels *et al.*, 1994). The relative uniformity of pseudopodia in size, boundary, frequency and lifetime has led to the suggestion that they are self-organizing structures (Verkhovsky *et al.*, 1999; Postma *et al.*, 2004; Van Haastert and Devreotes, 2004). A recent study in *D. discoideum* linked this basal random cell polarization to a Ras-PI3 kinase feedback loop which also depends on F-actin (Sasaki *et al.*, 2007).

In the *in vivo* situation, motile cells respond to gradients of nutrients and chemoattractants with directed chemotaxis. Eukaryotic cells can perceive- and respond to differences in chemoattractant levels as shallow as 2-10% between the front and the back of the cell (Van Haastert and Devreotes, 2004). Two sets of signals are necessary for subsequent directional migration: one set of stimulatory signals at the leading edge and another set of inhibitory signals which act at the sides and the trailing edge of cells (Xu *et al.*, 2003). Chemoattractants are mainly detected by seven transmembrane spanning serpentine-receptors which signal through heterotrimeric G-proteins (Parent *et al.*, 1998; Pierce *et al.*, 2002). Other important receptors are the receptor-tyrosine kinases which couple to a plethora of signaling proteins.

Amplification of the initial signal is thought to involve a local generation of phosphoinositides via activation of phosphatidylinositol-3 kinases (PI3 kinases). Activation of PI3 kinases leads to a local rise in PtdIns (3,4,5)P<sub>3</sub> and PtdIns (3,4)P<sub>2</sub> concentration (Parent *et al.*, 1998; Servant *et al.*, 2000; Rickert *et al.*, 2000). The small GTPases Rac and Ras have been reported to establish positive feedback loops with PI3 kinase activation (Srinivasan *et al.*, 2003; Wang *et al.*, 2002a; Weiner *et al.*, 2002; Sasaki *et al.*, 2004; Sasaki *et al.*, 2007). At the sides and the trailing edge of migrating *D. discoideum* cells, phosphoinositides are rapidly degraded by the phosphatidylinositol 3-phosphatase PTEN (phosphatase and tensin homologue) and by several

## Introduction

phosphatidylinositol 5-phosphatases and this is essential for chemotaxis (Funamoto *et al.*, 2002; Chung *et al.*, 2001). Cdc42 signaling at the leading edge of leukocytes excludes PTEN whereas RhoA is able to stimulate PTENs phosphatase activity via the RhoA effector molecule ROCK (Li *et al.*, 2005). However, localized activity of PTEN could not be found in migrating neutrophils (Xu *et al.*, 2003). Rho signaling at the trailing edge is in part responsible for regulated actomyosin contraction.

Different families of lipid kinases, which catalyze the addition of a phosphate to the sugar-moiety of inositolphosphate are known. Seven different metabolically active phosphoinositides have been identified up to now (Fig. 10, reviewed by (Parker, 2004). Different phosphoinositolphosphates are specifically recognized by a number of protein domains e.g. the PH-, ENTH, FERM-, FYVE- and PX domains (reviewed in (Lemmon, 2003), of which the PH-domain is often found in proteins involved in signaling to the actin cytoskeleton and hence will be introduced here.

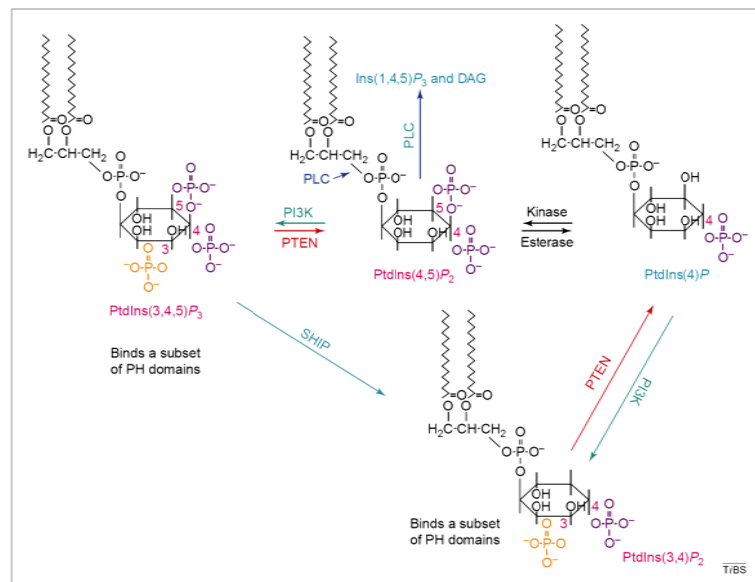


**Fig. 10. Interconversion of selected phosphatidylinositides through the activity of kinases and phosphatases (from Chung *et al* 2001).**

### 1.7.2 PH-domains as important links between gradient sensing and signaling

The PH-domains derive their name from the platelet protein *pleckstrin* in which this motif was first discovered. Pleckstrin-Homology (PH) domains are modules of ~120 amino acids that occur once or, more rarely, several times, in a protein sequence. While the amino acid sequences are poorly conserved, PH domains share a common core structure which consists of a seven-stranded  $\beta$ -sandwich formed from two near-perpendicular  $\beta$ -sheets (Ferguson *et al.*, 1995). A characteristic C-terminal  $\alpha$ -helix covers one open corner

between the  $\beta$ -sheets while the other open corner is covered by three loops between the strands. Basic residues of these loops -especially the  $\beta 1/\beta 2$  loop- are crucial for the specific binding to the phosphates in the headgroup of phosphoinositides. Phosphoinositides comprise only about one percent of the total lipid content of a cell, the most abundant phosphoinositide being PtdIns(4,5)P<sub>2</sub> and PtdIns(4)P.

A very rare but physiologically important phosphoinositide is PtdIns (3,4,5)P<sub>3</sub> the product of phosphatidylinositol 3-kinase (PI3 kinase). PtdIns (3,4,5)P<sub>3</sub> is recognized predominantly by PH-domains (Lemmon, 2003). It is present at very low levels in the membranes of unstimulated cells, but upon stimulation levels can rise to an estimated local concentration of around 150  $\mu$ M (Stephens *et al.*, 1993). PI3 kinase activity is important for directed cell migration by recruiting signaling proteins that contain PH-domains (e.g. kinases like Protein Kinase B (PKB) and Bruton's tyrosine kinase (Btk) as well as Dbl-family GEFs (guanine nucleotide-exchange factors, see below) for the Rho family of small GTPases like Tiam and SOS. During neutrophil chemotaxis, type I PI3 kinases are required for lamellipodium extension and migration towards inflammatory signals (Hirsch *et al.*, 2000; Li *et al.*, 2000; Sasaki *et al.*, 2000). Another phosphoinositide, PtdIns (3,4)P<sub>2</sub> derives from the initial product of class I PI3 kinases (PtdIns(3,4,5)P<sub>3</sub>) through 5-dephosphorylation. The inositol 5-phosphatase SHIP2 is a major contributor to PtdIns (3,4)P<sub>2</sub> generation from PtdIns (3,4,5)P<sub>3</sub> and plays a critical role for this conversion during oxidative stress (Zhang *et al.*, 2007). PtdIns(3,4)P<sub>2</sub> is also produced by class II PI3-kinases from PtdIns (4)P. Class II PI3 kinases are the most enigmatic family members of the three PI3 kinase classes to date. They preferentially phosphorylate phosphatidylinositol (PI) and PtdIns (4)P to form PtdIns(3)P and PtdIns(3,4)P<sub>2</sub>, respectively (Foster *et al.*, 2003). PtdIns (3,4)P<sub>2</sub> accumulates in cells after treatment with H<sub>2</sub>O<sub>2</sub> and this phosphoinositide has been shown to directly activate Protein Kinase B (PKB/Akt; Franke *et al.*, 1997; Klippel *et al.*, 1997).

### 1.7.3 Small GTPases are regulators of the actin cytoskeleton

#### 1.7.3.1 *Small GTPases*

The Ras (*rat sarcoma*) family of *small GTPases* belongs to a large superfamily of GTP-binding switch proteins characterized by a conserved structure and mechanism. This superfamily comprises a wide range of molecules that control a vast number of processes. Conserved GTPase core structures were found in elongation factors (e.g. EF-Tu and EF-G), the  $\alpha$ -subunits of heterotrimeric G-proteins, in large GTPases like dynamin, the *signal recognition particle* (SRP) and its receptor (SR) (Bourne *et al.*, 1990; Bourne *et al.*, 1991; Vetter and Wittinghofer, 2001).

The family of small GTPases, sometimes called the 'Ras superfamily' with reference to their in 1979 identified founding member, are divided into five major subfamilies according to their sequence and functional similarities: Ras, Rho, Rab, Ran and Arf

(Wennerberg *et al.*, 2005). To date, more than 150 small GTP-binding proteins have been identified in human. Small GTPases which have a molecular mass of 20-25 kDa are found in all eucaryotes (Takai *et al.*, 2001).

The Ras family comprises 36 members. Ras proteins are associated with the regulation of cell growth, proliferation and differentiation. Three Ras proteins, H-Ras, K-Ras and N-Ras, have been found to be frequently mutated in human cancer, implying an important role for aberrant Ras protein function in carcinogenesis. Mutations of Ras genes are especially prevalent in pancreatic (90%), lung (30%) and colorectal (50%) carcinomas (Downward, 2003), Takai *et al.*, 2001).

A vast number of studies (a PubMed search for “Ras” during this writing delivers 34327 hits, among them 4822 reviews) have attributed a central role to Ras in signal transduction pathways activated by diverse extracellular stimuli regulating gene expression. However, 10 years ago the Ras signaling pathway seemed much clearer than it is today.

The Rho (Ras homologues) subfamily comprises 20 mammalian members which in comparison to the Ras proteins share a conserved structural insert. Rho GTPases have been subgrouped into 8 subfamilies for which Rac is the evolutionary founder (Boureaux *et al.*, 2006). Some authors include mitochondrial Rho (Miro) and RhoBTB proteins within the RhoGTPases thus stating that there are 10 subfamilies (Wennerberg and Der, 2004). Rho GTPases are specific for eukaryotes and they are an evolutionary well conserved class of cellular signaling proteins (Boureaux *et al.*, 2007). Rho GTPases were identified as signaling molecules important for the organization of the actin cytoskeleton. The best characterized Rho-family-GTPases in respect to actin cytoskeleton reorganization are Rac, RhoA and Cdc42. In pioneering studies from Ridley, Nobes and Hall, it was shown that Rho regulates the assembly of stress fibers and focal adhesions, Rac induces lamellipodia formation and membrane ruffles and Cdc42 causes filopodium formation (Ridley and Hall, 1992; Ridley *et al.*, 1992; Ridley *et al.*, 1992; Nobes and Hall, 1995). Although Rho family members were first described as signaling proteins responsible for actin cytoskeleton reorganization (Hall, 1998; Mackay and Hall, 1998), they contribute to a variety of other cellular functions including adhesion, proliferation and differentiation, apoptosis, gene expression and vesicular trafficking (Ridley, 2001a; Ridley, 2001b; Takai *et al.*, 2001; Etienne-Manneville and Hall, 2002).

### **1.7.3.2 Structure and function of small GTPases**

The common catalytic domain of small GTPases (named *G*-domain) is a ~20 kDa module built of five  $\alpha$ -helices (marked A1-A5), 6  $\beta$ -strands (B1-B6) and 5 loops (G1-G5). Interestingly, the loops are the most structurally conserved motifs of the *G*-domain (Fig. 11 A,B). The loops contain amino acids that are essential for GTP/GDP-binding, e.g. coordination of  $Mg^{2+}$ -ions by the G2 and G3 loop, and nucleotide binding by the G1-loop (also called P-loop) (Wittinghofer and Pai, 1991; Saraste *et al.*, 1990; Bourne *et al.*, 1991;

## Introduction

Paduch *et al.*, 2001). Small GTPases act as molecular switches, cycling between an active GTP-bound state and an inactive GDP-bound state. Comparison of structural data revealed significant conformational changes between these two states. Two regions of particular importance have been described in the G-domain: the *Switch I* and *Switch II* regions. Switch I which corresponds to the G2-loop is called the effector loop because it is a binding site for effector molecules and GAPs (GTPase activating protein). Switch II corresponds to the third loop (G3) and part of the A2 alpha-helix. It is the structurally most flexible part of the G-domain. The mechanism behind the conformational switch of these regions has been described as *loaded spring mechanism* (Vetter and Wittinghofer, 2001). In the GTP-bound state, invariant residues of the switch-regions (for Ras: Thr35/Gly60 for switch I and II, respectively) form hydrogen bonds with oxygens of the nucleotide  $\gamma$ -phosphate (see Fig. 11C). Upon GTP hydrolysis, the  $\gamma$ -phosphate dissociates resulting in a “relaxation” of the switch regions into the GDP-specific conformation (Vetter and Wittinghofer, 2001).

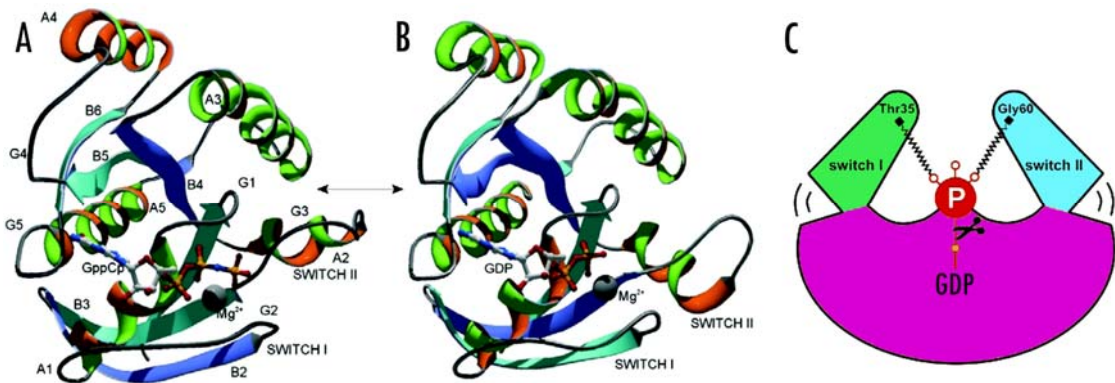


**Fig. 11. A:** Ribbon diagram of the G-domain crystal structure from Ras in complex with the nonhydrolyzable GTP analogue GppCp **B:** Ribbon diagram of the crystal structure from a GDP bound Ras. Note the different conformations of the switch II region (Source: Paduch *et al.*, 2001); **C:** cartoon representation of the “loaded spring mechanism” which is based on the interactions of the switch regions with the  $\gamma$ -phosphate from the nucleotide (Source: Vetter and Wittinghofer, 2001).

Small GTPases have poor hydrolase activities with a  $k_{\text{cat}}$  in the range of  $0.03 \text{ min}^{-1}$  for Ras to  $0.003 \text{ min}^{-1}$  for Arf1A (Paduch *et al.*, 2001). Thus, the catalytic activity is too slow to be compatible with the fast and transitory cellular signaling processes (Bourne *et al.*, 1989). Another class of GTP-binding switch proteins, the  $\alpha$ -subunits of heterotrimeric G-proteins, exhibit faster hydrolysis of bound GTP. Structural analysis revealed that an intrinsic invariant arginine-residue stabilizes the conformational transition state during hydrolysis. This arginine is missing in small GTPases of the Ras superfamily. The GTP hydrolase activity is abolished by mutations of conserved Glycins (Glycin 12 in H-Ras) and Glutamins (glutamine 61 in Ras). Substitution of these residues interferes with the  $S_N2$

mechanism of GTP-hydrolysis, therefore, the small GTPase stays in the activated conformation even in the absence of stimulatory signals (see below).

### **1.7.3.3 Regulation of small GTPases**

Since Ras family small GTPases are key mediators of signaling pathways, their correct function is essential for cellular physiology. The low intrinsic catalytic activity and slow GDP-dissociation rate of small GTPases are of physiological importance because they enable positive- as well as negative regulation through other factors (Paduch *et al.*, 2001). Some of these regulatory strategies are introduced in this chapter.

#### ***Posttranslational modifications contribute to membrane association***

Obviously, small GTPases need to be in the right place to fulfill their function in signaling pathways. Many of the small GTPases associate with cellular membranes. This association is in most cases dependent on a post-translational modification. The majority of small GTPases harbour a so-called CAAX-box at their C-terminus (C=Cys, A= aliphatic, x=any amino acid). This tetrapeptide serves as the recognition sequence for farnesyltransferase and geranylgeranyltransferase I that catalyze the covalent addition of farnesyl- or geranylgeranyl isoprenoids, respectively, to the cysteine residue of the motif. The addition of isoprenoids facilitates membrane association. Divergent C-terminal sequences of members of the small GTPases have been classified into at least four different groups for which divergent and/or additional modifications like myristoylation or palmitoylation were reported. This is especially important for farnesylated GTPases, since farnesylation alone can not stably anchor proteins to lipid bilayers (Hancock *et al.*, 1990).

H- and N-Ras GTPases are in addition to isoprenylation reversibly palmitoylated. Palmitic acid, a C16 saturated fatty acid, is esterified to the free thiol group of cysteines in the majority of cases. Palmitoylation is catalyzed by membrane-bound palmitoyl transferases (PATs) and therefore can be seen as a secondary membrane-association signal, since other factors are needed to bring the protein to the membrane in the first place (Greaves and Chamberlain, 2007). Post-translational addition of palmitic acid is not restricted to small GTPases but has been reported for many peripheral and integral membrane proteins. Palmitoylation is a reversible modification (Bijlmakers and Marsh, 2003). Cytosolic proteins can undergo cycles of depalmitoylation and repalmitoylation and consequently can shuttle between a membrane associated and a cytosolic state (Goodwin *et al.*, 2005), (Rocks *et al.*, 2005).

#### ***Degradation of small GTPases***

Cells can modulate local signaling of small GTPases at the plasma membrane by decreasing the local pool of GTPases through degradation or internalization. For example,

RhoA is ubiquitinated and degraded at the lamellipodium front through the ubiquitin-ligase Smurf1. This lowers the local RhoA level and prevents RhoA induced signaling during dynamic membrane protrusions (Wang *et al.*, 2003). Upon detachment of adherent cells, the plasma membrane association of Rac is abolished through integrin triggered internalization of low-density cholesterol rich membranes to which Rac localizes preferentially (del Pozo *et al.*, 2004). Another example for regulation of small GTPases through proper localization is the recycling of Rac. Rac is internalized and recycled via an Arf6 dependent endosomal pathway (Radhakrishna *et al.*, 1999). If internalization of Rac is inhibited by dominant-negative dynamin, Rac accumulates at the plasma membrane at aberrant dorsal membrane ruffles and lamellipodium formation at the periphery of the cell ceases (Schlunck *et al.*, 2004).

### **Activation of small GTPases by guanine nucleotide exchange factors**

Guanine nucleotide exchange factors (GEFs) or Guanine releasing proteins (GRPs) activate small GTPases by accelerating the exchange of GDP for GTP by several orders of magnitude (Vetter and Wittinghofer, 2001). GEFs are far more numerous than their “substrates” probably reflecting the need for specificity in regulation of different processes. Recent reviews state 85 GEFs for the 20 Rho family GTPases (Hall, 2005; Rossman *et al.*, 2005). Structural studies revealed that the action of GEFs is not due to a conserved catalytic domain but nonetheless based on a similar principal mechanism. Binding of GEFs to small GTPases induces conformational changes in the switch regions and the P-loop, while leaving the remainder of the structure mostly unperturbed. As a consequence of GEF-binding, the magnesium binding site of the GTPase is sterically occluded leading to a conformational change in the phosphate binding region. Therefore, GEFs reduce the affinity of the small GTPases to the bound nucleotide by deforming the phosphate binding site of the nucleotide binding pocket (Bos *et al.*, 2007). The catalytic cycle of GDP-GTP exchange involves the transition of a binary nucleotide-GTPase complex into a ternary nucleotide-GTPase-GEF complex and finally into a binary GEF-GTPase complex without bound nucleotide (Fig. 12). These competitive allosteric series of reactions can be reversed by the binding of a new nucleotide (Vetter and Wittinghofer, 2001). Since the intracellular concentration of GTP exceeds the concentration of GDP by ~10 times, the newly bound nucleotide is in the majority of cases a GTP. The resulting equilibrium of GTP/GDP bound GTPases depends not only on the concentration of these nucleotides, but also on the relative affinity of the GTPase for the two nucleotides. Furthermore, binding of effector proteins can stabilize the GTP bound form, pulling the equilibrium towards this state (Vetter and Wittinghofer, 2001, Bos *et al.*, 2007).

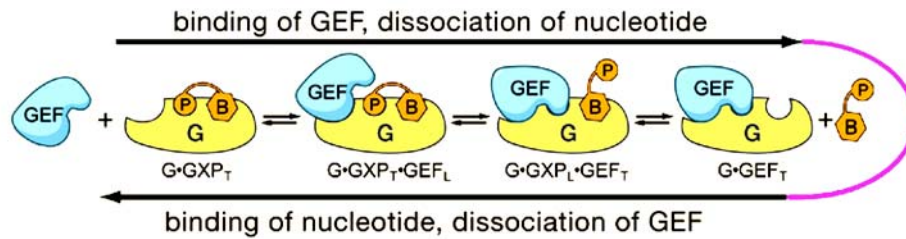


**Fig. 12. Mechanism of GEF dependent nucleotide exchange in small GTPases.** The exchange reaction occurs in successive reversible steps. The nucleotide (orange) interacts with the GTPase (G) via its base and the phosphate moieties (P). The GEF (blue) competes with the nucleotide for GTPase (yellow) binding and promotes nucleotide exchange via an intermediary ternary complex. Loose (subscript L) and tight (subscript T) interactions of the GTPase with the nucleotide and the GEF are formed during this reaction (Source: (Bos *et al.*, 2007)).

A large group of Rho-GTPase GEFs belong to the Dbl-homology (DH) family that was named after the first representative, a transforming gene from a *diffuse B-cell Lymphoma* (Eva *et al.*, 1988). The DH-domain is the catalytically active part of the GEF-protein. Typical representatives for DH proteins share a common domain arrangement, namely a PH-domain (see above) located C-terminally to the DH-domain. The PH-domains are often involved in correct intracellular localization of the GEF proteins via interactions with membrane phospholipids or other proteins. A common theme in the regulation of Rho family GEFs is relief of intramolecular interactions that inhibit the function of the catalytic DH domain. The PH-domain is often involved in this regulation and the binding of phospholipids not only positions the GEF but also activates it at the same time. P-Rex1, a GEF for Rac is stimulated by  $PtdIns(3,4,5)_3P_3$  *in vitro* (Welch *et al.*, 2002). A similar kind of positive regulation has also been reported for the Rac GEF Vav in which a direct interaction between the PH and the DH domain is relieved upon binding of  $PtdIns(3,4,5)_3P_3$  (Aghazadeh *et al.*, 2000; Das *et al.*, 2000). The opposite regulation was found in the Rho-GEF Dbl. Binding of phosphoinositides to the PH-domain of this GEF inhibits its GEF activity towards Rho (Russo *et al.*, 2001). Most GEFs are multidomain proteins. Additional ways of GEF regulation will be discussed later.

### ***GTPase activating proteins: giving a helping finger for hydrolysis***

Since the intrinsic GTPase activity of small GTPases is very slow, efficient hydrolysis needs supportive GTPase activating protein (GAP) activity which accelerates the reaction by up to five orders of magnitude (Scheffzek and Ahmadian, 2005). Comparable to the GEFs, GAPs for the different Ras-protein family members are structurally not conserved, but they all support the intrinsic hydrolase activity via providing residues that stabilize the transition state of the  $S_N2$  reaction. Early structural analysis suggested a common mechanism for Ras- and Rho-GAPs. The interaction of these GAPs with the small



GTPases stabilizes the switch regions of the small GTPase through interactions with the P-loop and the switch I and II regions. Upon GAP binding to the GTPase, a conserved glutamine residue of the G3 loop (Glu 61 in Ras) is positioned in a way that allows the oxygen of a coordinated water molecule to initiate an in-line nucleophilic attack on the  $\gamma$ -phosphate of the nucleotide. The resulting transition state is in most cases stabilized by a so called arginine finger from the GAP. The arginine finger is inserted into the phosphate binding site and neutralizes the negative charge of the pentacoordinated  $\gamma$ -phosphate transition state, thereby lowering the energy barrier for this reaction (Fig. 13). Whereas the rate limiting step of the intrinsic GTPase reaction of Ras is the hydrolysis of GTP, the rate limiting factor for the GAP catalyzed reaction is the dissociation of the  $\gamma$ -phosphate (Allin *et al.*, 2001).

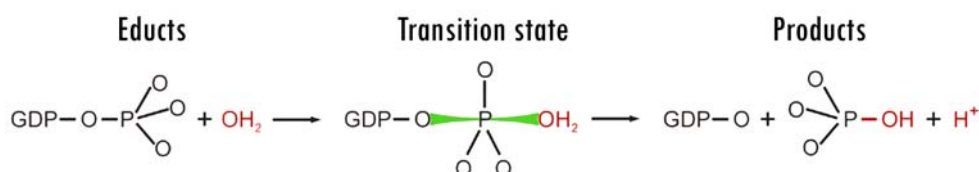


**Fig. 13. GTP-hydrolysis reaction.**

The catalytic arginine finger is conserved in many GAP molecules, so is the catalytic glutamine 61 of the small GTPases. Oncogenic substitution of the conserved glutamine results in catalytically inactive Ras and Rho GTPases. Substitution of the conserved glycine residue at position 12 of Ras sterically blocks the positioning of the arginine finger as well as the conserved glutamine (Scheffzek *et al.*, 1997). Interestingly, Small GTPases of the Rnd subfamily of Rho GTPases do not possess a conserved glutamine at position 61 and consequently are not able to hydrolyze GTP (Chardin, 2006).

### ***RhoGDIs control membrane association of small GTPases***

Small GTPases cycle between an active membrane bound state and an inactive cytosolic state (Fig. 14.). For some subfamilies of small GTPases, this cycle can be governed by the actions of GDP Dissociation Inhibitors (GDI). Three human RhoGDIs have been identified which form complexes with various members of the Rho family of small GTPases: 1) RhoGDI (or GDI $\alpha$ /GDI1), 2) Ly/D4GDI (also named GDI $\beta$ /GDI2) that is expressed in hematopoietic cells, and 3) RhoGDI $\gamma$  (or GDI3) that is specifically expressed in lung, brain and testis. RhoGDI proteins were originally named after their biochemical ability to inhibit the spontaneous dissociation of bound GDP from the GTPases. RhoGDIs main function is the extraction of the small GTPase from membranes and the subsequent formation of a cytosolic complex. Thus, RhoGDIs act as a cytosolic chaperone for geranylgeranyl modified small GTPases. The isoprenoid moiety present at the C-terminus of small GTPases is shielded from the solvent through binding to a hydrophobic pocket made of two  $\beta$ -sheets in the C-terminal part of the RhoGDI. The N-terminal part of RhoGDIs is

intrinsically unfolded but acquires a loop-structure upon GTPase binding. This loop binds to the switch 2 of the GTPase and an adjacent helix-turn-helix region binds to switch 1. RhoGDIs were also reported to bind to the GTP bound form of some GTPases, preventing intrinsic and GAP mediated GTP hydrolysis. Since the binding sites of small GTPases for RhoGDIs, GEFs and effectors overlap, RhoGDIs probably terminate GTP-GTPase signaling and prevent the GEF catalyzed reactivation of GDP-GTPases.

It has been speculated that RhoGDIs serve as factors for delivery of small GTPases to special membrane areas. The dissociation of RhoGDIs from GTPases is stimulated by *displacement factors*. ERM proteins were reported to stimulate RhoGDI release (Mammoto *et al.*, 2000) and evidences accumulates, that integrin receptors such as the neurotrophin receptor p75<sup>NTR</sup> can serve as displacement factors, too (Del Pozo *et al.*, 2002). Additionally, phosphorylation by diverse kinases of RhoGDIs might control and coordinate the dissociation and therefore, local Rho-GTPase activation (reviewed in (DerMardirossian and Bokoch, 2005; Dransart *et al.*, 2005).

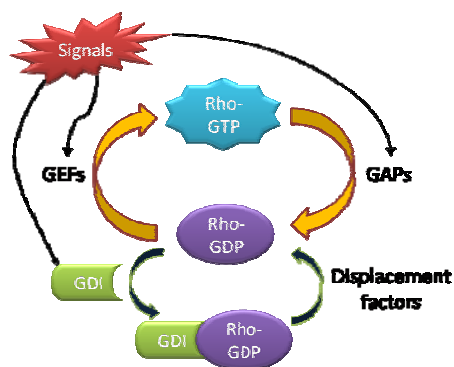


**Fig. 14. Cartoon drawing of the regulation of small GTPases from the Rho family.**

## 1.8 The protein SWAP-70

The protein SWAP-70 derives its name from a multiprotein complex identified in a screen for proteins involved in the DNA recombination events leading to the class-switch of antibody heavy chains (Borggreffe *et al.*, 1998). This switch associated protein (SWAP) complex was isolated from B-cells which were induced to switch and included the nuclear proteins nucleolin, nucleophosmin, poly (ADP-ribose) polymerase and an unknown protein of ~70 kDa which was named “SWAP-70”. Since this initial characterization as a nuclear protein, a number of studies have associated SWAP-70 with the actin cytoskeleton and signaling processes leading to the reorganization of this cytoskeletal element.

### 1.8.1 Structure and expression of SWAP-70

The gene of human SWAP-70 comprises 12 exons and encompasses over 89 kilobases on chromosome 11p15.2 (Masat *et al.*, 2000b; Rapalus *et al.*, 2001). The mouse gene is located on chromosome 7 (Masat *et al.*, 2000b). The mRNA codes for a protein of 585 amino acids with a molecular mass of ~70 kDa. Human SWAP-70 is 95% identical to the mouse protein. Database searches yield only a single close homologue which is called DEF6/IBP/SLAT (differentially expressed in FDCP-mix 6/IRF-4 binding protein/SWAP-70 like adaptor of T-cells). Human DEF6 consists of 631 residues and shows 46 % identity to SWAP-70 in a pairwise alignment.

The amino acid sequence of SWAP-70 contains several predicted motifs and domains also found in other proteins (Fig. 15). A predicted EF-hand domain is located in the N-terminal part of SWAP-70. EF-hand domains commonly bind calcium ions, but in the SWAP-70 sequence the calcium binding residues are not conserved. The amino acid D or E at position 12 of the EF-hand consensus sequence which provides oxygens for calcium binding is substituted for Q in the EF-hand motif of SWAP-70. For this reason it is unlikely that this domain of SWAP-70 has a high affinity for calcium. The sequence from amino acid 210 to 305 shows homology to PH-domains and indeed has been shown to bind to different phospholipids including PtdIns(3,4)P<sub>2</sub> and phosphatidic acid (PA) (Hilpelä *et al.*, 2003) or PtdIns(3,4,5)P<sub>3</sub> (Shinohara *et al.*, 2002; Wakamatsu *et al.*, 2006). SWAP-70 contains three regions in its C-terminal region that are predicted to adopt a coiled-coil structure (SMART-searches; Borggreffe *et al.*, 1998; Masat *et al.*, 2000a). A weak homology to Dbl homology domains (23.2% identity to DH domain of TIAM) was found in this C-terminal region (Shinohara *et al.*, 2002). DH-domains exhibit GEF activity for Rho-subfamily members. However, important residues that are necessary for GEF activity are not conserved. I will refer to this domain as DH-like (DHL) domain, as it was previously proposed for the homologous protein DEF6 (Mavrakis *et al.*, 2004). Moreover, three nuclear localization signal sequences, one nuclear export sequence and some phosphorylation sites were predicted in the amino acid sequence of SWAP-70.



**Fig. 15. Schematic drawing of the SWAP-70 domain structure.** Abbreviations in the boxes: EF= EF-hand, PH= PH-domain, CC=coiled coil region AT=Actin targeting sequence.

SWAP-70 is expressed in many tissues and cell lines (Ishikawa *et al.*, 1998; Hilpelä *et al.*, 2003). High expression levels are found in haematopoietic cells like macrophages, B-cells,

mast cells and dendritic cells. Its expression is strongly upregulated during *in vitro* differentiation of monocytes to dendritic cells (Oberbanscheidt *et al.*, 2007) and in extravillous trophoblasts during the processes of embryonic implantation and placentation (Liu *et al.*, 2007a).

### 1.8.2 Physiological functions of SWAP-70

Because SWAP-70 was originally identified as part of a nuclear complex of switching B-cells, the first studies on SWAP-70 focused on nuclear processes and B-cell physiology. Nuclear targeting of SWAP-70 was reported in LPS (lipopolysaccharide) stimulated spleen cells (Borggreffe *et al.*, 1999). Furthermore, upon CD40 and BCR stimulation, SWAP-70 relocalized from a cytosolic distribution in a sequential manner i) to the plasma membrane where it interacts with the BCR; ii) into the nucleus; and iii) back to the plasma membrane where SWAP-70 was then found to associate with IgG (Masat *et al.*, 2000a). Surprisingly, Shinohara *et al.*, (2002) reported a Rac-GEF activity of SWAP-70 and this finding implicated SWAP-70 in the reorganization of the actin cytoskeleton rather than in nuclear processes. However, the Rac-GEF activity could not be confirmed in subsequent studies and SWAP-70 was proposed to bind Rac-GTP. Another line of evidence for the involvement of SWAP-70 in actin cytoskeleton organization was found by Hilpelä *et al.*, (2003) who showed that SWAP-70 associates with a subset of loose actin-filament arrays commonly located behind the lamellipodium of motile cells and in so-called “*actin clouds*” (Ballestrem *et al.*, 1998) (see Fig. 16). The loose actin filament arrays labeled by SWAP-70 are located in close proximity to the ventral plasma membrane as shown by TIRF microscopy, and they do not contain myosin II or other F-actin associated proteins such as vinculin, tropomyosin or  $\alpha$ -actinin. In motile cells, the SWAP-70 labeled actin filament arrays follow the direction of movement, but do not extend into the lamellipodium. The association of SWAP-70 with F-actin depends on an F-actin targeting sequence that was shown to reside in the very C-terminal 60 amino acids of SWAP-70 (Hilpelä *et al.*, 2003). Recent studies provided evidence that SWAP-70 directly binds to non-muscle F-actin in an isoform dependent manner (Ihara *et al.*, 2006). The N-terminal region contributes to the specificity of the SWAP-70 association with the loose F-actin arrays, since the F-actin binding sequence alone as well as an N-terminally truncated construct starting with the PH-domain associate unselectively with cellular F-actin structures (Hilpelä *et al.*, 2003).

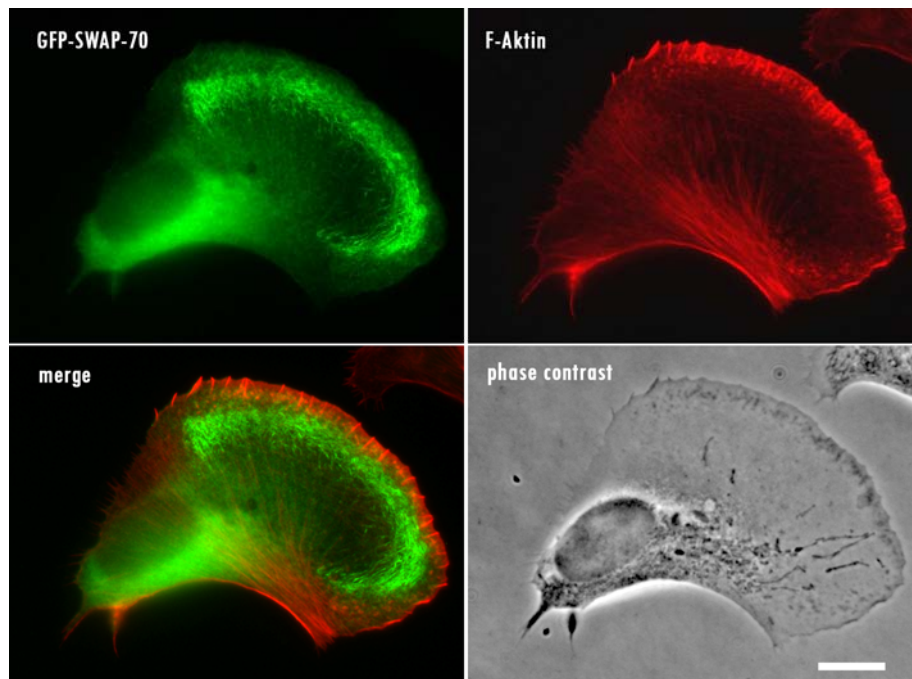


**Fig. 16. GFP-SWAP-70 associates with a subset of actin filaments in the lamella behind the protruding lamellipodium of a motile B16F1 cell.** B16F1 cells were replated on laminin 24 h post-transfection and fixed with 4% PFA after 5 hours. F-actin cytoskeleton was stained with Alexa 594 phalloidin. Cells were analyzed by fluorescence microscopy. Bar: 10  $\mu\text{m}$

### ***Regulation of SWAP-70***

While SWAP-70 colocalizes with F-actin arrays in motile cells, SWAP-70 was found to be mainly cytosolic in nonmotile cells. SWAP-70 contains a PH-domain that can bind to phosphoinositides. Shinohara *et al.* (2002) reported that SWAP-70 binds to the PI3 kinase product phosphoinositide 3,4,5 trisphosphate whereas Hilpelä *et al.* (2003) found evidence that SWAP-70 binds to phosphoinositide 3,4 bisphosphate. The association of the PH-domain with the plasma membrane is strongly increased by oxidative stress which is known to result in specific upregulation of PtdIns (3,4)P<sub>2</sub>. Mutations in the PH-domain of SWAP-70 abolish the plasma membrane association and prevent colocalization with F-actin. Currently, a working model hypothesizes that SWAP-70 resides in an inactive cytosolic form that can be recruited to the plasma membrane through binding to phosphoinositides. This binding is thought to promote the interaction of the C-terminal F-actin targeting sequence with F-actin.

### ***SWAP-70 deficient cells show defects in migration***

Since SWAP-70 is an F-actin binding protein that might link actin filaments with the plasma membrane, the loss of SWAP-70 could cause defects in actin dependent processes. Indeed, several defects have been reported for SWAP-70 deficient cells. B-cells of SWAP-70 deficient mice showed a kinetic delay in migration to lymph nodes during inflammation (Pearce *et al.*, 2006). SWAP-70 deficient B-cells had defects in polarization and formed unstable lamellipodia that were often simultaneously formed on several sides of the cell (Pearce *et al.*, 2006). Impaired *in vivo* migration has also been reported for SWAP-70<sup>-/-</sup> mast cells that migrated slower than wild-type mast cells into the peritoneum when injected in mice (Sivalenka and Jessberger, 2004).

### ***SWAP-70 is involved in integrin regulation***

SWAP-70 deficient B-cells and mast cells exhibit an abnormal, integrin-dependent homotypic association. Increased clustering of cells was observed *in vitro* (i.e. 20 fold increase of aggregates in mutant bone-marrow derived mast cells; Sivalenka and Jessberger, 2004; Pearce *et al.*, 2006). The homotypic association of cells depends on the integrin LFA-1 ( $\alpha_1\beta_2$ ) and extracellular calcium. Interestingly, SWAP-70 deficient bone-marrow derived mast cells adhere to fibronectin with lower efficiency than wildtype cells (Sivalenka and Jessberger, 2004). A direct association of DEF6, a close homologue of SWAP-70, with the integrin  $\alpha_7A$ -chain has been reported to be involved in myoblast differentiation (Samson *et al.*, 2007). SWAP-70 also interacted with this integrin chain, but with an affinity that was one order of magnitude lower than that for DEF6. The integrin  $\alpha_7A$  is specific for muscle and SWAP-70 expression is hardly detectable in muscle tissue (Hilpelä *et al.*, 2003).

### ***SWAP-70 affects the organization and dynamics of the actin cytoskeleton***

Overexpression of SWAP-70 induces alterations of the actin cytoskeleton in different cell lines. In B16F1 mouse melanoma cells, overexpression of GFP-SWAP-70 results in a loss of smooth lamellipodia. Lamellipodia of overexpressing cells exhibited strong ruffling activity and were less extended than lamellipodia of nontransfected control cells. In HtTa-1 HeLa cells, overexpression of GFP-SWAP-70 induced a loss of lamellipodia and the acquisition of highly refractile retraction fiber-like extensions (Hilpelä *et al.*, 2003).

Analysis of SWAP-70 deficient mast cells revealed alterations of actin dynamics upon stimulation of the receptor tyrosine kinase c-Kit. SWAP-70 deficient mast cells exhibited a faster accumulation and sustained elevation of F-actin upon c-Kit stimulation than wild type cells (Sivalenka and Jessberger, 2004). The authors suggested that this alteration is probably due to defects in the c-Kit signaling pathway. It could, however, be also a rather direct effect of the association of SWAP-70 with F-actin since there are hints that the

## Introduction

association with SWAP-70 might lead to the disassembly of some F-actin structures (Oberbanscheidt *et al.*, in preparation). SWAP-70 deficient fibroblasts were reported to form less lamellipodia and more stress fibers than wild-type control cells and to be impaired in the formation of ruffles induced by epidermal growth factor (EGF) (Shinohara *et al.*, 2002). Truncation constructs of SWAP-70 lacking the C-terminal actin-binding domain were reported to act in a dominant negative manner on the formation of membrane ruffles induced by EGF (Ihara *et al.*, 2006).

### ***SWAP-70 is important for macropinocytosis***

Ruffling of cells is often accompanied by macropinocytosis (Johannes and Lamaze, 2002) and live cell analyses revealed that SWAP-70 associates with newly formed macropinosomes in B16F1 and NIH/3T3 cells. In PDGF and phorbol ester stimulated NIH/3T3 cells, SWAP-70 association with the macropinosome is preceded by the accumulation of Rac-GTP and followed by the association of Rab5. To investigate whether SWAP-70 is necessary for macropinocytosis, Oberbanscheidt *et al.* (2007) compared macropinocytosis rates of bone marrow derived dendritic cells from SWAP-70 deficient- and wildtype mice. Dendritic cells exhibit constitutive macropinocytosis in immature stages of development. Indeed, macropinocytosis rate of SWAP-70 deficient cells was diminished by ~30% (Oberbanscheidt *et al.*, 2007).

### ***SWAP-70 is involved in signaling pathways***

SWAP-70 affects the actin cytoskeleton and various cellular functions (i.e. degranulation of mast cells, antibody class-switching and cell-survival upon  $\gamma$ -irradiation of B-cells, macropinocytosis, migration), but the underlying mechanisms are still not well understood. Since the actin cytoskeleton is involved in numerous processes, SWAP-70 might affect cell physiology directly through F-actin binding that might alter actin dynamics. More indirectly, SWAP-70 could also act as a signaling protein. There is evidence that SWAP-70 plays a role in several signaling pathways. It has been already mentioned that SWAP-70 was reported to associate with the small GTPase Rac and, in addition, is involved in c-Kit signaling of mast cells. Moreover, generation and analysis of SWAP-70 knockout mice provided evidence that SWAP-70 deficient B-cells are compromised in CD40 signaling. CD40 is a member of the tumor necrosis factor receptor (TNF) superfamily and its activation induces an antibody class switch in B-cells. SWAP-70 deficient B-cells are impaired in CD40 induced antibody class switching to the immunoglobulin  $\epsilon$  (IgE)-class (Borggreffe *et al.*, 2001). Moreover, the ko mice developed autoantibodies at a higher frequency than wild-typ mice and primary ko B-cells were two- to threefold more sensitive to  $\gamma$ -irradiation when activated by LPS (Borggreffe *et al.*, 2001). SWAP-70 also plays a role in mast cell function. Although mature mast cells degranulated normally upon Fc $\epsilon$ RI activation, immature mast cells exhibited a defect in IgE receptor

## Introduction

(FcεRI) mediated degranulation. The authors suggested that SWAP-70 functions in the signaling pathway downstream of FcεRI (Gross *et al.*, 2002). Furthermore, SWAP-70 deficient mice had fewer mast cells that were defective in c-Kit signaling (Sivalenka and Jessberger, 2004). Downstream effects of c-Kit signaling such as calcium release from intracellular stores, Rac and Akt localization and activation and Erk activation were aberrant in primary mast cells from SWAP-70<sup>-/-</sup> mice.



## **2. Aims of the present study**

The protein SWAP-70 binds to a special subset of actin filament arrays. In order to better understand the functions of SWAP-70 in the actin cytoskeleton dynamics, its association with actin and its influence on actin organization was investigated in this study, using biochemical and microscopy approaches. Since the association of SWAP-70 with loose actin filament arrays depends on a functional PH-domain capable to interact with 3-phosphoinositides, artificial targeting to the plasma membrane was used as a model system to study “activated” SWAP-70. To analyze the contributions of different domains of SWAP-70 on cell morphology and actin organization, different artificially plasma membrane targeted truncation constructs of SWAP-70 were examined. Small GTPases are key signaling proteins for the organization of the actin cytoskeleton. To investigate the influence of membrane targeted SWAP-70 on signaling pathways, the activation levels of different small GTPases were measured by pull down assays. Vice versa, the influence of different dominant active GTPases of the Ras superfamily on the molecular distribution of SWAP-70 was investigated. Bacterial two-hybrid screens were used to find interaction partners for SWAP-70. One of them was further characterized.

### **3. Materials**

#### **3.1 Equipment**

<b>Name</b>	<b>Company</b>
Balance 1412	Sartorius, Göttingen
CCD camera Imago	TILL Photonics, Gräfelfing
CCD camera Orca C4742-95 12G04	Hamamatsu Photonics (Herrsching/Ammersee)
Centrifuge 1-13	Sigma, Osterode
Centrifuge 5402	Eppendorf, Hamburg
Centrifuge 5415R	Eppendorf, Hamburg
Centrifuge 5804R	Eppendorf, Hamburg
Centrifuge Medifuge 15000	Heraeus Sepatech, Osterode
Centrifuge Sorvall <sup>®</sup> RC5C	DuPont, Bad Homburg
Chemiluminescence reader Fujifilm LAS-1000	Fujifilm, Straubenstadt
CO <sub>2</sub> Incubator Heraeus <sup>®</sup> BBD 6220	Thermo Electron, Langenselbold
DNA Gel documentation System BioDoc Analyse	Biometra, Göttingen
DNA electrophoresis chamber	Febikon, Köln
DNA electrophoresis chamber	
Gel dryer Speed Gel <sup>™</sup> System SGD210D	Thermo Savant, Waltham (MA, USA)
Gradient Mixer Minipuls2	Gilson, Villiers-Le-Bel (F)
Heater Block Heater	Stuart Scientific, Redhill (UK)
Heating magnetic stirrer Ikamag <sup>®</sup> RCT	Janke & Kunkel, Staufen
Heating waterbath 1083	GFL, Burgwedel
Heating waterbath MV-4	Julabo, Seelbach
Horizontal shaker Certomat <sup>®</sup> R	B. Braun, Melsungen
Incubator for bacteria	Bachhofer, Reutlingen
Laminar air flow cabinet Heraeus HERA <sup>®</sup> safe	Thermo Electron, Langenselbold
Microcentrifuge SD	Roth, Karlsruhe
Microscope Axiophot I	Zeiss, Jena
Microscope TDH	Nikon, Düsseldorf
Microscope CK 40	Olympus Optical Co. , Tokyo (J)
Microscope LSM 510	Zeiss, Jena
Microscope Axiovert 200M	Zeiss, Jena
Monochromator Polychrome IV	TILL Photonics, Gräfelfing

## Materials

Multitron shaking incubator	Infors, Aachen
PCR block	Biometra, Göttingen
pH meter Accumet Basic	Fisher Scientific, Schwerte
Photometer BioPhotometer (RE 232 C	Eppendorf, Hamburg
Photometer Wallac Victor <sup>2</sup> 1420	Perkin Elmer, Rodgau-Jügesheim
Photometer LS55	Perkin Elmer, Rodgau-Jügesheim
Photometer Ultrospec 2000	Pharmacia, Uppsala (S)
Pipettes (0,5-2,5 µl, 1-10 µl, 10-100 µl, 100-1000µl)	Eppendorf, Hamburg
Power supply PS 500XT	Hofer Scientific Instruments, San Francisco (CA, USA)
Power supply 1420A	Bio-Rad Laboratories, Hercules (CA, USA)
Precision Balance 1702	Sartorius, Göttingen
Quartz cells	Hellma, Mühlheim
Rotating mixer RM5	Karl Hecht KG, Sondheim
SDS gel-electrophoresis System SE600 Series	Hofer Scientific Instruments, San Francisco (CA, USA)
Sonicator Labsonic <sup>®</sup> M	B. Braun, Melsungen
Tank Blot apparatus (SE 600 series)	Hofer Scientific Instruments, San Francisco (CA, USA)
Ultracentrifuge L8-50 M/E	Beckman Coulter, Krefeld
Ultracentrifuge Optima <sup>™</sup> MAX-E	Beckman Coulter, Krefeld
UV stratalinker 1800	Stratagene, La Jolla (CA, USA)
UV Transilluminator UVT-20 LE	Herolab, Wiesloch
Vortex Genie 2	Bender & Hobein, Zürich (CH)

### 3.2 Chemicals

Standard chemicals were of analytical purity grade and were purchased from Applichem, (Darmstadt), Diagonal (Münster), MERCK (Darmstadt), Roth (Karlsruhe) and Sigma-Aldrich (Munich) if not quoted differently.

### 3.3 Molecular biology

#### 3.3.1 Prokaryotic cell lines

Table 1. Bacterial strains

<i>E. coli</i> strain	Genotype	Reference
<b>XL1-Blue MRF' Kan (strain harboring the pTRG cDNA library)</b>	$\Delta(\text{mcrA})183 \Delta(\text{mcrCB-hsdSMR-mrr}) 173$ $\text{endA1 supE44 thi-1 recA1 gyrA96 relA1}$ $\text{lac}[F' \text{ proAB lacI}^q \text{ HIS3 aadA Kan}^r]$	Stratagene, La Jolla (CA, USA)
<b>BacterioMatch<sup>®</sup> II Two-Hybrid System reporter strain</b>	$\Delta(\text{mcrA})183 \Delta(\text{mcrCB-hsdSMR-mrr}) 173$ $\text{endA1 hisB supE44 thi-1 recA1 gyrA96}$ $\text{relA1 lac}[F' \text{ proAB lacI}^q \text{ HIS3 aadA Kan}^r]$	Stratagene, La Jolla (CA, USA)
<b>DH5<math>\alpha</math></b>	$F^-$ , $\phi 80\text{dlacZ}\Delta\text{M15}$ , $\Delta(\text{lacZYA-argF})\text{U169}$ , $\text{deoR}$ , $\text{recA1}$ , $\text{endA1}$ , $\text{hsdR17}(\text{rK}^-, \text{mK}^+)$ , $\text{phoA}$ , $\text{supE44}$ , $\lambda^-$ , $\text{thi-1}$ , $\text{gyrA96}$ , $\text{relA1}$	Hanahan, 1983
<b>BL21(DE3)</b>	$F^- \text{ ompT hsdS}_B(\text{r}_B\text{-m}_B^-) \text{ gal dcm l}(\text{DE3})$	Studier and Moffatt, 1986
<b>NovaBlue Singles<sup>™</sup></b>		Merck (Novagen <sup>®</sup> ), Darmstadt

#### 3.3.2 Media for prokaryotes

Name	Composition
Luria-Bertani (LB) medium	10 g Bacto-Tryptone/Peptone, pH 7,4 5 g yeast extract 5 g NaCl 1 ml 1M NaOH H <sub>2</sub> O ad 1 l
LB Agar	1,8% agar (w/v) in LB medium
M9 salts (10x)	42,54 g Na <sub>2</sub> HPO <sub>4</sub> 15 g KH <sub>2</sub> HPO <sub>4</sub> 2,5 g NaCl

## Materials

	5 g NH <sub>4</sub> Cl H <sub>2</sub> O ad 1 l
M9 <sup>+</sup> His-dropout Broth (500 ml)	380 ml sterile, deionized H <sub>2</sub> O 50 ml of 10× M9 salts 67,5 ml M9 media additive H <sub>2</sub> O ad 500 ml
M9 Media Additives	<b>Solution I:</b> 10 ml of 20% glucose (filter-sterilized) 5 ml of 20 mM adenine HCl (filter-sterilized) 50 ml of 10× His dropout amino acid supplement <i>Note: Sterilize the 10× His dropout supplement by autoclaving at 121°C for 15 minutes prior to addition to solution I. Do not exceed 15 minutes</i>  <b>Solution II:</b> 0,5 ml of 1 M MgSO <sub>4</sub> 0,5 ml of 1 M Thiamine HCl 0,5 ml of 10 mM ZnSO <sub>4</sub> 0,5 ml of 100 mM CaCl <sub>2</sub> 0,5 ml of 50 mM IPTG <i>Note: Filter-sterilize the thiamine-HCl and the IPTG prior to use. Sterilize the remaining components of Solution II by autoclaving</i>
Nonselective Screening Medium (500 ml)	380 ml deionized H <sub>2</sub> O 7,5g Bacto agar Autoclave at 121°C for 20 minutes Cool the agar to 70 °C, and then add 50 ml of 10×M9 salts When the agar mixture has cooled to 50°C, <b>immediately</b> add one preparation of prewarmed (~45°C) M9 Media Additives (67,5 ml) containing the following agents: 0,5 ml of 25 mg/ml chloramphenicol 0,5 ml of 12,5 mg/ml tetracycline
Selective Screening Medium (5	In a 500-ml flask, combine:

## Materials

mM 3-AT) (500 ml)	<p>7,5g Bacto agar  380 ml H<sub>2</sub>O  Autoclave at 121°C for 20 minutes  Cool the agar to 70°C, then add  50 ml of 10× M9 salts  When the agar mixture has cooled to 50°C,  <b>immediately</b> add M9 Media Additives (67.5 ml)  plus  0,5 ml of 25 mg/ml chloramphenicol,  0,5 ml of 12,5 mg/ml tetracycline  2,5 ml of 1 M 3-AT (dissolved in DMSO)</p>
Dual Selective Screening Medium (5 mM 3-AT + Strep)(500 ml)	<p>In a 500-ml flask, combine:  7,5g Bacto agar  380 ml H<sub>2</sub>O  Autoclave at 121°C for 20 minutes  Cool the agar to 70 °C, and then add  50 ml of 10× M9 salts  When the agar mixture has cooled to 50°C,  <b>immediately</b> add M9 Media Additives (67.5 ml)  plus  0,5 ml of 25 mg/ml chloramphenicol  0,5 ml of 12,5 mg/ml tetracycline  2,5 ml of 1 M 3-AT (dissolved in DMSO)</p>
3-AT Stock-solution 1M	<p>0,5 ml of 12,5 mg/ml streptomycin  Dissolve 840,8 mg of 3-AT in 10 ml of  DMSO</p>
S.O.C. medium	<p>20 g Bacto Tryptone, pH 7,0  0,5 g NaCl  5g Bacto yeast extract  10 ml 250 ml KCl,  H<sub>2</sub>O ad 1 l</p>

### 3.3.3 Antibiotics

Ampicillin	100 µg ml <sup>-1</sup> medium	Roth, Karlsruhe
Chloramphenicol	12,5 µg ml <sup>-1</sup> medium	
Kanamycin	50 µg ml <sup>-1</sup> medium	Omnilab, Bremen







### 3.3.8 Oligonucleotides

Primers for PCR and sequencing were obtained from Biomers (Ulm).

**Table 2. Oligonucleotides used in this study**

Name	Sequence	Application
MB687	AAGGAAACTAGCGGCCGCAATGGGGAGCTTGAAG GAGGA	Construction of SWAP-70:pBT; 1 <sup>st</sup> part:pBT etc.
MB688	GGAATTCCTCACTCCGTGGTCTTTTTCT	Construction of DH:pTRG; C:pTRG; C:pBT
MB695	CGCGGATCCTCACTCCGTGGTCTTTTTCTC	Construction of SWAP-70:pBT
MB714	AAGGAAACTAGCGGCCGCGATGGCAACTAATAAG ACCAAG	Construction of C- term :pBT
MB732	AAGGAAACTAGCGGCCGCTCATCTGTTGAAGCTGG GCAG	Construction of DH:pTRG
MB705	CGCGGATCCGATGTGTAAAGCAGGGTTACA	Construction of PH:pTRG
MB715	CGCGGATCCGATGTGTAAAGCAGGGTTACA	Construction of PH:pTRG
MB716	GGAATTCATATAAATAAGGCATGTAGCCCT	Construction of EF:pBT; EF:pTRG
MB721	CGCGGATCCTCACACATCTAATATAAGTTCATT AA	Construction of 1 <sup>st</sup> part:pBT
MB711	TCCGTTGTGGGAAAGTTATC	FW Sequencing primer for pBT
MB712	GGTAGCCAGCAGCATCC	RV Sequencing primer for pBT
MB706	TGGCTGAACAACTGGAAGCT	FW Sequencing primer for pTRG
MB707	AAACTGCCAAGCTTGCATGC	RV Sequencing primer for pTRG
MB671	TCCCCGGGTATGGGGAGCTTGAAGGAGG	SWAP-70:pGEX- 4T-1
MB672	CCGCTCGAGTCACTCCGTGGTCTTTTTCT	SWAP-70:pGEX- 4T-1

### 3.3.9 Plasmids

#### Plasmids for BacterioMatch<sup>®</sup> Two-Hybrid System

Name	Reference
pBT	Stratagene, La Jolla (CA, USA)
pBT-LGF2	Stratagene, La Jolla (CA, USA)
pTRG	Stratagene, La Jolla (CA, USA)
pTRG-GAL11P	Stratagene, La Jolla (CA, USA)
SWAP-70:pBT	This work
SWAP-70 (1-211):pBT	This work
SWAP-70 (1-211):pTRG	This work
SWAP-70 (306-585):pTRG	This work
SWAP-70 (211-306):pTRG	U. Honnert
SWAP-70 (1-78):pBT	This work
SWAP-70 (1-78):pTRG	This work
SWAP-70 (525-585):pBT	This work
SWAP-70 (526-585):pTRG	This work
<b>Bacterial expression vectors</b>	
pGEX-4T-1	Pharmacia
pGEX-SWAP-70	This work
pGEX-SWAP-70 (525-585)	M. Lasic
pGEX-RAF-RBD	C. Block
pGEX-Rhotekin-C21	Reid <i>et al.</i> , 1996
pGEX-Pak-CRIB	Sander <i>et al.</i> , 1998
<b>Eukaryotic expression vectors</b>	
pEGFP-C1	BD Biosciences (Clontech), Heidelberg
pEGFP-SWAP-70	Hilpelä <i>et al.</i> , 2003
pEGFP-SWAP-70 (R230C)	Hilpelä <i>et al.</i> , 2003
pEGFP-SWAP-70 (RR 223,224 EE)	Hilpelä <i>et al.</i> , 2003
pEGFP-SWAP-70 (1-525)	Hilpelä <i>et al.</i> , 2003
mCherry-SWAP-70	F. Van den Boom, B. Terstegge
pEGFP-DEF6	U. Honnert
pMJC39 (RasGRP2-pEGFP-C1)	M.J. Caloca
pMJC40 (RasGRP1-pEGFP-C1)	M.J. Caloca
mCherry-RasGRP1	This work

## Materials

BJJ3 (PM-GFP-SWAP-70)	M.M. Kessels & B. Qualmann
BJL3 (PM-GFP-SWAP-70 [RR 223,224 EE])	M.M. Kessels & B. Qualmann
BYD8 (PM-GFP-SWAP-70 [1-525])	M.M. Kessels & B. Qualmann
PM-GFP-SWAP-70 (1-210)	J. Dang
PM-GFP-SWAP-70 (305-585)	J. Dang
PM-GFP-SWAP-70 (305-525)	J. Dang
PM-GFP	This work
mRFP-Rac1 (12V, 17N) dominant negative Rac1	U. Honnert
Myc-R-Ras (38V) dominant active R-Ras	A. Hall
Myc-H-Ras (12V) dominant active H-Ras	A. Hall
pLHA 110 CAAX (constitutively active PI3K)	M. Thelen
Myc-Rac1 (12V) dominant active Rac1	A. Hall
Myc-Rap1 (12V) dominant active Rap	A. Hall
mRFP-actin	Klemens Rottner

### 3.4. Proteins

#### 3.4.1 Proteins and enzymes for molecular biology

Taq DNA polymerase	NEB, Beverly (MA, USA)
Pfu DNA polymerase	Fermentas, St. Leon-Rot/NEB, Beverly (MA, USA)
Vent DNA polymerase	NEB, Beverly (MA, USA)
Restriction endonucleases	Fermentas, St. Leon-Rot / Roche Diagnostics, Mannheim
Lysozym	Sigma-Aldrich, Munich
RNase A	Roche Diagnostics, Mannheim
T4 DNA ligase	NEB, Beverly (MA, USA)/Promega, Mannheim
Thrombin	Sigma-Aldrich, Munich

### 3.4.2 Antibodies

Primary Antibody	Dilution	Obtained from
$\alpha$ -Cdc42, mAK, mouse,	WB 1:250	BD Biosciences, Heidelberg
$\alpha$ -Rac, mAK, 23A8, mouse	WB 1:1000	Upstate, Charlottesville, (VA, USA)
$\alpha$ -Rho, mAK, 26C4, mouse	WB 1:250	Santa Cruz, Heidelberg
$\alpha$ -Pan-Ras, mAK	WB 1:400	Calbiochem,
$\alpha$ -SWAP-70 pAK, GK2, rabbit	WB 1:250; IF 1:100	G. Kalhammer, AG Bähler
$\alpha$ -GST, pAK, rabbit	WB 1:2000	Sigma, Aldrich, Munich
$\alpha$ -GFP, mAK, 264-449-2, mouse	WB 1:7	Gift from M. Maniak
$\alpha$ -RasGRP1, pAK sc-28581, rabbit	WB 1:100	Santa Cruz, Heidelberg
$\alpha$ -HA-tag (HA.11)	IF 1:100	BabCo, Freiburg
$\alpha$ -c-myc, mAK, 9E10, mouse	IF 1:1000	Roche Diagnostics, Mannheim
$\alpha$ -vinculin, mAK hVIN-1, mouse	IF 1:300	Sigma-Aldrich, Munich
goat $\alpha$ -mouse IgG, Cy3 coupled	IF 1:1000	Jackson ImmunoResearch (Soham, Cambridgeshire, UK) distributed by Dianova, Hamburg
goat $\alpha$ -rabbit IgG, Cy3 coupled	IF 1:2000	Jackson ImmunoResearch (Soham, Cambridgeshire, UK) distributed by Dianova, Hamburg
goat $\alpha$ -mouse IgG, HRP coupled,	WB 1: 5000-1:10000	Jackson ImmunoResearch (Soham, Cambridgeshire, UK) distributed by Dianova, Hamburg
goat $\alpha$ -rabbit IgG, HRP coupled,	WB 1: 5000-1:10000	Jackson ImmunoResearch (Soham, Cambridgeshire, UK) distributed by Dianova, Hamburg

### 3.4.3 Phalloidins

Name	Dilution	Obtained from
------	----------	---------------

## Materials

Alexa Fluor 594 Phalloidin	1:100	Molecular Probes, Leiden (NL)
Alexa Fluor 350 Phalloidin	1:75	Molecular Probes, Leiden (NL)

### 3.5 Cell culture

#### 3.5.1 Cell lines

Name	Description	Organism
B16F1	Melanoma cells	<i>Mus musculus</i>
HEK 293T	Fibroblasts derived from kidney. Genomic integration of a copy of the large T'-antigens of SV-40 virus	<i>Homo sapiens</i>
NIH/3T3	Fibroblasts	<i>Mus musculus</i>
HeLa	Cervix carcinoma cells	<i>Homo sapiens</i>

#### 3.5.2 Cell culture materials

Description	Obtained from
Cell culture flasks and dishes	Techno Plastic Products (TPP <sup>®</sup> ), Trasadingen (CH)
Multi-Well Plates	Techno Plastic Products (TPP <sup>®</sup> ), Trasadingen (CH)
Sterile filters	Millipore Corporation, Bedford (MA, USA)
Coverslips	Roth, Karlsruhe
Kryo-tubes	Techno Plastic Products (TPP <sup>®</sup> ), Trasadingen (CH)

#### 3.5.3 Media for eukaryotic cells

Name	Composition	Obtained from
MEM culture medium ( <i>Minimal Essential Medium</i> )	MEM 2 mM L-glutamin 50 U ml <sup>-1</sup> penicillin G 50 µg ml <sup>-1</sup> streptomycin sulfate FCS (10% v/v, heat inactivated)	Invitrogen, Karlsruhe Invitrogen, Karlsruhe Invitrogen, Karlsruhe Invitrogen, Karlsruhe Biochrom, Berlin

## Materials

DMEM culture medium ( <i>Dulbecco's modified Eagle's Medium</i> )	DMEM 2 mM L-Glutamine 50 U ml <sup>-1</sup> penicillin G 50 µg ml <sup>-1</sup> streptomycin sulfate FCS (10% v/v, heat inactivated)	Invitrogen, Karlsruhe Invitrogen, Karlsruhe Invitrogen, Karlsruhe Invitrogen, Karlsruhe Biochrom, Berlin
HAM'S F-12 Medium (N8641)	HAM'S F-12 Medium 2 mM L-Glutamine 50 U ml <sup>-1</sup> penicillin G 50 µg ml <sup>-1</sup> streptomycin sulfate FCS (10% v/v, heat inactivated)	Sigma-Aldrich, Munich Invitrogen, Karlsruhe Invitrogen, Karlsruhe Invitrogen, Karlsruhe Biochrom, Berlin

**3.5.4 Solutions and reagents for eukaryotic cell culture**

<b>Name</b>	<b>Composition</b>	<b>Obtained from</b>
Freezing solution for cells	90% (v/v) heat-inactivated FCS 10 % (v/v) DMSO	Biochrom, Berlin Sigma-Aldrich, Munich
PBS	137 mM NaCl 2,7 mM KCl 10,2 mM Na <sub>2</sub> HPO <sub>4</sub> 1,8 mM KH <sub>2</sub> PO <sub>4</sub> pH 6,95	
HBSS	50 mM HEPES, pH 7.0 1,5 mM Na <sub>2</sub> PO <sub>4</sub> /HCl 280 mM NaCl	
Trypsin solution	0,05 % (w/v) trypsin 0,53 mM EDTA·4 Na in HBSS	
2x BBS	50 mM BES, pH 6.95 1,5 mM Na <sub>2</sub> HPO <sub>4</sub> 280 mM NaCl	
Superfect <sup>®</sup> Transfection Reagent		Qiagen, Hilden
Polyfect <sup>®</sup> Transfection Reagent		Qiagen, Hilden
Effectene <sup>®</sup> Transfection Reagent		Qiagen, Hilden
PMA (Phorbol 12-myristate 13-acetate)		Sigma-Aldrich, Munich
LY294002		Sigma-Aldrich, Munich
Wortmannin		Sigma-Aldrich, Munich

### 3.6 Solutions and materials for immuno-histochemical methods

Name	Composition
Laminin coating buffer	50 mM Tris/HCl pH 7,5 150 mM NaCl
Fixing solution	4% paraformaldehyde in PBS
Quench-solution for scavenging of free aldehyde groups	0,1 M Glycin in PBS
Permeabilization solution	0,05% (w/v) Saponin 5% (v/v) NGS in PBS
Blocking solution	5% NGS (v/v) in PBS
Phalloidin	Coupled to Alexa Fluor <sup>®</sup> 350 or Alexa Fluor <sup>®</sup> 594 (Molecular Probes) in methanol
Embedding medium	Mowiol
Coverslips (diameter: 12 or 18 mm)	Roth, Karlsruhe
Microscopy-slides SuperFrost <sup>®</sup> Plus	Roth, Karlsruhe

### 3.7 Proteinbiochemie

#### 3.7.1 Proteins and materials for biochemical experiments

Name	Company
Actin (from platelets)	Cytoskeleton, Denver (USA)
Actin (from rabbit muscle)	S. Struchholz
Bovine serum albumin (Fraction V)	Applichem, Darmstadt
Fat-free milk powder	Granovity, Lüneburg
Lysozyme	Sigma-Aldrich, Munich
Thrombin	Sigma-Aldrich, Munich



## Materials

Aprotinin	Sigma-Aldrich, Munich
Bio-Rad Protein Assay	Bio-Rad, Munich
Dialysis tubes Spectra/Por <sup>®</sup>	Spectrum Lab. Europe, Breda (NL)
Membrane MWCO 6,000-8,000	
DTT	Gerbu, Gaiberg
Leupeptin	Sigma-Aldrich, Munich
GSH-Sepharose 4B	GE-Healthcare, Uppsala (S)
PageRuler <sup>™</sup> Protein Ladder	Fermentas
Roti <sup>®</sup> PVDF membrane	Roth, Karlsruhe
Sigma Marker low range	Sigma-Aldrich, Munich
Sigma Marker high range	Sigma-Aldrich, Munich
Sigma Marker wide range	Sigma-Aldrich, Munich
SuperSignal <sup>®</sup> West Pico- Chemiluminescent Substrate	Pierce Perbio Science, Bonn
TEMED	Sigma-Aldrich, Munich
Whatman paper	Schleicher & Schuell, Dassel

### 3.7.2 Solutions for biochemical methods

#### 3.7.2.1 Polyacrylamide gels and SDS-PAGE

Name	Composition
AMBA (Acrylamide solution)	30% (w/v) acrylamide 0,8 % (w/v) bisacrylamide
Separation gel buffer 4x	1.5 M Tris/HCl, pH 6.8 0,4 % (w/v) SDS
Stacking gel buffer 4x	0.5 M Tris/HCl, pH 8.8 0,4 % (w/v) SDS
Radical starter (APS)	10 % (w/v) ammonium persulfate
Laemmli buffer 5x	0,2 M Tris/HCl, pH 6.8 5 mM EDTA 40 % (w/v) saccharose 15 % (w/v) SDS 10 % (v/v) 2-mercaptoethanol 0,02 % Bromphenol Blue
SDS running buffer	200 mM glycine 25 mM Tris

## Materials

Coomassie staining Solution	0,1 % SDS (w/v) 50 % methanol 3 % acetic acid 0,25 % Coomassie Brilliant Blue R250
Destaining solution	50 % methanol, 3% acetic acid

### 3.7.2.2 Solutions for Western Blotting

Name	Composition
Transfer buffer (tank-blot-buffer)	25 mM Tris/HCl 190 mM glycine 20 % methanol (v/v)
Staining solution for PVDF membranes	0.075 % Coomassie Brilliant Blue R250 in methanol
Destaining solution for PVDF membranes	40 % ethanol 10 % glacial acetic acid
TBS	10 mM Tris/HCl, pH 7.5 100 mM NaCl
TBS-T	0,05 % (v/v) Tween 20 in TBS
Blocking solution	5 % (w/v) fat-free milk powder in TBS-T
Stripping buffer	62,5 mM Tris/HCl, pH 6.7 100 mM 2-mercaptoethanol 2 % (v/v) SDS

### 3.7.2.3 *Solutions for actin cosedimentation assays and actin polymerization assays*

<b>Name</b>	<b>Composition</b>
Buffer A	2 mM Tris/HCl 0,2 mM CaCl <sub>2</sub> 0,2 mM ATP 0,5 mM DTT      pH 8.0
Actin polymerization buffer 1 PB1 (10X) (Cytoskeleton)	500 mM KCl 20 mM Mg Cl <sub>2</sub> 10 mM ATP      pH 8,0
Actin polymerization buffer 2 PB2 (10X) (S. Struchholz)	100 mM Hepes 300 mM KCl 0,5 mM MgCl <sub>2</sub>
Pyrene solution	10 mM Pyrene in Dimethylformamide (DMF)
General actin buffer (GAB)	5 mM Tris/HCl 0,2 mM CaCl <sub>2</sub> pH 8.0
Dialysis buffer for GST-SWAP-70 (525-585)	9 parts GAB plus 1 part Actin polymerization buffer 1 (10X)

### 3.7.3.4 *Solutions for GST-fusion-protein purification*

<b>Name</b>	<b>Composition</b>
GST-Fish-buffer for GST-fusion-protein purification	25 mM Tris/HCl pH 7,8 50 mM NaCl 0,1 mM EGTA 1 mM β-mercaptoethanol 1 mM NaN <sub>3</sub> 1 mM MgCl <sub>2</sub> (sometimes modified by 10% (v/v) glycerol and/or 1% (v/v) NP-40)

## Materials

GST wash buffer For washing of bead-coupled fusion GST-fusion proteins	25 mM Tris/HCl pH 7,8 400 mM KCl 0,1 mM EGTA 1 mM $\beta$ -mercaptoethanol 1 mM MgCl <sub>2</sub> (sometimes modified by 10% (v/v) glycerol and/or 1% (v/v) NP-40)
Lysis buffer for eukaryotic cells (used for GST pull-downs)	20 mM Hepes pH 7,35 100 mM NaCl 2 mM MgCl <sub>2</sub> 1 mM EGTA 1 mM DTT 1% NP40
Lysis buffer for eukaryotic cells (used for GTPase pull-downs)	50 mM Tris pH 7,4 50 mM NaCl 1 mM NaN <sub>3</sub> 0,1 mM EGTA 1 mM MgCl <sub>2</sub> 1 mM DTT 1% NP40

## 3.8 Software

Name	Software producer
Adobe Photoshop CS2	Adobe
Axio Vision LE 4.4	Zeiss
ImageJ	Freeware
Image Reader LAS-1000 Pro 2.6	Fujifilm
MetaMetamorph offline 6.1	Universal Imaging Corporation
Microsoft Office suite	Microsoft
TILLvisION 4.0	Till Photonics, Gräfelfing
Vector NTI 7.1	InforMax, Inc.
Wasabi 1.3	Hamamatsu, Herrsching

## **4. Methods**

### **4.1 Molecular biology**

Standard methods for molecular biology were adapted from the standard laboratory manual books (Sambrook *et al.*, 2001).

#### ***Transformation***

Transformation of chemically competent *E. coli* DH 5 $\alpha$  and BL21(DE3) was done according to the calcium-phosphate precipitation protocol of Hanahan (1985). Competent *E. coli* DH 5 $\alpha$  or BL21(DE3) were thawed on ice. 10 ng plasmid DNA were given to 100  $\mu$ l cells. After a further incubation time of 30 min on ice, DNA uptake was forced by a heat shock for 90 s at 42 °C. Cells were placed back on ice for 2 min and 900  $\mu$ l prewarmed, antibiotic-free LB or S.O.C. medium were added. After growth for 1 h at 37 °C, 10  $\mu$ l and 100  $\mu$ l cell suspension were plated on selective agar.

#### ***DNA Plasmid Preparation***

Plasmid DNA was prepared by alkaline extraction or with mini- and maxi-preparation kits, following the protocols of the manufacturer (Macherey-Nagel, Düren; Qiagen, Hilden). Plasmid concentrations were determined by spectrophotometry at 260 nm using Lambert-Beer Law. OD<sub>260</sub>/OD<sub>280</sub> ratios were used to evaluate protein contamination.

#### ***Restriction and electrophoretic separation of DNA on agarose gels***

Plasmids or PCR products were cut site-specifically by restriction enzymes using buffer conditions and temperatures recommended by the manufacturer. 5-10 U of restriction enzyme were used per microgram DNA. To DNA extracted by alkaline lysis, 40 ng of RNase A per microgram of DNA were added. DNA fragments were separated by horizontal agarose-gel electrophoresis. Agarose gels were poured by melting agarose in 1x TAE buffer together with 2-3  $\mu$ l ethidium bromide for visualization of DNA under UV-light. Dependent on the size of the fragment, differently concentrated (0,5%-3%) agarose-gels were used. DNA was mixed with 10x loading buffer, transferred to the gel and separated at 50-80 V. DNA was visualized using the BioDocAnalyse gel documentation system from Biometra.

DNA separated for preparative purposes was visualized with UV light using a transilluminator from Herolab. DNA was excised with a clean scalpel and separated from the agarose using the QIAquick Gel Extraction Kit (Qiagen).

## Methods

### **Ligation of DNA**

DNA T4 ligase was utilized for the covalent ligation of restricted DNA fragments. 100 ng vector DNA was added to a 2-5 molar excess of insert DNA in a end-volume of 10  $\mu$ l and ligated either over night at 4°C or for 1 h at room temperature by 0,5  $\mu$ l ligase in buffer conditions recommended by the manufacturer.

### **Polymerase chain reaction (PCR)**

PCR reactions (Mullis *et al.*, 1986) were used for selective amplification and modification of DNA sequences *in vitro*. The amplification is based on repeated cycles of duplication of a DNA sequence between two short DNA oligonucleotides by a thermostable DNA polymerase. A typical 50  $\mu$ l reaction was set up like this:

DNA-template	100 ng
DNA-polymerase (5 U ml <sup>-1</sup> )	1 $\mu$ l
dNTPs (10 mM)	2 $\mu$ l
5' primer (10 $\mu$ M)	2,5 $\mu$ l
3' primer (10 $\mu$ M)	2,5 $\mu$ l
10x Polymerase buffer	5 $\mu$ l
Aqua bidest	Ad 50 $\mu$ l

### **Typical program for PCR reactions**

Initial	95°C	5 min	
Denaturation			
Denaturation	95°C	1 min	} 25-35 cycles
Annealing	variable*	45 s	
Elongation	72°C	1 min/kb (Vent/Taq) 2 min/kb (Pfu)	
Extension	72°C	5 min	
End	4°C	$\infty$	

\* The annealing temperatures of primers mainly depends on the length and the G/C-content of the oligonucleotide.

## 4.2 Generation of SWAP-70 constructs

Several constructs comprising the full length sequence or different regions of human SWAP-70 were generated to carry out the screen of the mouse-spleen cDNA library and to search for intramolecular interactions between different domains of SWAP-70. All constructs were checked for correct insertion by restriction analysis and sequencing (GATC, Konstanz). A GST-SWAP-70 fusion construct was cloned using the pGEX4T-1 vector for bacterial expression and purification via glutathione coupled sepharose beads.

### **Construction of SWAP-70 : pBT**

The full length SWAP-70 sequence was amplified by PCR with primers MB695 and MB687 using the “GFP-DEF6-like” plasmid as template. The purified PCR product was restricted with Not I and BamH I and directly cloned into the restricted pBT vector.

### **Construction of SWAP-70 (1-211) : pBT**

The sequence encompassing aa 1-211 of the SWAP-70 sequence was amplified by PCR with primers MB687 and MB721 using the “GFP-DEF6-like” plasmid as template. The amplificate was ligated into the pT7-blue vector using Novagen’s “perfectly blunt-kit”. After amplification, the insert was excised using Not I and EcoR I and sub-cloned into the restricted pBT vector.

### **Construction of SWAP-70 (1-75) : pBT**

PCR-amplification of the sequence using primer-pair MB 716 + 687 on the template “GFP-DEF6-like” was followed by blunt-end cloning into pT7-blue vector. Insert was excised after amplification with Not I and EcoR I and ligated into the pBT vector.

### **Construction of SWAP-70 (526-585) : pBT**

The C-terminal sequence was amplified by PCR with primer pair MB714 + MB688, ligated into the pT7-blue vector and subcloned via EcoR I and Not I into the pBT vector.

### **Construction of SWAP-70 (306-585) : pTRG**

To construct this plasmid, the sequence coding for aa 306-585 was amplified by PCR using primers MB688 and MB732. The amplificate was ligated into the pT7 vector of the “perfectly blunt cloning” kit and after amplification excised by restriction with Not I and EcoR I followed by ligation into the Not I and EcoR I restricted pTRG vector.

### **Construction of SWAP-70 (1-75) : pTRG**

PCR-amplification of the sequence using primer-pair MB 716 + 687 on the template “GFP-DEF6-like” was followed by blunt-end cloning into pT7-blue vector. Insert was excised after amplification with Not I and EcoR I and ligated into the pTRG vector.

### **Construction of SWAP-70 (526-585) : pTRG**

The C-terminal sequence was amplified by PCR with primer pair MB714 + MB688, ligated into the pT7-blue vector and subcloned via EcoR I and Not I into the EcoR I and Not I restricted pTRG vector.

### **Construction of pGEX-4T-1 : SWAP-70 for GST-fusion protein expression**

The full length SWAP-70 sequence was amplified by PCR using primer pair MB671 and MB672 and the template “GFP-DEF6-like”. The amplicate was restricted with Sma I and Xho I after purification via Gel-extraction. The excised DNA fragment was cloned into SmaI and Xho I restricted pGEX-4T-1 vector.

## **4.3 BacterioMatch® Two-Hybrid System.**

The principle of the bacterial two-hybrid system is the detection of protein-protein interactions via the activation of transcription of specific genes. In the case of the BacterioMatch® two-hybrid system, a protein of interest (the bait) is fused to the full-length bacteriophage  $\lambda$  repressor protein, containing the amino-terminal DNA-binding domain and the carboxylterminal dimerization domain. The corresponding target protein is fused to the N-terminal domain of the  $\alpha$ -subunit of RNA polymerase. Interaction of the bait with a target protein leads to the recruitment and stabilization of the RNA polymerase at the promoter of a reporter gene. Expression of this His3 reporter gene confers growth on a selection medium containing the compound 3-amino-1,2,4-triazole (3-AT). 3-AT acts as a competitive inhibitor of the *HIS3* gene product which is essential for the bacterial synthesis of the essential amino acid histidine. (instruction manual, Stratagene). Successful cotransformation of a specialized *E. coli* reporter strain with two vectors coding for interacting bait and target proteins confers bacterial growth on selective medium containing 3-AT, Chloramphenicol, Tetracyclin and Streptomycin.

To amplify the mouse spleen cDNA- library, the purchased bacteria containing the library were plated on 35 plates ( $\varnothing$  150 mm) at a density of 30 000 colonies per plate. Cells were grown at 30°C for 30 hours and then carefully scraped off the plates after addition of 0,5 ml sterile S.O.C. medium. Half of the pooled bacteria were subjected to Maxi-Prep DNA-extraction to gather the plasmids. The remainder of the pooled bacteria were aliquoted and snap frozen with 20% (v/v) sterile glycerol and subsequently stored at -80°C.

The library was screened according to the manufacturer's instructions. In short: Electrocompetent BacterioMatch® reporter cells were transformed by adding 50 ng of mouse spleen cDNA library plus 50 ng of bait vector to prechilled microcentrifuge tubes. Electrocompetent cells were thawed on ice and 40  $\mu$ l of cells were added to each tube. After gently mixing, aliquots were transferred to a chilled electroporation cuvette and immediately electroporated followed by fast addition of 960  $\mu$ l of prewarmed (37°C) S.O.C. medium. Cells were transferred to sterile 14 ml polypropylene tubes and incubated



## Methods

for 90 minutes at 37°C followed by centrifugation at 2000 x g for 10 minutes. The supernatants were carefully removed and the cells were washed twice in 1 ml M9<sup>+</sup> His-dropout broth, collecting the cells by centrifugation between the washing steps. After aspirating the supernatants from the second wash step, the cells were resuspended in a fresh 1 ml of M9<sup>+</sup> His-dropout broth and incubated for 2 hours. Aliquots of the cell suspension were carefully plated on selective screening medium. Cells cotransformed with the empty pBT and pTRG served as negative control, cells cotransformed with the plasmids pBT-LGF2 and pTRG-Gal11<sup>P</sup> served as positive control for interaction dependent growth on selective medium.

24 hours later, grown colonies were transferred to “enrichment-plates” to grow for additional 24 hours. The original screening plates were incubated for additional 16 hours and the slower growing colonies were also transferred to an enrichment plate and grown for 24 hours. Bacteria from the enrichment plates were then transferred to dual selective medium to verify the interaction. Dual-selective screening plates were incubated overnight and each of the grown colonies was used to inoculate a 2 ml tetracycline containing liquid culture. Plasmid DNA was extracted from these cultures and retransformed into chemocompetent XL1-Blue MRF<sup>+</sup> Kan cells which subsequently were plated on kanamycin containing plates. On the next day, three colonies of each plate were transferred onto two plates: one plate containing LB-chloramphenicol and the other LB-tetracycline. Bacteria able to grow on tetracycline, but failing to grow on chloramphenicol have lost the bait vector and do solely contain the target-vector plasmid with the interacting sequence of the cDNA-library. Such colonies were used for inoculation of 4 ml tetracycline containing medium and then subjected to DNA extraction by alkaline lysis protocol.

The isolated plasmid DNA was used for retransformation of chemocompetent BacterioMatch<sup>®</sup> reporter cells together with the bait vector used in the original screen. Colony formation on selective screening medium after cotransfection rules out that a bacterial mutation was the reason for growth in the original screen.

Plasmid DNA of verified interactors was amplified by PCR with target-vector specific primers using Taq-polymerase and analysed by gel-electrophoresis. The amplified DNA was subjected to two different 4 base pair recognition restriction enzymes (BsuR I, Taq I) and the fragment patterns were compared. Only one clone from clones with identical band patterns was given to sequencing in 96 well-plates to GATC (Konstanz).

### **4.4 Cloning of palmitoylated SWAP-70 constructs**

PM-SWAP-70 constructs (Fig.17) were cloned by Dr. M. Kessels and Dr. B. Qualmann except for PM-SWAP-70 (305-585) and PM-SWAP-70 (305-525) which were cloned by diploma student J. Dang.

Palmitoylated constructs of SWAP-70 were cloned into the BamH I and Xho I sites of the pCMV Tag2b vector (Stratagene). This vector was modified by Kessels and Qualmann to

## Methods

incorporate an N-terminal palmitoylation sequence derived from the palmitoylation signal sequence of GAP43 (*growth associated protein 43*).

M L C C M R R T K Q V E K N D E D Q K I

This sequence is followed by the FLAG tag from the original vector and a GFP-tag in front of the gene of interest.

To obtain the palmitoylated GFP without a sequence from SWAP-70, PM-GFP-SWAP-70 was cut with BamH I and Xho I to excise the insert followed by blunting of the sticky ends and subsequent ligation. The vector contains multiple stop codons for each reading frame in the 3' part of the multiple cloning site.

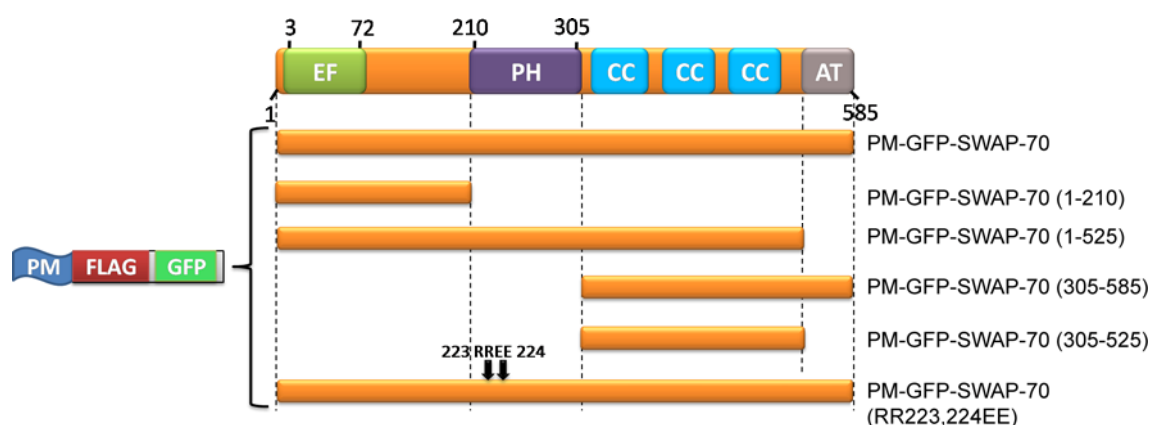


Fig. 17. Schemes of palmitoylated constructs of SWAP-70 used in this study

## 4.5 Cultivation and storage of bacteria

*E. coli* DH 5 $\alpha$  and BL21(DE3) were grown for 16 h at 37 °C. Incubation of suspension cultures in selective LB medium was performed in a shaking incubator (180 rpm), single colonies were grown on selective agar plates. For preparation of glycerol stocks bacteria were resuspended in LB medium containing 20 % (v/v) sterile glycerol, quickly frozen in liquid nitrogen and stored at -80 °C.

## 4.6 Biochemical Methods

### 4.6.1 GST-fusion protein expression and purification

Different GST-fusion proteins for pull-down experiments and actin co-sedimentation assays were prepared during this work. The cDNAs for the different proteins were cloned into pGEX vectors which provide an N-terminal Glutathione-S-Transferase protein (GST) from *Schistosoma japonicum* as tag. GST binds with high affinity to glutathione (GSH) and in many cases increases the solubility of the fusion protein. Restriction sites for

## Methods

proteases like Thrombin are inserted between the GST-tag and the protein of interest. This allows the purification of the protein of interest without the GST-tag. For bacterial expression, the *E. coli* strain BL21(DE3) was used because of the deficiencies in bacterial protease systems. Bacteria were transfected and a single clone was grown overnight in 15 ml ampicillin containing LB medium. On the next day, Erlenmeyer flasks with 500 ml LB medium containing ampicillin were inoculated with 5 ml of the overnight bacteria culture and incubated in a rotary shaker at 37°C until the bacteria cultures reached an optical density of OD<sub>600</sub> 0,6. For the GST-SWAP-70 construct, 3% ethanol was added before inoculation to promote the expression of bacterial chaperones. At an OD<sub>600</sub> of 0,6, expression of fusion protein was induced by 100-250 µM IPTG and cultures were either grown for additional 3-4 hrs at 37°C or overnight at room temperature. The cells were then collected by centrifugation for 20 min with 4500 rpm at 4°C using a SORVALL® RC5C centrifuge and a GSA rotor. After discarding the supernatant, the pellet was resuspended in 30 ml of ice-cold PBS and centrifuged in a Falcon tube for 10 minutes at 4°C (Eppendorf 5702R, Rotor: A-4-38). Cell pellets were either frozen at -20°C or the pelleted cells were directly lysed.

Bacteria were resuspended in bacterial lysis buffer containing protease inhibitors leupeptin (10 µg/ml), PEFA-bloc (100 µg/ml) and aprotinin (2,9 µg/ml) and incubated for 10 min with 50 µg/ml Lysozyme. Cells were then further lysed on ice by sonication with the Sonicator Labsonic®M (10-12 pulses à 45 seconds) with full amplitude (100%) and intervals of 0,6 s. The lysate was centrifuged for 30 min with 16 000 rpm, using a SS34 rotor in a Sorvall® RC5C centrifuge. The supernatant was carefully transferred to an ultracentrifugation tube and centrifuged for additional 45-60 min at 45 000 rpm (~186 000 x g) in a Beckmann L8-50 Ultracentrifuge and the 70.1Ti rotor.

Bacterially expressed fusion proteins were purified by the batch-purification method following the instructions of the manufacturer. Glutathione-sepharose 4B fast flow (equilibrated in GST-fish buffer or lysis buffer for GTPase pull-downs, dependent on the purpose) was added to the supernatant of the ultracentrifugation step and incubated for 90 minutes on a rotary shaker at 4°C. After binding, beads were collected by centrifugation with 600 rpm at 4°C. After carefully removing the supernatant, beads were washed thrice with: i) GST-fish buffer/lysis buffer for GTPase pull-downs, ii) GST-wash buffer iii) GST-fish buffer/ lysis buffer for GTPase pull-downs/GST-pull downs, respectively. Alternatively, GST-fusion proteins were competitively eluted 1-3 times with 0,5 -1 ml of 20 mM free glutathione containing GST-Fish-buffer for at least 2 hrs for each elution step. Eluted fusion-protein was dialyzed over night and a second time for 3 hours against at least 2 l of the buffer of choice for the following experiments. The dialyzed protein was centrifuged at 4°C for 20 min at 75 000 rpm and the supernatant was carefully gathered and protein concentration was measured according to the method of Bradford (1976)

### 4.6.2 Qualitative binding-assay (GST-pull down assay)

GST-pull down assays utilize GST-fusion proteins immobilized on glutathione-sepharose beads to catch interacting proteins from e.g. eukaryotic cell- or tissue lysates. Lysates were incubated with 30-60  $\mu\text{l}$  of fusion-protein-loaded beads for 30-60 minutes on a rotary shaker at 4°C. Beads were collected by centrifugation (600 rpm at 4°C) and washed thrice with an excess of lysis buffer for eukaryotic cells. Beads were collected by centrifugation after each washing step. After carefully removing the supernatant of the last washing step using a Hamilton-syringe, the remaining beads were boiled in 30-50  $\mu\text{l}$  of 2x Laemmli-buffer. Analysis for bound proteins was carried out by SDS-PAGE, western blotting and immunodetection.

GTPase pull down assays are a variant of the GST-pull down assay. Effectors of small GTPases bind preferentially and with high affinity to the GTP bound (activated) form of small GTPases. Hence, pull downs with the GTPase Binding Domain (GBD) of effectors fused to GST can be used to detect and compare activated levels of specific small GTPases in cell lysates. In this work, the GBD of Pak1 was used to bind activated Rac and Cdc42, the GBD of Raf binds to Ras and the C21 domain of the Rho effector Rhotekin pulls down activated Rho.

### 4.6.3 Bradford protein assay

Protein concentrations were determined using the Bradford Protein Microassay (Bio-Rad). The assay was performed in 96-well micro-plates in an end-volume of 200  $\mu\text{l}$  containing 40  $\mu\text{l}$  Bradford solution. After mixing by pipetting, the samples were incubated for 10 min at room temperature. The Bradford-reagent (Coomassie-brilliant-blue G-250) forms complexes with cationic and hydrophobic amino acids, leading to a shift of the light-absorbance maximum from 465 nm to 595 nm. This increase in absorption at 595 nm was measured by photometry using the micro-plate reader WallacVictor<sup>2</sup> 1420 (Perkin Elmer). BSA (0,5-2,5  $\mu\text{g}$ ) was used as a standard.

### 4.6.4 F-actin cosedimentation assays

F-actin cosedimentation assays make use of the fact, that F-actin sediments due to its high molecular weight in ultracentrifugation steps whereas G-actin and other intact cytosolic proteins do not. F-actin binding proteins will co-sediment with F-actin and hence will be found in the pellet after centrifugation whereas negative controls without F-actin will not show sedimentation.

F-actin was polymerized either from frozen and fast thawed rabbit-muscle G-actin or from commercially purchased platelet G-actin in general actin buffer (5 mM Tris, 0,2 mM  $\text{CaCl}_2$ ). G-actin solutions (5  $\mu\text{M}$ ) were polymerized in ultracentrifugation tubes by adding 1/10 volume of polymerization buffer (PB1) followed by 60 minutes of incubation at room

## Methods

temperature. During this incubation period, GST-SWAP-70 (525-585) was clarified by ultracentrifugation (217 000 x g for 15 minutes at 4°C) to remove aggregates. The protein concentration of the supernatant was measured via a Bradford-assay to calculate the volume necessary for 5 µM GST-fusion construct in the assay. Muscle- or nonmuscle F-actin were each mixed with either the GST-SWAP-70 (525-585) fusion protein or GST alone in an end-volume of 93 µl and incubated for 60 minutes to allow for eventual binding. After this period, the tubes were centrifuged (217 000 x g for 15 minutes at 4°C). Supernatant and pellet were separated and boiled in equal endvolumes of 1x Laemmli-buffer. Protein distribution was analyzed by SDS-PAGE, western blotting and immunodetection using an α-GST antibody.

### 4.6.5 SDS-polyacrylamide gel electrophoresis of proteins (SDS-PAGE)

The SDS-PAGE is a method for the separation of proteins by their molecular weight (Laemmli, 1970). SDS-PAGE was performed using vertical gel units (Hofer). Electrophoresis was run at 100 V in the stacking gel (4 % acrylamide, 0.125 M Tris/HCl pH 6.8, 0.1 % SDS, 0.33 % APS, 0.1 % TEMED) and at 200 V in the separating gel (7.5-15 % acrylamide, 0.375 M Tris/HCl pH 8.8, 0.1 % SDS, 0.8 % APS, 0.08 % TEMED). The gels were either fixed and stained in Coomassie solution, destained and dried or they were subjected to western blotting.

### 4.6.6 Immunoblotting

Proteins were electrophoretically transferred from SDS-PAGE-gels to PVDF membranes (Millipore) (Renart *et al.*, 1979). All components for the transfer-sandwich (Whatman-paper, PVDF-membrane, gel, sponge) were equilibrated in blotting buffer and subsequently assembled in the order: sponge- 2 sheets of Whatman-Paper, PVDF membrane, running gel, 2 sheets of Whatman-Paper, sponge. This sandwich was held together by a plastic cassette and vertically inserted in a Hofer tank-blot chamber and the transfer was run either for 2 h at 30 V or over night at 12 V. The transfer of proteins was visualized by staining the membrane with PVDF-staining solution and destaining. To document the transfer of the proteins, the membrane was scanned. The membrane was washed in TBS and unspecific binding sites were blocked with 5% BSA in TBS-T. The blots were incubated for 2 hours at RT or alternatively over night at 4°C with the primary antibody diluted in blocking solution (see: Materials and Methods: Antibodies). Afterwards, the membrane was washed 4 times with TBS-T and incubated for 45 min with the secondary antibody at RT. Membranes were again washed 4 times with TBS-T followed by a short incubation with ECL-solution (SuperSignal, Pierce). Signals were detected with the chemiluminescence reader Fujifilm LAS-1000 (Fujifilm). All washing steps were performed at RT on a shaker.

### 4.6.7 Pyrene-actin polymerization assay

Pyrene is a fluorescent marker and can be used to follow actin polymerization/depolymerization dynamics when covalently linked to actin. Pyrene labeled actin exhibits increased fluorescence intensity when incorporated in F-actin (factor of 7-10:1 for F-actin vs. G-actin).

Pyrene actin was produced by incubating muscle F-actin with a 7,5x molar excess of pyrene-iodoacetamide for 18 h at room temperature. F-actin was sedimented by ultracentrifugation for 15 minutes. For depolymerization, the F-actin pellet was resuspended in 1 ml buffer A and dialyzed against the same buffer 48 h at 4°C with two buffer changes. Precipitated pyrene and non depolymerized F-actin was sedimented by another ultracentrifugation step and the supernatant was used for experiments. Pyrene-labeling efficiency for actin was measured according to Cooper (Cooper *et al.*, 1983). 87% labeling efficiency was achieved.

Polymerization experiments were performed by the bachelor students J. Hettinger, M. Storbeck and C. Pieper. GST-SWAP-70 (525-585) (or GST as control) in dialysis buffer was ultracentrifuged and the supernatant was transferred into a quartz-cuvette. 12 µl polymerization buffer was added to give an end concentration of 50 mM KCl and 2 mM MgCl<sub>2</sub>. Samples were mixed in quartz-cuvettes and the reaction was started by adding muscle- or non-muscle G-actin each mixed 10:1 with pyrene-labeled muscle actin. Actin concentration was 2 µM in an endvolume of 120 µl. Pyrene fluorescence representing actin polymerization kinetics was analyzed with a *Luminescence Spectrometer LS 55* (Perkin-Elmer). The wavelengths used for this experiment were 365 nm for excitation and 407 nm for measurement of emission. Data were analyzed using Sigma-Plot.

## 4.7 Cell culture

### 4.7.1 Cultivation of cells

Cells were cultivated in cell-culture flasks (75cm<sup>2</sup>) or Ø 10cm culture-dishes at 37°C, 90% humidity and 5% CO<sub>2</sub>. HeLa cells, B16F1 cells and NIH/3T3 cells were cultivated in DMEM supplemented with 10% fetal calf serum, 100 µg ml<sup>-1</sup> streptomycin and 100 U ml<sup>-1</sup> penicillin. HEK 293T cells were cultivated in MEM supplemented with 10% fetal calf serum, 100 µg ml<sup>-1</sup> streptomycin and 100 U ml<sup>-1</sup> penicillin. Cells were passaged at ~80% confluence and diluted 1:20-1:30 (B16F1, NIH/3T3), 1:6 (HEK 293T) or 1:10 (HeLa). For video-microscopy, cells were transferred to HEPES containing Ham's F-12 Medium.

For cryoconservation, cells were collected by centrifugation (1000 x g, 5 min, RT), resuspended in sterile FCS (10<sup>6</sup> cells in 900 µl) followed by slow addition of 100 µl sterile DMSO. Cells were stored at -20 C in a styropor-box overnight, transferred to -80°C for another day and then frozen in liquid nitrogen. Frozen cells were thawed quickly at 37°C in

a water bath and immediately transferred into a sterile Falcon-tube containing 10 ml of growth medium. Cells were collected by centrifugation (1000 x g, 5 min, RT) and plated after resuspension in an appropriate volume of growth medium.

### **4.7.2 Transfection of cells**

#### **4.7.2.1 *Transfection of B16F1 cells with Superfect*<sup>®</sup>**

B16F1 cells were seeded in 6-well plates and transfected 24 h later at a confluence of 50%-70%. For one transfection, 300 µl DMEM, 1 µg plasmid-DNA and 6 µl Superfect<sup>®</sup> reagent were mixed in a 2 ml tube, vortexed for 10 s and incubated for 15 min at room temperature. Afterwards, 1,5 ml culture medium was added and the solution was pipetted to PBS washed cells in a well of the multiwell-plate. 6 to 12 hours later the DNA containing medium was exchanged for fresh culture-medium.

#### **4.7.2.2 *Transfection of NIH/3T3 cells with Polyfect*<sup>®</sup>**

NIH/3T3 cells were seeded in 6-well plates and transfected 16 h later at a confluence of ~40%. For one transfection, 60 µl DMEM, 1 µg plasmid-DNA and 10 µl Polyfect<sup>®</sup> reagent were mixed in a 2 ml tube and incubated for 15 minutes at room temperature. 1,5 ml culture medium was added to the mixture and the solution was pipetted in a well of PBS washed cells. 6-8 hours later, the DNA containing medium was exchanged for fresh culture-medium.

#### **4.7.2.3 *Transfection of HeLa cells with Effectene*<sup>®</sup>**

HeLa cells were transfected in a 6-well plate at a confluence of 50%- 70%. 0,5 µg DNA was mixed by vortexing with 3,5 µl of “enhancer”-solution in a microcentrifuge tube. After 5 minutes of incubation at RT, 10 µl of effectene-reagent was added to the solution, vortexed for 10 seconds and incubated for additional 10 minutes. During this time, HeLa cells were washed once with warm PBS and supplemented with fresh culture medium (1,6 ml). 0,6 ml culture medium were then added to the DNA-complex solution which was subsequently added drop-wise to the cells.

#### **4.7.2.4 *Transfection of HEK 293T cells (calcium-phosphate precipitation)***

For the purpose of pull downs, HEK 293T cells were transiently transfected in 15 cm Ø plates at a confluence of 60%-75%. For each plate, 25 µg plasmid-DNA were mixed with 562 µl 1M CaCl<sub>2</sub> and sterile H<sub>2</sub>O was added to an end volume of 2,25 ml in a Falcon tube. The DNA-solution was added drop-wise to 2,25 ml 2x BBS into another vial under weak air-bubbling produced by a pasteur pipette. The mixture was incubated for 30 min at room temperature to allow for complex formation before 10 ml MEM culture medium was

added. The old medium was aspirated from the cells followed by a careful washing step with PBS. 12 ml MEM culture medium were added to the cells followed by the evenly distributed, drop-wise addition of DNA-precipitate containing medium. After 5-6 h of incubation at 37°C and 3% CO<sub>2</sub>, the transfection medium was replaced by new MEM culture medium after a washing step with warm PBS. Cells were incubated for additional 40 hours in new MEM culture medium.

### **4.8 Preparation of cells for microscopy**

#### **4.8.1 Seeding of cells**

When not indicated differently, B16F1 cells were seeded on laminin coated coverslips. Laminin coating was done with 25 µg ml<sup>-1</sup> laminin in 50 mM Tris/HCl (pH 7,5), 150 mM NaCl solution for 1 h. HeLa and NIH/3T3 cells were either seeded on uncoated- or on fibronectin coated coverslips. Coating of coverslips with fibronectin was done by placing coverslips on drops of a 25 µg ml<sup>-1</sup> fibronectin in PBS solution for 1 h at room temperature. Laminin- or fibronectin coated coverslips were washed two times with an excess of PBS before they were used for cell seeding.

For microscopy, 5 x 10<sup>4</sup> NIH/3T3 cells were plated on 18 mm coverslips 24 h before fixation or video microscopy. B16F1 cells were plated on laminin or fibronectin 4-5 h before fixation or video microscopy

#### **4.8.2 Pharmacological treatment of cells**

Pharmaceuticals (PMA, Wortmannin, LY294002) were used according to the descriptions of the manufacturer. Before addition to the cells, stock solutions of the substances were diluted to the proper end-concentration in the corresponding culture medium (DMEM or alternatively Ham's F-12 for video-microscopy). If medium was added during video-microscopy, the substance was diluted to 5x higher than the end-concentration. 200 µl of this mixture were carefully and equally added to 800 µl of Ham's F-12 medium in the observation chamber.

#### **4.8.3 Fixation and staining**

Cells were washed once with warm 1x PBS (37°C) followed by fixation with 4% (w/v) PFA for 30 minutes. Free aldehyde groups were then blocked with 0,1 M glycine in PBS for 10 minutes followed by two washing steps with 1x PBS. For antibody- or phalloidin staining, cells were routinely permeabilized for 30 min with 0,05% Saponin and 5% NGS buffered in PBS. For F-actin staining, cells were directly incubated with Alexa-595 or Alexa-350 coupled phalloidin (Molecular Probes, Leiden) for 1 hour followed by 3



washing steps with PBS. Coverslips were then mounted with Mowiol and dried in the dark for 24 h at 4°C.

For antibody-staining, cells were incubated after permeabilization for an additional hour with 5% NGS in PBS to block unspecific binding sites. Afterwards, cells were incubated for at least 1 h with the primary antibody followed by 3-4 washing steps with PBS 10 min each. After 1 hour of incubation with the secondary antibody, cells were again washed 3 times with PBS and mounted with Mowiol. If phalloidin staining and antibody staining were combined, phalloidin was mixed with the secondary antibody.

### **4.9 Microscopy**

#### **4.9.1 Epifluorescence microscopy**

Fixed cells were analyzed with an Axiophot I microscope (Zeiss) using either a 100x Plan-NEOFLUAR oil-objective with a numerical aperture of 1.3 or a 63x/NA 1,25 Plan-Neofluar oil-objective. Images were taken with a digital CCD camera (Hamamatsu Orca C4742-95) controlled via the corresponding WASABI-Software. Images were processed using Photoshop CS2 (Adobe).

#### **4.9.2 Confocal laser-scanning microscopy**

Three-dimensional visualization of fixed cells was done using a LSM 510 scanning unit in combination with an Axiovert 200M microscope (Zeiss). The system was equipped with 543 nm Helium/Neon single wavelength laser and a 450-514 nm Argon multi wavelength laser (Lasos, Ebersberg). The objective used was a 63x/1,4 Plan-APOCHROMAT oil-objective. Multicolor-images were taken by excitation of individual fluorophores at a time. The optical keyholes were adjusted for each fluorophore to provide confocal planes of the same thickness. Data were processed with LSM software, MetaMorph software and ImageJ.

#### **4.9.3 Life-cell microscopy**

Living cells were analyzed in an open chamber on a heatable object-table at 37°C. Ham's F-12 medium was used for live cell analysis because of its low autofluorescence. Additionally, Ham's F-12 medium contains 25 mM HEPES buffer that provides more effective buffering in the optimum pH range of 7.2-7.4. Images were taken with an Axiovert 200 microscope (Zeiss) equipped with an IMAGO CCD camera (TILL Photonics). Fluorophores were excited by a XBO-lamp filtered by a polychrome IV monochromator (TILL Photonics). A heatable 63x/NA 1.25 Plan-NEOFLUAR oil-objective was used. Every 4-8 seconds, phase contrast and fluorescence images were taken

## Methods

with a delay of 10 ms. Fluorescence images were taken using exposure times of 500-900 ms dependent on the fluorescence intensity. Data were processed with TILL VisION 4.0 Software and MetaMorph 6.1. software was used for the generation of videos.

### **4.9.4 TIRF-microscopy**

TIRF (*total internal reflection fluorescence*) is a technique that allows a high axial resolution because it specifically excites fluorophores immediately adjacent to the interface between two media with different refractive indices. An exciting *evanescent field* originates by the total reflection of a laser beam and excites fluorophores in the area of 100-200 nm next to the interface. Images were taken with a Nikon TDH microscope, a Cascade II CCD camera (Photometrics) and a 100x/NA 1.49 APOCHROMAT oil-objective. The system was equipped with T-RCP electronic shutters and the *Perfect Focus System* (all Nikon, Düsseldorf). Two lasers, a 50 mW solid-state laser and a 150 mW 514 nm Ion laser (Melles Griot, Carlsbad, USA) provided the source for the evanescent field.

## 5. Results

### 5.1 The C-terminal part of SWAP-70 binds to non-muscle F-actin

SWAP-70 colocalizes with a special subset of loose actin filament arrays that are commonly located behind protruding lamellipodia of motile cells (Hilpelä *et al.*, 2003). Despite the clear colocalisation of SWAP-70 with F-actin *in vivo*, a direct binding of SWAP-70 to F-actin could neither be shown in spin-down experiments using purified muscle actin nor in spin-down experiments with F-actin from cell lysates. SWAP-70 is expressed in various cell lines and tissues, however, it is only weakly expressed in muscle cells. Ihara and colleagues (2006) reported recently that SWAP-70 binds isoform specifically to non-muscle F-actin. In order to verify these results and to further investigate, whether the binding of SWAP-70 to F-actin influences actin dynamics, spin-down experiments were performed with muscle actin and commercially available platelet-actin. The C-terminal part of SWAP-70 contains actin targeting information. Therefore, GST-SWAP-70 (525-585) was bacterially expressed and purified as described in Materials and Methods. The C-terminal part of SWAP-70 bound to non-muscle actin in F-actin cosedimentation assays while it did not bind to muscle actin (Fig 18.). A degradation product of the GST-tagged C-terminal 60 amino acids failed to bind to non-muscle F-actin, suggesting that the very C-terminal amino acids are crucial for F-actin binding.

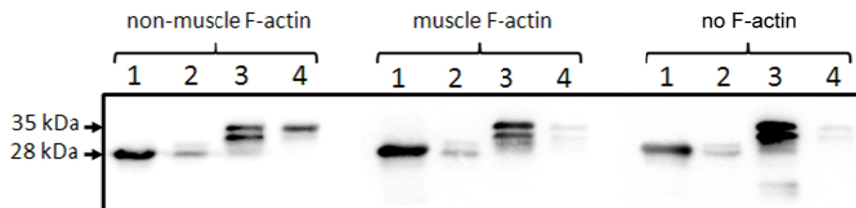


**Fig. 18. The C-terminal 60 amino acids of SWAP-70 bind selectively to non-muscle F-actin.** F-actin-cosedimentation assays were performed with purified bacterially expressed GST and GST-SWAP-70 (525-585) fusion protein. Western blots were probed with  $\alpha$ -GST-antibody. **1.** GST supernatant **2.** GST pellet **3.** GST-SWAP-70 (525-585) supernatant **4.** GST-SWAP-70 (525-585) pellet. Note that in the non-muscle actin spin-down only the upper band of GST-SWAP- (525-585) is visible in the F-actin pellet. SWAP-70 (525-585) does not cosediment with muscle actin.

To investigate, whether the binding of the C-terminal 60 amino acids to non-muscle F-actin influences actin polymerization, the polymerization of pyrene-labeled actin was followed photometrically. Polymerization of pyrene-labeled G-actin into F-actin results in a rise in fluorescence. 2  $\mu$ M G-actin (1,8  $\mu$ M non-muscle actin + 0,2  $\mu$ M pyrene labeled

## Results

muscle actin) was polymerized in the presence of different concentrations of GST-SWAP-70 (525-585). No significant changes in actin polymerization kinetics were observed (Fig. 19). Taken together, the C-terminal 60 amino acids of SWAP-70 bind directly to non-muscle F-actin. This binding did not have any obvious effect on the polymerization nor did it quench pyrene fluorescence.

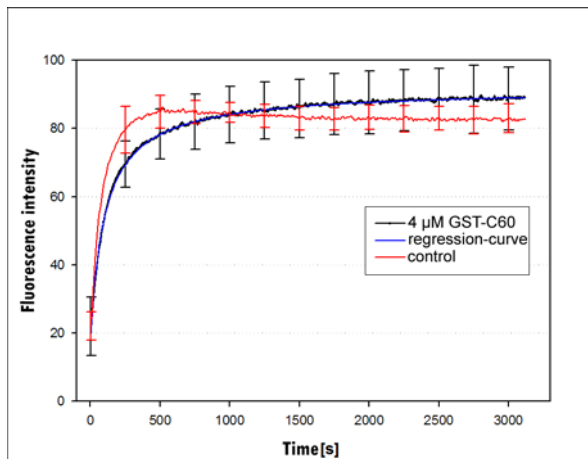


**Fig. 19. The polymerization of non-muscle actin is not altered in the presence of GST-SWAP-70 (525-585).** Graphs showing results from pyrene-actin assays of non-muscle actin polymerization. 2 μM G-actin were polymerized in a buffer containing 30 mM KCl and 2 mM MgCl<sub>2</sub> with- or without the addition of GST-SWAP-70 (525-585). Experiments were carried out by the cand. Bsc. Hettinger, Storbeck, Pieper.

## 5.2 Artificial plasma membrane targeting of SWAP-70 results in alterations of the actin cytoskeleton and cell morphology.

### 5.2.1 Palmitoylated SWAP-70 localizes to the plasma membrane

If the cellular function of SWAP-70 is dependent on- or mediated by its binding to the membrane, the artificial targeting of the protein to the plasma membrane might result in a “dominant active” form of SWAP-70. Even if the membrane localization is not sufficient for appropriate activation of SWAP-70, there should be an increased probability of interaction between the PH domain and phosphoinositides, when SWAP-70 is artificially tethered to the membrane. Cells direct proteins via different mechanisms to the plasma membrane. One mechanism is the post-translational addition of palmitate to the N-terminus of proteins which tethers them predominantly to the plasma membrane and the Golgi-apparatus (Bijlmakers and Marsh, 2003). A GFP-SWAP-70 construct with an additional N-terminal palmitoylation signal-sequence from GAP-43 (growth associated protein 43) was used to study the effects of artificially membrane-targeted SWAP-70 (PM-

## Results

SWAP-70). The palmitoylation signal indeed led to the localization of SWAP-70 on the plasma membrane (Fig. 20). A control construct with palmitoylated GFP was predominantly localized on the plasma membrane.

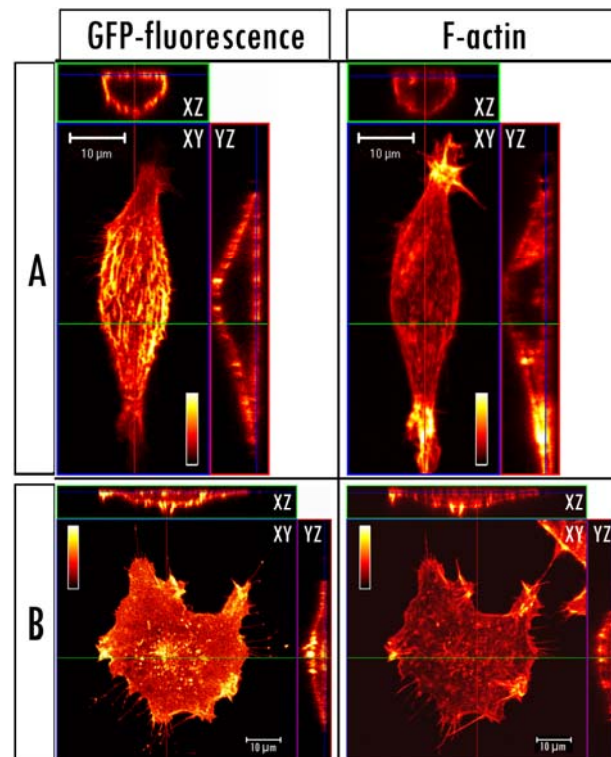


**Fig. 20. Palmitoylation of SWAP-70 leads to membrane association of the fusion protein and to changes in cell morphology.** HEK 293T cells were fixed with 4% PFA 24 h after transfection and permeabilized with 0,05% Saponin. F-actin was stained with Alexa594 Phalloidin. Depicted in each image is one ventral confocal section of the cell (XY) and the orthogonal projections of the stack in Z-direction (XZ, YZ). For better visualization, the fluorescence intensity is visualized in the “orange hot” scale for which the gradient is depicted in the colored bar. **A:** PM-GFP-SWAP-70 transfected HEK-293T cell plated on fibronectin coated coverslips. PM-SWAP-70 localizes to longitudinal filamentous actin underneath the plasma membrane but does not localize to the F-actin rich ruffles at the ends of the cell. Note that PM-GFP-SWAP-70 is predominantly localized to the membrane **B:** PM-GFP transfected HEK-293T cell showing normal cellular morphology.

### 5.2.2 PM-SWAP-70 induces morphological alterations

The expression of PM-SWAP-70 resulted in morphological alterations of transfected cells. The effects were dependent on the expression level of the construct which was judged by the exposure time that was necessary to obtain a well exposed picture.

In B16F1 cells with PM-GFP-SWAP-70 expression levels that were barely visible by eye and took over ~5s exposure time with additional electronic gain for adequate exposition in the Axiophot-microscope, a fraction of the fusion protein was still localized at the typical

## Results

loose actin filament arrays behind ruffling lamellipodia, but most of the fusion-protein was found at the membrane in the area of the cell body. (Fig. 21, video S1).

In B16F1 and NIH/3T3 cells that showed intermediate expression levels that could be visualized with exposure times between ~1,5-5 s without electronic gain, staining for F-actin with Alexa 594 Phalloidin revealed a colocalization of palmitoylated SWAP-70 with F-actin mainly in the region of the cell body but not at protrusions of cells. In NIH3T3 cells plated on glass, PM-SWAP-70 clearly colocalized with F-actin while non-palmitoylated SWAP-70 usually showed a cytosolic localization (data not shown). In B16F1 or NIH/3T3 cells expressing stronger intermediate levels of PM-SWAP-70 the fusion protein often colocalized with longitudinally oriented F-actin fibers located mainly in the range of the often elongated cell body (Figs. 21 and 22), but was not found to accumulate in the lamella of the cells. With higher expression levels, lamellipodia were mostly small or absent. The cells often showed a bulge-like swelling (see supplemental video S23).

High expression levels of palmitoylated SWAP-70 typically resulted regularly in an elongated, often spindle-shaped cellular morphology and disturbed actin-organization both in NIH/3T3 and B16F1 cells. Transfected cells appeared less spread and adherent than non-transfected cells and they frequently exhibited thin protrusions which either ended in a thorn or small ruffles. The cells were immotile as judged by time lapse video microscopy (video S18) and often showed strong ruffling activity at the ends of the spindle shaped cells. Transfected cells were covered with microspikes and fine, elongated protrusions reminiscent of filopodia or retraction fibers. The palmitoylated GFP-SWAP-70 fusion protein colocalized with F-actin in the mentioned microspikes and also in membranous structures (Figs. 20, 21; for a summary of expression-level dependent effects of PM-SWAP-70 see Table 3). The F-actin organization of cells expressing high levels of PM-SWAP-70 differs from non-transfected cells. Prominent stress fibers were absent and almost all long filaments appeared disrupted. Instead, F-actin was found predominantly in microspikes and was also found in structures maybe resembling actin aggregates at the cell cortex (see Figs. 21 “high” and 23). Very high expression of PM-SWAP-70 mostly led to cell rounding and probably cell death.

## Results

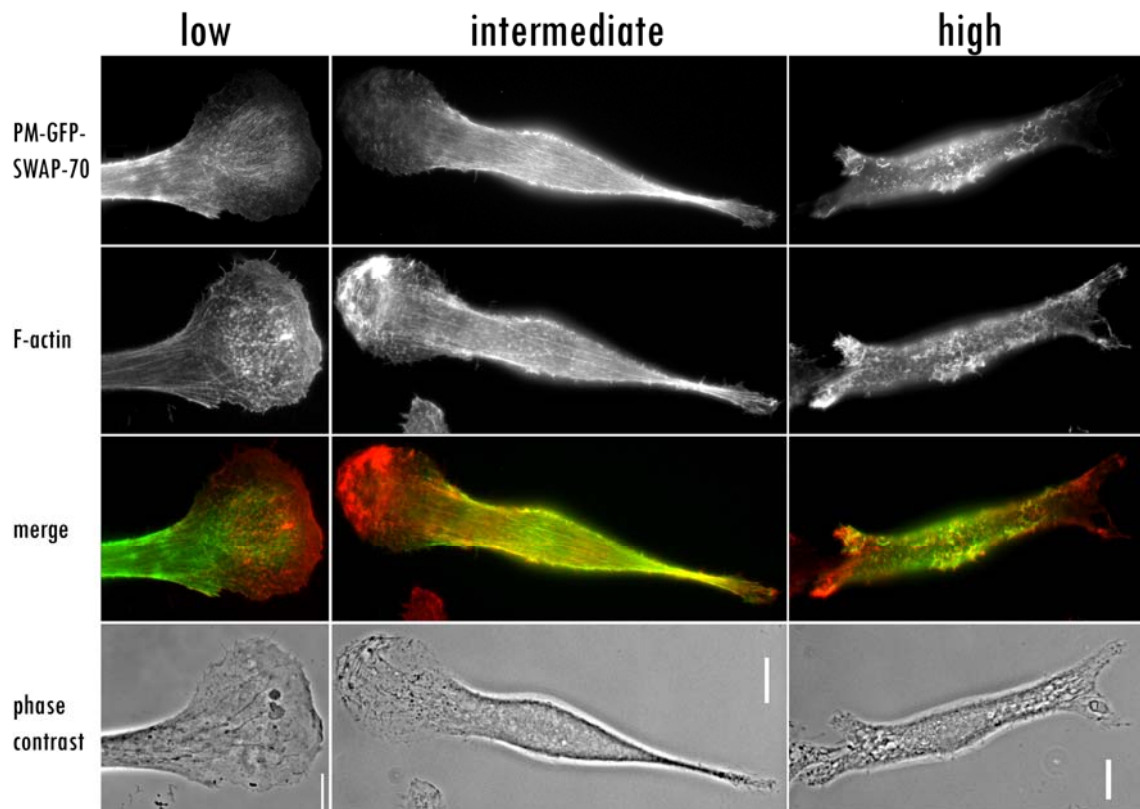


**Fig. 21. Dependent on the expression level of PM-SWAP-70, cells exhibit an altered morphology.** Low expression levels of PM-SWAP-70 do not have a strong effect on cell morphology. PM-SWAP-70 labels longitudinally oriented actin filaments in the cell body and sometimes localizes to the lamella. In cells expressing intermediate levels of the construct, PM-SWAP-70 is predominantly oriented along longitudinal actin filaments in elongated B16F1 cells and is almost absent from the lamella. High expression level of the construct results in complete loss of lamellipodia and misorganization of the actin cytoskeleton. PM-SWAP-70 localizes to microspikes and membrane crinkles. B16F1 cells were transfected with PM-GFP-SWAP-70, replated 24 h later on laminin coated coverslips and fixed after 5 h with 4% PFA. Cells were permeabilized with 0,05% Saponin and stained for F- actin with Alexa594 Phalloidin. Expression levels were judged by the exposure-time necessary for proper exposition Bars: 10  $\mu$ m

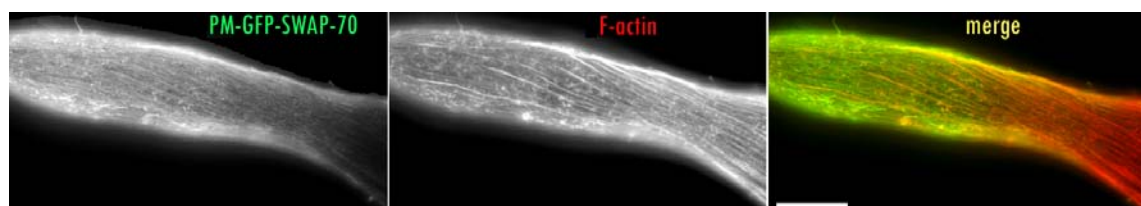


**Fig. 22. PM-GFP-SWAP-70 associates with longitudinal oriented F-actin in moderately expressing B16F1 cells.** B16F1 cells were transfected with PM-GFP-SWAP-70, replated 24 h later on laminin coated coverslips and fixed after 5 h with 4% PFA. Cells were permeabilized with 0,05% Saponin and stained for F-actin with Alexa594-phalloidin. Bar: 10  $\mu$ m

## Results

Table 3. Summary of expression level dependent morphological effects of PM-SWAP-70

Low expression	Moderate expression	High expression
<ul style="list-style-type: none"> <li>• No alterations of cell morphology</li> <li>• PM-GFP-SWAP-70 localizes to F-actin mainly in the region of the cell body and only on occasion to the lamella</li> <li>• Occasional enrichment of PM-GFP-SWAP-70 at thorn-like protrusions which do not widen into a lamellipodium.</li> </ul>	<ul style="list-style-type: none"> <li>• Elongated cells</li> <li>• sometimes with smaller protrusions</li> <li>• loss of broad lamellipodia</li> <li>• Less spread than control cells</li> <li>• Actin cytoskeleton often organized in longitudinal oriented, corset-like actin filament arrays that are labeled by PM-GFP-SWAP-70</li> </ul>	<ul style="list-style-type: none"> <li>• Elongated, often spindle-shaped cells</li> <li>• small ruffles at the ends of the cell</li> <li>• loss of stress fibers</li> <li>• formation of microspikes, filopodia and longitudinal oriented membrane crinkles.</li> <li>• Loss of focal adhesions</li> </ul>



### 5.2.3 PM-SWAP-70 induces morphological changes in different cell lines

Transfections of different cell lines were carried out to investigate possible cell type specific influences of the PM-SWAP-70 construct on cell morphology and actin-rearrangements. Microspike formation, elongated, often spindle shaped morphology and crinkled membrane structures were visible in transfected HEK-293T, NIH/3T3, B16F1, Cos7 and HeLa cells (Figs. 20, 21, 23). Therefore, the artificial membrane targeting of the actin binding protein SWAP-70 does alter cellular morphology independently of the cell-type.

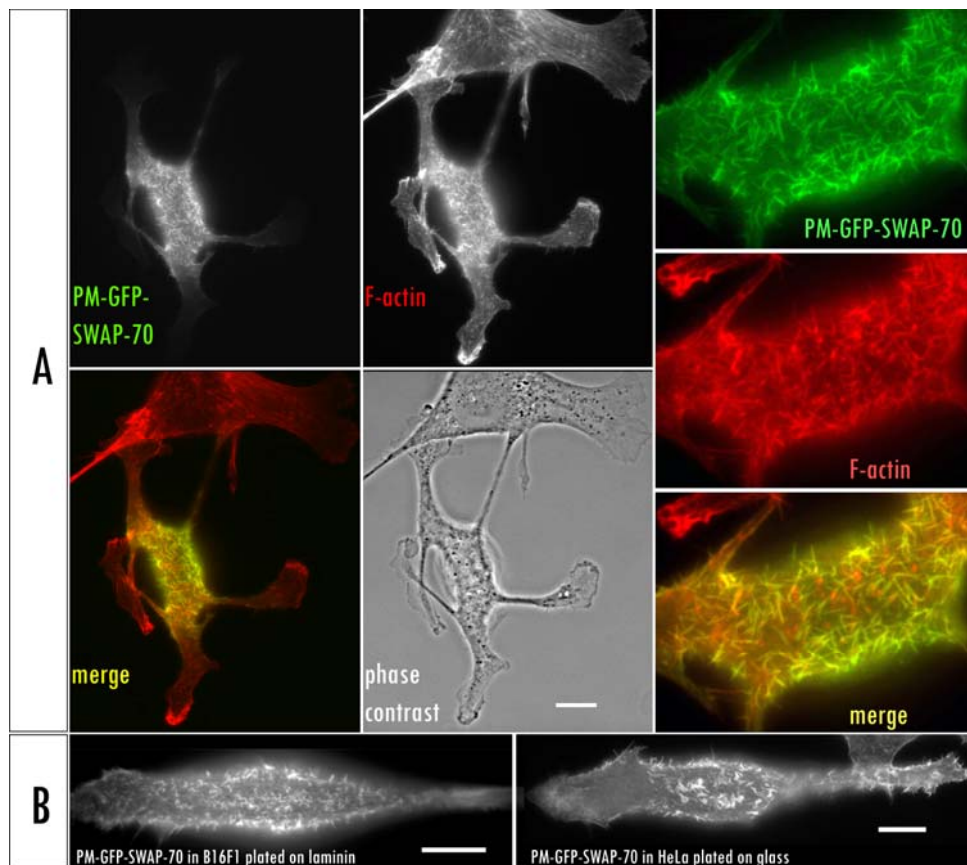


**Fig. 23. Palmitoylated GFP-SWAP-70 causes morphological changes and a distorted actin cytoskeleton in transfected NIH/3T3, B16F1 and HeLa cells.** **A:** Fluorescence images showing the colocalisation of PM-GFP-SWAP-70 with various short F-actin bundles in the area of the cell body but not in ruffling areas of various protrusions. Images on the right-hand side are higher magnifications of the transfected cell rotated 90° clockwise. NIH/3T3 cells were transfected with PM-GFP-SWAP-70, replated on glass coverslips and fixed after 24 h with 4% PFA. Cells were permeabilized with 0,05% Saponin and stained for F-actin with Alexa594 phalloidin. **B:** High expression levels of PM-GFP-SWAP-70 induce a similar phenotype in B16F1 and HeLa cells. Depicted is the GFP-fluorescence of PM-GFP-SWAP-70. Notice the microspike and membrane-crinkle formation. B16F1 cells and HeLa cells were transfected with PM-GFP-SWAP-70 and replated 24 h later on laminin or glass, respectively. Cells were fixed with 4% PFA after 5 h for B16F1 cells and 16 h for HeLa cells and analyzed by fluorescence microscopy. Bars: 10 µm

### 5.2.4 Palmitoylated SWAP-70 alters cell morphology independently of the extracellular matrix

Cells reside in the extracellular matrix (ECM) to which they bind and adhere. Activated adhesion receptors, e.g. integrins, bind to the ECM and link intracellularly to components of the cytoskeleton (Adams, 2002). Most known integrins are indirectly associated with the actin cytoskeleton, some are linked to intermediate filaments (Reznicek *et al.*, 1998). Integrin signaling represents a major pathway for cells to gather information about the surrounding ECM. Therefore, the type and composition of the ECM in which the cells reside has a profound influence on cell behavior and morphology.

To study whether the morphological changes induced by PM-GFP-SWAP-70 are influenced by the ECM, transfected cells were plated on different extracellular matrices and analyzed by fluorescence microscopy. The PM-GFP-SWAP-70 induced morphological changes were independent of the extracellular matrix, since transfected B16F1 mouse melanoma cells (plated on laminin or fibronectin; see Fig. 24), NIH/3T3 fibroblasts (plated on glass or fibronectin) and HeLa cells (plated on glass or fibronectin) all exhibited an identical phenotype.

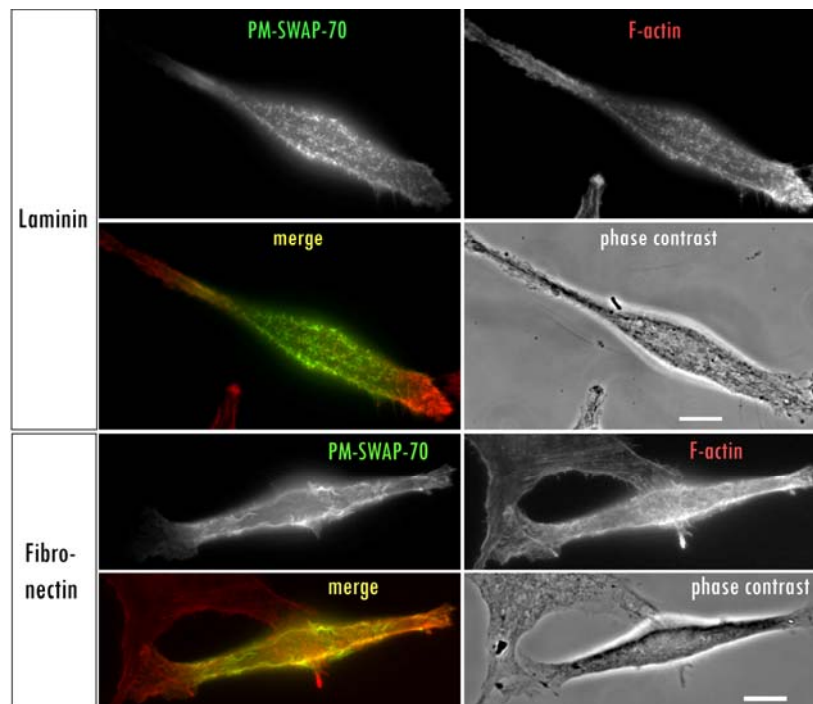


**Fig. 24. High expression levels of palmitoylated GFP-SWAP-70 induce spindle shaped morphologies and a distorted actin cytoskeleton independently of the extracellular matrix.** B16F1 cells plated on laminin or on fibronectin show an identical phenotype. High expression levels of PM-GFP-SWAP-70 cause a disorganization of the actin cytoskeleton and formation of microspikes and membranous crinkles. B16F1 cells were transfected with PM-GFP-SWAP-70 and replated on laminin or fibronectin coated coverslips 24 h after transfection. Cells were fixed after 5 h with 4% PFA and permeabilized with 0,05% Saponin. F-actin was stained with Alexa594 Phalloidin. Cells were analyzed by fluorescence microscopy. Bars: 10  $\mu$ m

### **5.2.5 Formation of vinculin containing focal adhesions is reduced in PM-SWAP-70 transfected NIH/3T3 cells.**

Focal adhesions are cell-matrix-contacts and their formation and regulation are strongly dependent on Rho GTPase signaling (Barry and Critchley, 1994; Hall, 2005; Ridley and Hall, 1992). Because the morphology of cells expressing PM-SWAP-70 was reminiscent of a downregulation of Rho signaling (Ward *et. al.* 2002), cells were stained against a marker for focal adhesions. Vinculin is an important protein in focal adhesions where it links F-actin to  $\beta$ -integrins in a complex with talin and paxillin. NIH/3T3 cells (plated on fibronectin) still showed focal adhesions as judged by vinculin staining. Palmitoylated SWAP-70 did not localize to vinculin stained focal adhesions at the periphery of the cells. In PM-SWAP-70 transfected cells with a high expression level, vinculin was predominantly cytosolic and no distinct focal adhesions could be observed. Nontransfected cells and cells transfected with palmitoylated GFP contained numerous focal adhesions (Fig. 25).

## Results

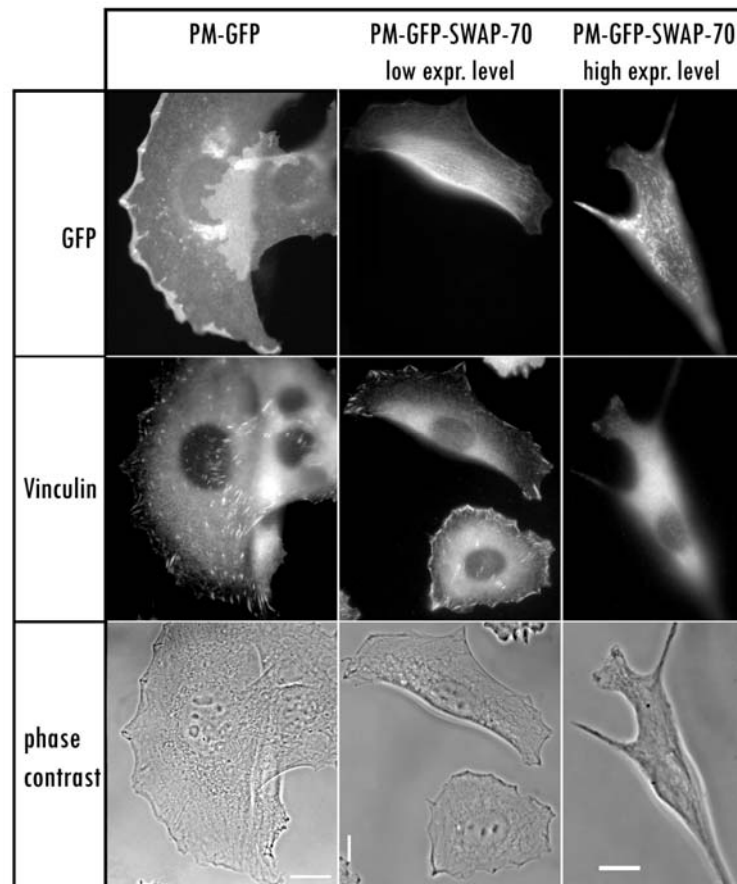


**Fig. 25. Formation of focal adhesion is affected in PM-GFP-SWAP-70 transfected NIH/3T3 cells.** Vinculin stained focal adhesions were visible in nontransfected cells, cells transfected with PM-GFP and in cells expressing low levels of PM-SWAP-70. Vinculin stained focal adhesions are hardly visible in cells expressing higher levels of PM-GFP-SWAP-70. Note the typical cell morphology of the strongly expressing cell. NIH/3T3 cells were replated on fibronectin coated coverslips 16 h after transfection. 24 h later, cells were fixed with 4% PFA and permeabilized with 0,05% Saponin. Staining for vinculin was obtained with the monoclonal antibody hVin-1 and a Cy3 coupled secondary antibody.

### 5.2.6 Plasma-membrane localization of SWAP-70 is sufficient for F-actin binding

The PH-Domain of SWAP-70 has been shown to bind to different phosphoinositides *in vitro* and to be necessary for correct intracellular localization and F-actin binding *in vivo* (Hilpelä *et al.*, 2003). Mutations in the PH domain result in decreased F-actin binding. To examine whether the membrane association of SWAP-70 is sufficient for F-actin binding, we used an artificially membrane targeted PM-SWAP-70 construct with mutations in the

## Results

PH-domain. Two amino acids (RR223, 224) in the  $\beta 1/\beta 2$  loop of the PH-domain have been shown to be essential for phosphoinositide binding *in vitro* (Hilpelä *et al.*, 2003). A palmitoylated construct with mutations in these two residues still localized to the cortical F-actin corset. Moreover, transfection of NIH/3T3 cells with this construct resulted in morphological changes similar to its non-mutated counterpart (Fig. 26). However, the F-actin colocalisation of the fusion protein and the microspike formation induced by the construct were not as clear-cut as seen for the non-mutated palmitoylated construct. The fusion protein was sometimes found in the perinuclear region, presumably at the Golgi-apparatus (data not shown).

Taken together, in the artificially membrane targeted PM-SWAP-70 a functional PH-domain is not necessary for F-actin binding and the induction of morphological alterations.

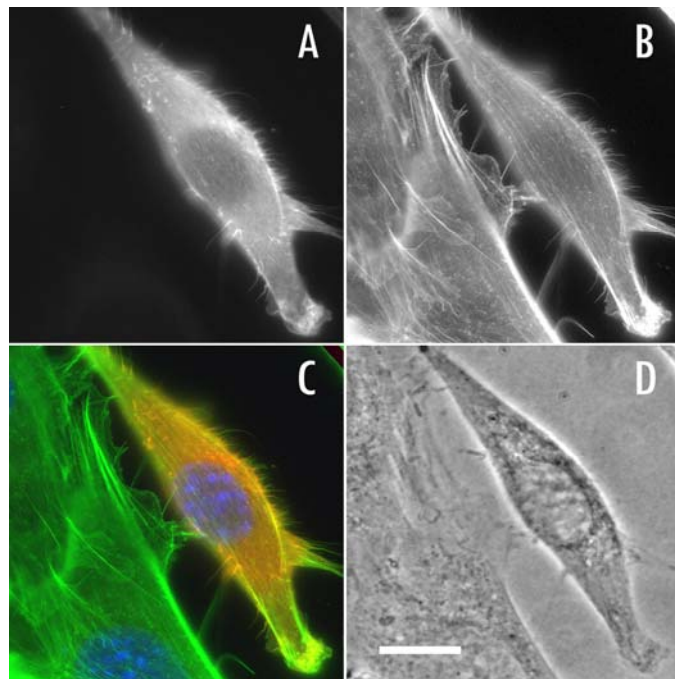


**Fig. 26. Palmitoylated SWAP-70 with mutations in the PH-domain still binds to F-actin and causes morphological changes in NIH/3T3 cells.** Left side: **A:** PM-GFP-SWAP-70 (RR223,224EE). **B:** F-actin **C:** Merged image showing the GFP-signal together with F-actin **D:** Phase contrast. NIH/3T3 cells were transfected with a PM-GFP-SWAP-70 (RR223,224EE) construct and replated on glass coverslips 16 h after transfection. After 24 h cells were fixed with 4% PFA and permeabilized with 0,05% saponin. Cells were stained for F-actin using Alexa594-Phalloidin and analyzed by fluorescence microscopy.

### 5.2.7 Dominant negative Rac does not rescue the phenotype induced by PM-GFP-SWAP-70

Ihara *et al.* (2006) reported that SWAP-70 binds to Rac-GTP in an effector-like manner while an earlier paper proposed that SWAP-70 might act as a Rac-GEF. If SWAP-70 really

## Results

acts as a Rac-GEF (Shinohara *et al.*, 2002), then the effects of palmitoylated SWAP-70 might be caused by the activation of Rac-signaling. If SWAP-70 was a Rac-GEF, coexpressed dominant negative Rac should compete with endogenous Rac for binding to SWAP-70. In this case, SWAP-70 would be partly sequestered and its effects might be blocked.

Disagreeing with this hypothesis, most of the NIH/3T3 cells expressing high levels of palmitoylated SWAP-70 exhibited the elongated ruffling phenotype even when cotransfected with dominant negative mRFP-Rac (Fig. 27). Therefore, it is unlikely, that the morphological changes induced by SWAP-70 are due to a Rac-GEF activity. Furthermore, the elongated cell morphology without prominent lamellipodia is not typical for a Rac-GEF. mRFP-Rac (N17) cotransfected cells with a low expression level of PM-SWAP-70 were still spread and exhibited a colocalisation of PM-SWAP-70 with F-actin, probably stress fibers.

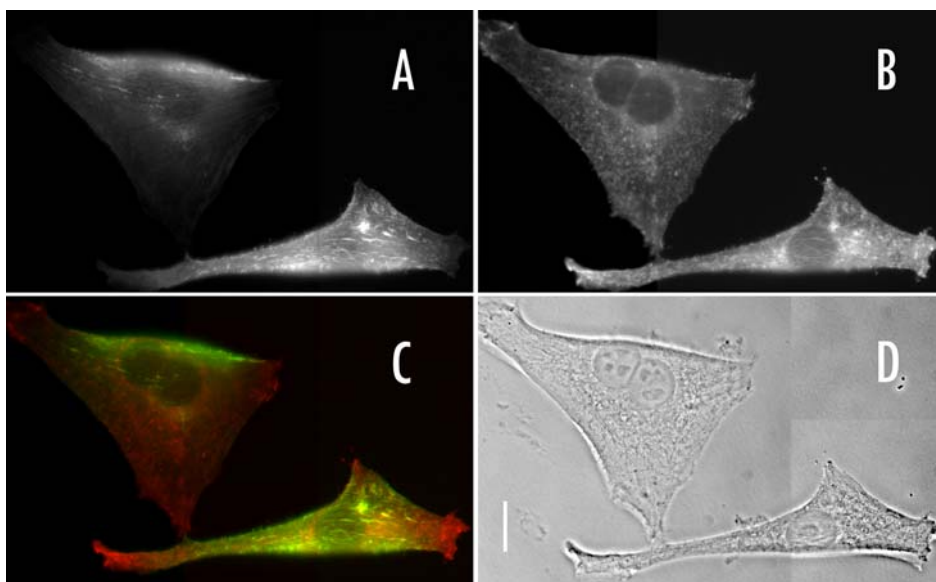


**Fig. 27. Dominant negative Rac does not prevent PM-SWAP-70 induced morphological changes in NIH/3T3 cells.** NIH/3T3 cells cotransfected with dominant negative Rac (17N) and PM-GFP-SWAP-70 plated on glass. **A:** PM-GFP-SWAP-70. Higher expression-levels of the fusion protein result in the typical elongated phenotype **B:** mRFP-Rac (17N) **C:** Merge of GFP and mRFP fluorescence. **D:** Phase contrast. Bar: 10  $\mu\text{m}$

### 5.3 Different domains of SWAP-70 induce distinctive changes in cell morphology

SWAP-70 is a multidomain protein and its different domains contribute in different ways to its *in vivo* localization (Hilpelä, *et al.*, 2003; Oberbanscheidt *et al.*, 2007) and probably

to the physiological function of SWAP-70. The N-terminal region localizes to macropinosomes but the C-terminal part enhances the affinity (Oberbanscheidt *et al.*, 2007). The PH domain is dispensable for macropinosomes association, but necessary for localization to the special subset of actin-filaments SWAP-70 localizes with. F-actin colocalisation critically depends on the C-terminal F-actin binding domain. In order to investigate the contributions of different domains of SWAP-70 for the changes in the actin cytoskeleton and the morphology of the cells, a variety of constructs were used:

### **5.3.1 PM-SWAP-70 (1-525) that lacks the actin binding domain of SWAP-70 induces dramatic morphological changes**

To find out, whether the morphological changes seen in cells transfected with the palmitoylated SWAP-70 depend on the ability of SWAP-70s C-terminal part to bind to non-muscle F-actin, a C-terminal truncation construct was used in which the actin-targeting sequence had been deleted.

Transfections of B16F1 and NIH/3T3 cells with this PM-SWAP-70 (1-525) construct resulted in a different phenotype from that of the PM-SWAP-70 construct. Colocalisation with F-actin was completely abolished. The fusion protein was localized evenly at the plasma membrane. The cells did not show the spindle shaped morphology characteristic for the palmitoylated SWAP-70 full-length construct but instead were still spread and only occasionally rounded up. Nevertheless, the fusion-protein had a severe influence on cell morphology. Transfected cells showed a ragged and frayed plasma membrane surface and apparently could not extend smooth lamellipodia. Instead, they often exhibited rather spiky protrusions (Figs. 28 and 29). Cells expressing high levels of this construct showed dorsal bleb-formation not seen with the full-length construct. This was especially obvious in NIH/3T3 and HeLa cells (Figs. 30 and 31). Interestingly, the ventral actin cytoskeleton organisation of dorsally blebbing B16F1 and HeLa cells did not differ much compared to adjacent non-transfected cells (Figs. 30 and 31).

## Results

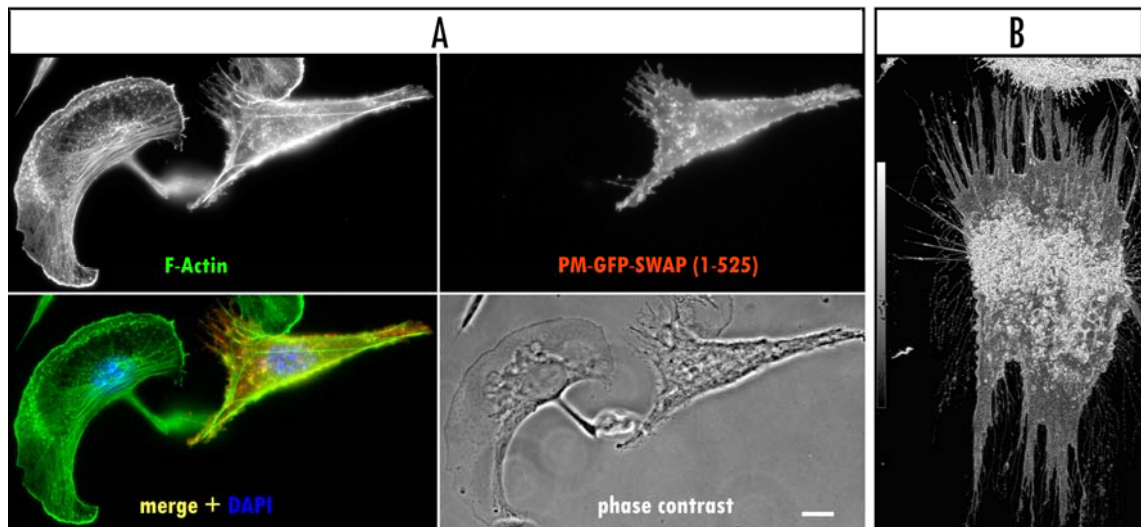


**Fig. 28. Irregular surface formation and lack of lamellipodia in cells transfected with artificially membrane targeted PM-GFP-SWAP-70 without the F-actin targeting sequence.** **A:** Fluorescence microscopy images of B16F1 cells transfected with PM-GFP-SWAP-70 (1-525). Cells were plated on Laminin coated coverslips 24 h after transfection and fixed after additional 5 h with 4% PFA. F-actin was stained with Alexa594-Phalloidin after permeabilization with 0,05% Saponin.. **B:** 3D-projection of a confocal stack of a PM-GFP-SWAP-70 (1-525) transfected NIH/3T3 cell. Depicted is the rendered GFP-fluorescence using a Sobel-edge filter for 3D projection. Note the thin membrane protrusions, the lack of lamellipodia and the various dorsal blebs.

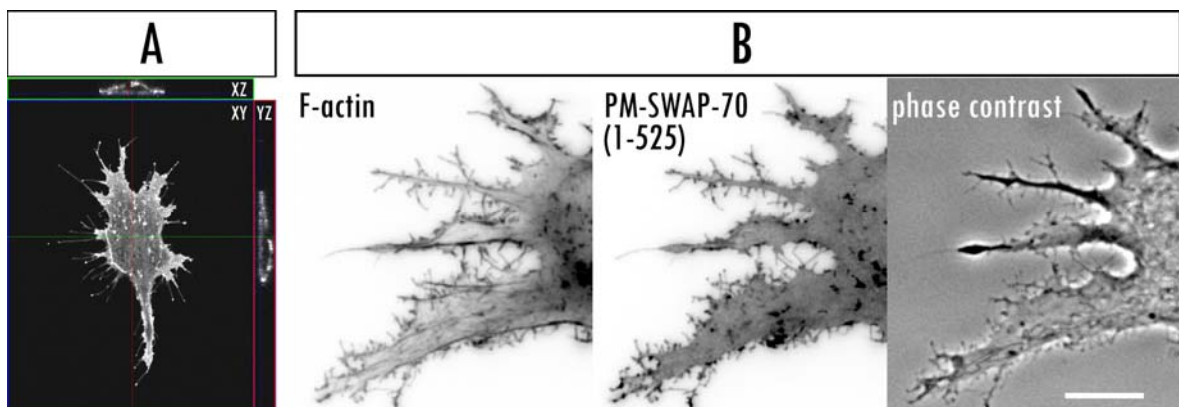


**Fig. 29. PM-GFP-SWAP-70 (1-525) induces prominent morphological alterations.** **A:** Single ventral plane of a confocal stack of a PM-SWAP-70 (1-525) transfected B16F1 cell. Note the irregular membrane morphology at the periphery of the cell and the membrane localization of the construct in the orthogonal projections (XZ, YZ). The GFP-signal highlights thin membrane extensions and their distal tips. **B:** Typical jagged membrane morphology of B16F1 cells expressing a high level of PM-GFP-SWAP-70 (1-525). Cells were plated on Laminin coated coverslips 24 h after transfection, and fixed after additional 5 h with 4% PFA. F-actin was stained with Alexa594-Phalloidin after permeabilization with 0,05% Saponin. Bar 10  $\mu\text{m}$



## Results

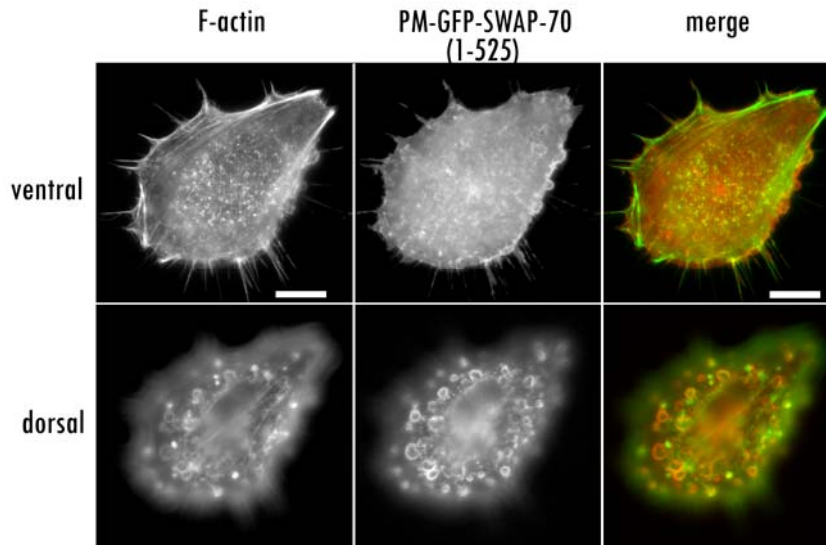


**Fig. 30. Palmitoylated SWAP-70 (1-525) frequently causes dorsal bleb formation in B16F1 cells.** Fluorescence images of a B16F1 cell plated on fibronectin. Cells were replated on fibronectin 24 h after transfection and fixed after additional 5 hours. Note that the ventral part of the cell still shows F-actin staining. F-actin was stained with Alexa594-Phalloidin after permeabilization with 0,05% Saponin. Bar 10  $\mu\text{m}$

### ***Palmitoylated SWAP-70 devoid of the F-actin binding domain localizes to tubular structures in HeLa cells***

In HeLa cells expressing low levels of PM-SWAP-70 (1-525), the fusion-protein localized frequently adjacent to- or colocalized with tubular structures which could not clearly be identified to be F-actin, but sometimes run along stress-fibers in the region of the nucleus. The same tubular or filamentous structures are observed with PM-SWAP-70 in HeLa cells with moderate expression levels. The localization of PM-SWAP-70 (1-525) to tubular structures was found predominantly in the region of the nucleus, whereas PM-SWAP-70 also labels more peripherally located filamentous structures. However, PM-SWAP-70 (1-525) could not be detected on such tubular structures in other cell-types. In HeLa cells cotransfected with GFP-SWAP-70 and dominant active H-Ras (12V), the GFP-signal also could be detected on similar tubular structures (data not shown).

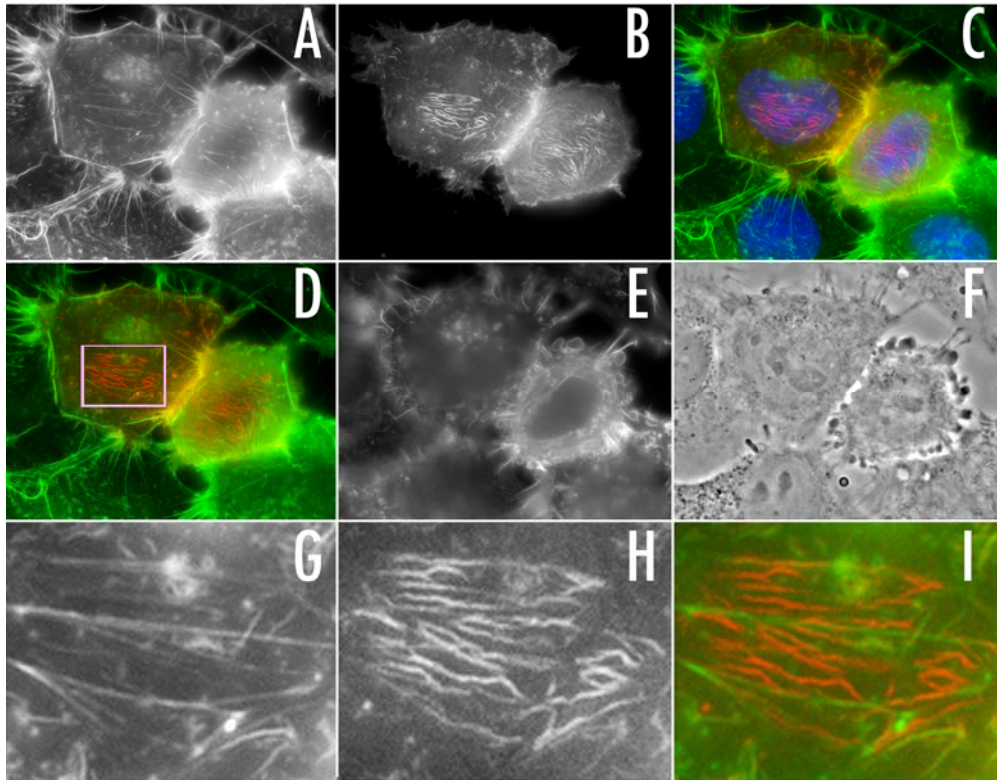


**Fig. 31 PM-GFP-SWAP-70 (1-525) localizes to tubular structures at the ventral side of HeLa cells.** **A-F:** HeLa cells plated on fibronectin were transfected with PM-GFP-SWAP-70 (1-525) and fixed after 24 h. After permeabilization cells were stained with Alexa 594-Phalloidin and DAPI. **A:** F-actin; **B:** PM-GFP-SWAP-70 (1-525); **C:** Merge of PM-GFP-SWAP-70 (1-525), F-actin and DAPI; **D:** Merge of PM-GFP-SWAP-70 (1-525) and F-actin. Higher magnification of the boxed area is shown in G-I; **E:** F-actin at the dorsal side of the cells. Note the bleb formation; **F:** Phase contrast; **G:** F-actin; **H:** PM-GFP-SWAP-70 (1-525); **I:** Merge of G and H.

### **5.3.2 PM-SWAP-70 (305-525) induces similar changes in cell morphology as PM-SWAP-70 (1-525).**

Confocal microscopy revealed that the PM-SWAP-70 (305-525) GFP-fusion protein localizes evenly to the plasma membrane of transfected NIH/3T3-cells and does not colocalize with F-actin (Fig. 32). In NIH/3T3 cells expressing moderate levels of the construct, PM-SWAP-70 (305-525) strongly localized to ruffles, vesicles and macropinosomes (see video S19). Interestingly, transfected cells frequently showed abundant macropinocytosis even without induction via PMA or PDGF.

In accordance with the results of the PM-SWAP-70 (1-525) construct, the NIH/3T3 cells expressing higher levels of the PM-SWAP-70 (305-525) construct revealed spiky membrane protrusions instead of smooth lamellipodia. Phalloidin staining shows F-actin

## Results

running through the axis of the spiky protrusions while few F-actin bundles were visible in the flat and membranous areas surrounding the axis of the protrusions (Fig. 32). Transfected cells also frequently exhibited bleb formation at the dorsal membrane surface. Also in B16F1 cells, the PM-SWAP-70 (305-525) construct was distributed at the plasma membrane, macropinosomes and smaller vesicles as visualized by confocal microscopy. High expression levels of the construct led to a loss of lamellipodia and similar long and spiky protrusions as seen in NIH/3T3 cells. Since spots of the GFP-signal were visible in these protrusions, cells were stained for phosphotyrosine to label focal adhesions. The fluorescent spots of PM-SWAP-70 (305-525) did not colocalize with spots stained by P-Tyr antibodies in B16F1 cells (Fig. 32).

HeLa cells transfected with PM-GFP-SWAP-70 (305-525) exhibited bleb-formation at the dorsal membrane without showing obvious differences in the ventral actin cytoskeleton (Fig. 32). No filamentous association of the construct was observed. Palmitoylated SWAP-70 devoid of the last 60 amino acids localized in HeLa cells to tubular structures which sometimes colocalized with F-actin (Fig. 31). This localization must depend on the N-terminal part of the protein, because no association with these tubular structures was seen for the PM-GFP-SWAP-70 (305-525) construct.

## Results

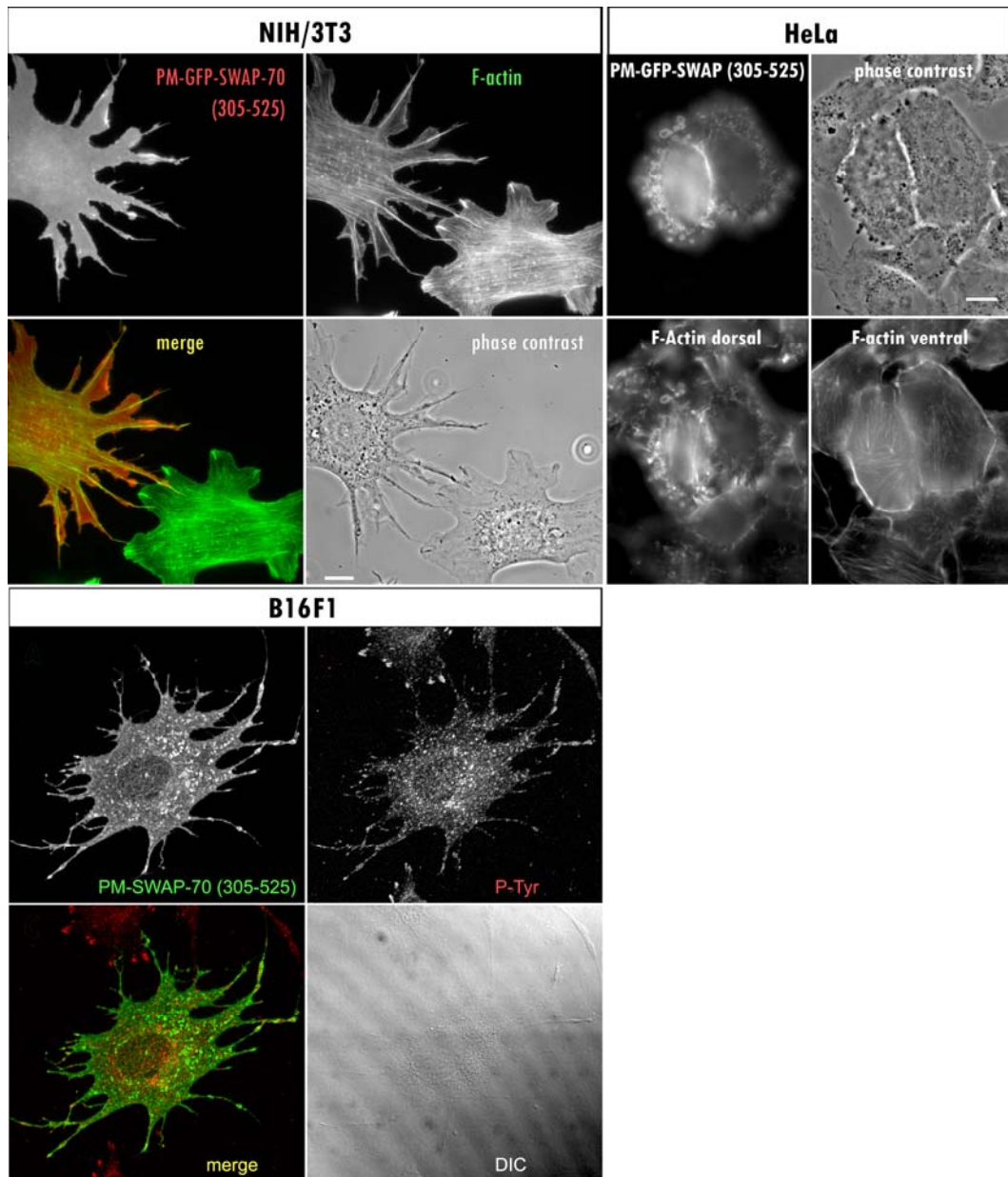


**Fig. 32. Effects on cell morphology induced by the palmitoylated C-terminal fragment of SWAP-70 devoid of the actin binding information.** Fluorescence images of PM-GFP-SWAP-70 (305-525) transfected and F-actin stained cells. **NIH/3T3:** Transfection of NIH/3T3 cells with the PM-GFP-SWAP-70 (305-525) construct results in loss of rounded lamellipodia and induces an irregular cell surface with long and spiky protrusions. **HeLa:** HeLa cells transfected with the construct frequently exhibit bleb-formation at the dorsal membrane. Note that the ventral F-actin cytoskeleton of blebbing HeLa cells does not show obvious alterations compared to nontransfected cells. **B16F1:** Transfection of B16F1 cells with the construct results in a loss of lamellipodia. An irregular cell surface with extended spiky protrusions is characteristic as seen also for NIH/3T3 cells. Aggregates of PM-GFP-SWAP-70 (305-525) do not colocalize with  $\alpha$ -phosphotyrosine stained focal adhesions. B16F1 cells were replated on fibronectin coated coverslips 16 hours after transfection and fixed after additional 5 h. Cells were stained for phosphotyrosine and analyzed by confocal microscopy. 3-D projection of a confocal stack of the GFP-fluorescence from PM-GFP-SWAP-70 (305-525) was obtained by using a Sobel-edge filter.

### 5.3.3 The palmitoylated C-terminal part of SWAP-70 (305-585) induces a phenotype similar to the palmitoylated full-length construct

The morphology of cells transfected with a truncation construct of SWAP-70 beginning directly behind the PH-domain of SWAP-70 (PM-SWAP-305-585) resembled that seen with the palmitoylated GFP-SWAP-70 construct. Transfected cells were not as well spread as the nontransfected control cells. Often, ruffling of the cell could be observed at small lamellipodial protrusions at the ends of the spindle shaped cells. The palmitoylated C-terminal part of SWAP-70 (305-585) colocalised with F-actin. Frequently, an accumulation of the GFP-signal in the perinuclear region was apparent. As with the full-length construct, the severity of the phenotype of the cells was dependent on the expression level. In NIH/3T3 cells, the fusion protein predominantly localized to the area of the cell body and only weakly stained ruffling areas and smaller lamellipodia (Fig. 33A). In B16F1 cells the construct sometimes also localized to ruffles (Fig. 33B). However, it induced similar changes in cell morphology in B16F1 cells and in NIH/3T3 cells

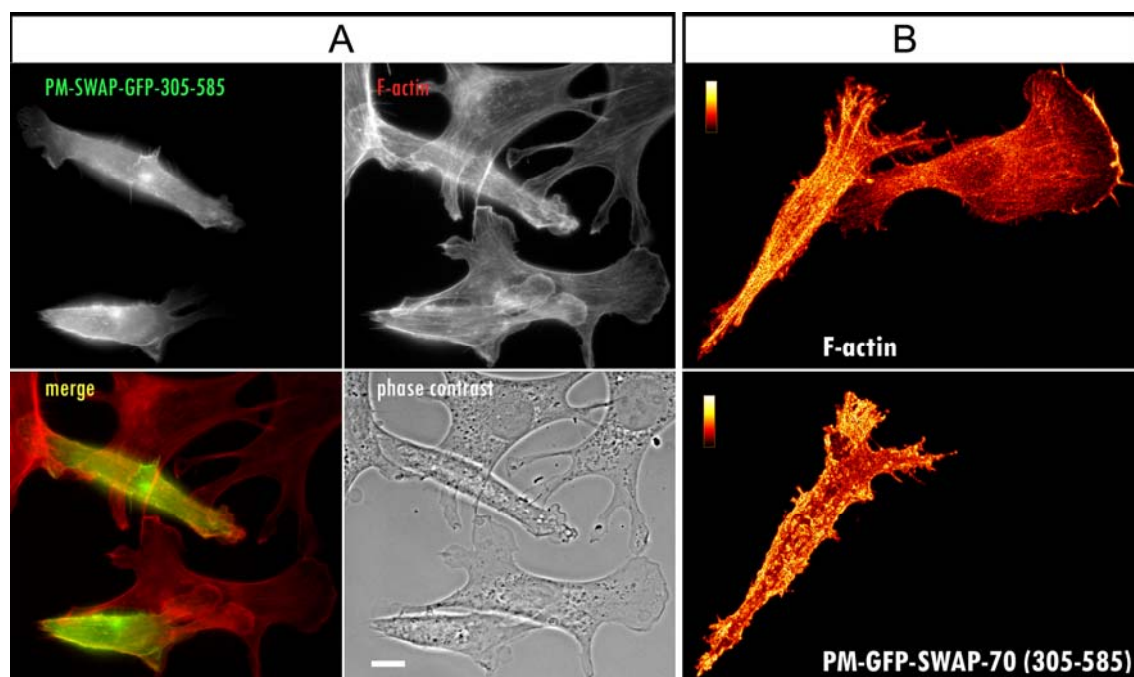


**Fig. 33.** The palmitoylated C-terminal part of SWAP-70 induces morphological changes resembling the alterations seen with the palmitoylated full-length construct. **A:** NIH/3T3 cells expressing PM-SWAP-70 (305-525) are not as spread as non-transfected cells and show a spindle shaped morphology. Cells were transfected with PM-GFP-SWAP-70 (305-585), replated on fibronectin coated coverslips and fixed after 24 h with 4% PFA. Cells were permeabilized with 0,05% Saponin and stained for F-actin with Alexa594 Phalloidin. Bar: 10  $\mu$ m. **B:** Projections of a confocal stack from a B16F1 cell expressing a high level of PM-GFP-SWAP-70 (305-585). Note that the truncation construct also localizes to the ruffling area which is not seen for the full-length construct.

### 5.3.4 The palmitoylated N-terminal part of SWAP-70 does not induce morphological changes

The N-terminal part of SWAP-70 (amino acids 1- 210) has been reported to associate with macropinosomes and to contain information for the correct intracellular localization of SWAP-70 to the loose actin arrays behind protruding lamellipodia in motile cells. B16F1 and NIH/3T3 cells transfected with the construct PM-SWAP-70 (1-210) did not show obvious morphological changes or alterations in the actin cytoskeleton compared to nontransfected control cells (Fig. 34). Transfected B16 F1 cells were still able to migrate in contrast to cells transfected with the PM-SWAP-70 construct and showed no alterations in phospho-tyrosine staining compared to non-transfected cells (data not shown). Fixation of B16F1 cells 90 minutes after replating on Laminin did not reveal differences in the spreading area or actin organization compared to non-transfected cells. In addition to B16F1 cells, no severe effects were visible in NIH/3T3 cells when transfected with the palmitoylated N-terminus, apart from various thin membranous threads that were probably visible due to the artificially membrane bound GFP-SWAP-70-construct.

The PM-SWAP-70 (1-210) GFP-fusion protein was evenly distributed at the plasma membrane and in the perinuclear region, probably the Golgi-apparatus. No colocalisation with F-actin was observed. Noticeably, the construct was not concentrated in the lamellae of migrating B16F1 cells but still associated with macropinosomes and - in contrast to the full-length PM-SWAP-70 construct- ruffling areas in both cell types (Fig. 34).

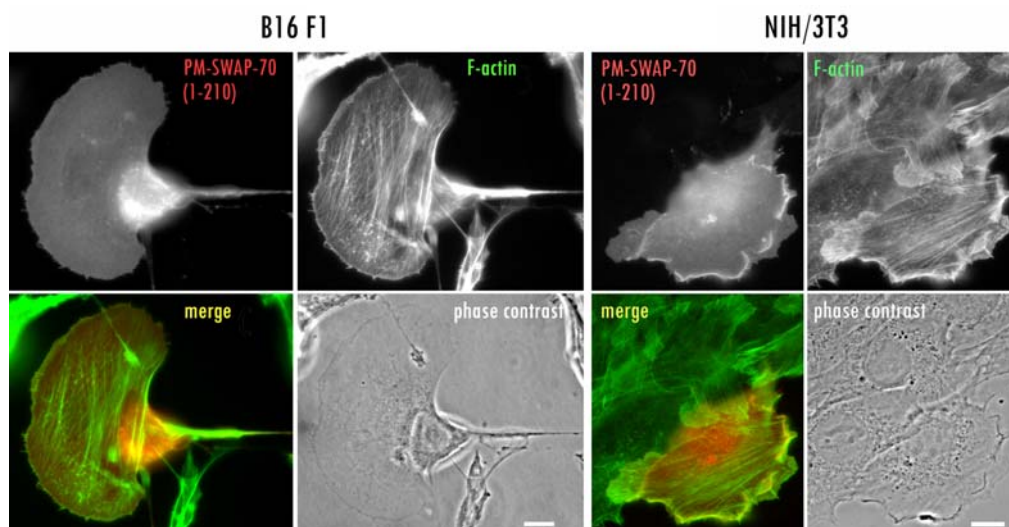


**Fig. 34. Artificial targeting of the N-terminal 210 amino acids from SWAP-70 to the plasma membrane does not influence cell morphology or actin organization.** Fluorescence images of cells transfected with PM-GFP-SWAP-70 (1-210). B16F1 cells were replated 24 h after transfection on laminin coated coverslips. Cells were fixed 5 h after replating with 4% PFA, permeabilized with 0,05% Saponin and stained for F-actin with Alexa-594-phalloidin. **A:** PM-GFP-SWAP-70 (1-210); **B:** F-actin; **C:** merge of the two fluorescence images; **D:** phase contrast. NIH/3T3 cells were replated on glass 16 h after transfection and fixed the next day with 4% PFA, permeabilized with 0,05% Saponin and stained for F-actin with Alexa-594-phalloidin. Bars: 10  $\mu$ m

## Results

Taken together, artificial membrane tethering of SWAP-70 through introduction of an N-terminal palmitoylation signal affected the actin cytoskeleton, cell adhesion and cell morphology in a dose dependent manner. Transfected cells developed a spindle-shaped morphology and showed an association of PM-SWAP-70 with a corset-like cortical F-actin system in moderately expressing cells. F-actin binding of membrane tethered SWAP-70 might contribute to the typical spindle shaped morphology of transfected cells. Stronger expression levels of PM-SWAP-70 ultimately led to a loss of lamellipodia, stress fibers and the formation of various microspikes and small ruffles. The expression of high levels of PM-SWAP-70 interfered with formation of vinculin stainable focal adhesions. Unexpectedly, the palmitoylated SWAP-70 fusion protein did neither localize to the lamella nor to membrane rich peripheral ruffling areas even though SWAP-70 has been implicated in the formation of ruffles. Phosphoinositide binding of PM-SWAP-70 was not essential, since a palmitoylated construct of SWAP-70 with a mutated PH-domain still bound F-actin and induced the typical phenotype.

Expression of different truncation constructs demonstrated that the C-terminal part of SWAP-70 starting behind the PH-domain is responsible for the morphological alterations. The morphological effects depend on the actin-binding information since a deletion of the C-terminal 60 amino acids lead to a diminished microspike formation and a complete loss of F-actin colocalisation in NIH/3T3 and B16F1 cells. Overexpression of the PM-GFP-SWAP-70 (1-525) construct abolished lamellipodia formation and induced blebbing of cells. Consistent with the notion that the C-terminal part is responsible for the observed alterations, a palmitoylated C-terminal fragment (amino acid 305-525) was sufficient whereas a palmitoylated N-terminal fragment of SWAP-70 (1-210) did not induce any alterations in cell morphology.

### **5.4 Artificially membrane targeted SWAP-70 affects the activation levels of RhoA, Ras and Cdc42 but not Rac**

SWAP-70 binds to actin and the palmitoylated SWAP-70 construct has a strong influence on the actin cytoskeleton leading to morphological changes of cells. How SWAP-70 contributes to these cellular alterations is not clear. SWAP-70 has been implicated in various signaling pathways originating from receptor tyrosine kinases. If SWAP-70 acts as a Rac GEF or a Rac effector as proposed, the overexpression of a palmitoylated SWAP-70 construct would probably have an influence on the activation status of this small GTPase. As SWAP-70 regulates the actin cytoskeleton, it is likely to influence the activity of other small GTPases known to regulate the actin cytoskeleton, e.g. Ras, Rho, Cdc42. To compare the activation status of the mentioned small GTPases, pull down experiments were carried out from lysates of HEK 293T cells transfected with PM-SWAP-70 or PM-GFP. Transfection efficiency was regularly in the range of ~40% (Fig. 35).

## Results

The results illustrate that expression of membrane targeted SWAP-70 has an influence on the signaling of small GTPases. Interestingly, the activation level of Rac did not change upon transfection of cells with membrane targeted SWAP-70. This result confirms previous findings that SWAP-70 does not have GEF activity for Rac. If SWAP-70 would be a GEF for Rac or a Rac-GTP stabilizing factor, then Rac-levels should change. Instead, the activation levels of RhoA, Ras and Cdc42 were affected (Fig. 35). In accordance with the morphology of PM-SWAP-70 transfected cells, the activity of RhoA was found to be downregulated. The activities of Cdc42 and Ras were upregulated. These changes could either be responsible for the morphological changes or reflect secondary effects of another mechanism (e.g. disturbance of integrin-adherence).

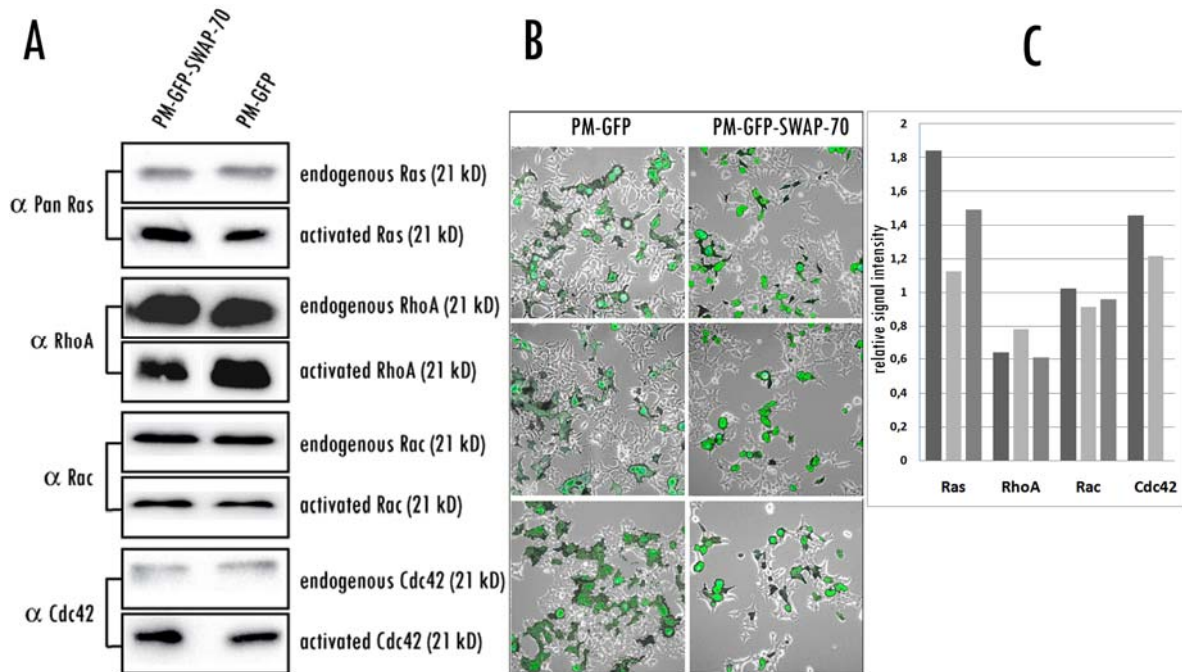


**Fig. 35. Expression of artificially membrane targeted SWAP-70 influences the activities of different small GTPases.** **A:** HEK 293T-cells were transiently transfected with the expression plasmids for PM-GFP-SWAP-70 or PM-GFP and lysed after 48 h of expression. The levels of activated GTPases were analysed by subjecting the cell lysates to precipitation with GST-coupled GTPase binding domains followed by Western blotting with GTPase specific antibodies. Results are representative examples of independent experiments (for Ras N=3; RhoA N=3; Rac N=3; Cdc42 N=2) **B:** For examination of the transfection efficiency, transfected cells were analyzed by fluorescence microscopy. Depicted are fluorescence images merged with the corresponding brightfield images of three random regions of culture dishes from different transfections. **C:** Quantifications of the relative chemiluminescence intensity of the western-blot for the GTPase-pull-downs. The intensity-quotient of the chemiluminescence signal of the activated small GTPase from pull-downs of PM-SWAP-70 transfected vs. the signal intensity of pull-downs from PM-GFP transfected is depicted in arbitrary units on the Y-axis.



## 5.5 Ras regulates the subcellular localization of SWAP-70

### 5.5.1 Dominant active Ras induces the association of SWAP-70 with F-actin arrays

SWAP-70 has been hypothesized to bind to actin-filaments generated in the lamellipodium that are in transition before incorporation into contractile F-actin bundles. SWAP-70 has also been implicated in receptor tyrosine-kinase signaling pathways and in coordinated cell migration (Pearce *et al.*, 2006). Endogenous SWAP-70 relocates to the plasma membrane under conditions of high levels of phosphatidylinositol 3,4 bisphosphate (Hilpelä *et al.*, 2003).

The small G-protein Ras might have a severe influence on SWAP-70 due to direct activation of PI3-kinases leading to enhanced 3-phosphoinositide production. Additionally, Ras activation stimulates the production of reactive oxygen species that have been shown to raise the levels of phosphoinositide (3,4) bisphosphate and to inactivate Rho-signaling (van der Kaay *et al.*, 1999); (Shinohara *et al.*, 2007). Furthermore, activated Ras leads to dissociation of stress fibers (Sahai *et al.*, 2001) and this probably favors the existence of more delicate actin bundles to which SWAP-70 preferentially associates (Hilpelä *et al.*, 2003; Oberbanscheidt *et al.*, in preparation).

The influence of dominant active H-Ras and R-Ras on the localization of SWAP-70 was investigated in B16F1 and NIH/3T3 cells.

Dominant active R-Ras and H-Ras often induced abundant lamellipodial actin polymerization judged by the peripheral bright F-actin staining seen for phalloidin stainings and mRFP-actin fluorescence in fixed cells (Fig. 36). SWAP-70 and dominant active R-Ras (38V) cotransfected B16F1 cells plated on laminin were well spread (Figs. 36 and 37). The cells were often immotile judged by their rounded and unpolarized morphology (Fig. 37) and had few stress fibers. B16F1 cells transfected with dominant active H-Ras (12V) exhibited strongly enhanced lamellipodium formation and were generally more polarized than dominant active R-Ras (38V) transfected cells. H-Ras (12V) cotransfected cells showed very few stress fibers (Fig. 36). Fluorescence microscopy showed that GFP-SWAP-70 localized to extended F-actin arrays oriented parallel to the plasma membrane of cotransfected cells. The localization of GFP-SWAP-70 was characteristic for dominant active R-Ras (38V) and dominant active H-Ras (12V) cotransfected cells and was not observed in cells not cotransfected with dominant active Ras. The actin filament arrays could not be visualized with mRFP-actin in dominant active H-Ras (12V) cotransfected cells (Fig. 36 L). To analyze the dynamics of these F-actin arrays, kymographs were generated from time-lapse movies (Fig. 37). A 1-pixel-wide line was drawn perpendicular to the membrane front in the same position for each picture. Individual lines were then stacked in series, creating a kymograph with the  $x$ -axis

## Results

representing the GFP-fluorescence intensity and the y-axis representing individual frames and therefore time. The SWAP-70 labeled actin filaments appeared  $\sim 1-5 \mu\text{m}$  behind the tip of lamellipodia and moved away perpendicular from the membrane border without losing the membrane parallel orientation (video S3, S4). In motile cells cotransfected with dominant active H-Ras (12V), SWAP-70 labeled filaments originated behind the leading edge and moved slowly towards the cell center. In R-Ras (38V) cotransfected immotile cells, the filaments moved slowly inwards in continuous parallel waves (Fig. 37 R-Ras cotransfected cell; video S5). The speed of actin filament movement away from the membrane towards the cell center was between  $0,1 \mu\text{m}/\text{min}$  and  $0,18 \mu\text{m}/\text{min}$  according to the kymographs. The speed of the inward movement decreased near the cell center and the filaments appeared to arrive in a convergence zone adjacent to the cell body (Fig. 37). In this zone, the filaments condensed and either SWAP-70 dissociated from the filaments, the filaments themselves disassembled or both.

Results

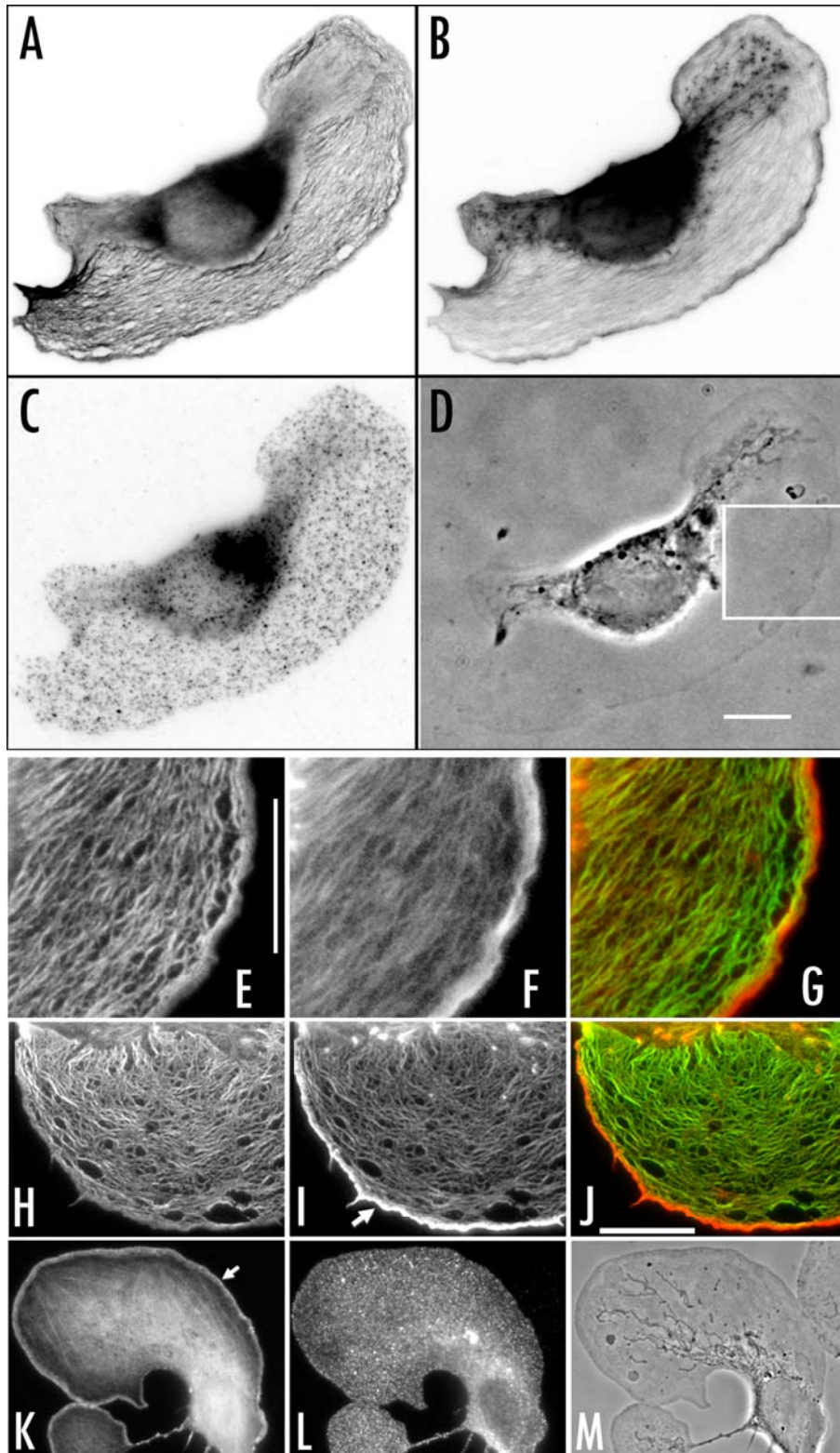


**Fig. 36. GFP-SWAP-70 localizes to F-actin arrays oriented parallel to the plasma membrane behind a zone of high lamellipodial actin polymerization in B16F1 cells cotransfected with dominant active R-Ras (38V) (A-G) or dominant active H-Ras (12V) (H-J).** Fluorescence microscopy images of a cotransfected B16F1 cell are shown. A: GFP-SWAP-70; B: Alexa350-phalloidin stained F-actin; C: Cy3

## Results

staining against the myc-tag of the myc-R-Ras (38V) fusion protein; **D**: Phase contrast image. Boxed area is shown in higher magnification in E-G; **E**: GFP-SWAP-70; **F**: F-actin; **G**: Merge (GFP-SWAP-70 in red, F-actin in green); **H**: GFP-SWAP-70; **I**: Alexa 594-phalloidin stained F-actin. The arrow points at the bright rim of actin staining at the tip of the lamellipodium; **J**: Merge (GFP-SWAP-70 in green, F-actin in red); **K-M**: B16F1 cell cotransfected with mRFP-actin and myc-H-Ras (12V). **K**: mRFP-fluorescence. Note the strong lamellipodia formation around the cell periphery (arrow) and the very few stress-fibers **L**: Alexa488 staining against the myc-tag of the myc-H-Ras (12V) fusion protein. **M**: Phase contrast image. B16F1 cells were cotransfected and after 24 h replated on laminin coated coverslips. Cells were fixed with 4% PFA after 4 hours and permeabilized with 0,05% Saponin. The expression of the myc-tagged Ras constructs was detected by staining with the primary mouse antibody 9e10 and subsequent staining with a Cy3 or Alexa488 coupled secondary antibody. F-actin was stained with Alexa 350 or Alexa 594 coupled phalloidin. Fluorescence images of **A-C** were inverted for better visualization.

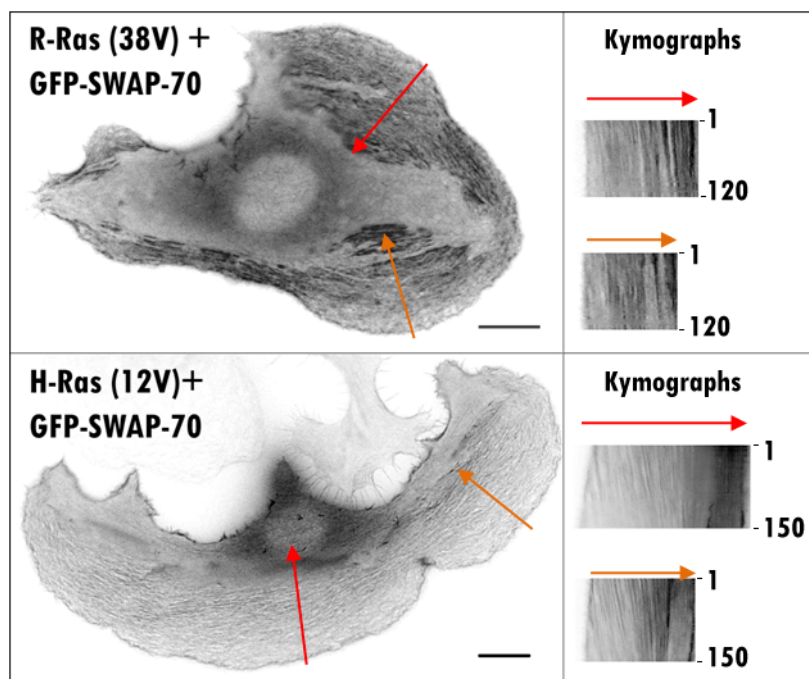


**Fig. 37. In dominant active Ras cotransfected B16F1 cells, the SWAP-70 labeled F-actin arrays move towards the cell interior.** Images to the left are single frames of live cell imaging depicting inverted GFP-SWAP-70 fluorescence in Ras cotransfected B16F1 cells. Colored arrows show the direction and the position of the lines which were used for generating kymographs. Kymographs to the right depict the fluorescence intensity along these single-pixel wide lines for each frame of the video. These lines were stacked the first frame on top and the last frame at the bottom of the kymograph (120 frames for R-Ras (38V) and 150 frames for H-Ras (12V), respectively). Frames were taken in intervals of 8 s. The position of fluorescent GFP-SWAP-70 dependent on the time reveals a movement of the filaments from the leading edge towards the cell center. Some of these GFP-SWAP-70 labeled filaments are stable for at least 16 min. Cells were cotransfected with GFP-SWAP-70 and myc-tagged R-Ras (38V) or myc-tagged H-Ras (12V) and replated on laminin 16 h after transfection. After additional 4 hours, cells were analysed using live cell imaging. Cotransfected cells were chosen by their characteristic morphology and GFP-SWAP-70 labeled filaments.

## Results

The Ras induced filaments could also be visualized by TIRF microscopy, implying a close proximity to the adherent plasma membrane (Fig 38).

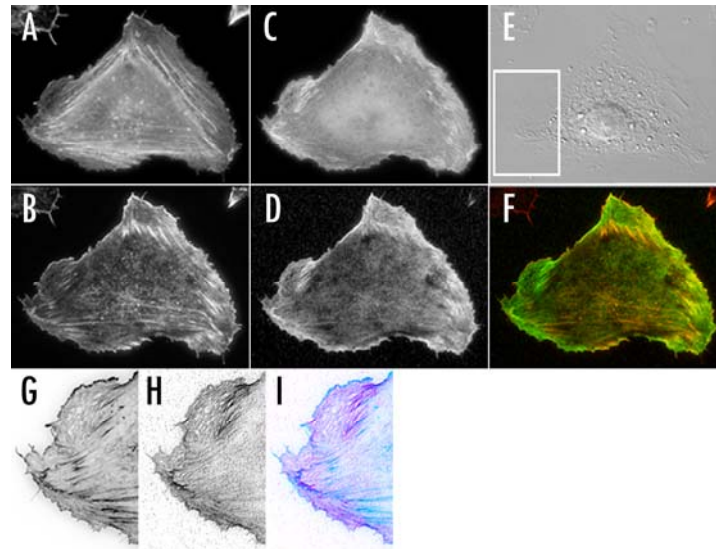


**Fig. 38. GFP-SWAP-70 labeled filaments in B16F1 cells cotransfected with dominant active R-Ras (38V) are visible in TIRF microscopy implying a ventral localization near the plasma membrane. A:** F-actin epifluorescence image. **B:** F-actin TIRF-image. **C:** GFP-SWAP-70 epifluorescence image. **D:** GFP-SWAP-70 TIRF-image. **E:** DIC-contrast image. **F:** overlay of the TIRF fluorescence images for F-actin and GFP-SWAP-70. **G,H,I:** higher magnifications of the boxed region depicted in E. **G:** F-actin, **H:** GFP-SWAP-70, **I:** merge. Images were inverted for better contrast.

The effects of dominant active Ras could not be substituted by Ras-GEFs such as SOS, RasGRF2, and RasGRP1 (data not shown). Interestingly, a constitutively membrane targeted and therefore dominant active form of the p110 subunit of the PI3 kinase could not substitute for dominant active Ras activity, implying that dominant active Ras influences SWAP-70 localization not only through induction of phosphoinositide production. Cotransfections of mCherry-SWAP-70 with the GFP-tagged Ras-effector Raf-kinase did not induce a similar phenotype as dominant active H- or R-Ras.

Many studies reported a downstream activation of Rac by activated Ras. Cotransfections of B16F1 cells with dominant active Rac (V12) and GFP-SWAP-70 led to well spread cells with large lamellipodia closely resembling the morphological phenotype induced by dominant active R-Ras. However, the localization of SWAP-70 was not affected. Instead, GFP-SWAP-70 localized to typical loose actin filament arrays in the lamella region behind large lamellipodia.

The closest homologue of Ras proteins is the small GTPase Rap1. Cotransfections of B16F1 cells with dominant active Rap1a and GFP-SWAP-70 did not induce alterations in the SWAP-70 localization comparable to the effects of dominant active Ras. Rap1 binds to some of the same effector proteins as Ras. In more recent studies Rap1 has attracted much

## Results

attention in the context of integrin dependent cell adhesion. Rap1 signaling regulates integrin avidity (integrin clustering) and activity (affinity).

Interestingly, the dominant active R-Ras induced association of SWAP-70 with actin filament arrays is cell type specific. NIH/3T3 cells cotransfected with dominant active R-Ras and GFP-SWAP-70 did not exhibit the prominent filamentous localization of GFP-SWAP-70. Cotransfected NIH/3T3 cells showed increased accumulation of macropinosomes labeled with dominant active R-Ras (38V) (Fig. 39).

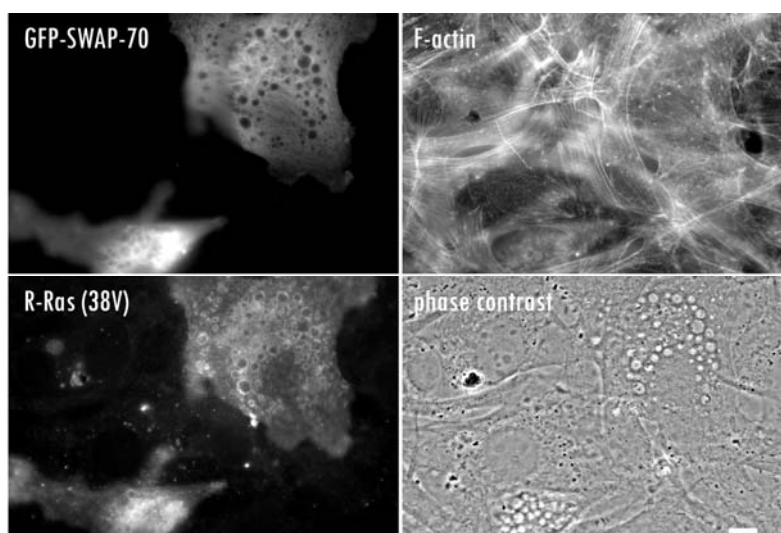


**Fig. 39. R-Ras (38V) induces the accumulation of macropinosomes in transfected NIH/3T3.** Cells were cotransfected with myc-tagged R-Ras (38V) and GFP-SWAP-70, replated on glass-coverslips and fixed after 24 h with 4% PFA. Cells were permeabilized with 0,05% saponin and stained for F- actin with Alexa350-phalloidin and for the myc-tag with the primary antibody 9E10 and a Cy3 coupled secondary antibody. Bar: 10  $\mu$ m

### 5.5.2 Ras dependent activation of PI3 kinase is crucial for the localization of SWAP-70

Ras interacts directly with the p110 catalytic subunit of phosphatidylinositol 3-kinases and thereby activates these enzymes, leading to a rise in 3-phosphoinositide levels at membranes. To investigate, whether the SWAP-70 association with the filaments induced by dominant active Ras can be suppressed by the PI3 kinase inhibitors LY29004 and Wortmannin, cotransfected B16F1 cells were either visualized by live-cell video microscopy (see video S6) or alternatively fixed at different times after addition of the inhibitors and analyzed by fluorescence microscopy.

Addition of 50  $\mu$ M LY29004 led to the dissociation of GFP-SWAP-70 from filamentous actin in the lamella beginning  $\sim$ 3 min after addition of the inhibitor resulting in almost complete absence of GFP-SWAP-70 from filaments  $\sim$ 30 min after addition (Video S6; Fig.

## Results

40). The dissociation from peripheral filaments was accompanied by a rise in the cytosolic GFP-SWAP-70 fluorescence intensity. The addition of PI3-K inhibitors and the subsequent dissociation of GFP-SWAP-70 did not cause any visible morphological changes. Neither did the large surrounding lamella of the observed cells collapse nor did the cell shape change noticeably.

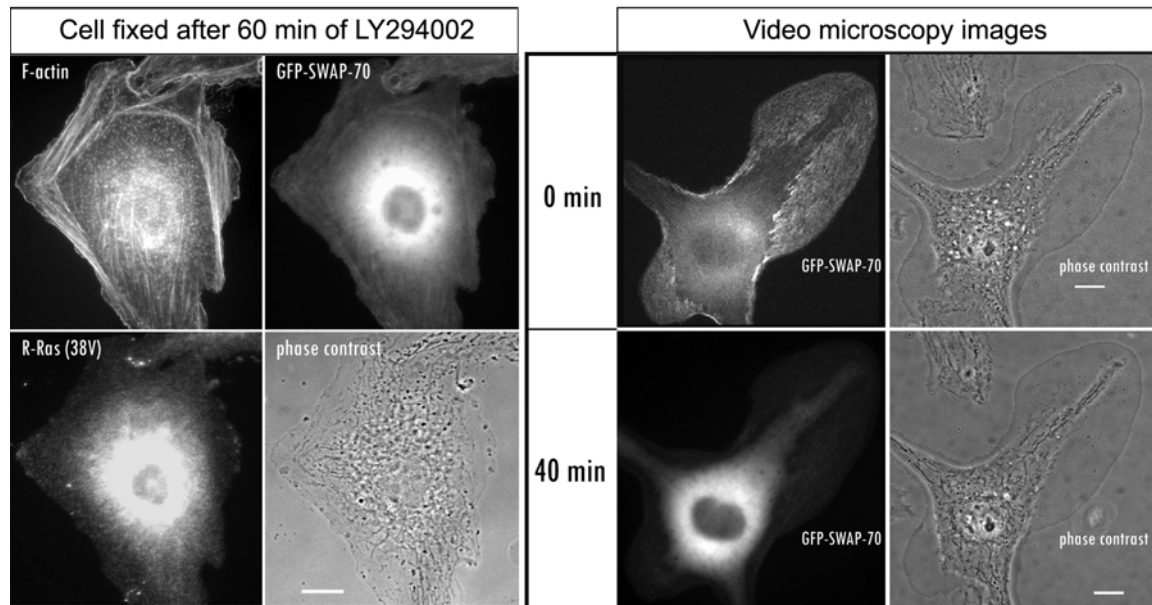


**Fig. 40 PI3-kinase inhibitor LY294002 causes a dissociation of SWAP-70 from filaments induced by dominant active R-Ras.** B16F1 cells were cotransfected with dominant active R-Ras (38V)-myc and GFP-SWAP-70 and replated on laminin coated coverslips. Cells were either fixed different times after addition of 50  $\mu$ M LY294002 or analyzed by live cell imaging 4 h after replating (video S6). **Left:** Fluorescence images of a cell fixed 60 min after addition of LY294002. **Right:** Fluorescence images taken from a living cell before- and 40 min after addition of 50  $\mu$ M LY294002. Living cells were judged to express R-Ras based on the characteristic morphology and the GFP-SWAP-70 distribution.

Interestingly, the degree of dissociation of GFP-SWAP-70 from actin filaments differed for H-Ras (12V) and R-Ras (38V) transfected cells. While R-Ras induced filament association of GFP-SWAP-70 was blocked nearly completely, cells cotransfected with H-Ras (12V) still showed some labeling of filaments with SWAP-70 even after 45 min of incubation. This difference was also observed for Wortmannin.

### 5.5.3 A functional PH-domain is necessary for Ras-induced F-actin binding of SWAP-70

To further verify that the association of SWAP-70 with Ras induced F-actin arrays is directly dependent on the activation of PI3-kinase in dominant active Ras expressing cells,

## Results

SWAP-70 constructs defective in phosphoinositide binding were cotransfected. GFP-SWAP-70 RR(223,224)EE contains mutations in the PH-domain known to abolish the binding to phosphoinositides *in vitro*. Another mutation, GFP-SWAP-70 (R230C), selectively inhibits binding to PI (3,4) P<sub>2</sub> *in vitro* (Hilpelä *et al.*, 2003). Upon cotransfection with dominant active R-Ras (38V), both SWAP-70 mutant PH-domain constructs showed a diffuse cytosolic localization (Fig. 41). However, dominant R-Ras (38V) cotransfected cells were still well spread and had large lamellipodia. Since the SWAP-70 (R230C) mutation selectively inhibits binding to PI (3,4) P<sub>2</sub>, this phosphoinositide is probably crucial for association of SWAP-70 with dominant active R-Ras (38V) induced actin filament arrays.

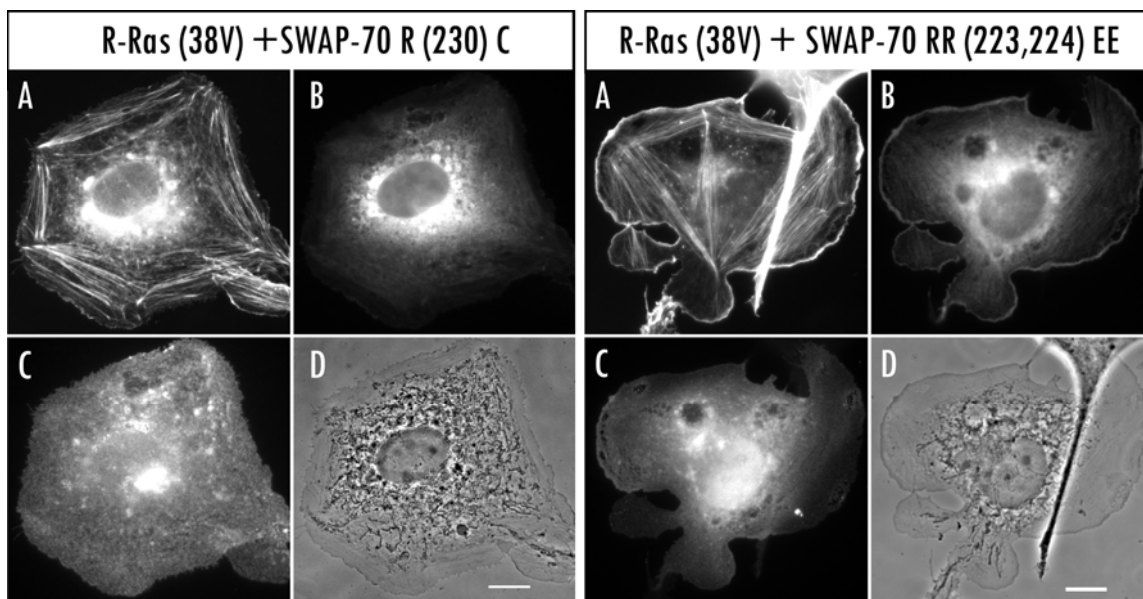


**Fig. 41. Mutations in the PH-domain of SWAP-70 abolish its localization to F-actin arrays oriented parallel to the plasma membrane.** B16F1 cells were cotransfected with GFP-tagged PH-domain mutants of SWAP-70 as indicated above each panel and myc R-Ras (38V). 24 h after transfection, cells were replated on laminin coated coverslips and fixed after additional 4 hours. Cells were fixed with 4% PFA and permeabilized with 0,05% Saponin. The expression of the myc tagged R-Ras (38V) construct was detected by staining with the primary mouse antibody 9E10 and subsequent staining with a Cy3 coupled secondary antibody. F-actin was stained with Alexa 350 coupled phalloidin. Letter-code in the images: **A:** F-actin; **B:** GFP-fluorescence; **C:** R-Ras (38V) **D:** phase contrast. Bar: 10  $\mu$ m



## 5.6 SWAP-70 interacts with RasGRP1

### 5.6.1 Bacterial-Two-Hybrid-screen

Earlier work on SWAP-70 did not find a direct binding of SWAP-70 to F-actin despite the clear colocalisation with F-actin *in vivo*. Furthermore, it could be shown that SWAP-70 associates with macropinosomes independently of phosphoinositide- or actin binding (Oberbanscheidt *et al.*, 2007). Since the N-terminal part also contributes to correct intracellular localization, other factors than phosphoinositides and F-actin are likely to interact with SWAP-70.

For these reasons a screen for interacting proteins was undertaken. The method used was the BacterioMatch II-two-hybrid-system (Stratagene) which detects protein-protein interactions based on transcriptional activation.

Two screens were carried out with different baits using a premade mouse spleen cDNA library (see Table 4.).

Control cotransformations using bait and target vectors encoding the dimerization domain of the Gal4 transcriptional activator protein and a domain of the Gal11 protein, respectively, consistently resulted in bacterial growth on selective medium. Cotransformations with empty vectors did not result in bacterial growth on selective medium at all. However, the bacterial-two-hybrid screens had a high background of nonphysiological interactions since most of the interacting sequences turned out to be out of frame or to be fragments of untranslated regions. Restriction analysis of PCR products obtained from plasmids of interacting proteins ruled out many redundant clones. The DNA sequences that were not in the correct reading frame, were also translated for a sequence homology BLAST against Protein-Databases. This approach did not reveal any conserved binding motifs.

Table 4. Summary of the bacterial two-hybrid-screens

bait	screened clones	colonies grown on selective medium	colonies on selective medium after retransformation	Validated clones in correct reading frame
SWAP-70 (1-585)	1,114*10 <sup>6</sup>	149	145	9
SWAP-70 (1-211)	8,6*10 <sup>5</sup>	346	304	5

The two screens yielded together 14 interacting sequences of which six coded for a complete protein sequence whereas the other interacting sequences coded for C-terminal

## Results

fragments of proteins (see Table 5). None of the interactors was identified in both screens. A physiological context for an interaction with SWAP-70 was not obvious for most of the interacting proteins. The interacting proteins did not share any obvious physiological role with each other nor with SWAP-70.

## Results

Table 5. Results of the Two-Hybrid-screens

Interactor	Bait	Interacting sequence (aa)	Full length protein (aa)
G-Protein Coupled Receptor 175	N-term	52	373
Nucleoporin 188	N-term	104	1759
Ras Guanyl releasing protein 1	N-term	135	795
Ubiquitin like protein 4	N-term	157	157
Hemoglobin alpha chain	N-term	142	142
Coronin 7	FL	192	922
Ig heavy Chain gamma 2a	FL	38	398
Erythroid association factor (Eraf)	FL	103	103
lysosomal thiol reductase	FL	193	193
Smooth muscle associated protein-1	FL	139	944
Peptidylprolyl-isomerase isoform 1	FL	164	164
HESB-domain-like protein	FL	129	129
Smith-Magenis syndrome candidate 7	FL	18	454
myeloid batenecin (F1)	FL	161	167

### 5.6.2 RasGRP1 interacts with SWAP-70 in the bacterial-two-hybrid system

One of the interacting sequences for the SWAP-70 (1-211) bait turned out to encode the C-terminal part (amino acids 661-795) of the RasGEF Ras Guanyl releasing protein 1 (RasGRP1). Its sequence was found in 11 different clones even though many identical clones had already been ruled out based on fragment patterns from digestions of the PCR-products with 4-base-pair cutters. In contrast, most of the clones with sequences in the wrong reading-frame were found once or twice.

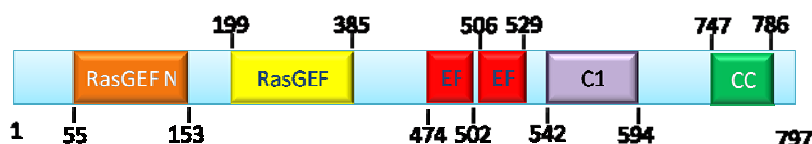












Fig. 42. Domain structure of the human RasGRP1 protein

RasGRP1 activates the exchange activity of the small GTPases TC21, M-Ras, and Ras proteins. However, it is inactive on Rap GTPases (Ohba *et al.*, 2000; Ebinu *et al.*, 1998, Ebinu *et al.*, 2000). RasGRP1 contains a Cdc25 homology domain typical for RasGEFs and an N-terminal RasGEF-N domain found in most Ras-GEFs (Fig. 42). Moreover, RasGRP1 encompasses two EF-hand regions known to bind calcium and a diacylglycerol-binding C1 domain. A weak homology to a basic region leucine zipper coiled-coil region is predicted in the C-terminal part. Since it interacted with the N-terminal part of SWAP-70,

## Results

an unspecific interaction of the coiled-coil domain of RasGRP1 with the coiled-coil domains of SWAP-70 could be ruled out.

Bacterial growth on selective medium can have different reasons. Apart from an interaction between bait- and target sequence, it can also be caused by spontaneous bacterial mutations leading to resistance towards the selective medium or it can be due to auto-activation by the target sequence alone. To rule out these possibilities, the plasmid DNAs of the two different vectors were isolated and separated according to the manufacturers instructions. Retransformation of reporter cells with the vector containing the interacting sequence and the original bait-construct were plated on either nonselective medium or selective medium. As control, the interacting sequence containing vector and the empty bait-vector were retransformed in parallel. These retransformation experiments showed that the C-terminal part of RasGRP1 (661-795) interacted with the N-terminal fragment of SWAP-70 and the full-length protein in the bacterial two-hybrid system (Fig. 43). The identified part of the RasGRP1 protein has been shown to relocate RasGRP1 to the plasma membrane in B-cells after B cell receptor (BCR) stimulation (Beaulieu *et al.*, 2007).

Target Medium	SWAP-70		SWAP-70 (1-211)		Vector control
	RasGRP1 661-795	Vector control	RasGRP1 661-795	Vector control	RasGRP1 661-795
Nonselective medium					
Selective medium					

**Fig. 43. RasGRP1 (661-795) interacts in retransformation experiments with the full-length SWAP-70 and the N-terminal part of SWAP-70 (SWAP-70 1-211).** Reporter cells of the BacterioMatch-II-Two-Hybrid system were cotransformed with pBT (Bait)- and isolated pTRG (Target) vectors with different combinations of insert or empty vector for control. Transformed bacteria were plated on selective and nonselective agar. Growth of bacteria on nonselective agar displays successful cotransformation. Growth on selective agar displays an interaction of the vector inserts.

## Results

### 5.6.3 Bacterially expressed GST-SWAP-70 binds to RasGRP1

To validate this interaction, pull-down experiments using bacterially expressed GST-SWAP-70 coupled to Glutathione-Sepharose-beads were carried out. The available RasGRP1 antibody M120 could not detect RasGRP1 in tissue homogenates and lysates, but RasGRP1 was readily detected in pulldowns from lysates of spleen and brain of sacrificed mice (Fig. 44). The negative control with GST coupled to Glutathione-Sepharose did not show any signal.

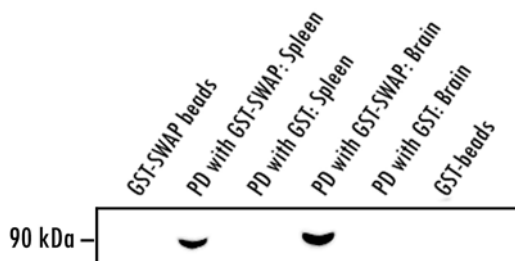


**Fig. 44 GST-SWAP-70 specifically pulls down endogenous RasGRP1 from homogenates of mouse spleen and brain.** Tissue from sacrificed mice was homogenized in lysis buffer containing 1% NP-40 using a potter. After centrifugation for 20 min at 15000 g, the supernatants were carefully transferred to a new tube and incubated for 1 h with bacterially expressed GST-SWAP-70 coupled to glutathione-sepharose beads or GST coupled to glutathione-sepharose beads as a control. After washing thrice, the beads were boiled in 1x Laemmli-buffer. After Gel-electrophoresis and Western blotting using a PVDF membrane, RasGRP1 was detected by using the M120 antibody from Santa Cruz.

### 5.6.4 SWAP-70 interacts specifically with the C-terminal part of RasGRP1

RasGRP1 is a member of a protein family with 4 different members (RasGRP1-RasGRP4) that further exist in differentially spliced isoforms. The C-terminal part of RasGRP1 that interacted with SWAP-70 is not conserved between the family members.

Bacterially expressed GST-SWAP-70 pulls down GFP-RasGRP1 from lysates of transfected HEK-293T cells. To verify that this interaction is not only due to unspecific binding, GFP-RasGRP2 was taken as a control for pull down experiments. The two family members RasGRP1 and RasGRP2 differ in their C-terminal parts.

After centrifugation of the homogenate, most of the GFP-RasGRP1 protein was found in the pellet and only a small amount was detected in the lysate. This was probably due to the association of RasGRP1 with membranes. However, GST-SWAP-70 specifically pulled down GFP-RasGRP1- but not GFP-RasGRP2 from lysates of transfected cells (Fig. 45). As with the pull-downs of endogenous RasGRP1, the protein was enriched in the GST-SWAP-70 pull-down compared with the lysates.

## Results

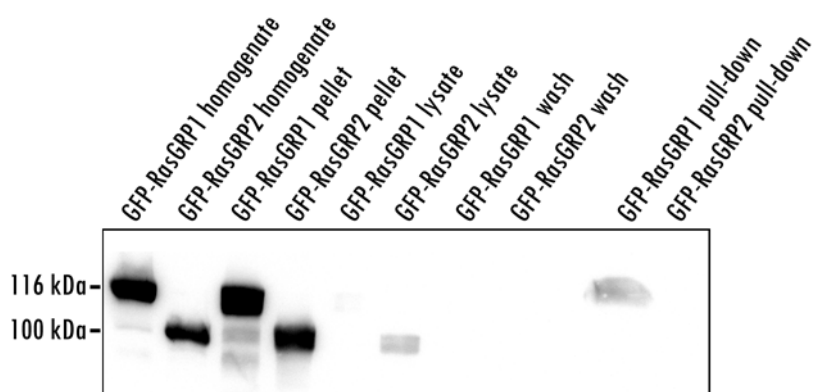


**Fig. 45. GST-SWAP-70 binds to GFP-RasGRP1 but not to GFP-RasGRP2 *in vitro*.** HEK-293T cells were transfected with either GFP-RasGRP1 or GFP-RasGRP2 and harvested 24 h after transfection. Cell lysates were prepared by squeezing the homogenate through a 26G-needle in lysis buffer containing 1% NP-40. After centrifugation for 20 min at 14000 rpm in a cooled microcentrifuge, the supernatants were carefully transferred to a new tube and incubated for 1 h with bacterially expressed GST-SWAP-70 coupled to glutathione-sepharose beads. After washing thrice, the beads were boiled in 1x Laemmli-buffer. The GFP-fusion constructs were visualized by immunoblot using an  $\alpha$ -GFP antibody.

## 5.7 Colocalization studies of RasGRP1 with SWAP-70

### 5.7.1 GFP-RasGRP1 partially colocalizes with endogenous SWAP-70

RasGRP1 has been shown to localize to different cellular compartments depending on the cell type and on the activation state. The protein contains different domains that contribute to its subcellular localization: A C1 domain (amino acids 542 to 594) binds to DAG and thereby targets RasGRP1 to membranes. An association with endomembranes of the Golgi-apparatus as well as with the endoplasmatic reticulum has been reported. Very recently, Bealieu *et al.*, (2007) reported that two additional C-terminal regions of RasGRP1 are necessary for the regulated targeting to the plasma membrane upon B-cell receptor stimulation. To investigate, whether RasGRP1 colocalizes with SWAP-70 *in vivo*, B16F1 cells were transfected with GFP-RasGRP1 and plated on laminin. Consistent with the literature, GFP-RasGRP1 often localized to endomembranes. Nevertheless, in living B16F1 cells GFP-RasGRP1 also localized to the lamella region behind ruffling lamellipodia (Fig. 46A) in numerous spots with a diameter of  $<1 \mu\text{m}$ . These spots accumulated behind- and followed the extension of the ruffling lamellipodium (videos S10, S11). Staining of endogenous SWAP-70 in GFP-RasGRP1 transfected B16F1 cells showed a partial colocalisation of both proteins in the lamella region (Fig. 46B).

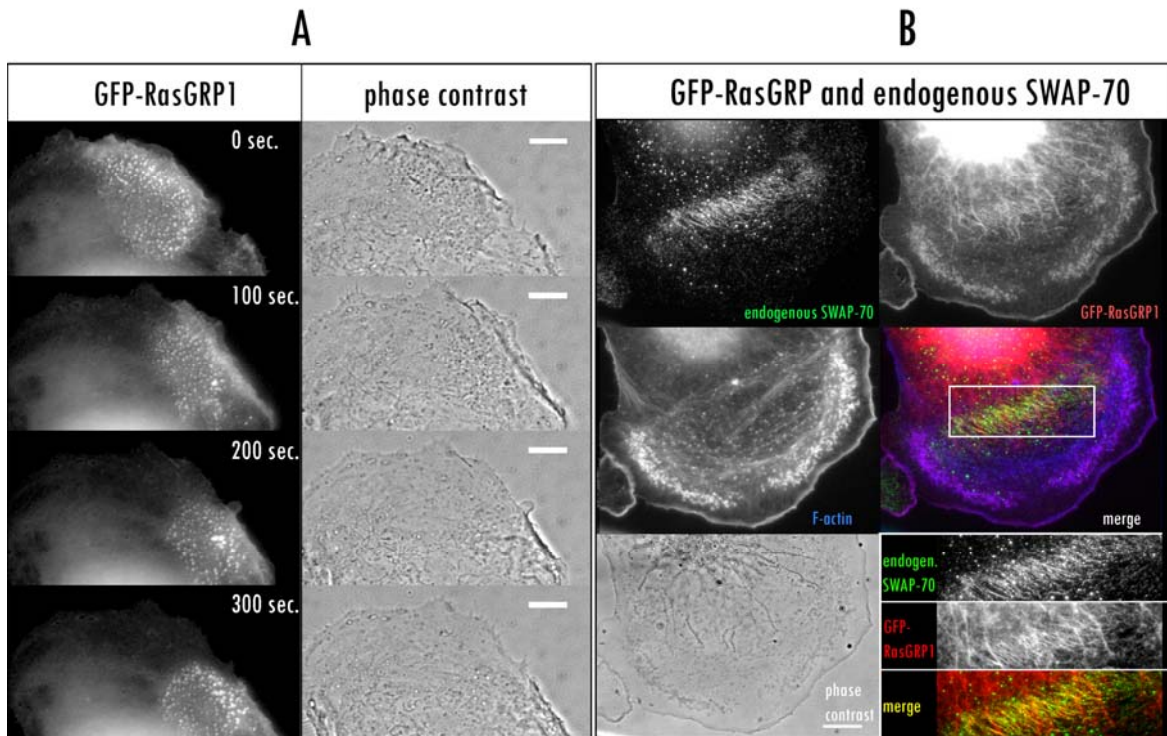


**Fig. 46. GFP-RasGRP1 localizes to the lamella region and partially colocalizes with endogenous SWAP-70** **A:** Fluorescent images taken from a live cell. GFP-RasGRP1 localizes to small spots located in the lamella behind a ruffling lamellipodium and follows the direction of ruffling. B16F1 cells were replated on glass coverslips 24 h after transfection and analyzed by live cell imaging on the next day. **B:** GFP-RasGRP1 colocalizes partially with endogenous SWAP-70. B16F1 cells were replated on laminin coated coverslips 24 h after transfection with RasGRP1. Cells were fixed with 4% PFA 5 hours after replating and stained with the SWAP-70 specific antibody GK2 and a Cy3 coupled secondary antibody. F-actin was stained with Alexa350-phalloidin. Images in the lower right corner are higher magnifications of the boxed region in the merged image.

### 5.7.2 Fluorophore tagged SWAP-70 and RasGRP1 colocalize in cotransfected B16F1 and NIH/3T3-cells.

To determine the influence of RasGRP1 on the subcellular distribution of SWAP-70 and vice versa, NIH/3T3 and B16F1 cells were cotransfected with mCherry-SWAP-70 and GFP-RasGRP1 and plated on different extracellular matrices. A strong colocalisation was observed for the fusion proteins in both cell lines (Fig. 47).

Cotransfections of B16F1 cells with both proteins resulted in morphological changes depending on the extracellular matrix. In B16F1 cells plated on fibronectin, the proteins colocalised at filaments throughout the cell (Fig. 47A). Cotransfected cells were often more spread than nontransfected cells. Fluorophore tagged SWAP-70 had a higher cytosolic background than fluorophore tagged RasGRP1. Whenever lamellipodia were visible, SWAP-70 and RasGRP1 labeled the same filaments in the lamella but SWAP-70

## Results

localized in addition to filaments closer to the lamellipodium that were not labeled with RasGRP1. RasGRP1 occasionally labeled tubular structures that probably represented endomembranes, but the signal intensity was much lower in comparison to the filaments. Cotransfected B16F1 cells that were plated on laminin often showed a colocalisation of fluorophore tagged SWAP-70 and RasGRP1 at filamentous structures in cell protrusions that mostly ended in a small ruffle or lamellipodium (Fig. 47A). Cotransfected cells were immotile and the broad protrusions as well as the filaments with which both proteins associated appeared quite stable. In the lamellipodial ends of the protrusions, both proteins often localized to unstable membranous structures (see Video S20). Interestingly, RasGRP1 could be detected on numerous small vesicles which moved into the protrusion on filaments labeled with RasGRP1 and SWAP-70. In NIH/3T3 cells, a multitude of small vesicles labeled with RasGRP1 emerged at the periphery of cotransfected cells and moved towards the cell center. When plated on glass, SWAP-70 colocalized with RasGRP1 in the majority of cases in well spread cells. In motile cells, RasGRP1 partially colocalized with SWAP-70 at filament-arrays in the lamella that resembled the loose F-actin arrays with which SWAP-70 typically colocalizes (see video S13 and S14). Confocal imaging as well as TIRF microscopy revealed that both proteins were associated with filaments at the ventral plane of cells (Fig. 47E and data not shown).



## Results

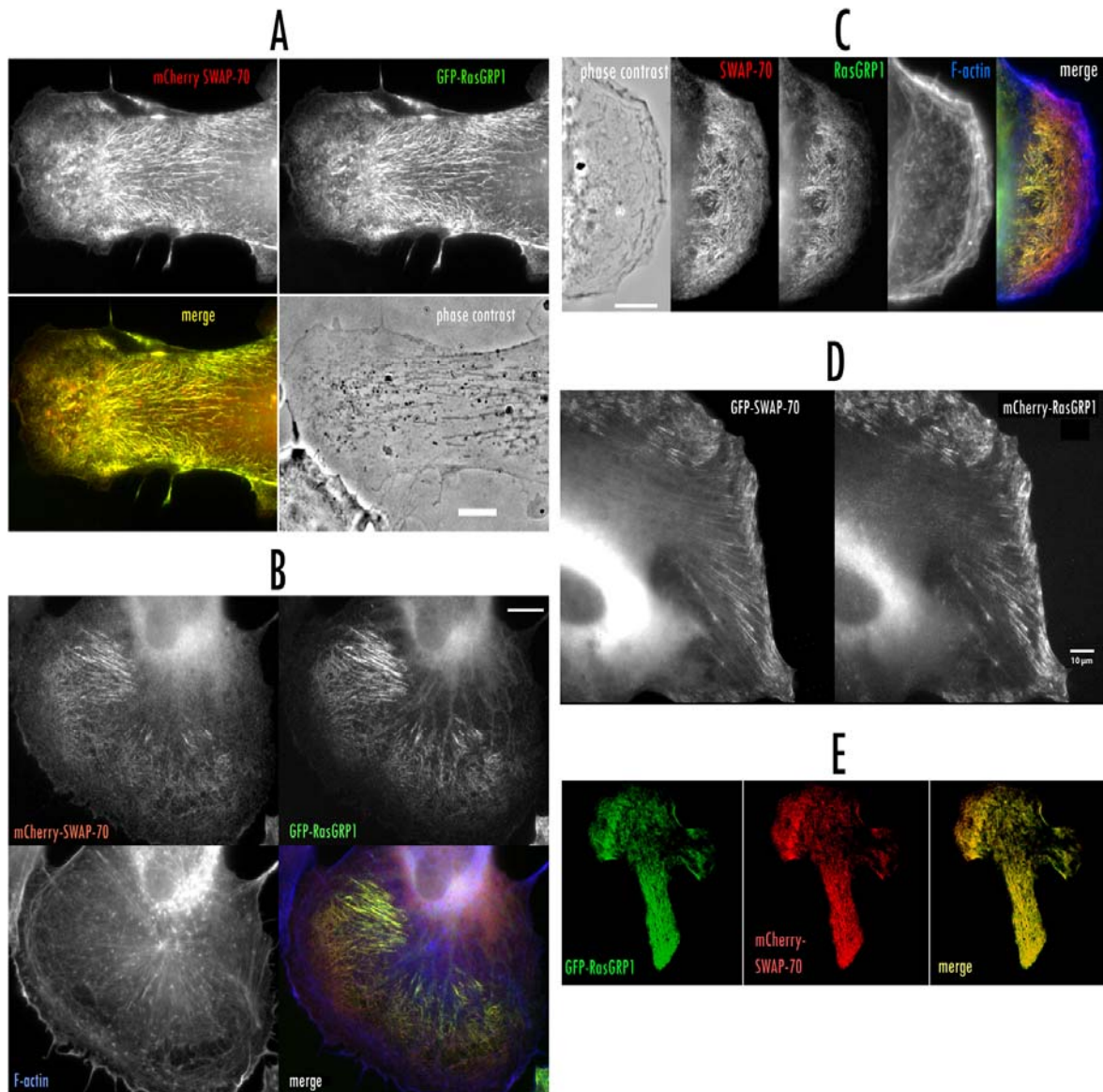


**Fig. 47. In cotransfected cells, SWAP-70 and RasGRP1 colocalize at filaments.** B16/F1 or NIH/3T3 cells were transfected with the indicated plasmids and 24 hrs later replated on coverslips. B16F1 cells were fixed and processed after additional 4 hours. NIH/3T3 cells were either fixed and processed for fluorescence microscopy or viewed directly by live cell imaging on the next day. **A:** mCherry-SWAP-70 and GFP-RasGRP1 colocalize in a filamentous pattern in broad protrusions of a B16F1 cell plated on laminin. **B:** mCherry-SWAP-70 and GFP-RasGRP1 colocalize in the lamella of a strongly spread B16F1 cell plated on fibronectin. Note that GFP-RasGRP1 also stains tubular structures closer to the cell center. **C:** mCherry SWAP-70 and GFP-RasGRP1 partially colocalize in the lamella behind a ruffling lamellipodium of a B16F1 cell plated on glass. Note that SWAP-70 is associated to filaments closer to the F-actin rich ruffling zone than RasGRP1. **D:** Fluorescent images taken from a live cell video of a GFP-SWAP-70 and mCherry-RasGRP1 cotransfected NIH/3T3 cell plated on glass. Both proteins colocalize at structures probably resembling focal adhesions. This localization is rarely seen for GFP-SWAP-70 alone in NIH/3T3 cells plated on glass. **E:** Fluorescence images of a single ventral confocal plane of a confocal stack from a transfected B16F1 cell plated on laminin confirming the ventral colocalisation of SWAP-70 with RasGRP1 at filaments.

### ***SWAP-70 and RasGRP1 colocalize at ruffles and macropinosomes of NIH/3T3 cells***

SWAP-70 has been reported to associate with closed macropinosomes (Oberbanscheidt *et al.*, 2007) and its N-terminal part including the PH-domain is sufficient for localization to these vesicles. This association is independent of phosphoinositide generation at the vesicle membrane and consistently does not need a functional PH-domain. Macropinocytosis can be induced by PDGF and phorbol esters in NIH/3T3 cells. Phorbol esters are analogues of the second messenger diacylglycerol and bind directly to the C1 domain of RasGRP1. Phorbol ester treatment of GFP-RasGRP1 transfected NIH/3T3 cells resulted in the relocalization of GFP-RasGRP1 to the plasma membrane as well as to endomembranes about 20 min after treatment (video S21). Nevertheless, RasGRP1 also localized to ruffling areas and vesicles in some cells treated with the phorbol ester (see supplemental video S22).

When fluorophore-tagged SWAP-70 and RasGRP1 were both cotransfected, they colocalized in NIH/3T3 cells with F-actin-fibers, focal adhesions and membrane ruffles. On few occasions, both proteins were enriched on macropinosomes, but frequent macropinosome formation could not be observed in cells cultured in Hams F12 medium. To investigate, whether SWAP-70 and RasGRP1 bind simultaneously to macropinosomes, cotransfected cells were treated with 10 nM PMA to induce macropinocytosis. On the few occasions in which cotransfected cells exhibited macropinocytosis, both proteins colocalized at ruffles (Fig. 48 A) and at macropinosomes (Fig. 48 B, video S15). However, the fluorescence intensity of RasGRP1 peaked after that of SWAP-70 (Fig. 48 B).

## Results

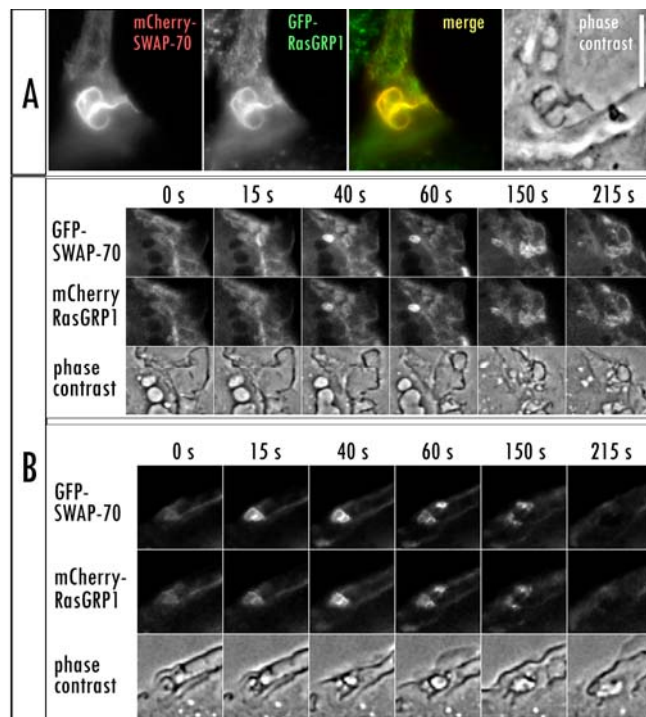


**Fig. 48. Fluorophore-tagged SWAP-70 colocalizes with fluorophore-tagged RasGRP1 at ruffles and macropinosomes in NIH/3T3 cells** **A:** Fluorescence microscopy image of a fixed NIH/3T3 cell plated on glass. Both fusion proteins colocalize in a ruffling region at the periphery of the cell. Cells were cotransfected with mCherry-SWAP-70 and GFP-RasGRP1 and plated on glass coverslips 16 h after transfection and fixed after additional 24 hours **B:** Live-cell microscopy images at different time-points of PMA-induced macropinocytosis. Both fusion proteins colocalize at macropinosomes. Note that the peak of mCherry-RasGRP1 fluorescence intensity is delayed compared to GFP-SWAP-70 fluorescence. Cells were cotransfected with GFP-SWAP-70 and mCherry-RasGRP1 and replated on glass coverslips 16 h after transfection. Cells were analysed by live-video microscopy after additional 24 hours. Macropinocytosis was induced with 10 nM PMA. The times given refer to the beginning of the video analysis ~5 min after PMA addition.

### 5.7.3 SWAP-70 colocalizes with RasGRP1 but not with RasGRP2

RasGRP1 as well as RasGRP2 have been reported to bind directly to F-actin via an N-terminal region (Caloca *et al.*, 2003; Caloca *et al.*, 2004). Therefore, colocalization of SWAP-70 and RasGRP1 could be independent of each other by binding of both proteins to F-actin. Both GEFs have otherwise different properties concerning their regulation, localization and their target GTPases (Clyde-Smith *et al.*, 2000; Ohba *et al.*, 2000). Because the two proteins share the F-actin binding property but are likely to have different physiological functions, a colocalisation of SWAP-70 with RasGRP2 would argue against a specific interaction of RasGRP1 with SWAP-70. For this reason, B16F1 cells were cotransfected with mCherry-SWAP-70 and GFP-RasGRP2 and analyzed by fluorescence microscopy. No colocalisation could be detected. GFP-RasGRP2 was predominantly cytosolic and sometimes localized to the lamellipodium and the F-actin rich areas of actin

## Results

clouds in migrating B16F1 cells. mCherry-SWAP-70 intensely labeled the loose actin filament arrays as in untransfected cells (Fig. 49).

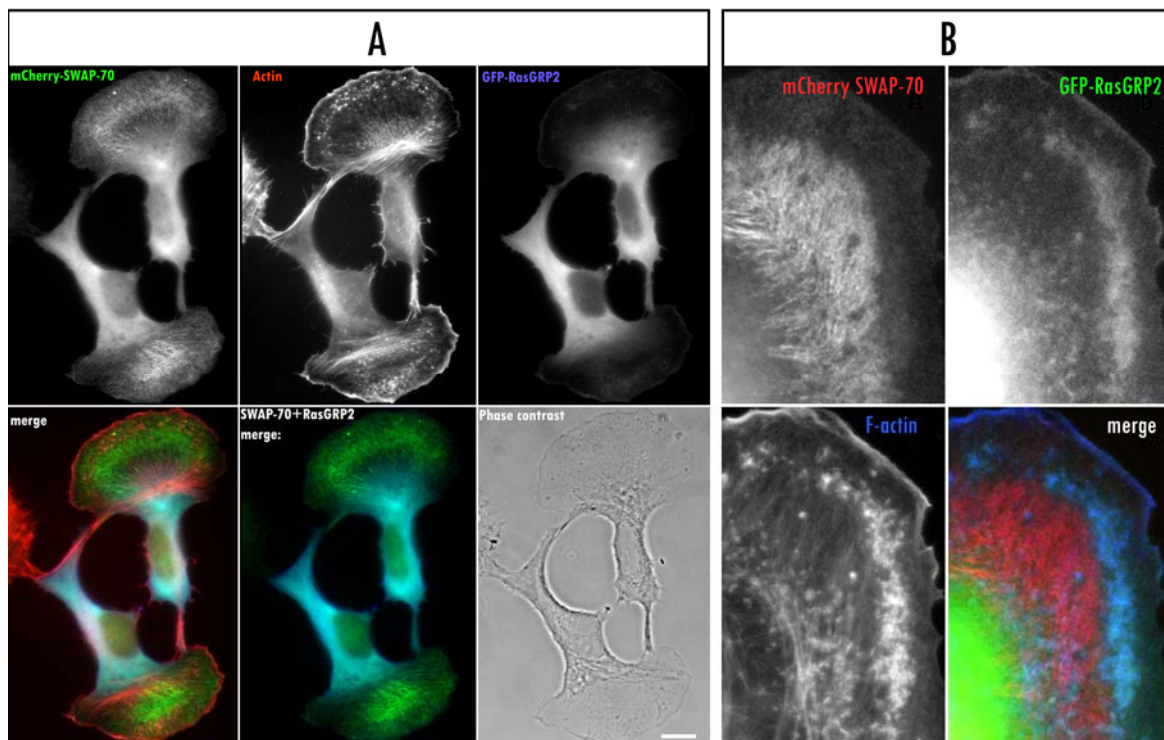


**Fig. 49. mCherry-SWAP-70 does not colocalize with GFP-RasGRP2.** B16F1 cells were cotransfected and replated on laminin coated coverslips 16 h after transfection. Cells were fixed 5 hours after replating and stained for F-actin with Alexa-350 Phalloidin. **A:** Lower left (merge) image includes all three fluorescences, lower middle image is a merge without F-actin Bar: 10  $\mu\text{m}$ . **B:** Higher magnification of a lamella region of a cotransfected B16F1 cell.

Taken together, SWAP-70 did interact with RasGRP1 but not RasGRP2 *in vitro* and partially colocalized with RasGRP1 but not RasGRP2 *in vivo*.

### 5.7.4 Colocalization of fluorophore tagged RasGRP1 and SWAP-70 depends on the actin binding properties of SWAP-70

Binding of SWAP-70 to F-actin is mediated by its 60 C-terminal amino acids. A GFP-tagged truncation construct of SWAP-70 lacking the C-terminal 60 amino acids has been reported to localize mainly to the cytosol (Hilpelä *et al.*, 2003). In migrating B16F1 cells, this truncation construct is sometimes enriched in the lamella region but in a rather diffuse or spotty appearance instead of the clearly filamentous appearance of the full length SWAP-70. Since RasGRP1 was hardly observed at actin filaments without coexpression of SWAP-70 even though it can bind to F-actin via its N-terminal region, it was investigated whether the F-actin binding domain of SWAP-70 is necessary for their colocalisation. The

## Results

clearly filamentous localization of mCherry-RasGRP1 was abolished when it was coexpressed with the GFP-tagged truncation construct of SWAP-70. Instead, mCherry-RasGRP1 localized diffusely in small spots, probably vesicles, throughout the cell (Fig. 50). Accumulation of GFP-SWAP-70 (1-525) in the lamella region of motile cells did not coincide with an accumulation of mCherry-RasGRP1 in this area (Fig. 50B). Therefore, the F-actin binding properties of SWAP-70 are necessary for colocalization with RasGRP1 and F-actin might be an important mediator of the interaction at least at the plasma membrane.

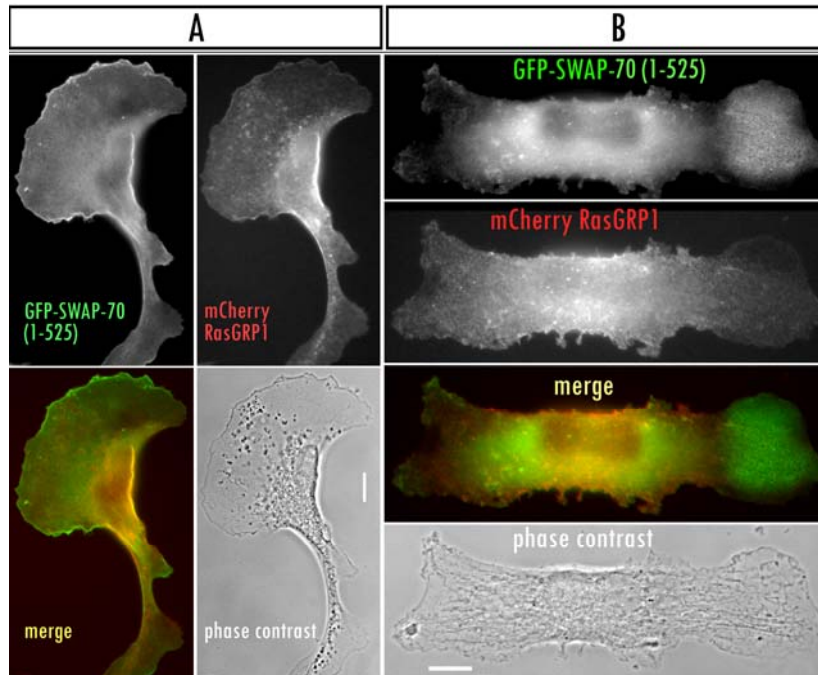


**Fig. 50. Filamentous localization of mCherry RasGRP1 is abolished when it is cotransfected with a truncation mutant of SWAP-70 missing the C-terminal F-actin binding domain. A:** B16F1 cell plated on laminin exhibiting a lamellipodium. Strong GFP-SWAP-70 signal at the leading edge but not in the typical region of the lamella is observed. mCherry-RasGRP1 localizes to small vesicles throughout the cell. **B:** B16F1 cell with a small lamellipodium to the right of the cell. GFP-SWAP-70 (1-525) concentrates in the region of the lamella but does not show a filamentous staining. mCherry-RasGRP1 does not concentrate in the same region. B16F1 cells were replated on laminin coated coverslips 24 hours after cotransfection. Cells were fixed after 5 hours and analysed by fluorescence microscopy. Bars: 10  $\mu$ m

## **6 Discussion**

### **6.1 SWAP-70 binds directly to nonmuscle actin**

Previous results from Hilpelä *et al.* (2003) had shown that a GFP-fusion protein of the C-terminal 60 amino acids of SWAP-70 colocalizes with F-actin in transfected cells. However, SWAP-70 did not bind to muscle actin (Oberbanscheidt, 2005). Ihara *et al.* (2006) reported a direct binding of a His-tagged SWAP-70 (448-585) construct to non-muscle actin in an isoform specific manner. They reported that SWAP-70 (448-585) binds to F-actin in a stoichiometric 1:1 ratio with a dissociation constant (Kd) of 0,74  $\mu$ M. His-tags contain positively charged residues and hence might interact with the negatively charged actin (Stock *et al.*, 1999). For this reason we used GST-tagged proteins to circumvent potential nonspecific binding. A bacterially expressed GST-tagged SWAP-70 (525-585) construct cosedimented with non-muscle F-actin, but not with muscle F-actin in our experiments. This result confirms the reported actin-isoform-specificity. In our F-actin binding experiments we observed that a degradation fragment of GST-tagged SWAP-70 (525-585) failed to bind to non-muscle F-actin. This is consistent with results obtained by Ihara *et al.*, (2006) that the loss of the last 20 amino acids (amino acids 448-564) abolished actin binding. They postulated that the very C-terminal SWAP-70 sequence consisting of basic amino acids is related to the actin binding sequence of gelsolin. This stretch of basic amino acids is conserved in SWAP-70 from different organisms. However, a GFP-fusion protein of the very C-terminal peptide (20 AS) containing this postulated F-actin binding sequence did not colocalize with F-actin (Hülsmann, 2004). Therefore, it appears that the postulated F-actin binding sequence is not sufficient for F-actin binding. Furthermore, sequence alignments with DEF6 revealed that this motif is not conserved. Nevertheless, DEF6 colocalized in a very similar way with F-actin (Fig. 51; sequence alignments not shown). It appears that SWAP-70 and DEF6 contain a novel F-actin binding motif.

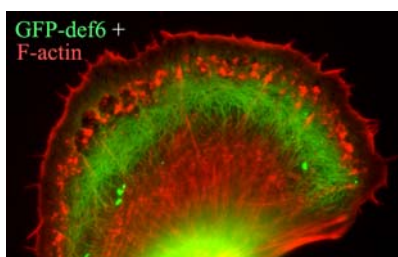


**Fig. 51. GFP-DEF6 localizes in the lamella of a motile B16F1 cells similar to SWAP-70.**

The actin-isoform specific binding of SWAP-70 is very interesting.  $\alpha$ -,  $\beta$ -, and  $\gamma$ -actin are highly conserved proteins and most actin binding proteins do not distinguish between the isoforms. Isoform specific binding to  $\beta$ -actin has been reported for another actin-membrane linking protein, the ERM protein Ezrin (Hirao *et al.*, 1996; Shuster and Herman, 1995; Yao *et al.*, 1996). Different actin isoforms differ in intracellular localization and contribute to different F-actin structures *in vivo*. The mRNA of  $\beta$ -actin is actively delivered to- and translated at sites of strong actin dynamics for

## Discussion

example the leading edge where  $\beta$ -actin is predominantly found (Drenckhahn *et al.*, 1991; Hofer *et al.*, 1997).  $\beta$ -actin is also found in circular F-actin structures in B16F1 cells called actin clouds (Ballestrem *et al.*, 1998). Furthermore,  $\beta$ -actin has been shown to have functions in the nucleus of cells. It associates with the RNA-Polymerase II and markedly stimulates transcription (Hofmann *et al.*, 2004; Philimonenko *et al.*, 2004). This, and actin containing nuclear complexes (Bettinger *et al.*, 2004) might provide a link to SWAP-70 accumulation in the nucleus of activated B-cells (Masat *et al.*, 2000).

A posttranslational isoform specific modification of  $\beta$ -actin contributes to differences with other actin isoforms. Approximately 40% of  $\beta$ -actin is posttranslationally modified by addition of arginyl from a tRNA onto the Asp3 of the  $\beta$ -actin sequence (Karakozova *et al.*, 2006). This arginylation is important for lamella formation and for cell migration. While non-arginylated actin filaments are mildly negatively charged due to the presence of Asp/Glu side chains and N-terminal acetyl groups, the addition of an Arg residue at the N-terminal part of  $\beta$ -actin introduces a bulky, positively charged group onto the filament surface. This modification would probably prevent filaments from bundling and formation of aggregates. Since  $\beta$ -actin is predominantly found at the leading edge (Condeelis and Singer, 2005; Karakozova *et al.*, 2006) where SWAP-70 does not localize to, it could be speculated that arginylation is a sorting mechanism marking filaments which survive the lamellipodium severing zone and become incorporated into filaments labeled by SWAP-70.

Actin polymerization assays with pyrene labeled muscle actin mixed with non-muscle actin (1:10 respectively) did not reveal effects of GST-SWAP-70 (525-585) fusion protein on actin polymerization. Thus, the C-terminal part of SWAP-70 probably binds to existing actin filaments but has no capping-, nucleating- or severing activity. It would be interesting to determine whether the full length SWAP-70 has a direct influence on F-actin dynamics because artificially membrane targeted SWAP-70 leads to a loss of stress fibers and live cell video microscopy has provided hints for an association of SWAP-70 with disassembling stress fibers (Hilpelä, personal communication; Oberbanscheidt *et al.*, submitted). On the other hand, the association of SWAP-70 with long-lived filaments as seen in dominant active Ras-cotransfected cells or the specific actin arrays in the lamella of motile cells argue against an inherent filament-severing activity. The association of SWAP-70 with dissolving stress fibers could as well be a secondary effect due to the dissociation of other actin binding proteins or the disintegration into loose actin arrays. Nonetheless, the occasional stable association of SWAP-70 with stress fibers is informative, because it suggests that SWAP-70 and myosin II association are not mutually exclusive like e.g. fimbrin and myosin II. The specific actin filament arrays labeled by SWAP-70 behind protruding lamellipodia do not contain myosin II, but SWAP-70 is probably not the reason for this absence.

## 6.2 Activation of SWAP-70

Based on previous work it is hypothesized that SWAP-70 resides in an inactive cytosolic conformation and that it can be activated by various signaling pathways that induce a rise in phosphoinositide levels (Hilpelä *et al.*, 2003; Shinohara *et al.*, 2002). Membrane association of SWAP-70 through interaction of the PH-domain with phosphoinositides results in accessibility of its C-terminal region for binding to preformed F-actin. Support for this hypothesis was provided by the observation that exposure of cells to oxidative stress caused a quantitative PI3-kinase dependent translocation of SWAP-70 to loose actin arrays and the plasma membrane (Hilpelä *et al.*, 2003). Furthermore, GFP-SWAP-70 constructs harboring mutations in its PH-domain that abolish the binding to phosphoinositides show a strongly reduced association with F-actin. Palmitoylation of a SWAP-70 mutant unable of binding to phosphoinositides revealed colocalisation of this artificial protein with F-actin. Thus, the binding of the PH-domain to phosphoinositides is not necessary for F-actin association and can be replaced by artificial targeting of SWAP-70 to the plasma membrane. Therefore, it appears that the main function of the PH domain is the targeting and tethering of SWAP-70 to the correct microenvironment on the plasma membrane. However, since the palmitoylated SWAP-70 construct is already tethered to the plasma membrane, the high local concentration of phosphoinositides could be sufficient to bind to the mutant PH-domain in spite of its low affinity for phosphoinositides.

The hypothesized inactive conformation might be due to intramolecular interactions. Evidence for such a regulation is provided by the F-actin binding experiments: the C-terminal 60 amino acids of SWAP-70 bind to nonmuscle F-actin while a SWAP-70 (305-585) construct failed to bind (data not shown). Ihara *et al.*, (2006) reported that a myc-tagged SWAP-70 (448-585) construct binds to non-muscle F-actin with a much higher affinity than the full-length protein. Therefore, the region of SWAP-70 starting from amino acid 305 to 448 might be necessary for the postulated intramolecular interactions. On the other hand, preliminary pull-down experiments suggested a possible interaction of the N-terminal part (1-210) of SWAP-70 with the C-terminal part (305-585) (Lasic, 2003). An attempt to detect intramolecular interactions by means of the BacterioMatch-II-Two-Hybrid system with different combinations of domains of SWAP-70 was not successful (data not shown).

## 6.3 Targeting of SWAP-70 to the membrane by palmitoylation

The basic idea behind the use of palmitoylated constructs of SWAP-70 is the targeting to the plasma membrane independently of phosphoinositide levels. Palmitoylation is a reversible modification carried out by multiple palmitoyl transferases (PATs) at the Golgi apparatus and the plasma membrane. The membrane affinity of a palmitoylated protein is



## Discussion

~15 times higher than for a myristoylated protein (Peitzsch and McLaughlin, 1993). Artificial membrane targeting has been used in other studies to elucidate the influence of membrane localization on signaling activity. The addition of a CAAX-box to the RasGEF SOS has been shown to activate downstream signaling (Quilliam *et al.*, 1994). Artificial membrane targeting of the integrin linked kinase (ILK) through addition of a farnesylation site from H-Ras resulted in enhanced Rac activation and to an 1,8x larger spreading area (Boulter *et al.*, 2006). Artificially membrane targeted PI3 kinase augmented the direct association with alphaPIX resulting in increased activity of this Rac-GEF (Yoshii *et al.*, 1999).

The palmitoylation signal sequence used for modification of SWAP-70 is derived from the *growth associated protein 43* (GAP43). The sites of palmitoylation of GAP-43 were suggested to be the endoplasmic reticulum intermediate compartment (ERGIC) and the Golgi apparatus (McLaughlin and Denny, 1999). Palmitoylation at the third and at the fourth cysteine confers association with the plasma membrane of growth cones (Skene and Virag, 1989). Dually palmitoylated GAP43 peptide (amino acids 1-20) fused to YFP is equally distributed between the plasma membrane and the Golgi apparatus in Madin-Darby canine kidney cells (Rocks *et al.*, 2005).

Confocal microscopy of PM-GFP-SWAP-70 transfected cells revealed that the fusion protein was localized predominantly at the plasma membrane. Routinely, cells were fixed 4-5 hours after replating on fibronectin or laminin. Only little PM-SWAP-70 was detected in the cytosol. The preferential localization of PM-SWAP-70 at the plasma membrane is probably dependent on cell adhesion because the fusion construct was often detected in the perinuclear region of newly plated and spreading B16F1 cells. This might reflect a difference in palmitoylation in non-adherent cells. B16F1 cells transfected with PM-SWAP-70 showed normal spreading and lamellipodia while in cells adherent for some time the actin cytoskeleton and cellular morphology were altered. This suggests that plasma membrane localization is crucial for the effects of PM-SWAP-70.

PM-SWAP-70 localizes predominantly on the plasma membrane, whereas palmitoylated GFP alone did localize to the plasma membrane but was also found in the cytosol and at the Golgi apparatus of transfected HEK-293T cells even at later time points (Fig. 20; Rocks *et al.*, 2005). This could be explained by the fact that palmitoylation is carried out by membrane-bound PATs. Therefore, it is seen as a secondary membrane association signal and other factors are crucial to target the protein to the membrane in the first place (Greaves and Chamberlain, 2006). Hence, it is possible that the plasma membrane localization of PM-SWAP-70 compared with PM-GFP is due to localization signals in the SWAP-70 sequence. Subsequent palmitoylation of both cysteines in the GAP-43 peptide may then contribute to prolonged association with the membrane. Moreover, PM-SWAP-70 colocalizes with cortical F-actin probably due to direct binding. This binding is likely to further stabilize the plasma membrane association of PM-SWAP-70. If

already tethered to the membrane, the chances of interaction between the PH-domain of SWAP-70 and even low levels of phosphoinositides should be high and could contribute to plasma membrane association. The importance of the PH-domain for plasma membrane targeting and association could also explain why palmitoylated truncation constructs lacking the PH-domain [PM-SWAP-70 (305-585) and PM-SWAP-70 (1-210)] were localized not only on the plasma membrane but also on the Golgi apparatus. In agreement with this hypothesis, the palmitoylated SWAP-70-PH-domain mutant was frequently localized to the Golgi-apparatus, too. The importance of the PH-domain for plasma membrane localization does not rule out the existence of another more specific localization-signal for the association with the loose actin filament arrays in motile cells. The N-terminal region encompassing amino acids 1-205 of SWAP-70 is crucial for the preferential association of SWAP-70 to the loose actin filament arrays. A truncation construct of SWAP-70 lacking this region associates with actin filament bundles in general (Hilpelä *et al.*, 2003).

### **6.4 Effects of overexpression of palmitoylated SWAP-70 on cellular morphology and the actin cytoskeleton**

Expression of palmitoylated GFP-SWAP-70 constructs led to aberrant F-actin organization and changes in cell morphology. Both effects were dependent on the expression level of the construct. Overexpression of palmitoylated SWAP-70 resulted in filopodia and microspike formation in generally elongated and poorly spread cells. The cells did not form large lamellipodia and cell migration could not be observed. PM-SWAP-70 transfected cells expressing moderate levels of the fusion protein exhibited an elongated phenotype with corset-like, PM-GFP-SWAP-70 labeled, longitudinally oriented cortical F-actin bundles (Figs. 21 and 22). Whether myosin II is incorporated into these structures needs to be determined. These alterations in actin organization depend on the actin binding properties of palmitoylated SWAP-70 since the deletion of the C-terminal 60 amino acids abrogated the corset-like F-actin staining and the elongated phenotype. Cells transfected with this truncation construct still exhibited frequent filopodia formation. The induction of microspikes and filopodia is a hallmark of Cdc42 signaling. This matches the higher Cdc42-GTP levels in PM-SWAP-70 transfected cells as observed in the small-GTPase-pulldowns (see next chapter). PM-SWAP-70 induced this phenotype in a variety of cell lines and independently of the extracellular matrix. Therefore, the engagement of different integrins by different ECMs did not influence the phenotype seen with the palmitoylated SWAP-70 construct. This differs from results from cells transfected with non-palmitoylated GFP-SWAP-70 plated on different ECMs. GFP-SWAP-70 localized to focal adhesions and sometimes stress fibers in B16F1 cells plated on fibronectin while such structures were not detected in B16F1 cells plated on laminin (Oberbanscheidt, 2005;

## Discussion

Oberbanscheidt *et al.*, submitted). The independence of PM-SWAP-70 localization on the extracellular matrix, the constitutive targeting of the fusion protein to the plasma membrane and its constitutive F-actin binding suggest that PM-SWAP-70 acts in a dominant active manner.

Overexpression of SWAP-70 has been reported to promote spreading of transiently transfected HeLa cells (Arthur *et al.*, 2004). This is in contrast to the observations with PM-SWAP-70 during this work and results obtained by Hilpelä *et al.* (2003) that SWAP-70 transfected HfTa Hela cells show a loss of lamellipodia and the acquisition of highly refractile retraction fiber like extensions. Furthermore, SWAP-70<sup>-/-</sup> B-cells exhibit a significantly larger spreading area as compared with wildtype B-cells (Pearce *et al.*, 2006). Furthermore, B-cells mast-cells exhibit an enhanced homotypic association that depends on the misregulation of the integrin LFA-1 (Pearce *et al.*, 2006; Sivalenka and Jessberger, 2004). These results suggested that SWAP-70 influences the activation level of integrins. Therefore, the less spread phenotype of PM-SWAP-70 transfected cells could be due to misregulation of integrins. During adhesion, binding of heterodimeric integrins to their extracellular matrix ligands causes the sequential activation of small GTPases by outside-in signaling. Cdc42 and Rac activation precede the activation of Rho during spreading and this succession mediates cell spreading (Price *et al.*, 1998; Defilippi *et al.*, 1999). Recently, adhesion and early spreading of fibroblasts was shown to be largely dependent on the formation of long radial filopodia that contain integrins (Partridge and Marcantonio, 2006). During this early adhesion and spreading, RhoA signaling is initially decreased through phosphorylation and activation of p190RhoGAP in a c-src dependent manner (Arthur *et al.*, 2000). PM-SWAP-70 transfected HEK293-T cells have decreased RhoA-GTP levels. Assuming that the effect of PM-SWAP-70 on Rho activity is the reason for the phenotype, the morphological changes would probably begin to occur when RhoA is normally activated after the initial spreading period.

Transfected NIH/3T3 cells expressing low levels of PM-GFP-SWAP-70 exhibited constitutive labeling of F-actin structures under conditions in which non-palmitoylated SWAP-70 is mostly cytosolic. Therefore, the membrane association probably leads to “activation” of SWAP-70 in agreement with the hypothetical model for SWAP-70. However, localization of the fusion protein differed from the subcellular localization of endogenous SWAP-70. PM-GFP-SWAP-70 localized to the region of the cell body and was hardly ever found in ruffles or enriched in the lamella of smaller protrusions. Association of palmitoylated SWAP-70 with loose actin filament arrays in the lamella of cells has been observed only on few occasions in B16F1 cells with very low expression levels. The palmitoylation of SWAP-70 interferes with its phosphoinositide-dependent transitory recruitment to the plasma membrane. SWAP-70 was speculated to bind to F-actin bundles that are in transition between generation in the lamellipodium and incorporation in other F-actin structures. If the binding of SWAP-70 to F-actin loses its

transitory character it could change the fate of actin-filaments labeled by PM-SWAP-70. This could lead to misorganization of the F-actin cytoskeleton.

PM-SWAP-70 transfected B16F1, NIH/3T3 and HEK-293T cells often showed extensive F-actin rich ruffles at the ends of spindle shaped cells (e.g. Fig. 20). Ihara *et al.* (2006) and Shinohara *et al.* (2002) reported that SWAP-70 is a necessary component in tyrosine kinase dependent ruffle formation and accumulates in these F-actin rich compartments. However, PM-SWAP-70 was very rarely seen in ruffles. This indicates that PM-SWAP-70 acts indirectly and interferes with a signaling pathway.

## 6.5 Regulation of small GTPases by palmitoylated SWAP-70

SWAP-70 has been implicated in regulating the activity of the small GTPase Rac (Shinohara *et al.*, 2002; Ihara *et al.*, 2006; Sivalenka and Jessberger, 2004). However, overexpression of SWAP-70 or PM-SWAP-70 did not result in morphological alterations typically associated with Rac activation (this work; Hilpelä *et al.*, 2003). The poorly spread cellular morphology induced by PM-SWAP-70 together with a loss of stress fibers and decreased focal adhesion formation resemble phenotypes reported for downregulated Rho-signaling, Rac<sup>-/-</sup> cells (Guo *et al.*, 2006) and oncogenic H-Ras (Dartsch *et al.*, 1994; Uberall *et al.*, 1999). GTPase pull downs were carried out to investigate, whether overexpression of palmitoylated SWAP-70 affects levels of Rac or Rho activity. GTPase pull-downs revealed no changes in Rac activity but an upregulation of active Ras and Cdc42 and a downregulation of Rho in PM-SWAP-70 transfected HEK-293T cells. This is in agreement with the observed morphological changes, since microspike- and filopodia formation is a hallmark of Cdc42 signaling and the loss of stress fibers and focal adhesions is a sign for a low Rho-GTP-level. Very interestingly, the phenotype of Rat1 cells cotransfected with dominant active Ras and dominant active Cdc42 also looks quite similar to the phenotype induced by PM-SWAP-70 (Izawa *et al.*, 1998).

Rho signals to the actin cytoskeleton via several effectors including formins and Rho dependent kinases. The Rho dependent pathways leading to the formation of stress fibers have been a focus of intense research. An important signal transduction branch downstream from activated Rho is the direct binding of Rho associated coiled-coil forming serine/threonine kinase ROCK (Fujisawa *et al.*, 1996; Matsui *et al.*, 1996). Activated ROCK causes the activation of myosin II either directly via phosphorylation of myosin light chain or indirectly through enhanced phosphorylation and inactivation of the myosin binding subunit of the myosin light-chain phosphatase (MLCP). Both effects synergize to amplify the activity of myosin II resulting in increased stress fiber formation (Kawano *et al.*, 1999; Pellegrin and Mellor, 2007). Activation of formins by Rho signaling probably contributes to stress fiber formation since formins are involved in actin polymerization at focal contacts giving rise to dorsal stress fibers which eventually fuse to form ventral stress fibers (Hotulainen and Lappalainen, 2006). Binding of activated Rho to ROCK enables the kinase to phosphorylate a threonine residue in the activation loop of LIM-kinase enabling

## Discussion

this kinase to phosphorylate cofilins (Sumi *et al.*, 1999). Phosphorylation of cofilins inactivates their F-actin severing activity resulting in a net increase in the cellular filamentous actin and less dynamic F-actin (Maekawa *et al.*, 1999; Sumi *et al.*, 2001a; Sumi *et al.*, 2001b).

How SWAP-70 affects the activity of Rho, Ras and Cdc42 remains to be determined. Possible explanations regarding Ras and Rho include the possible interactions of SWAP-70 with the RasGEF RasGRP1 and myosin 9b that contains a RhoGAP in its C-terminal part. If SWAP-70 would directly influence one GTPase it could indirectly affect the activation state of other GTPases (see next chapter).

### **Signaling interplay of small GTPases**

Signaling pathways of small GTPases are interconnected and there exists crosstalk between different members of the superfamily. Apart from the fact, that many highly related small GTPases share the same effectors and regulators, different members are suggested to modulate or counteract the pathway of their “relatives”. Rho can be inactivated through downstream signaling of Arf6, Rac, Cdc42, RhoD, Rnd proteins and Ras. Ras signaling affects not only stress fiber formation but also focal adhesion formation via the extensively investigated Ras-Raf-Mek-ERK signaling cascade. Activated Erk1/2 enhances the turnover rate of focal adhesions in *Src* transformed cells (Fincham *et al.*, 2000).

The level of activated Ras is elevated in PM-SWAP-70 transfected HEK293-T cells. Whether this is an effect of the interaction of SWAP-70 with the RasGEF RasGRP1 remains to be elucidated. RasGRP1 expression has not been shown for HEK293-T cells and the antibody used in this work did not detect endogenous RasGRP1 in HEK293-T cell homogenates, but neither did it in homogenates from spleen and brain where RasGRP1 is known to be expressed. Ras signaling can result in the disruption of stress fibers and the downregulation of Rho signaling via several mechanisms. Some authors suggest a direct downregulation of Rho-GTP levels through Ras signaling. Ras signaling could affect Rho activation via activation of the serin/threonin kinase p21 activated kinase (Pak1) by a PI3 kinase dependent pathway (Chaudhary *et al.*, 2000). Pak1 is an effector of Ras, Rac and Cdc42 (Tang *et al.*, 1999) and is able to influence Rho-signaling by negatively regulating the activity of the Rho GEF NET1 (Alberts *et al.*, 2005). This might be one explanation why Cdc42 signaling can downregulate Rho-activity (Sander *et al.*, 1999).

Other factors disturbing the Rho dependent formation of stress fibers include Src kinases which probably interfere with signaling from ROCK to LIM kinase, thereby leading to activation of cofilins. Furthermore, Rho activation levels are sensitive to reactive oxygen species (ROS). Recently, Shinohara *et al.* (2007) reported that NOX1 dependent generation of ROS contributes to the disruption of stress fibers downstream of Ras. ROS inactivate the low molecular weight protein-tyrosine phosphatase resulting in a subsequent elevation

## Discussion

of the tyrosine-phosphorylated active form of p190RhoGAP. Activated p190RhoGAP ultimately leads to decreased Rho-signaling at least in NIH/3T3 cells (Shinohara *et al.*, 2007). A quite similar mechanism is known for Rac signaling: In phagocytic cells, Rac associates with the NADPH oxidase which is necessary for the oxidative burst of macrophages and neutrophils. Recent studies provided evidence that homologues of this ROS generating flavoenzyme exist in non-phagocytic cells and are activated by Rac-GTP. The concomitant rise in ROS inactivates the low-molecular weight protein tyrosine phosphatase (LMW-PTP) resulting in increased activity of p190RhoGAP (Nimnual *et al.*, 2003). However, transfection of 293-T cells with PM-SWAP-70 did not alter Rac-GTP levels and the transfected cells did not resemble an activated Rac phenotype. Therefore, it is unlikely that Rac is the reason for PM-SWAP-70 induced cellular alterations. Furthermore, preliminary experiments on the susceptibility of 129SvEM-SWAP-70 ko mice towards infections with *Leishmania mexicana* did not reveal differences in the disease time-course compared to infected wildtype mice (cooperation with Dr. Ehrchen, data not shown). *Leishmania* are intracellular parasites residing in macrophages and NADPH oxidase dependent generation of ROS is crucial for the elimination of the intracellular parasites and the survival of the immune cell.

There are conflicting reports concerning the effects of Ras on Rho-GTP levels. Some authors found increased Rho activity in NIH/3T3 cells expressing oncogenic Ras (Chen *et al.*, 2003). According to these results, the loss of stress fibers is due to uncoupling Rho-GTP signaling from stress fiber formation downstream of Ras signaling. For example, oncogenic H-Ras (12V) impacts Rho-GTP signaling via the MEK dependent cytoplasmic relocalization of p21(Cip1) which inhibits ROCK (Lee and Helfman, 2004; Sahai *et al.*, 2001). Besides inhibition of ROCK at the protein level, Ras transformed fibroblasts exhibit post-transcriptional down-regulation of ROCK through a MEK dependent pathway (Pawlak and Helfman, 2002). Inhibition of Rho and ROCK is crucial for the disruption of actin stress fibers and cell adhesions by oncogenic Ras (V12), since these alterations could be restored by cotransfections of dominant active Rho (V14) or constitutively active ROCK I (Izawa *et al.*, 1998). Furthermore, the inhibition of ROCK1 induced an elongated phenotype in A375 cells that was attributed to an aberration of the cortical acto-myosin network (Pinner and Sahai, 2008). For these reasons, it would be informative to cotransfect PM-SWAP-70 with dominant active Rho/ROCK to investigate whether these constructs could rescue the phenotype induced by PM-SWAP-70.

Of course, the downregulation of Rho activity is not necessarily a consequence of the upregulation of Ras and Cdc42 in PM-SWAP-70 transfected cells. The effects on GTPase activity levels could be independent of each other and the morphological effects induced by PM-SWAP-70 could also depend on other signaling pathways or solely on the ability of PM-SWAP to cross-link F-actin with the plasma membrane. Interestingly, a similar phenotype as with PM-SWAP-70 overexpression has been observed in NIH-3T3 cells as a

consequence of Rho downregulation in cooperation with an F-actin plasma membrane linker. The atypical small GTPase GEM is able to associate with activated Ezrin and the Rho-GAP Gmip. This leads to increased cortical F-actin formation and Rho downregulation in GEM and Ezrin cotransfected cells. The elongated phenotype is dependent on the cooperation of both proteins (Hatzoglou *et al.*, 2007). Therefore, it is likely that the Ezrin mediated binding of cortical F-actin to the plasma membrane is crucial for the elongated cell morphology in combination with low Rho-activity. One could speculate that overexpression of PM-SWAP-70 is able to substitute for Ezrin, since PM-SWAP-70 transfected cells frequently exhibit strong corset-like cortical F-actin arrays labeled by the fusion protein. This linkage between F-actin and plasma membrane together with the low Rho activity could have the same effect on cell morphology as activated Ezrin and GEM. Interestingly, activated Ezrin recruits the dual Cdc42/Rho GEF db1 and promotes specifically the activation of Cdc42 which by competition could additionally lower Rho-GTP levels (Prag *et al.*, 2007). Activation of Cdc42 is also a consequence of PM-SWAP-70 expression.

Another possibility how SWAP-70 could affect Rho-GTP levels is its putative interaction with myosin 9b. SWAP-70 was originally identified in a yeast-two-hybrid screen as a binding partner of myosin 9b. Myosin 9b contains a Rho-GAP domain in its C-terminal part and is suggested to be a motorized signaling molecule. Overexpression of the Rho-GAP-domain leads to low Rho GTP levels *in vivo* (Uhlenbrock, 2006; van den Boom *et al.*, 2007). If SWAP-70 is indeed a binding partner of myosin 9b, the constitutive plasma membrane targeting of SWAP-70 might result in recruitment of myosin 9b to the plasma membrane and Rho inactivation. Further studies are necessary to determine the exact molecular mechanisms through which SWAP-70 acts. Whether the effect of PM-SWAP-70 is due to upregulation of Ras- and Cdc42 activities or the downregulation of Rho activity in combination with the tethering of actin to the plasma membrane or a combination of all these factors remains to be elucidated.

### **6.6 The palmitoylated C-terminal region of PM-SWAP-70 induces actin reorganization**

SWAP-70 is a multidomain protein and the actual physiological roles of the domains are currently not completely understood. Expression of different artificially plasma membrane targeted truncation constructs were used to elucidate the contributions of the different domains to the phenotype induced by PM-SWAP-70.

Actin association of palmitoylated SWAP-70 and resulting morphological changes of cells did no longer depend on phosphoinositide binding by the PH-domain. The PH-domain might contribute to the “activation” of SWAP-70, because the palmitoylated PH-mutant construct showed a somewhat “milder” phenotype concerning microspike- and filopodia formation. This result supports a model in which the PH-domain is crucial as a signal

## Discussion

sensing, membrane targeting and anchoring domain but not necessarily for the downstream effects of membrane associated SWAP-70. Given that the PH-domain is not necessary for induction of the phenotype, artificial membrane association through palmitoylation can substitute for the PH-domain.

Two results are of major importance: 1) A palmitoylated C-terminal fragment (305-585) of SWAP-70 was sufficient to induce a similar phenotype as the full-length protein; 2) Loss of the actin binding sequence resulted in an altered phenotype.

Expression of the palmitoylated C-terminal part induced a similar phenotype as the palmitoylated full-length construct. Given that palmitoylated constructs of SWAP-70 resemble constitutively active versions of SWAP-70, the C-terminal part acts as “effector” part of SWAP-70. The C-terminal part of SWAP-70 exhibits weak homology to DH-domains. However, all results of our lab argue against a GEF activity for SWAP-70. The C-terminal part of SWAP-70 contains three regions that are predicted to form coiled-coils. These motifs of  $\alpha$ -helical structure contain heptad repeat sequences and associate in various ways including parallel- or antiparallel dimers, trimers and tetramers (Woolfson, 2005). The association is stabilized via hydrophobic interactions at the contact sites between the helices. Coiled-coil regions can mediate intramolecular- as well as intermolecular interactions. Intermolecular interactions mediated by coiled-coil domains can be either homo- or heterotypic. Homotypic interactions are known from the filament formation of skeletal muscle myosin and intermediate filaments and were found to be crucial for stress fiber formation mediated by the formin FHOD1 (Madrid *et al.*, 2005). Heterotypic interactions were found e.g. between the Arf-GEF cytohesin and the scaffolding protein CASP (Mansour *et al.*, 2002). SWAP-70 runs as a monomer in sucrose density gradients and in gel filtration (Hilpelä, 2002). These results favor an intramolecular coiled-coil formation. How this predicted structure mediates the changes in cell morphology remains to be elucidated.

### **6.7 Deletion of the F-actin binding sequence results in a different phenotype**

SWAP-70 binds directly to nonmuscle actin via its very C-terminal amino acids. PM-SWAP-70 (1-525) and PM-SWAP-70 (305-525) fusion proteins did not associate with F-actin in NIH/3T3 and B16F1 cells. This result further supports the crucial role of the C-terminal 60 amino acids for F-actin targeting. Loss of the F-actin binding information through deletion of the last 60 amino acids resulted in strong alterations of the phenotype induced by PM-SWAP-70 and PM-SWAP-70 (305-585). PM-SWAP-70 (1-525) and PM-SWAP-70 (305-525) transfected cells exhibited a comparable phenotype. PM-SWAP-70 (1-525) and PM-SWAP-70 (305-525) transfected cells were not elongated or spindle shaped, but exhibited ragged plasma membranes, blebs and a loss of lamellipodia. The formation of smooth and broad lamellipodia was abolished in stronger expressing cells.



## Discussion

Expression of high levels of PM-SWAP-70 (1-525) or PM-SWAP-70 (305-525) resulted in frequent bleb formation at the dorsal plasma membrane. Blebs are spherical protrusions with a diameter of 1-10  $\mu\text{m}$ . Blebs are formed during cytokinesis (Fishkind *et al.*, 1991), at the onset of apoptosis (Mills *et al.*, 1998) and are a feature of amoeboid migration (Sahai and Marshall, 2003). Palmitoylated SWAP-70 devoid of the F-actin binding sequence could promote blebbing through different mechanisms, as bleb formation depends on different factors, namely outward pressure of cytoplasm, adhesion between cortical F-actin and the plasma membrane, and plasma membrane tension. As a consequence, F-actin membrane-linking- and F-actin cross-linking proteins play major roles in bleb-formation. For example, blebs have been noted in Filamin depleted melanoma (M2) cells (Cunningham, 1995; Alberts *et al.*, 2004). The expression of palmitoylated constructs of SWAP-70 that lack the F-actin binding sequence could interfere with the cortical F-actin cytoskeleton by acting in a dominant-negative manner. This could for example be due to sequestration of proteins that normally interact with endogenous SWAP-70 and are directly necessary for the stability of cortical F-actin or the linkage to the plasma membrane. It could as well depend on signaling pathways that are influenced by artificially membrane targeted SWAP-70 truncation constructs. Overexpression of palmitoylated SWAP-70 (1-525) fusion protein could also act as phosphoinositide-sequestering/scavenging factor. Membrane blebbing as a consequence of an artificially membrane targeted phosphoinositide binding protein has been reported for myristoylated alanine rich C kinase substrate (MARCKS). Artificial N-terminal palmitoylation using the GAP-43 palmitoylation signal sequence targets MARCKS to blebs at the plasma membrane and prevents cell spreading (Myat *et al.*, 1997). However, expression of the PM-SWAP-70 (305-525) construct lacking the PH-domain induced a similar blebbing effect as PM-SWAP-70 (1-525) in cells. Therefore, the coiled-coil containing C-terminal region of SWAP-70 is sufficient to induce blebbing when artificially targeted to the membrane and phosphoinositide sequestering can not be the reason for this phenotype. If the Dbl homology like (DHL) domain of SWAP-70 is sufficient for induction of blebs, it could be via an intrinsic activity or the binding of other proteins. The proposed Rac-GEF activity of SWAP-70 has been mapped to the DHL domain and GEF-activity measurements showed higher activity for the isolated domain compared with the full-length SWAP-70 (Shinohara *et al.*, 2002). However, bleb formation depends rather on Rho- than on Rac activity. Rho signaling pathway dependent myosin II activation and the corresponding contractility increases intracellular pressure and consequently can drive bleb formation in susceptible cells. Recently, the Rac-GAP FilGAP which directly binds to the actin cross-linker Filamin has been identified to mediate bleb-formation upon phosphorylation by ROCK (Ohta *et al.*, 2006) and hence has been implicated in RhoA-Rac antagonism. The Rho-ROCK-LIM-kinase pathway is a major factor for bleb formation, since LIM kinase 2 induces not only stress fiber formation but also membrane blebs

## Discussion

(Amano *et al.*, 2001). Elevated Rho-GTP levels due to expression of a PM-SWAP-70 (1-525) construct are unlikely. Thus, a misregulation of the binding of cortical actin to the plasma membrane is favored as an explanation. Interestingly, many transfected cells showing blebs on their dorsal plasma membrane exhibited a ventral F-actin architecture that did not differ much from non-transfected cells.

An alternative interpretation regarding the induction of bleb-formation is based on the observation that vertebrate cells can use two different modes of migration: Amoeboid or mesenchymal (Sahai and Marshall, 2003). While mesenchymal migration is based on the formation of well regulated protrusions and degradation of the extracellular matrix via proteases, the amoeboid-like motility is based on bleb formation and squeezing through the three dimensional extracellular matrix. Amoeboid migration in 3-D matrices depends on the activity of the Rho-effector ROCK1. Inhibition of ROCK1 in A375 cells results in an elongated phenotype with multiple long protrusions (Pinner and Sahai, 2008). ROCK1 inhibition was found to be due to the direct interaction of ROCK1 with RhoE. This inhibition could be released by a direct and competitive interaction of ROCK1 with the 3-phosphoinositide dependent kinase 1 (PDK1). Interestingly, the phenotype of cells with low ROCK1 activity closely resembles the phenotype induced by PM-SWAP-70. However, the morphological alterations induced through inhibition of ROCK1 were reported for 3-D matrices. Knockdown of PDK1 reduced the amoeboid motility of cells in 3-D matrices (Pinner and Sahai, 2008). It would be informative to investigate, whether cells transfected with PM-SWAP constructs also show this phenotype in a 3-D environment. Furthermore, since cells transfected with PM-SWAP-70 constructs devoid of the actin binding sequence frequently exhibit membrane blebs, it would be interesting to find out, whether these cells are able to migrate in an amoeboid manner in three-dimensional matrices and if there are differences to cells transfected with PM-SWAP-70.

Surprisingly, PM-SWAP-70 (1-525) still associated with filamentous structures in HeLa cells but not in other cell types. If these filamentous structures turn out to be actin filaments, SWAP-70 might possess a second actin binding site as suggested by Ihara *et al.*, (2006). Alternatively, HeLa cells might express a binding partner of SWAP-70 that recruits it to F-actin even in the absence of SWAP-70's actin-targeting domain. However, the filamentous structures resemble also tubular structures or membrane folds underneath the nucleus. The structures sometimes run along straight stress fibers but lose the straight orientation of the stress fibers giving rise to small variations between the localization of PM-SWAP-70 (1-525) and F-actin. It can not be ruled out that PM-SWAP-70 (1-525) is associated with more delicate F-actin bundles that are connected with the stress fibers, but not visible in the F-actin staining.

## 6.8 Effects of dominant active Ras on the actin cytoskeleton and localization of SWAP-70

Dominant active Ras has a profound effect on the actin cytoskeleton in B16F1 cells. Disruption of stress fibers is characteristic for Ras activation (Bar-Sagi and Feramisco, 1986; Dartsch *et al.*, 1994) and can be caused by different downstream effects that interfere with the Rho signaling pathway (see above). Oncogenic mutations of Ras-genes result in constitutively active Ras-proteins. Cancer cell migration can lead to metastasis. Because SWAP-70 is important for cell migration (Pearce *et al.*, 2006) and Ras signaling results in conditions that might favor the association of SWAP-70 with F-actin (e.g. activation of PI3 kinase) it was investigated how SWAP-70 behaves in cells transfected with dominant active Ras.

As demonstrated previously, R-Ras (38V) transfected B16F1 cells showed enhanced spreading and did not migrate (Self *et al.*, 2001; Wozniak *et al.*, 2005; Ada-Nguema *et al.*, 2006). H-Ras (12V) transfected cells exhibited very strong lamellipodia formation but were still able to migrate and often had long and thin protrusions (Self *et al.*, 2001). Irrespective of lamellipodial forward protrusion, GFP-SWAP-70 labeled F-actin bundles behind the leading edge that were oriented parallel to the plasma membrane. These F-actin arrays moved slowly (0,1-0,18  $\mu\text{m}/\text{min}$ ) towards the cell center. One could speculate that these F-actin arrays resemble transverse arcs because these structures are also oriented parallel to the leading edge in the lamella of U2OS cells (Hotulainen and Lappalainen, 2006). Formation of transverse arcs is based on the end-to-end annealing of alternating short alpha-actinin- and myosin containing bundles probably derived from the lamellipodial actin network (Hotulainen and Lappalainen, 2006). If the dominant active Ras-induced F-actin arrays labeled by SWAP-70 contain myosin II remains to be elucidated.

It is known that Ras activates several signaling cascades. H-Ras signals via its direct binding partner Raf-kinase to mitogen activated protein kinases (MAPK). R-Ras, which shares ~55% sequence homology with its three close paralogue Ras proteins (H-,N-,K-Ras) can bind to many of the same effectors as H-Ras albeit its downstream signaling pathway differs from H-Ras. The proto-oncogene H-Ras and the Ras family GTPase R-Ras share an identical 9 amino acid core effector domain and therefore, bind to many of the same signaling proteins in vitro, such as the p110 catalytic subunit of phosphatidylinositol 3-kinase, (Marte *et al.*, 1997), p101 PI3K (Suire *et al.*, 2002), c-Raf (Rey *et al.*, 1994; Spaargaren *et al.*, 1994) and Nore1 (Vavvas *et al.*, 1998; Oertli *et al.*, 2000). However, H-Ras and R-Ras differ in their ability to activate downstream signaling cascades like the Erk-kinase pathway. R-Ras does not activate the conventional extracellular signal-regulated kinase 1/2 (Erk1/2) pathway (Marte *et al.*, 1997; Oertli *et al.*, 2000); moreover, it has even been reported that R-Ras can antagonize this pathway (Sethi *et al.*, 1999). A shared effector of H- and R-Ras is the PI3-kinase (Rincon-Arano *et al.*, 2003; Mora *et al.*,

## Discussion

2007; Wozniak *et al.* 2005). Since dominant H- and R Ras both cause a similar effect on SWAP-70 association with F-actin arrays, the PI3 kinase pathway, but not the Erk1/2 pathway is important for the effect on SWAP-70 localization.

In agreement with the hypothesis that SWAP-70 is activated by 3-phosphoinositide binding, the very strong recruitment of SWAP-70 to the plasma membrane and F-actin colocalisation in B16F1 cells transfected with H-Ras (12V) and R-Ras (38V) could be reversed by the PI3-kinase inhibitors LY294002 and Wortmannin. SWAP-70 binding to F-actin seems not to be essential for cellular morphology, as cells treated with the PI3-kinase inhibitors did not collapse or show any other morphological changes on a time scale of ~45 min. Even cells with extremely cytosolic SWAP-70 localization due to PI3 kinase inhibition still showed a well spread morphology.

While the addition of 50  $\mu$ M LY294002 or 10 nM Wortmannin led to an almost complete dissociation of SWAP-70 from the filaments in dominant active R-Ras (38V) cotransfected cells, the dissociation was not as complete in dominant active H-Ras (12V) cotransfected cells. This may be explained by activation of different classes of PI3 kinases by H- vs. R-Ras. Three different classes of PI3 kinases exist which differ in their substrate specificity and intracellular localization. The class II PI3 kinases are relatively resistant to Wortmannin and LY294002 (reviewed in (Shepherd *et al.*, 1998; Foster *et al.*, 2003). Hence, it could be speculated that H-Ras (12V) activates class II PI3-kinases more efficiently than R-Ras (38V). Currently, no data are available about H-/R-Ras activation of class II PI3-kinases. Class I PI3 kinases reside mainly in the cytoplasm and are recruited to membranes upon appropriate signals whereas the class II enzymes are constitutively membrane associated (Foster *et al.*, 2003). *In vivo*, the class I PI3-kinases predominantly produce PtdIns (3,4,5)<sub>3</sub>P from their preferred substrate PtdIns (4,5)P<sub>2</sub>, while the class II PI3-kinases can produce PtdIns (3,4)P<sub>2</sub> directly through phosphorylation of PtdIns (4)P. Since there is evidence that SWAP-70 binds to PtdIns (3,4)P<sub>2</sub>, it could be speculated that the class II PI3-kinases are important activators of SWAP-70. They are implicated in growth factor receptor signaling from e.g. c-Kit, the receptor for *stem cell factor* (SCF) (Lennartsson and Ronnstrand, 2006). c-Kit signaling is severely inhibited in SWAP-70<sup>-/-</sup> mast cells (Sivalenka and Jessberger, 2004). Especially the PI3 kinase C2 $\beta$  which constitutively associates with c-Kit mediates signaling from SCF leading i.e. to the activation of the PtdIns (3,4) P<sub>2</sub> binding kinase Akt (Arcaro *et al.*, 2002). In this context it is of interest that expression of artificially membrane targeted class I catalytic p110-subunit (PI3K-CAAX) did not result in a strong increase in SWAP-70-F-actin association. The p110-subunit is a class I PI3-kinase and its main product is PtdIns (3,4,5)<sub>3</sub>P. This phosphoinositide can be converted to PtdIns (3,4)P<sub>2</sub> by phosphatase activity of enzymes like the inositol 5-phosphatase SHIP2. It would be interesting to investigate, whether coexpression of SHIP2 would change the effect of PI3K-CAAX. Furthermore, the association of Pak1 with PI3-kinase leads to phosphorylation of actin by Pak1 and a

## Discussion

subsequent dissolution of stress fibers (Papakonstanti and Stournaras, 2002). The PI3-kinase effector Akt/PKB which specifically binds PtdIns (3,4) bisphosphate (Klippel *et al.*, 1997) has recently also been shown to phosphorylate actin, too (Vandermoere *et al.*, 2006). Therefore, it represents an interesting idea that SWAP-70 may preferentially bind to phosphorylated F-actin.

Since PI3-Kinase activity is necessary but not sufficient for the effects of dominant active Ras on SWAP-70 localization, other downstream effectors of Ras contribute to the F-actin reorganization and SWAP-70 association with F-actin. R-Ras and H-Ras have both the ability to activate Rac via various mechanisms, most importantly by the activation of GEFs via PI3-kinase activation, and all three small GTPases are implicated in lamellipodia formation. Rac can also be activated independently of Ras. Ras and Rac signaling converge on some downstream effectors such as Pak protein kinase that acts as a hub for signal integration of different small GTPases (Tang *et al.*, 1999). Moreover, Rac has also been shown to activate PI3-kinases in a positive feedback-loop (Bourne and Weiner, 2002; Srinivasan *et al.*, 2003; Wang *et al.*, 2002b). To find out whether Rac has a similar influence on the localization of SWAP-70, B16F1 cells were cotransfected with GFP-SWAP-70 and dominant active Rac (12V). Rac (12V) did not show a similar effect on SWAP-70 localization and apart from strong induction of large lamellipodia did not change SWAP-70 localization in the lamella. The effects of dominant active Ras on the actin cytoskeleton and SWAP-70 are probably the result of the combination of different downstream-effectors. Additionally, the interaction of Ras proteins with Ena/VASP via the protein PREL (Proline Rich EVH1 Ligand) might contribute to the specific effects on the F-actin reorganization (Jenzora *et al.*, 2005).

Dominant active Ras does not hydrolyze bound GTP and therefore does not cycle between active and inactive states. To find out, whether dominant active Ras can be substituted by enhanced GEF activity *in vivo*, different Ras-GEFs were cotransfected with SWAP-70. Since the phenotype induced by dominant active Ras could not be substituted by the Ras-GEFs RasGRP1, RasGRP2, SOS and RasGRF2, it seems unique for non-cycling Ras proteins. Cotransfections of B16F1 cells with SWAP-70 and RasGRP2 or RasGRF2 resulted in polar and motile cells with prominent SWAP-70 labeling of the typical loose F-actin arrays in the lamella of cells (data not shown).

### ***Why is the effect of oncogenic Ras on SWAP-70 cell type specific?***

In contrast to B16F1 cells, dominant active R-Ras (38V) transfected NIH/3T3 did not form similar F-actin structures labeled with SWAP-70. Whereas in many cell types R-Ras has been shown to activate the PI3-kinase, there exist conflicting reports concerning PI3-kinase activation in fibroblasts. In Swiss 3T3 fibroblasts, R-Ras (38V) fails to activate PI3 kinase (Self *et al.*, 2001). Furthermore, Ras can activate the Pak kinase in Rat-1 cells through a signal cascade Ras > PI3 kinase > Rac/Cdc42 > Pak, but this signaling pathway does not

exist in NIH/3T3 cells as measured by kinase-assays with immunoprecipitated Pak from cell lysates (Tang *et al.*, 1999). In NIH/3T3 fibroblasts, R-Ras (38V) mediated spreading is independent of PI3-kinase binding (Holly *et al.*, 2005). Instead, it probably depends on the activation of Rac via the R-Ras specific effector RLIP76 and subsequent Arf6 activation (Goldfinger *et al.*, 2006). Cotransfection of NIH/3T3 cells with SWAP-70 and dominant active R-Ras (38V) resulted in accumulation of macropinosomes (Fig. 39). These large translucent vesicles were labeled by R-Ras (38V) but GFP-SWAP-70 was not detected on them in fixed cells. However, SWAP-70 association to macropinosomes is transient (Oberbanscheidt *et al.*, 2007) and therefore probably has been missed. As mentioned, R-Ras activates Rac but not PI3-kinase in NIH/3T3 cells and Rac activation is linked to peripheral membrane ruffling and macropinocytosis (Johannes and Lamaze, 2002; Lanzetti *et al.*, 2004). The Rac effector Pak1 stimulates macropinocytosis in NIH/3T3 cells and a constitutive active mutant is able to induce macropinocytosis (Dharmawardhane *et al.*, 2000). This might be an explanation, why NIH/3T3 cells expressing R-Ras (38V) exhibit increased numbers of macropinosomes.

## 6.9 RasGRP1, an interactor of SWAP-70?

The interaction of SWAP-70 with RasGRP1 has been found in a bacterial two-hybrid screen. The C-terminal region of murine RasGRP1 (amino acids 661-795) interacted with SWAP-70 in the two-hybrid assay. The interaction could be confirmed by *in vitro* pull-down assays using bacterially expressed GST-SWAP-70. Endogenous RasGRP1 from mouse-tissue lysates was enriched specifically on GST-SWAP-70-beads. The specificity for the interaction of SWAP-70 with the C-terminal part of RasGRP1 could further be substantiated by pull-down-experiments showing that bacterially expressed GST-SWAP-70 interacts with GFP-RasGRP1, but not GFP-RasGRP2 from transfected HEK-293-T-cells. Thus, RasGRP1 interacts via its C-terminal part with at least the N-terminal part of SWAP-70. When transfected alone, RasGRP1 was sometimes found in the lamella behind ruffling lamellipodia (Fig. 46A), but more frequently associated with internal membranes. However, cotransfections of SWAP-70 and RasGRP1 resulted in extensive colocalisation. In motile cells, RasGRP1 colocalized partially with SWAP-70 on actin filaments. However, it did not extend as far towards the leading edge as SWAP-70 does. F-actin is polymerized predominantly at the leading edge of lamellipodia and actin filaments flow backwards into the lamella. SWAP-70 associates with preformed actin filaments (Oberbanscheidt *et al.*, submitted). The association of SWAP-70 with filaments located closer to the leading edge than RasGRP1 could therefore also be a result of an earlier recruitment of SWAP-70 to F-actin and subsequent recruitment of RasGRP1. Cells cotransfected with a truncation construct of SWAP-70 devoid of the C-terminal actin binding sequence and RasGRP1 do not exhibit a localization of either protein at filaments. This suggests that SWAP-70 recruits RasGRP1 to actin filaments. However, SWAP-70 lacking the F-actin targeting sequence occasionally colocalized with RasGRP1 on some

larger vesicles. RasGRP1 is expressed in mast cells and B-cells that also express SWAP-70. However, RasGRP1 is also highly expressed in T-cells that do not express SWAP-70 but its only homologue DEF6.

Even though the cotransfection of SWAP-70 with RasGRP1 led in most cases to stable filamentous colocalisation, a consecutive association of SWAP-70 and RasGRP1 could be observed on macropinosomes in cotransfected NIH/3T3 cells. SWAP-70 accumulated slightly before RasGRP1 (Fig. 48B). If this association is dependent on actin filaments remains to be elucidated. SWAP-70 associates with macropinosomes shortly after activated Rac (Oberbanscheid, 2005; Oberbanscheidt *et al.*, 2007). Rac-GTP is a strong activator of the WAVE-complex at the leading edge and responsible for generation of new actin filaments. It would be interesting to find out whether Rac activation on macropinosomes is crucial for SWAP-70 recruitment. It is currently unclear if Rac-GTP leads to F-actin generation on existing macropinosomes. However, no accumulation of actin on macropinosomes could be observed before the vesicles were labeled by SWAP-70 (Oberbanscheidt *et al.*, 2007).

Taken together, SWAP-70 interacts with the C-terminal part of RasGRP1 and this is suggested to recruit RasGRP1 to actin filaments (Figs. 52 and 55)



**Fig. 52. Hypothetical model of SWAP-70 and RasGRP1 interaction with F-actin.** SWAP-70 binds to non-muscle actin with its C-terminal F-actin targeting sequence. The N-terminus of SWAP-70 interacts with the C-terminal region of RasGRP1 and this recruits RasGRP1 to F-actin. Additionally, RasGRP1 binds to the actin filament by an N-terminal F-actin binding region.

### ***What could be the physiological relevance of the interaction between SWAP-70 and RasGRP1?***

SWAP-70 was reported to specifically bind Rac-GTP in an effector-like manner (Ihara *et al.*, 2006). If SWAP-70 was indeed an effector of Rac and an interactor of RasGRP1, binding and activation of RasGRP1 could provide a link between Rac and Ras signaling. This Rac dependent Ras activation via RasGRP1 would be unusual in that it places Ras activation downstream of Rac activation. However, such a signaling pathway has been reported to exist in B-cells and T-cells (Caloca *et al.*, 2003; Zugaza *et al.*, 2004). Intriguingly, this pathway depends on RasGRP1.

RasGRP1 can be activated by the Rac-GEF Vav or dominant active Rac (Caloca *et al.*, 2003; Zugaza *et al.*, 2004). Vav is activated by receptor tyrosine kinases like c-Kit (Alai *et*

## Discussion

*al.*, 1992; Bustelo, 2000) and BCR-signaling (Caloca *et al.*, 2003; Bustelo, 2000). Assuming that SWAP-70 interacts with RasGRP1 *in vivo*, either binding of SWAP-70 to F-actin (maybe in a Rac dependent manner) or direct binding of SWAP-70 to activated Rac in an effector like manner could influence RasGRP1 localization and/or activity and consequently the activation status of small GTPases for which RasGRP1 shows GEF activity. However, the Vav induced RasGRP1 dependent Ras activation does also exist in T-cells that do not express SWAP-70 but the related protein DEF6. Both proteins share a high sequence homology especially in the N-terminal part (Fig. 53).

```

humDEF6      -MALRKELLLKSIWYAFTALDVEKSGKVSQKLVLSHNLYTVLHHPHDPVALEEHRDDD 59
humSWAP      MGSLLKEELLKAIWHAFTALDQDHSGKVSQKLVLSHNLCVTKVPHDPVALEEHRDDD 60
              *:.****:*:***** :***** ***** :.*****

humDEF6      DGPVSSQGYMPYLNKYIILDKVEGAFVKEHFDELCWTLTAKKNYRADSNGNSMLSNQDAF 119
humSWAP      EGPVSNQGYMPYLNRFILKVKQD-NFDKIEFNRCWTLCKKNTKN---PLLI TEEDAF 116
              :****.*****:***:* : * * ..:**** .*** : :. :***

humDEF6      RLWCLFNFLSEDKYPLIMVPDEVEYLLKVLSSMSLEVSLEGELEELLAQEAQVAQTGGGL 179
humSWAP      KIWVIFNFLSEDKYPLIIVSEEIEYLLKLTTEAMGGGWQQEQFEHYKINF---DSKNGL 173
              :.* :* *****:***:..:*****. :*. . :.* : :. *:

humDEF6      SVWQFLELFNSGRCLRGVGRDTLSMAIHEVYQ
humSWAP      SAWELIELIGNGQFSKGMDRQTVSMAINEVFN
              :.* :*:..* :* :*:*****.*:

```

**Fig. 53. Sequence alignment of the N-terminal part of human SWAP-70 that interacted with RasGRP1 in the two-hybrid system and the corresponding sequence of the related human protein DEF6.** Stars indicate identical amino acids, colons indicate conserved amino acids with similar properties.

GFP-DEF6 partly colocalized with mCherry-RasGRP1 in B16F1 cells similar to SWAP-70 (Fig. 54). However, the colocalisation of DEF6 with RasGRP1 was not as clear as with SWAP-70 and appeared more punctuated at the filaments. Interestingly, RasGRP1 deficient mice exhibit a phenotype very similar to that of DEF6 deficient mice. Both knockout mice develop a lymphoproliferative autoimmune syndrome and show defects in T-cell proliferation and Erk activation upon TCR activation (Fanzo *et al.*, 2006; Layer *et al.*, 2003). Furthermore, both knockout mice strains develop autoantibodies, a phenotype that also has been reported for SWAP-70 deficient mice (Borggreffe *et al.*, 2001).



## Discussion

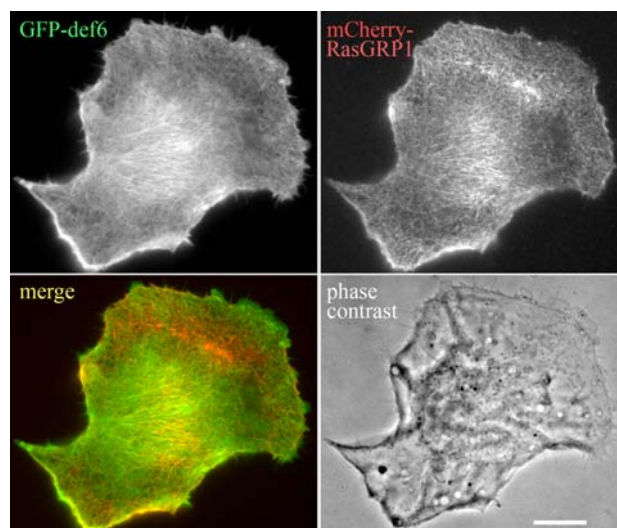


**Fig. 54. GFP-DEF6 and mCherry-RasGRP1 colocalize in cotransfected B16F1 cells plated on laminin.**

Ras activation by RasGRP1 has been reported to take place on the Golgi-apparatus membrane (Bivona *et al.*, 2003) and the plasma membrane (Coughlin *et al.*, 2005; Hancock, 2007). Recent findings have elucidated some important mechanisms for the correct localization of the RasGRP1 protein. Interestingly, the SWAP-70 interacting region of RasGRP1 is important for the recruitment of the RasGRP1 to the plasma membrane.

RasGRP1 is recruited to endomembranes and the plasma membrane by BCR and TCR signaling. The membrane binding of RasGRP1 has been attributed to RasGRP1's diacylglycerol (DAG) binding C1 domain. However, the C1-domain is not sufficient to localize RasGRP1 to the plasma membrane of WEHI-231 cells and DT-40 cells (Beaulieu *et al.*, 2007). A GFP-fusion construct of the isolated C1 domain of RasGRP1 accumulated on internal membranes but not on the plasma membrane in DT40 cells after BCR stimulation. Moreover, RasGRP1 truncation constructs lacking the C1 domain still relocated to the plasma membrane after BCR-stimulation of murine WEHI-231 cells (Beaulieu *et al.*, 2007). This is in accordance with results obtained by Caloca *et al.*, (2003) revealing that the C1 domain was not necessary for relocalization of RasGRP1 after Vav activation. In B-cells the C-terminal 101 amino acids of RasGRP1 were necessary and sufficient for BCR-stimulated relocalization to the plasma membrane (Beaulieu *et al.*, 2007). This region was named PT domain (for plasma membrane targeting). The PT-domain of RasGRP1 shares no similarity to known domains in the databases except for a weak homology with a basic region leucine zipper.

The PT domain of RasGRP1 is enclosed in the 135 amino acid fragment that interacted with SWAP-70 in the two-hybrid screen. When transfected without SWAP-70, RasGRP1 predominantly associated with tubular structures and was rarely found to colocalize with

## Discussion

actin filaments that are supposed to be labeled with endogenous SWAP-70. However, when cotransfected with SWAP-70, RasGRP1 almost exclusively associated with SWAP-70 labeled actin filaments at the plasma membrane. The cytosolic background of fluorophore-tagged RasGRP1 was very low in cotransfected cells, implying a strong recruitment of RasGRP1 to these filaments. It might be speculated that exogenous RasGRP1 alone binds predominantly to diacylglycerol-containing endomembranes but is recruited to F-actin through higher levels of actin filament associated SWAP-70 that probably exist in SWAP-70 cotransfected cells. However, SWAP-70 is probably not the only mediator of F-actin dependent Ras activation at the plasma membrane, because RasGRP1 can bind to F-actin on its own via its N-terminal region. Moreover, a truncation construct of RasGRP1 devoid of the C1 domain and the PT-domain still localizes to ruffles in COS1 cells cotransfected with active Vav (Caloca *et al.*, 2003). Yet, the interaction with SWAP-70 might contribute to a specificity of RasGRP1 for subsets of actin filaments and/or the interaction of both proteins increase the affinity of RasGRP1 for F-actin (Fig. 56). The presence of DAG might contribute to the interaction of RasGRP1 with SWAP-70 since binding of RasGRP1 to DAG probably relieves an intramolecular masking of the PT-domain by a C-terminal PT-suppressor domain (Beaulieu *et al.*, 2007). Furthermore, additional stabilization of RasGRP1 membrane binding might be provided by the interaction of the C1 domain with DAG. Thus, DAG binding contributes to plasma membrane localization even though the C1 domain is not sufficient for it.

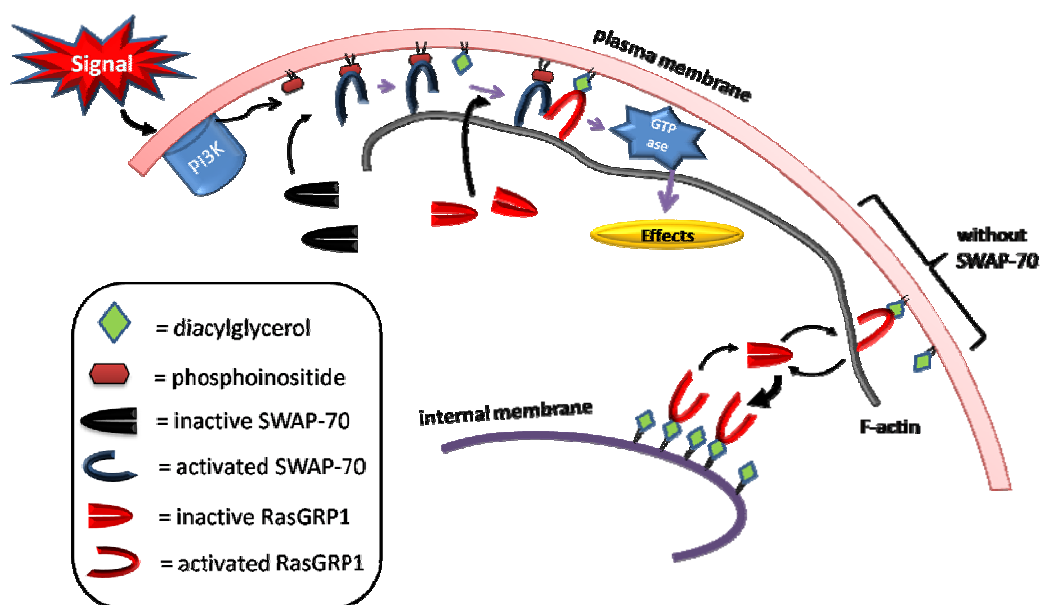


**Fig. 55. Hypothetical model for SWAP-70 dependent RasGRP1 recruitment at the plasma membrane.** PI3 kinase activation results in the generation of 3-phosphoinositides at the plasma membrane. SWAP-70 is recruited from an inactive cytosolic state to the plasma membrane by the interaction of the PH-domain with the 3-phosphoinositides. SWAP-70 associates with actin filaments and links them to the membrane. The interaction of SWAP-70 with the plasma membrane targeting domain (PT-domain) of RasGRP1 recruits RasGRP1 from an inactive state to F-actin at the plasma membrane. This interaction probably needs the presence of diacylglycerol that binds to the C1 domain of RasGRP1, thereby releasing an intramolecular interaction of the PT-domain. Furthermore, the binding of DAG by the C1 domain might stabilize the plasma membrane association. When not recruited by SWAP-70 to F-actin, RasGRP1 resides either in an inactive cytosolic state or is recruited preferentially to endomembranes because of a higher DAG concentration at these membranes compared with the plasma membrane.

Since RasGRP1 contains an F-actin binding sequence, it is possible that the colocalisation with SWAP-70 is by chance. Another member of the RasGRP protein family, RasGRP2, has the same intrinsic F-actin binding capacity (Caloca *et al.*, 2004). F-actin binding via its N-terminal region contributes to translocation of RasGRP2 into membrane ruffles in Vav cotransfected cells. However, RasGRP2 did not colocalize with SWAP-70 in cotransfected cells and moreover it did not interact in *in vitro* binding assays. These results argue for the specificity of SWAP-70-RasGRP1 interaction. However, it can not be excluded that the colocalisation with SWAP-70 is independent of a direct association between both proteins but rather by chance or due to a SWAP-70 dependent signaling pathway that leads to F-actin association of RasGRP1.

Given that SWAP-70 is directly involved in the recruitment of RasGRP1 to cortical actin filaments, SWAP-70 should be recruited to sites where RasGRP1 is necessary for Ras activation. Beaulieu and colleagues (2007) showed that RasGRP1 is directed to the plasma

## Discussion

membrane upon BCR stimulation. Intriguingly, BCR-signaling causes a sustained rise in PtdIns (3,4) bisphosphate concentration at the plasma membrane (Krahn *et al.*, 2004; Marshall *et al.*, 2002; Cheung *et al.*, 2007). PtdIns (3,4) P<sub>2</sub> is supposed to bind to the PH-domain of SWAP-70. SWAP-70 is relocalized to the plasma membrane immediately after B-cell receptor stimulation (Masat *et al.*, 2000). Interestingly, BCR activation induces a F-actin dependent- and Rac mediated relocalization of RasGRP1 to the plasma membrane (Caloca *et al.*, 2003). Could this dependency on F-actin be due to the recruitment of RasGRP1 through F-actin associated SWAP-70? If this was the case, SWAP-70 could contribute to BCR signaling through specific binding of RasGRP1 at the plasma membrane. However, it is currently still unclear whether the interaction of SWAP-70 with RasGRP1 influences Ras activity levels either in a positive or a negative manner. Experiments with cotransfections of SWAP-70 and RasGRP1 vs. single transfections of RasGRP1 or SWAP-70 did not show consistent differences in Erk activation levels. These experiments utilized NIH/3T3 and B16F1 cells in which a clear colocalisation of SWAP-70 with RasGRP1 was evident. While transfections with SWAP-70 alone did not result in Erk 1/2 phosphorylation, RasGRP1 transfected cells had elevated Erk 1/2 phosphorylation levels. However, the cotransfection rates were too low to decide whether the interaction of SWAP-70 with RasGRP1 does influence Ras downstream signaling to Erk. Activation of Ras could also be monitored with Raichu-probes in individual cells (Mochizuki *et al.*, 2001). Raichu-Rap1 probes revealed that Rac dependent interaction of RasGRP2 with F-actin does not change the basal activity of Rap1 but results in a regionalized activation of Rap1 leading to spatially regulated integrin activation (Caloca *et al.*, 2004). Given that the spatial control of Rap1 by RasGRP2 and F-actin would also hold true for the RasGRP1-F-actin association, this interaction could contribute to integrin regulation which is defective in SWAP-70<sup>-/-</sup> Mast- and B-cells (Sivalenka and Jessberger, 2004; Pearce *et al.*, 2006).

Cotransfections of SWAP-70 with dominant active Ras constructs resulted in enhanced association of SWAP-70 with F-actin. In contrast, cotransfection of dominant active Ras with RasGRP1 resulted in strong association of RasGRP1 with endomembranes and vesicles (videos S8, S9). Two findings could explain this difference. Caloca and colleagues (2003) reported that F-actin contributes to the optimal RasGRP1 dependent stimulation of the Ras pathway under conditions in which low amounts of DAG are present. However, Ras signaling increases the DAG-level of cells (Wolfman and Macara, 1987; Martin *et al.*, 1997). It might be that dominant active Ras induced high DAG levels at the internal membranes overcome the SWAP-70-RasGRP1 interaction at the plasma membrane because the diacylglycerol (DAG) binding C1 domain of RasGRP1 contributes to its localization. In this regard it is interesting that the preferential accumulation of a RasGRP1 construct devoid of the PT domain at internal membranes after BCR stimulation was suggested to reflect a higher affinity of the C1 domain of RasGRP1 for saturated DAGs.

## Discussion

They can be more abundant at internal membranes than at the plasma membrane (Beaulieu *et al.*, 2007; Carrasco and Merida, 2004).

Would the recruitment of RasGRP1 to the plasma membrane by SWAP-70 make a difference in Ras activation since other ubiquitous RasGEFs like SOS are thought to be the main activators of Ras at the plasma membrane? The canonical pathway for Ras activation at the plasma membrane includes the recruitment of the cytosolic Grb2-SOS complexes to activated RTKs. However, efficient Ras activation by SOS depends on RasGRPs in B- and T-cells (Roose *et al.*, 2007; Aiba *et al.*, 2004; Zheng *et al.*, 2005). SOS has a binding pocket specific for Ras-GTP and binding of RasGRP1-derived Ras-GTP elicits enhanced GEF-activity of SOS. Therefore, RasGRP1 is crucial for the initial generation of Ras-GTP and this promotes SOS activation via a positive feedback loop (Roose *et al.*, 2007).

Recruitment of SOS was long thought to depend on the interaction with the adaptor protein Grb2 at RTKs. In addition, SOS contains a PH-domain that can bind to phosphoinositides at the plasma membrane. A recent paper from Zhao and colleagues (2007) challenged the view on Ras activation at the plasma membrane upon growth factor stimulation in COS-1, HeLa and NIH/3T3 cells. They provided evidence that SOS recruitment to the plasma membrane upon EGFR stimulation does not depend on phosphoinositide binding or binding to Grb2. Instead, SOS's binding to phosphatidic acid (PA) is necessary and sufficient for SOS plasma membrane association and Ras activation *in vivo* (Zhao *et al.*, 2007). Interestingly, the PH domain of SWAP-70 binds to PA *in vitro* (Hilplelä *et al.*, 2003). It would be interesting to find out whether PA is also a targeting signal for SWAP-70 *in vivo*. Plasma membrane association of SOS upon EGFR activation depends on PA generation by phospholipase D2 (PLD2) (Zhao *et al.*, 2007). But since efficient SOS activation is also dependent on RasGRP1, one could speculate that SWAP-70 contributes to the cascade via recruitment of RasGRP1 to PA/phosphoinositide rich sites. Recruitment of RasGRP1 could then start a positive feedback loop with SOS, resulting in robust Ras activation and increased DAG levels that further stimulate RasGRP1. Therefore, if SWAP-70 recruited RasGRP1 to cortical F-actin filaments or to signaling complexes such as e.g. the B-cell-receptor, it could play an important role in the activation of Ras. Further studies are necessary to elucidate whether the interaction of SWAP-70 with RasGRP1 contributes to Ras regulation *in vivo*. The interpretation of the results is complicated by the findings that the RasGRP1-4 family members exhibit diverse functions (Coughlin *et al.*, 2005; Coughlin *et al.*, 2006; Layer *et al.*, 2003; Liu *et al.*, 2007b). SWAP-70 is a Rac-GTP binding protein and if it was important for Ras regulation, it would provide an interesting link between the Rac and the Ras signaling pathway.

## **7. References**

### **Books:**

Alberts, B., Johnson, A., Lewis, J., Raff, M., Roberts, K., Walter, P., Jaenicke, L. and Alberts-Johnson-Lewis-Raff-Roberts-Walter (2004). "Molekularbiologie Der Zelle" : [with: Cell Biology Interactive]. Weinheim: Wiley-VCH.

### **Diploma-theses:**

Lasić, Maja (2003). "Das Protein SWAP-70: Intramolekulare Interaktionen und GDP-Austauschaktivität für monomere G-Proteine der Rho-Familie."

Hülsmann, Bärbel (2004). „Untersuchungen zur subzellulären Lokalisation der Proteine Def6 (SLAT; IBP) und SWAP-70“

### **Dissertations:**

Hilpelä, Pirta (2002). „Identification of a transitional subset of fine actin filaments“

Oberbanscheidt, Pia (2005). „Charakterisierung der Funktion von SWAP-70 in der Makropinozytose und in Signalwegen, die das Aktinzytoskelett modulieren“

Uhlenbrock, Kathi (2006). „Untersuchungen zur Eingliederung von Myosin 9b in zelluläre Signalwege: Zielfindung, RhoGAP-Aktivität und Interaktionspartner“

Welsch, Thilo (2003). „Zur Rolle des CD2 assoziierten Proteins in Podozyten“

### **Scientific articles**

Rac downregulates Rho activity: reciprocal balance...[J Cell Biol. 1999] - PubMed Result.

Abercrombie, M., J.E. Heaysman, and S.M. Pegrum. 1970. The locomotion of fibroblasts in culture. I. Movements of the leading edge. *Exp Cell Res.* 59:393-8.

Adams, J.C. 2002. Molecular organisation of cell-matrix contacts: essential multiprotein assemblies in cell and tissue function. *Expert Rev Mol Med.* 4:1-24.

Ada-Nguema, A.S., H. Xenias, J.M. Hofman, C.H. Wiggins, M.P. Sheetz, and P.J. Keely. 2006. The small GTPase R-Ras regulates organization of actin and drives membrane protrusions through the activity of PLCepsilon. *J Cell Sci.* 119:1307-19.

Aghazadeh, B., W. Lowry, X. Huang, and M. Rosen. 2000. Structural basis for relief of autoinhibition of the Dbl homology domain of proto-oncogene Vav by tyrosine phosphorylation. *Cell.* 102:625-633.

Ahuja, R., R. Pinyol, N. Reichenbach, L. Custer, J. Klingensmith, M.M. Kessels, and B. Qualmann. 2007. Cordon-bleu is an actin nucleation factor and controls neuronal morphology. *Cell.* 131:337-50.

Aiba, Y., M. Oh-hora, S. Kiyonaka, Y. Kimura, A. Hijikata, Y. Mori, and T. Kurosaki. 2004. Activation of RasGRP3 by phosphorylation of Thr-133 is required for B cell receptor-mediated Ras activation. *Proc Natl Acad Sci U S A.* 101:16612-7.

Alai, M., A.L. Mui, R.L. Cutler, X.R. Bustelo, M. Barbacid, and G. Krystal. 1992. Steel factor stimulates the tyrosine phosphorylation of the proto-oncogene product, p95vav, in human hemopoietic cells. *The Journal of biological chemistry.* 267:18021-18025.

Alberts, A., H. Qin, H. Carr, and J. Frost. 2005. PAK1 negatively regulates the activity of the Rho exchange factor NET1. *The Journal of biological chemistry.* 280:12152-12161.

## References

- Allin, C., M. Ahmadian, A. Wittinghofer, and K. Gerwert. 2001. Monitoring the GAP catalyzed H-Ras GTPase reaction at atomic resolution in real time. *Proceedings of the National Academy of Sciences of the United States of America*. 98:7754-7759.
- Amano, T., K. Tanabe, T. Eto, S. Narumiya, and K. Mizuno. 2001. LIM-kinase 2 induces formation of stress fibres, focal adhesions and membrane blebs, dependent on its activation by Rho-associated kinase-catalysed phosphorylation at threonine-505. *Biochem J*. 354:149-59.
- Anton, I.M., M.A. de la Fuente, T.N. Sims, S. Freeman, N. Ramesh, J.H. Hartwig, M.L. Dustin, and R.S. Geha. 2002. WIP deficiency reveals a differential role for WIP and the actin cytoskeleton in T and B cell activation. *Immunity*. 16:193-204.
- Araki, N., T. Hatae, T. Yamada, and S. Hirohashi. 2000. Actinin-4 is preferentially involved in circular ruffling and macropinocytosis in mouse macrophages: analysis by fluorescence ratio imaging. *J Cell Sci*. 113 ( Pt 18):3329-40.
- Arcaro, A., U.K. Khanzada, B. Vanhaesebroeck, T.D. Tetley, M.D. Waterfield, and M.J. Seckl. 2002. Two distinct phosphoinositide 3-kinases mediate polypeptide growth factor-stimulated PKB activation. *Embo J*. 21:5097-108.
- Arnaout, M.A., S.L. Goodman, and J.-P. Xiong. 2007. Structure and mechanics of integrin-based cell adhesion. *Curr Opin Cell Biol*.
- Arthur, W., L. Petch, and K. Burridge. 2000. Integrin engagement suppresses RhoA activity via a c-Src-dependent mechanism. *Current biology : CB*. 10:719-722.
- Balcer, H.I., A.L. Goodman, A.A. Rodal, E. Smith, J. Kugler, J.E. Heuser, and B.L. Goode. 2003. Coordinated regulation of actin filament turnover by a high-molecular-weight Srv2/CAP complex, cofilin, profilin, and Aip1. *Curr Biol*. 13:2159-69.
- Ballestrem, C., B. Hinz, B.A. Imhof, and B. Wehrle-Haller. 2001. Marching at the front and dragging behind: differential alphaVbeta3-integrin turnover regulates focal adhesion behavior. *J Cell Biol*. 155:1319-32.
- Ballestrem, C., B. Wehrle-Haller, and B.A. Imhof. 1998. Actin dynamics in living mammalian cells. *J Cell Sci*. 111 ( Pt 12):1649-58.
- Bamburg, J.R. 1999. Proteins of the ADF/cofilin family: essential regulators of actin dynamics. *Annu Rev Cell Dev Biol*. 15:185-230.
- Bamburg, J.R., A. McGough, and S. Ono. 1999. Putting a new twist on actin: ADF/cofilins modulate actin dynamics. *Trends Cell Biol*. 9:364-70.
- Barkalow, K., W. Witke, D. Kwiatkowski, and J. Hartwig. 1996. Coordinated regulation of platelet actin filament barbed ends by gelsolin and capping protein. *The Journal of cell biology*. 134:389-399.
- Barry, S.T., and D.R. Critchley. 1994. The RhoA-dependent assembly of focal adhesions in Swiss 3T3 cells is associated with increased tyrosine phosphorylation and the recruitment of both pp125FAK and protein kinase C-delta to focal adhesions. *Journal of cell science*. 107 ( Pt 7):2033-2045.
- Bar-Sagi, D., and J.R. Feramisco. 1986. Induction of membrane ruffling and fluid-phase pinocytosis in quiescent fibroblasts by ras proteins. *Science (New York, N.Y.)*. 233:1061-1068.
- Bartles, J.R. 2000. Parallel actin bundles and their multiple actin-bundling proteins. *Curr Opin Cell Biol*. 12:72-8.
- Bartles, J.R., L. Zheng, A. Li, A. Wierda, and B. Chen. 1998. Small espin: a third actin-bundling protein and potential forked protein ortholog in brush border microvilli. *J Cell Biol*. 143:107-19.
- Baum, B., and P. Kunda. 2005. Actin nucleation: spire - actin nucleator in a class of its own. *Curr Biol*. 15:R305-8.
- Bear, J.E., T.M. Svitkina, M. Krause, D.A. Schafer, J.J. Loureiro, G.A. Strasser, I.V. Maly, O.Y. Chaga, J.A. Cooper, G.G. Borisy, and F.B. Gertler. 2002. Antagonism between Ena/VASP proteins and actin filament capping regulates fibroblast motility. *Cell*. 109:509-21.

## References

- Beaulieu, N., B. Zahedi, R.E. Goulding, G. Tazmini, K.V. Anthony, S.L. Omeis, D.R. de Jong, and R.J. Kay. 2007. Regulation of RasGRP1 by B cell antigen receptor requires cooperativity between three domains controlling translocation to the plasma membrane. *Mol Biol Cell*. 18:3156-68.
- Berrier, A.L., and K.M. Yamada. 2007. Cell-matrix adhesion. *J Cell Physiol*. 213:565-73.
- Bertling, E., O. Quintero-Monzon, P. Mattila, B. Goode, and P. Lappalainen. 2007. Mechanism and biological role of profilin-Srv2/CAP interaction. *Journal of Cell Science*. 120:1225-1234.
- Bettinger, B.T., D.M. Gilbert, and D.C. Amberg. 2004. Actin up in the nucleus. *Nat Rev Mol Cell Biol*. 5:410-5.
- Bhattacharya, N., S. Ghosh, D. Sept, and J.A. Cooper. 2006. Binding of myotrophin/V-1 to actin-capping protein: implications for how capping protein binds to the filament barbed end. *J Biol Chem*. 281:31021-30.
- Bijlmakers, M.J., and M. Marsh. 2003. The on-off story of protein palmitoylation. *Trends Cell Biol*. 13:32-42.
- Bivona, T.G., I. Perez De Castro, I.M. Ahearn, T.M. Grana, V.K. Chiu, P.J. Lockyer, P.J. Cullen, A. Pellicer, A.D. Cox, and M.R. Philips. 2003. Phospholipase Cgamma activates Ras on the Golgi apparatus by means of RasGRP1. *Nature*. 424:694-8.
- Borggreffe, T., S. Keshavarzi, B. Gross, M. Wabl, and R. Jessberger. 2001. Impaired IgE response in SWAP-70-deficient mice. *Eur J Immunol*. 31:2467-75.
- Borggreffe, T., L. Masat, M. Wabl, B. Riwar, G. Cattoretti, and R. Jessberger. 1999. Cellular, intracellular, and developmental expression patterns of murine SWAP-70. *Eur J Immunol*. 29:1812-22.
- Borggreffe, T., M. Wabl, A.T. Akhmedov, and R. Jessberger. 1998. A B-cell-specific DNA recombination complex. *J Biol Chem*. 273:17025-35.
- Borm, B., R.P. Requardt, V. Herzog, and G. Kirfel. 2005. Membrane ruffles in cell migration: indicators of inefficient lamellipodia adhesion and compartments of actin filament reorganization. *Exp Cell Res*. 302:83-95.
- Bos, J.L., H. Rehmann, and A. Wittinghofer. 2007. GEFs and GAPs: critical elements in the control of small G proteins. *Cell*. 129:865-77.
- Boulter, E., D. Grall, S. Cagnol, and E. Van Obberghen-Schilling. 2006. Regulation of cell-matrix adhesion dynamics and Rac-1 by integrin linked kinase. *Faseb J*. 20:1489-91.
- Boureaux, A., E. Vignal, S. Faure, and P. Fort. 2007. Evolution of the Rho family of ras-like GTPases in eukaryotes. *Molecular biology and evolution*. 24:203-216.
- Bourne, H., C. Landis, and S. Masters. 1989. Hydrolysis of GTP by the alpha-chain of Gs and other GTP binding proteins. *Proteins*. 6:222-230.
- Bourne, H., and O. Weiner. 2002. A chemical compass. *Nature*. 419:21.
- Bourne, H.R., D.A. Sanders, and F. McCormick. 1990. The GTPase superfamily: a conserved switch for diverse cell functions. *Nature*. 348:125-32.
- Bourne, H.R., D.A. Sanders, and F. McCormick. 1991. The GTPase superfamily: conserved structure and molecular mechanism. *Nature*. 349:117-27.
- Brakebusch, C., and R. Fassler. 2003. The integrin-actin connection, an eternal love affair. *Embo J*. 22:2324-33.
- Bretscher, A., K. Edwards, and R. Fehon. 2002. ERM proteins and merlin: integrators at the cell cortex. *Nature reviews. Molecular cell biology*. 3:586-599.
- Burtnick, L.D., D. Urosev, E. Irobi, K. Narayan, and R.C. Robinson. 2004. Structure of the N-terminal half of gelsolin bound to actin: roles in severing, apoptosis and FAF. *Embo J*. 23:2713-22.
- Buss, F., C. Temm-Grove, S. Henning, and B.M. Jockusch. 1992. Distribution of profilin in fibroblasts correlates with the presence of highly dynamic actin filaments. *Cell Motil Cytoskeleton*. 22:51-61.
- Bustelo, X.R. 2000. Regulatory and signaling properties of the Vav family. *Mol Cell Biol*. 20:1461-77.



## References

- Caloca, M.J., J.L. Zugaza, D. Matallanas, P. Crespo, and X.R. Bustelo. 2003. Vav mediates Ras stimulation by direct activation of the GDP/GTP exchange factor Ras GRP1. *Embo J.* 22:3326-36.
- Caloca, M.J., J.L. Zugaza, M. Vicente-Manzanares, F. Sanchez-Madrid, and X.R. Bustelo. 2004. F-actin-dependent translocation of the Rap1 GDP/GTP exchange factor RasGRP2. *J Biol Chem.* 279:20435-46.
- Carlier, M.F., C. Jean, K.J. Rieger, M. Lenfant, and D. Pantaloni. 1993. Modulation of the interaction between G-actin and thymosin beta 4 by the ATP/ADP ratio: possible implication in the regulation of actin dynamics. *Proc Natl Acad Sci U S A.* 90:5034-8.
- Carlier, M.F., C. Le Clainche, S. Wiesner, and D. Pantaloni. 2003. Actin-based motility: from molecules to movement. *Bioessays.* 25:336-45.
- Carlier, M.F., P. Nioche, I. Broutin-L'Hermite, R. Boujemaa, C. Le Clainche, C. Egile, C. Garbay, A. Ducruix, P. Sansonetti, and D. Pantaloni. 2000. GRB2 links signaling to actin assembly by enhancing interaction of neural Wiskott-Aldrich syndrome protein (N-WASp) with actin-related protein (ARP2/3) complex. *J Biol Chem.* 275:21946-52.
- Carrasco, S., and I. Merida. 2004. Diacylglycerol-dependent binding recruits PKCtheta and RasGRP1 C1 domains to specific subcellular localizations in living T lymphocytes. *Mol Biol Cell.* 15:2932-42.
- Chang, L., and R.D. Goldman. 2004. Intermediate filaments mediate cytoskeletal crosstalk. *Nat Rev Mol Cell Biol.* 5:601-13.
- Chardin, P. 2006. Function and regulation of Rnd proteins. *Nature reviews. Molecular cell biology.* 7:54-62.
- Chaudhary, A., W. King, M. Mattaliano, J. Frost, B. Diaz, D. Morrison, M. Cobb, M. Marshall, and J. Brugge. 2000. Phosphatidylinositol 3-kinase regulates Raf1 through Pak phosphorylation of serine 338. *Current biology : CB.* 10:551-554.
- Chen, J., S. Zhuang, T. Nguyen, G. Boss, and R. Pilz. 2003. Oncogenic Ras leads to Rho activation by activating the mitogen-activated protein kinase pathway and decreasing Rho-GTPase-activating protein activity. *The Journal of biological chemistry.* 278:2807-2818.
- Cheung, S.M., J.C. Kornelson, M. Al-Alwan, and A.J. Marshall. 2007. Regulation of phosphoinositide 3-kinase signaling by oxidants: hydrogen peroxide selectively enhances immunoreceptor-induced recruitment of phosphatidylinositol (3,4) bisphosphate-binding PH domain proteins. *Cell Signal.* 19:902-12.
- Chhabra, E.S., and H.N. Higgs. 2007. The many faces of actin: matching assembly factors with cellular structures. *Nat Cell Biol.* 9:1110-21.
- Chou, Y.H., F.W. Flitney, L. Chang, M. Mendez, B. Grin, and R.D. Goldman. 2007. The motility and dynamic properties of intermediate filaments and their constituent proteins. *Exp Cell Res.* 313:2236-43.
- Chung, C., S. Funamoto, and R. Firtel. 2001. Signaling pathways controlling cell polarity and chemotaxis. *Trends in biochemical sciences.* 26:557-566.
- Clyde-Smith, J., G. Silins, M. Gartside, S. Grimmond, M. Etheridge, A. Apolloni, N. Hayward, and J.F. Hancock. 2000. Characterization of RasGRP2, a plasma membrane-targeted, dual specificity Ras/Rap exchange factor. *J Biol Chem.* 275:32260-7.
- Co, C., D. Wong, S. Gierke, V. Chang, and J. Taunton. 2007. Mechanism of actin network attachment to moving membranes: barbed end capture by N-WASP WH2 domains. *Cell.* 128:901-913.
- Condeelis, J., and R.H. Singer. 2005. How and why does beta-actin mRNA target? *Biol Cell.* 97:97-110.
- Connolly, B.A., J. Rice, L.A. Feig, and R.J. Buchsbaum. 2005. Tiam1-IRSp53 complex formation directs specificity of rac-mediated actin cytoskeleton regulation. *Mol Cell Biol.* 25:4602-14.
- Cooper, J.A., S.B. Walker, and T.D. Pollard. 1983. Pyrene actin: documentation of the validity of a sensitive assay for actin polymerization. *J Muscle Res Cell Motil.* 4:253-62.

## References

- Cory, G.O., R. Cramer, L. Blanchoin, and A.J. Ridley. 2003. Phosphorylation of the WASP-VCA domain increases its affinity for the Arp2/3 complex and enhances actin polymerization by WASP. *Mol Cell*. 11:1229-39.
- Coughlin, J., S. Stang, N. Dower, and J. Stone. 2005. RasGRP1 and RasGRP3 Regulate B Cell Proliferation by Facilitating B Cell Receptor-Ras Signaling. *The Journal of Immunology*. 175:7179-7184.
- Coughlin, J.J., S.L. Stang, N.A. Dower, and J.C. Stone. 2006. The role of RasGRPs in regulation of lymphocyte proliferation. *Immunol Lett*. 105:77-82.
- Cunningham, C. 1995. Actin polymerization and intracellular solvent flow in cell surface blebbing. *The Journal of cell biology*. 129:1589-1599.
- Dartsch, P.C., M. Ritter, D. Haussinger, and F. Lang. 1994. Cytoskeletal reorganization in NIH 3T3 fibroblasts expressing the ras oncogene. *Eur J Cell Biol*. 63:316-25.
- Das, B., X. Shu, G. Day, J. Han, U. Krishna, J. Falck, and D. Broek. 2000. Control of intramolecular interactions between the pleckstrin homology and Dbl homology domains of Vav and Sos1 regulates Rac binding. *The Journal of biological chemistry*. 275:15074-15081.
- de la Fuente, M.A., Y. Sasahara, M. Calamito, I.M. Anton, A. Elkhali, M.D. Gallego, K. Suresh, K. Siminovitch, H.D. Ochs, K.C. Anderson, F.S. Rosen, R.S. Geha, and N. Ramesh. 2007. WIP is a chaperone for Wiskott-Aldrich syndrome protein (WASP). *Proc Natl Acad Sci U S A*. 104:926-31.
- Defilippi, P., C. Olivo, M. Venturino, L. Dolce, L. Silengo, and G. Tarone. 1999. Actin cytoskeleton organization in response to integrin-mediated adhesion. *Microscopy research and technique*. 47:67-78.
- del Pozo, M.A., N.B. Alderson, W.B. Kiosses, H.H. Chiang, R.G. Anderson, and M.A. Schwartz. 2004. Integrins regulate Rac targeting by internalization of membrane domains. *Science*. 303:839-42.
- Del Pozo, M.A., W.B. Kiosses, N.B. Alderson, N. Meller, K.M. Hahn, and M.A. Schwartz. 2002. Integrins regulate GTP-Rac localized effector interactions through dissociation of Rho-GDI. *Nat Cell Biol*. 4:232-9.
- Delon, I., and N.H. Brown. 2007. Integrins and the actin cytoskeleton. *Curr Opin Cell Biol*. 19:43-50.
- DeMali, K.A., C.A. Barlow, and K. Burridge. 2002. Recruitment of the Arp2/3 complex to vinculin: coupling membrane protrusion to matrix adhesion. *J Cell Biol*. 159:881-91.
- DerMardirossian, C., and G.M. Bokoch. 2005. GDIs: central regulatory molecules in Rho GTPase activation. *Trends Cell Biol*. 15:356-63.
- DeRosier, D., and L. Tilney. 2000. F-actin bundles are derivatives of microvilli: What does this tell us about how bundles might form? *The Journal of cell biology*. 148:1-6.
- DesMarais, V., M. Ghosh, R. Eddy, and J. Condeelis. 2005. Cofilin takes the lead. *J Cell Sci*. 118:19-26.
- Dharmawardhane, S., A. Schürmann, M. Sells, J. Chernoff, S. Schmid, and G. Bokoch. 2000. Regulation of macropinocytosis by p21-activated kinase-1. *Molecular biology of the cell*. 11:3341-3352.
- Disanza, A., A. Steffen, M. Hertzog, E. Frittoli, K. Rottner, and G. Scita. 2005. Actin polymerization machinery: the finish line of signaling networks, the starting point of cellular movement. *Cell Mol Life Sci*. 62:955-70.
- Djinovic-Carugo, K., M. Gautel, J. Ylanne, and P. Young. 2002. The spectrin repeat: a structural platform for cytoskeletal protein assemblies. *FEBS Lett*. 513:119-23.
- dos Remedios, C.G., D. Chhabra, M. Kekic, I.V. Dedova, M. Tsubakihara, D.A. Berry, and N.J. Nosworthy. 2003. Actin binding proteins: regulation of cytoskeletal microfilaments. *Physiol Rev*. 83:433-73.
- Downward, J. 2003. Targeting RAS signalling pathways in cancer therapy. *Nat Rev Cancer*. 3:11-22.
- Dransart, E., B. Olofsson, and J. Cherfils. 2005. RhoGDIs revisited: novel roles in Rho regulation. *Traffic (Copenhagen, Denmark)*. 6:957-966.

## References

- Drenckhahn, D., K. Engel, D. Höfer, C. Merte, L. Tilney, and M. Tilney. 1991. Three different actin filament assemblies occur in every hair cell: each contains a specific actin crosslinking protein. *The Journal of cell biology*. 112:641-651.
- Ebinu, J.O., D.A. Bottorff, E.Y. Chan, S.L. Stang, R.J. Dunn, and J.C. Stone. 1998. RasGRP, a Ras guanyl nucleotide-releasing protein with calcium- and diacylglycerol-binding motifs. *Science*. 280:1082-6.
- Ebinu, J.O., S.L. Stang, C. Teixeira, D.A. Bottorff, J. Hooton, P.M. Blumberg, M. Barry, R.C. Bleakley, H.L. Ostergaard, and J.C. Stone. 2000. RasGRP links T-cell receptor signaling to Ras. *Blood*. 95:3199-203.
- Eden, S., R. Rohatgi, A.V. Podtelejnikov, M. Mann, and M.W. Kirschner. 2002. Mechanism of regulation of WAVE1-induced actin nucleation by Rac1 and Nck. *Nature*. 418:790-3.
- Efimov, A., A. Kharitonov, N. Efimova, J. Loncarek, P.M. Miller, N. Andreyeva, P. Gleeson, N. Galjart, A.R. Maia, I.X. McLeod, J.R. Yates, 3rd, H. Maiato, A. Khodjakov, A. Akhmanova, and I. Kaverina. 2007. Asymmetric CLASP-dependent nucleation of noncentrosomal microtubules at the trans-Golgi network. *Dev Cell*. 12:917-30.
- Endlich, N., C.A. Otey, W. Kriz, and K. Endlich. 2007. Movement of stress fibers away from focal adhesions identifies focal adhesions as sites of stress fiber assembly in stationary cells. *Cell Motil Cytoskeleton*.
- Etienne-Manneville, S., and A. Hall. 2002. Rho GTPases in cell biology. *Nature*. 420:629-35.
- Eva, A., G. Vecchio, C.D. Rao, S.R. Tronick, and S.A. Aaronson. 1988. The predicted DBL oncogene product defines a distinct class of transforming proteins. *Proc Natl Acad Sci U S A*. 85:2061-5.
- Evans, E.A., and D.A. Calderwood. 2007. Forces and bond dynamics in cell adhesion. *Science*. 316:1148-53.
- Fanzo, J.C., W. Yang, S.Y. Jang, S. Gupta, Q. Chen, A. Siddiq, S. Greenberg, and A.B. Pernis. 2006. Loss of IRF-4-binding protein leads to the spontaneous development of systemic autoimmunity. *J Clin Invest*. 116:703-14.
- Felder, S., and E.L. Elson. 1990. Mechanics of fibroblast locomotion: quantitative analysis of forces and motions at the leading lamellas of fibroblasts. *J Cell Biol*. 111:2513-26.
- Ferguson, K., M. Lemmon, J. Schlessinger, and P. Sigler. 1995. Structure of the high affinity complex of inositol trisphosphate with a phospholipase C pleckstrin homology domain. *Cell*. 83:1037-1046.
- Fincham, V.J., M. James, M.C. Frame, and S.J. Winder. 2000. Active ERK/MAP kinase is targeted to newly forming cell-matrix adhesions by integrin engagement and v-Src. *Embo J*. 19:2911-23.
- Fishkind, D.J., L.G. Cao, and Y.L. Wang. 1991. Microinjection of the catalytic fragment of myosin light chain kinase into dividing cells: effects on mitosis and cytokinesis. *J Cell Biol*. 114:967-75.
- Footer, M., J. Kerssemakers, J. Theriot, and M. Dogterom. 2007. Direct measurement of force generation by actin filament polymerization using an optical trap. *Proceedings of the National Academy of Sciences*. 104:2181-2186.
- Foster, F.M., C.J. Traer, S.M. Abraham, and M.J. Fry. 2003. The phosphoinositide (PI) 3-kinase family. *J Cell Sci*. 116:3037-40.
- Fowler, V.M., N.J. Greenfield, and J. Moyer. 2003. Tropomodulin contains two actin filament pointed end-capping domains. *J Biol Chem*. 278:40000-9.
- Franco, S., and A. Huttenlocher. 2005. Regulating cell migration: calpains make the cut. *Journal of cell science*. 118:3829-3838.
- Franke, T.F., D.R. Kaplan, L.C. Cantley, and A. Toker. 1997. Direct regulation of the Akt proto-oncogene product by phosphatidylinositol-3,4-bisphosphate. *Science*. 275:665-8.
- Fujisawa, K., A. Fujita, T. Ishizaki, Y. Saito, and S. Narumiya. 1996. Identification of the Rho-binding domain of p160ROCK, a Rho-associated coiled-coil containing protein kinase. *J Biol Chem*. 271:23022-8.

## References

- Fujiwara, I., S. Takahashi, H. Tadakuma, T. Funatsu, and S. Ishiwata. 2002. Microscopic analysis of polymerization dynamics with individual actin filaments. *Nat Cell Biol.* 4:666-73.
- Fukuoka, M., S. Suetsugu, H. Miki, K. Fukami, T. Endo, and T. Takenawa. 2001. A novel neural Wiskott-Aldrich syndrome protein (N-WASP) binding protein, WISH, induces Arp2/3 complex activation independent of Cdc42. *The Journal of cell biology.* 152:471-482.
- Funamoto, S., R. Meili, S. Lee, L. Parry, and R. Firtel. 2002. Spatial and temporal regulation of 3-phosphoinositides by PI 3-kinase and PTEN mediates chemotaxis. *Cell.* 109:611-623.
- Galbraith, C.G., K.M. Yamada, and J.A. Galbraith. 2007. Polymerizing actin fibers position integrins primed to probe for adhesion sites. *Science.* 315:992-5.
- Galbraith, C.G., K.M. Yamada, and M.P. Sheetz. 2002. The relationship between force and focal complex development. *J Cell Biol.* 159:695-705.
- Galkin, V.E., A. Orlova, N. Lukyanova, W. Wriggers, and E.H. Egelman. 2001. Actin depolymerizing factor stabilizes an existing state of F-actin and can change the tilt of F-actin subunits. *J Cell Biol.* 153:75-86.
- Gautreau, A., H.Y. Ho, J. Li, H. Steen, S.P. Gygi, and M.W. Kirschner. 2004. Purification and architecture of the ubiquitous Wave complex. *Proc Natl Acad Sci U S A.* 101:4379-83.
- Geiger, B., A. Bershadsky, R. Pankov, and K. Yamada. 2001. Transmembrane crosstalk between the extracellular matrix--cytoskeleton crosstalk. *Nature reviews. Molecular cell biology.* 2:793-805.
- Ghosh, M., X. Song, G. Mouneimne, M. Sidani, D.S. Lawrence, and J.S. Condeelis. 2004. Cofilin promotes actin polymerization and defines the direction of cell motility. *Science.* 304:743-6.
- Giannone, G., B.J. Dubin-Thaler, O. Rossier, Y. Cai, O. Chaga, G. Jiang, W. Beaver, H.G. Dobereiner, Y. Freund, G. Borisy, and M.P. Sheetz. 2007. Lamellipodial actin mechanically links myosin activity with adhesion-site formation. *Cell.* 128:561-75.
- Giannone, G., P. Rondé, M. Gaire, J. Beaudouin, J. Haiech, J. Ellenberg, and K. Takeda. 2004. Calcium rises locally trigger focal adhesion disassembly and enhance residency of focal adhesion kinase at focal adhesions. *The Journal of biological chemistry.* 279:28715-28723.
- Goldfinger, L.E., C. Ptak, E.D. Jeffery, J. Shabanowitz, D.F. Hunt, and M.H. Ginsberg. 2006. RLIP76 (RalBP1) is an R-Ras effector that mediates adhesion-dependent Rac activation and cell migration. *The Journal of Cell Biology.* 174:877-888.
- Goldschmidt-Clermont, P.J., M.I. Furman, D. Wachsstock, D. Safer, V.T. Nachmias, and T.D. Pollard. 1992. The control of actin nucleotide exchange by thymosin beta 4 and profilin. A potential regulatory mechanism for actin polymerization in cells. *Mol Biol Cell.* 3:1015-24.
- Goley, E., and M. Welch. 2006. The ARP2/3 complex: an actin nucleator comes of age. *Nature reviews. Molecular cell biology.* 7:713-726.
- Goode, B.L., and M.J. Eck. 2007. Mechanism and function of formins in the control of actin assembly. *Annu Rev Biochem.* 76:593-627.
- Goodwin, J., K. Drake, C. Rogers, L. Wright, J. Lippincott-Schwartz, M. Philips, and A. Kenworthy. 2005. Depalmitoylated Ras traffics to and from the Golgi complex via a nonvesicular pathway. *The Journal of cell biology.* 170:261-272.
- Grashoff, C., I. Thievensen, K. Lorenz, S. Ussar, and R. Fässler. 2004. Integrin-linked kinase: integrin's mysterious partner. *Curr Opin Cell Biol.* 16:565-571.
- Greaves, J., and L. Chamberlain. 2007. Palmitoylation-dependent protein sorting. *The Journal of cell biology.* 176:249-254.
- Greaves, J., and L.H. Chamberlain. 2006. Dual role of the cysteine-string domain in membrane binding and palmitoylation-dependent sorting of the molecular chaperone cysteine-string protein. *Mol Biol Cell.* 17:4748-59.

## References

- Gross, B., T. Borggrefe, M. Wabl, R.R. Sivalenka, M. Bennett, A.B. Rossi, and R. Jessberger. 2002. SWAP-70-deficient mast cells are impaired in development and IgE-mediated degranulation. *Eur J Immunol.* 32:1121-8.
- Guo, F., M. Debidda, L. Yang, D. Williams, and Y. Zheng. 2006. Genetic deletion of Rac1 GTPase reveals its critical role in actin stress fiber formation and focal adhesion complex assembly. *The Journal of biological chemistry.* 281:18652-18659.
- Gupton, S.L., K.L. Anderson, T.P. Kole, R.S. Fischer, A. Ponti, S.E. Hitchcock-DeGregori, G. Danuser, V.M. Fowler, D. Wirtz, D. Hanein, and C.M. Waterman-Storer. 2005. Cell migration without a lamellipodium: translation of actin dynamics into cell movement mediated by tropomyosin. *J Cell Biol.* 168:619-31.
- Gupton, S.L., and C.M. Waterman-Storer. 2006. Spatiotemporal feedback between actomyosin and focal-adhesion systems optimizes rapid cell migration. *Cell.* 125:1361-74.
- Hall, A. 1998. Rho GTPases and the actin cytoskeleton. *Science.* 279:509-14.
- Hall, A. 2005. Rho GTPases and the control of cell behaviour. *Biochem Soc Trans.* 33:891-5.
- Hamada, K., T. Shimizu, S. Yonemura, S. Tsukita, and T. Hakoshima. 2003. Structural basis of adhesion-molecule recognition by ERM proteins revealed by the crystal structure of the radixin-ICAM-2 complex. *Embo J.* 22:502-14.
- Hamadi, A., M. Bouali, M. Dontenwill, H. Stoeckel, K. Takeda, and P. Rondé. 2005. Regulation of focal adhesion dynamics and disassembly by phosphorylation of FAK at tyrosine 397. *Journal of cell science.* 118:4415-4425.
- Hancock, J.F., H. Paterson, and C.J. Marshall. 1990. A polybasic domain or palmitoylation is required in addition to the CAAX motif to localize p21ras to the plasma membrane. *Cell.* 63:133-9.
- Harris, E.S., F. Li, and H.N. Higgs. 2004. The mouse formin, FRLalpha, slows actin filament barbed end elongation, competes with capping protein, accelerates polymerization from monomers, and severs filaments. *J Biol Chem.* 279:20076-87.
- Hashimoto, Y., M. Parsons, and J.C. Adams. 2007. Dual actin-bundling and protein kinase C-binding activities of fascin regulate carcinoma cell migration downstream of Rac and contribute to metastasis. *Mol Biol Cell.* 18:4591-602.
- Hatzoglou, A., I. Ader, A. Spingard, J. Flanders, E. Saade, I. Leroy, S. Traver, S. Aresta, and J. de Gunzburg. 2007. Gem associates with Ezrin and acts via the Rho-GAP protein Gmp1 to down-regulate the Rho pathway. *Mol Biol Cell.* 18:1242-52.
- Heath, J.P., and B.F. Holifield. 1993. On the mechanisms of cortical actin flow and its role in cytoskeletal organisation of fibroblasts. *Symp Soc Exp Biol.* 47:35-56.
- Hemmings, L., D.J. Rees, V. Ohanian, S.J. Bolton, A.P. Gilmore, B. Patel, H. Priddle, J.E. Trevithick, R.O. Hynes, and D.R. Critchley. 1996. Talin contains three actin-binding sites each of which is adjacent to a vinculin-binding site. *J Cell Sci.* 109 ( Pt 11):2715-26.
- Higashida, C., T. Miyoshi, A. Fujita, F. Ocegüera-Yanez, J. Monypenny, Y. Andou, S. Narumiya, and N. Watanabe. 2004. Actin polymerization-driven molecular movement of mDia1 in living cells. *Science.* 303:2007-10.
- Higgs, H.N., and T.D. Pollard. 2001. Regulation of actin filament network formation through ARP2/3 complex: activation by a diverse array of proteins. *Annu Rev Biochem.* 70:649-76.
- Hildebrand, J.D., M.D. Schaller, and J.T. Parsons. 1995. Paxillin, a tyrosine phosphorylated focal adhesion-associated protein binds to the carboxyl terminal domain of focal adhesion kinase. *Mol Biol Cell.* 6:637-47.
- Hilpelä, P., P. Oberbanscheidt, P. Hahne, M. Hund, G. Kalhammer, J.V. Small, and M. Bähler. 2003. SWAP-70 identifies a transitional subset of actin filaments in motile cells. *Mol Biol Cell.* 14:3242-53.

## References

- Hirao, M., N. Sato, T. Kondo, S. Yonemura, M. Monden, T. Sasaki, Y. Takai, and S. Tsukita. 1996. Regulation mechanism of ERM (ezrin/radixin/moesin) protein/plasma membrane association: possible involvement of phosphatidylinositol turnover and Rho-dependent signaling pathway. *J Cell Biol.* 135:37-51.
- Hirsch, E., V. Katanaev, C. Garlanda, O. Azzolino, L. Pirola, L. Silengo, S. Sozzani, A. Mantovani, F. Altruda, and M. Wymann. 2000. Central role for G protein-coupled phosphoinositide 3-kinase gamma in inflammation. *Science (New York, N.Y.)*. 287:1049-1053.
- Ho, H.Y., R. Rohatgi, A.M. Lebensohn, M. Le, J. Li, S.P. Gygi, and M.W. Kirschner. 2004. Toca-1 mediates Cdc42-dependent actin nucleation by activating the N-WASP-WIP complex. *Cell*. 118:203-16.
- Hofer, D., W. Ness, and D. Drenckhahn. 1997. Sorting of actin isoforms in chicken auditory hair cells. *J Cell Sci.* 110 ( Pt 6):765-70.
- Hofmann, W.A., L. Stojiljkovic, B. Fuchsova, G.M. Vargas, E. Mavrommatis, V. Philimonenko, K. Kysela, J.A. Goodrich, J.L. Lessard, T.J. Hope, P. Hozak, and P. de Lanerolle. 2004. Actin is part of pre-initiation complexes and is necessary for transcription by RNA polymerase II. *Nat Cell Biol.* 6:1094-101.
- Hogan, A., Y. Yakubchik, J.e. Chabot, C. Obagi, E. Daher, K. Maekawa, and S.H. Gee. 2004. The phosphoinositol 3,4-bisphosphate-binding protein TAPP1 interacts with syntrophins and regulates actin cytoskeletal organization. *The Journal of biological chemistry.* 279:53717-53724.
- Holmes, K.C., D. Popp, W. Gebhard, and W. Kabsch. 1990. Atomic model of the actin filament. *Nature.* 347:44-9.
- Hotulainen, P., and P. Lappalainen. 2006. Stress fibers are generated by two distinct actin assembly mechanisms in motile cells. *J Cell Biol.* 173:383-94.
- Hotulainen, P., E. Paunola, M. Vartiainen, and P. Lappalainen. 2005. Actin-depolymerizing factor and cofilin-1 play overlapping roles in promoting rapid F-actin depolymerization in mammalian nonmuscle cells. *Molecular biology of the cell.* 16:649-664.
- Hu, K., L. Ji, K. Applegate, G. Danuser, and C. Waterman-Storer. 2007. Differential transmission of actin motion within focal adhesions. *Science (New York, N.Y.)*. 315:111-115.
- Innocenti, M., A. Zucconi, A. Disanza, E. Frittoli, L.B. Areces, A. Steffen, T.E. Stradal, P.P. Di Fiore, M.F. Carrier, and G. Scita. 2004. Abi1 is essential for the formation and activation of a WAVE2 signalling complex. *Nat Cell Biol.* 6:319-27.
- Ishikawa, K., T. Nagase, M. Suyama, N. Miyajima, A. Tanaka, H. Kotani, N. Nomura, and O. Ohara. 1998. Prediction of the coding sequences of unidentified human genes. X. The complete sequences of 100 new cDNA clones from brain which can code for large proteins in vitro. *DNA Res.* 5:169-76.
- Izawa, I., M. Amano, K. Chihara, T. Yamamoto, and K. Kaibuchi. 1998. Possible involvement of the inactivation of the Rho-Rho-kinase pathway in oncogenic Ras-induced transformation. *Oncogene.* 17:2863-2871.
- Janmey, P.A., and U. Lindberg. 2004. Cytoskeletal regulation: rich in lipids. *Nat Rev Mol Cell Biol.* 5:658-66.
- Johannes, L., and C. Lamaze. 2002. Clathrin-dependent or not: is it still the question? *Traffic.* 3:443-51.
- Kabsch, W., H.G. Mannherz, D. Suck, E.F. Pai, and K.C. Holmes. 1990. Atomic structure of the actin:DNase I complex. *Nature.* 347:37-44.
- Karakozova, M., M. Kozak, C.C. Wong, A.O. Bailey, J.R. Yates, 3rd, A. Mogilner, H. Zebroski, and A. Kashina. 2006. Arginylation of beta-actin regulates actin cytoskeleton and cell motility. *Science.* 313:192-6.
- Kawano, Y., Y. Fukata, N. Oshiro, M. Amano, T. Nakamura, M. Ito, F. Matsumura, M. Inagaki, and K. Kaibuchi. 1999. Phosphorylation of myosin-binding subunit (MBS) of myosin phosphatase by Rho-kinase in vivo. *J Cell Biol.* 147:1023-38.

## References

- Khaitlina, S., and H. Hinssen. 2002. Ca-dependent binding of actin to gelsolin. *FEBS Lett.* 521:14-8.
- Klippel, A., W. Kavanaugh, D. Pot, and L. Williams. 1997. A specific product of phosphatidylinositol 3-kinase directly activates the protein kinase Akt through its pleckstrin homology domain. *Molecular and cellular biology.* 17:338-344.
- Kovar, D., and T. Pollard. 2004. Insertional assembly of actin filament barbed ends in association with formins produces piconewton forces. *Proceedings of the National Academy of Sciences of the United States of America.* 101:14725-14730.
- Krahn, A.K., K. Ma, S. Hou, V. Duronio, and A.J. Marshall. 2004. Two distinct waves of membrane-proximal B cell antigen receptor signaling differentially regulated by Src homology 2-containing inositol polyphosphate 5-phosphatase. *J Immunol.* 172:331-9.
- Krueger, E., J. Orth, H. Cao, and M. McNiven. 2003. A Dynamin-Cortactin-Arp2/3 Complex Mediates Actin Reorganization in Growth Factor-stimulated Cells. *Molecular Biology of the Cell.* 14:1085-1096.
- Kuhn, J.R., and T.D. Pollard. 2007. Single molecule kinetic analysis of actin filament capping. Polyphosphoinositides do not dissociate capping proteins. *J Biol Chem.* 282:28014-24.
- Kurokawa, K., and M. Matsuda. 2005. Localized RhoA activation as a requirement for the induction of membrane ruffling. *Mol Biol Cell.* 16:4294-303.
- Lammers, M., R. Rose, A. Scrima, and A. Wittinghofer. 2005. The regulation of mDia1 by autoinhibition and its release by Rho\*GTP. *Embo J.* 24:4176-87.
- Lanzetti, L., A. Palamidessi, L. Areces, G. Scita, and P.P. Di Fiore. 2004. Rab5 is a signalling GTPase involved in actin remodelling by receptor tyrosine kinases. *Nature.* 429:309-14.
- Lauffenburger, D.A., and A.F. Horwitz. 1996. Cell migration: a physically integrated molecular process. *Cell.* 84:359-69.
- Laukaitis, C., D. Webb, K. Donais, and A. Horwitz. 2001. Differential dynamics of alpha 5 integrin, paxillin, and alpha-actinin during formation and disassembly of adhesions in migrating cells. *The Journal of cell biology.* 153:1427-1440.
- Layer, K., G. Lin, A. Nencioni, W. Hu, A. Schmucker, A.N. Antov, X. Li, S. Takamatsu, T. Chevassut, N.A. Dower, S.L. Stang, D. Beier, J. Buhlmann, R.T. Bronson, K.B. Elkon, J.C. Stone, L. Van Parijs, and B. Lim. 2003. Autoimmunity as the consequence of a spontaneous mutation in Rasgrp1. *Immunity.* 19:243-55.
- Lazarides, E., and K. Burridge. 1975. Alpha-actinin: immunofluorescent localization of a muscle structural protein in nonmuscle cells. *Cell.* 6:289-98.
- Lee, S., and D. Helfman. 2004. Cytoplasmic p21Cip1 is involved in Ras-induced inhibition of the ROCK/LIMK/cofilin pathway. *The Journal of biological chemistry.* 279:1885-1891.
- Legate, K.R., E. Montanez, O. Kudlacek, and R. Fassler. 2006. ILK, PINCH and parvin: the tIPP of integrin signalling. *Nat Rev Mol Cell Biol.* 7:20-31.
- Lemmon, M.A. 2003. Phosphoinositide recognition domains. *Traffic.* 4:201-13.
- Lennartsson, J., and L. Ronnstrand. 2006. The stem cell factor receptor/c-Kit as a drug target in cancer. *Curr Cancer Drug Targets.* 6:65-75.
- Li, Z., X. Dong, X. Dong, Z. Wang, W. Liu, N. Deng, Y. Ding, L. Tang, T. Hla, R. Zeng, L. Li, and D. Wu. 2005. Regulation of PTEN by Rho small GTPases. *Nature cell biology.* 7:399-404.
- Li, Z., H. Jiang, W. Xie, Z. Zhang, A.V. Smrcka, and D. Wu. 2000. Roles of PLC-beta2 and -beta3 and PI3Kgamma in chemoattractant-mediated signal transduction. *Science.* 287:1046-9.
- Liu, J., D. Li, B. Cao, Y.X. Li, R. Herva, Y.S. Piao, and Y.L. Wang. 2007a. Expression and localization of SWAP-70 in human fetomaternal interface and placenta during tubal pregnancy and normal placentation. *J Histochem Cytochem.* 55:701-8.
- Liu, Y., M. Zhu, K. Nishida, T. Hirano, and W. Zhang. 2007b. An essential role for RasGRP1 in mast cell function and IgE-mediated allergic response. *J Exp Med.* 204:93-103.

## References

- Loomis, P., L. Zheng, G. Sekerková, B. Changyaleket, E. Mugnaini, and J. Bartles. 2003. Espin cross-links cause the elongation of microvillus-type parallel actin bundles in vivo. *The Journal of cell biology*. 163:1045-1055.
- Luo, B.-H., C.V. Carman, and T.A. Springer. 2007. Structural basis of integrin regulation and signaling. *Annual review of immunology*. 25:619-647.
- Machesky, L.M., and K.L. Gould. 1999. The Arp2/3 complex: a multifunctional actin organizer. *Curr Opin Cell Biol*. 11:117-21.
- Mackay, D.J., and A. Hall. 1998. Rho GTPases. *J Biol Chem*. 273:20685-8.
- Madrid, R., J. Gasteier, J. Bouchet, S. Schröder, M. Geyer, S. Benichou, and O. Fackler. 2005. Oligomerization of the diaphanous-related formin FHOD1 requires a coiled-coil motif critical for its cytoskeletal and transcriptional activities. *FEBS letters*. 579:441-448.
- Maekawa, M., T. Ishizaki, S. Boku, N. Watanabe, A. Fujita, A. Iwamatsu, T. Obinata, K. Ohashi, K. Mizuno, and S. Narumiya. 1999. Signaling from Rho to the actin cytoskeleton through protein kinases ROCK and LIM-kinase. *Science*. 285:895-8.
- Mallik, R., and S.P. Gross. 2004. Molecular motors: strategies to get along. *Curr Biol*. 14:R971-82.
- Mammoto, A., K. Takahashi, T. Sasaki, and Y. Takai. 2000. Stimulation of Rho GDI release by ERM proteins. *Methods in enzymology*. 325:91-101.
- Mansour, M., S. Lee, and B. Pohajdak. 2002. The N-terminal coiled coil domain of the cytohesin/ARNO family of guanine nucleotide exchange factors interacts with the scaffolding protein CASP. *The Journal of biological chemistry*. 277:32302-32309.
- Marchand, J.B., D.A. Kaiser, T.D. Pollard, and H.N. Higgs. 2001. Interaction of WASP/Scar proteins with actin and vertebrate Arp2/3 complex. *Nat Cell Biol*. 3:76-82.
- Marshall, A.J., A.K. Krahn, K. Ma, V. Duronio, and S. Hou. 2002. TAPP1 and TAPP2 are targets of phosphatidylinositol 3-kinase signaling in B cells: sustained plasma membrane recruitment triggered by the B-cell antigen receptor. *Mol Cell Biol*. 22:5479-91.
- Marte, B.M., P. Rodriguez-Viciana, S. Wennstrom, P.H. Warne, and J. Downward. 1997. R-Ras can activate the phosphoinositide 3-kinase but not the MAP kinase arm of the Ras effector pathways. *Curr Biol*. 7:63-70.
- Martin, A., P.A. Duffy, C. Liossis, A. Gomez-Munoz, L. O'Brien, J.C. Stone, and D.N. Brindley. 1997. Increased concentrations of phosphatidate, diacylglycerol and ceramide in ras- and tyrosine kinase (fps)-transformed fibroblasts. *Oncogene*. 14:1571-1580.
- Masat, L., J. Caldwell, R. Armstrong, H. Khoshnevisan, R. Jessberger, B. Herndier, M. Wabl, and D. Ferrick. 2000a. Association of SWAP-70 with the B cell antigen receptor complex. *Proc Natl Acad Sci U S A*. 97:2180-4.
- Masat, L., R.A. Liddell, B.A. Mock, W.L. Kuo, R. Jessberger, M. Wabl, and H.C. Morse, 3rd. 2000b. Mapping of the SWAP70 gene to mouse chromosome 7 and human chromosome 11p15. *Immunogenetics*. 51:16-9.
- Matsui, T., M. Amano, T. Yamamoto, K. Chihara, M. Nakafuku, M. Ito, T. Nakano, K. Okawa, A. Iwamatsu, and K. Kaibuchi. 1996. Rho-associated kinase, a novel serine/threonine kinase, as a putative target for small GTP binding protein Rho. *The EMBO journal*. 15:2208-2216.
- Mattila, P., A. Pykalainen, J. Saarikangas, V. Paavilainen, H. Vihinen, E. Jokitalo, and P. Lappalainen. 2007. Missing-in-metastasis and IRSp53 deform PI(4,5)P<sub>2</sub>-rich membranes by an inverse BAR domain-like mechanism. *The Journal of Cell Biology*. 176:953-964.
- Mavrikakis, K.J., K.J. McKinlay, P. Jones, and F. Sablitzky. 2004. DEF6, a novel PH-DH-like domain protein, is an upstream activator of the Rho GTPases Rac1, Cdc42, and RhoA. *Exp Cell Res*. 294:335-44.
- McGough, A.M., C.J. Staiger, J.K. Min, and K.D. Simonetti. 2003. The gelsolin family of actin regulatory proteins: modular structures, versatile functions. *FEBS Lett*. 552:75-81.



## References

- McLaughlin, R.E., and J.B. Denny. 1999. Palmitoylation of GAP-43 by the ER-Golgi intermediate compartment and Golgi apparatus. *Biochim Biophys Acta*. 1451:82-92.
- McLean, B.G., S.R. Huang, E.C. McKinney, and R.B. Meagher. 1990. Plants contain highly divergent actin isoforms. *Cell Motil Cytoskeleton*. 17:276-90.
- Michelot, A., J. Berro, C. Guerin, R. Boujemaa-Paterski, C.J. Staiger, J.L. Martiel, and L. Blanchoin. 2007. Actin-filament stochastic dynamics mediated by ADF/cofilin. *Curr Biol*. 17:825-33.
- Miki, H., H. Yamaguchi, S. Suetsugu, and T. Takenawa. 2000. IRSp53 is an essential intermediate between Rac and WAVE in the regulation of membrane ruffling. *Nature*. 408:732-735.
- Mills, J., N. Stone, J. Erhardt, and R. Pittman. 1998. Apoptotic membrane blebbing is regulated by myosin light chain phosphorylation. *The Journal of cell biology*. 140:627-636.
- Mochizuki, N., S. Yamashita, K. Kurokawa, Y. Ohba, T. Nagai, A. Miyawaki, and M. Matsuda. 2001. Spatio-temporal images of growth-factor-induced activation of Ras and Rap1. *Nature*. 411:1065-1068.
- Mora, N., R. Rosales, and C. Rosales. 2007. R-Ras promotes metastasis of cervical cancer epithelial cells. *Cancer Immunol Immunother*. 56:535-44.
- Mullins, R.D., J.A. Heuser, and T.D. Pollard. 1998. The interaction of Arp2/3 complex with actin: nucleation, high affinity pointed end capping, and formation of branching networks of filaments. *Proc Natl Acad Sci U S A*. 95:6181-6.
- Myat, M., S. Anderson, L. Allen, and A. Aderem. 1997. MARCKS regulates membrane ruffling and cell spreading. *Current biology : CB*. 7:611-614.
- Neuhaus, J.M., M. Wanger, T. Keiser, and A. Wegner. 1983. Treadmilling of actin. *J Muscle Res Cell Motil*. 4:507-27.
- Nimnual, A.S., L.J. Taylor, and D. Bar-Sagi. 2003. Redox-dependent downregulation of Rho by Rac. *Nat Cell Biol*. 5:236-41.
- Nobes, C.D., and A. Hall. 1995. Rho, rac, and cdc42 GTPases regulate the assembly of multimolecular focal complexes associated with actin stress fibers, lamellipodia, and filopodia. *Cell*. 81:53-62.
- Oberbanscheidt, P., S. Balkow, J. Kuhl, S. Grabbe, and M. Bähler. 2007. SWAP-70 associates transiently with macropinosomes. *Eur J Cell Biol*. 86:13-24.
- Oertli, B., J. Han, B.M. Marte, T. Sethi, J. Downward, M. Ginsberg, and P.E. Hughes. 2000. The effector loop and prenylation site of R-Ras are involved in the regulation of integrin function. *Oncogene*. 19:4961-9.
- Ohba, Y., N. Mochizuki, S. Yamashita, A.M. Chan, J.W. Schrader, S. Hattori, K. Nagashima, and M. Matsuda. 2000. Regulatory proteins of R-Ras, TC21/R-Ras2, and M-Ras/R-Ras3. *The Journal of biological chemistry*. 275:20020-20026.
- Ohta, Y., J. Hartwig, and T. Stossel. 2006. FilGAP, a Rho- and ROCK-regulated GAP for Rac binds filamin A to control actin remodelling. *Nat Cell Biol*. 8:803-814.
- Oikawa, T., H. Yamaguchi, T. Itoh, M. Kato, T. Ijuin, D. Yamazaki, S. Suetsugu, and T. Takenawa. 2004. PtdIns(3,4,5)P3 binding is necessary for WAVE2-induced formation of lamellipodia. *Nat Cell Biol*. 6:420-6.
- Ono, S. 2003. Regulation of actin filament dynamics by actin depolymerizing factor/cofilin and actin-interacting protein 1: new blades for twisted filaments. *Biochemistry*. 42:13363-70.
- Orth, J.D., and M.A. McNiven. 2006. Get off my back! Rapid receptor internalization through circular dorsal ruffles. *Cancer Res*. 66:11094-6.
- Paduch, M., F. Jelen, and J. Otlewski. 2001. Structure of small G proteins and their regulators. *Acta Biochim Pol*. 48:829-50.
- Pantaloni, D., R. Boujemaa, D. Didry, P. Gounon, and M.F. Carlier. 2000. The Arp2/3 complex branches filament barbed ends: functional antagonism with capping proteins. *Nat Cell Biol*. 2:385-91.

## References

- Pantaloni, D., C. Le Clainche, and M.F. Carlier. 2001. Mechanism of actin-based motility. *Science*. 292:1502-6.
- Papakonstanti, E., and C. Stournaras. 2002. Association of PI-3 kinase with PAK1 leads to actin phosphorylation and cytoskeletal reorganization. *Molecular biology of the cell*. 13:2946-2962.
- Parent, C.A., B.J. Blacklock, W.M. Froehlich, D.B. Murphy, and P.N. Devreotes. 1998. G protein signaling events are activated at the leading edge of chemotactic cells. *Cell*. 95:81-91.
- Parker, P.J. 2004. The ubiquitous phosphoinositides. *Biochem Soc Trans*. 32:893-8.
- Partridge, M., and E. Marcantonio. 2006. Initiation of attachment and generation of mature focal adhesions by integrin-containing filopodia in cell spreading. *Molecular biology of the cell*. 17:4237-4248.
- Pawlak, G., and D.M. Helfman. 2002. Post-transcriptional down-regulation of ROCK1/Rho-kinase through an MEK-dependent pathway leads to cytoskeleton disruption in Ras-transformed fibroblasts. *Mol Biol Cell*. 13:336-47.
- Pearce, G., V. Angeli, G.J. Randolph, T. Junt, U. von Andrian, H.J. Schnittler, and R. Jessberger. 2006. Signaling protein SWAP-70 is required for efficient B cell homing to lymphoid organs. *Nat Immunol*. 7:827-34.
- Pearson, M., D. Reczek, A. Bretscher, and P. Karplus. 2000. Structure of the ERM protein moesin reveals the FERM domain fold masked by an extended actin binding tail domain. *Cell*. 101:259-270.
- Peitzsch, R.M., and S. McLaughlin. 1993. Binding of acylated peptides and fatty acids to phospholipid vesicles: pertinence to myristoylated proteins. *Biochemistry*. 32:10436-43.
- Pellegrin, S., and H. Mellor. 2007. Actin stress fibres. *J Cell Sci*. 120:3491-9.
- Philimonenko, V.V., J. Zhao, S. Iben, H. Dingova, K. Kysela, M. Kahle, H. Zentgraf, W.A. Hofmann, P. de Lanerolle, P. Hozak, and I. Grummt. 2004. Nuclear actin and myosin I are required for RNA polymerase I transcription. *Nat Cell Biol*. 6:1165-72.
- Pierce, K.L., R.T. Premont, and R.J. Lefkowitz. 2002. Seven-transmembrane receptors. *Nat Rev Mol Cell Biol*. 3:639-50.
- Pinner, S., and E. Sahai. 2008. PDK1 regulates cancer cell motility by antagonising inhibition of ROCK1 by RhoE. *Nat Cell Biol*. 10:127-37.
- Pollard, T.D. 1986. Assembly and dynamics of the actin filament system in nonmuscle cells. *J Cell Biochem*. 31:87-95.
- Pollard, T.D., L. Blanchoin, and R.D. Mullins. 2000. Molecular mechanisms controlling actin filament dynamics in nonmuscle cells. *Annu Rev Biophys Biomol Struct*. 29:545-76.
- Pollard, T.D., and G.G. Borisy. 2003. Cellular motility driven by assembly and disassembly of actin filaments. *Cell*. 112:453-65.
- Ponti, A., M. Machacek, S.L. Gupton, C.M. Waterman-Storer, and G. Danuser. 2004. Two distinct actin networks drive the protrusion of migrating cells. *Science*. 305:1782-6.
- Postma, M., J. Roelofs, J. Goedhart, H.M. Looovers, A.J. Visser, and P.J. Van Haastert. 2004. Sensitization of Dictyostelium chemotaxis by phosphoinositide-3-kinase-mediated self-organizing signalling patches. *J Cell Sci*. 117:2925-35.
- Prag, S., M. Parsons, M. Keppler, S. Ameer-Beg, P. Barber, J. Hunt, A. Beavil, R. Calvert, M. Arpin, B. Vojnovic, and T. Ng. 2007. Activated ezrin promotes cell migration through recruitment of the GEF Dbl to lipid rafts and preferential downstream activation of Cdc42. *Molecular biology of the cell*. 18:2935-2948.
- Prass, M., K. Jacobson, A. Mogilner, and M. Radmacher. 2006. Direct measurement of the lamellipodial protrusive force in a migrating cell. *The Journal of Cell Biology*. 174:767-772.
- Price, L.S., J. Leng, M.A. Schwartz, and G.M. Bokoch. 1998. Activation of Rac and Cdc42 by integrins mediates cell spreading. *Mol Biol Cell*. 9:1863-71.

## References

- Qian, F., Z.C. Zhang, X.F. Wu, Y.P. Li, and Q. Xu. 2005. Interaction between integrin alpha(5) and fibronectin is required for metastasis of B16F10 melanoma cells. *Biochem Biophys Res Commun.* 333:1269-75.
- Quilliam, L.A., S.Y. Huff, K.M. Rabun, W. Wei, W. Park, D. Broek, and C.J. Der. 1994. Membrane-targeting potentiates guanine nucleotide exchange factor CDC25 and SOS1 activation of Ras transforming activity. *Proc Natl Acad Sci U S A.* 91:8512-6.
- Quinlan, M.E., J.E. Heuser, E. Kerkhoff, and R.D. Mullins. 2005. Drosophila Spire is an actin nucleation factor. *Nature.* 433:382-8.
- Radhakrishna, H., O. Al-Awar, Z. Khachikian, and J.G. Donaldson. 1999. ARF6 requirement for Rac ruffling suggests a role for membrane trafficking in cortical actin rearrangements. *J Cell Sci.* 112 ( Pt 6):855-66.
- Rapalus, L., Y. Minegishi, A. Lavoie, C. Cunningham-Rundles, and M.E. Conley. 2001. Analysis of SWAP-70 as a candidate gene for non-X-linked hyper IgM syndrome and common variable immunodeficiency. *Clin Immunol.* 101:270-5.
- Renart, J., J. Reiser, and G.R. Stark. 1979. Transfer of proteins from gels to diazobenzyloxymethyl-paper and detection with antisera: a method for studying antibody specificity and antigen structure. *Proc Natl Acad Sci U S A.* 76:3116-20.
- Revenu, C., R. Athman, S. Robine, and D. Louvard. 2004. The co-workers of actin filaments: from cell structures to signals. *Nat Rev Mol Cell Biol.* 5:635-46.
- Rey, I., P. Taylor-Harris, H. van Erp, and A. Hall. 1994. R-ras interacts with rasGAP, neurofibromin and c-raf but does not regulate cell growth or differentiation. *Oncogene.* 9:685-92.
- Rezniczek, G.A., J.M. de Pereda, S. Reipert, and G. Wiche. 1998. Linking integrin alpha6beta4-based cell adhesion to the intermediate filament cytoskeleton: direct interaction between the beta4 subunit and plectin at multiple molecular sites. *J Cell Biol.* 141:209-25.
- Rickert, P., O.D. Weiner, F. Wang, H.R. Bourne, and G. Servant. 2000. Leukocytes navigate by compass: roles of PI3Kgamma and its lipid products. *Trends Cell Biol.* 10:466-73.
- Ridley, A.J. 2001a. Rho family proteins: coordinating cell responses. *Trends Cell Biol.* 11:471-7.
- Ridley, A.J. 2001b. Rho proteins: linking signaling with membrane trafficking. *Traffic.* 2:303-10.
- Ridley, A.J., and A. Hall. 1992. The small GTP-binding protein rho regulates the assembly of focal adhesions and actin stress fibers in response to growth factors. *Cell.* 70:389-99.
- Ridley, A.J., H.F. Paterson, C.L. Johnston, D. Diekmann, and A. Hall. 1992. The small GTP-binding protein rac regulates growth factor-induced membrane ruffling. *Cell.* 70:401-10.
- Rincon-Arano, H., R. Rosales, N. Mora, A. Rodriguez-Castaneda, and C. Rosales. 2003. R-Ras promotes tumor growth of cervical epithelial cells. *Cancer.* 97:575-85.
- Riveline, D., E. Zamir, N. Balaban, U. Schwarz, T. Ishizaki, S. Narumiya, Z. Kam, B. Geiger, and A. Bershadsky. 2001. Focal contacts as mechanosensors: externally applied local mechanical force induces growth of focal contacts by an mDia1-dependent and ROCK-independent mechanism. *The Journal of cell biology.* 153:1175-1186.
- Robinson, R.C., K. Turbedsky, D.A. Kaiser, J.B. Marchand, H.N. Higgs, S. Choe, and T.D. Pollard. 2001. Crystal structure of Arp2/3 complex. *Science.* 294:1679-84.
- Rocks, O., A. Peyker, M. Kahms, P.J. Verveer, C. Koerner, M. Lumbierres, J. Kuhlmann, H. Waldmann, A. Wittinghofer, and P.I. Bastiaens. 2005. An acylation cycle regulates localization and activity of palmitoylated Ras isoforms. *Science.* 307:1746-52.
- Rohatgi, R., H. Ho, and M. Kirschner. 2000. Mechanism of N-WASP activation by CDC42 and phosphatidylinositol 4, 5-bisphosphate. *The Journal of cell biology.* 150:1299-1310.

## References

- Rohatgi, R., L. Ma, H. Miki, M. Lopez, T. Kirchhausen, T. Takenawa, and M. Kirschner. 1999. The interaction between N-WASP and the Arp2/3 complex links Cdc42-dependent signals to actin assembly. *Cell*. 97:221-231.
- Rohatgi, R., P. Nollau, H. Ho, M. Kirschner, and B. Mayer. 2001. Nck and phosphatidylinositol 4,5-bisphosphate synergistically activate actin polymerization through the N-WASP-Arp2/3 pathway. *The Journal of biological chemistry*. 276:26448-26452.
- Romero, S., C. Le Clainche, D. Didry, C. Egile, D. Pantaloni, and M.F. Carlier. 2004. Formin is a processive motor that requires profilin to accelerate actin assembly and associated ATP hydrolysis. *Cell*. 119:419-29.
- Roose, J.P., M. Mollenauer, M. Ho, T. Kurosaki, and A. Weiss. 2007. Unusual interplay of two types of Ras activators, RasGRP and SOS, establishes sensitive and robust Ras activation in lymphocytes. *Mol Cell Biol*. 27:2732-45.
- Rosales-Nieves, A.E., J.E. Johndrow, L.C. Keller, C.R. Magie, D.M. Pinto-Santini, and S.M. Parkhurst. 2006. Coordination of microtubule and microfilament dynamics by Drosophila Rho1, Spire and Cappuccino. *Nat Cell Biol*. 8:367-76.
- Rose, R., M. Weyand, M. Lammers, T. Ishizaki, M.R. Ahmadian, and A. Wittinghofer. 2005. Structural and mechanistic insights into the interaction between Rho and mammalian Dia. *Nature*. 435:513-8.
- Rossman, K.L., C.J. Der, and J. Sondek. 2005. GEF means go: turning on RHO GTPases with guanine nucleotide-exchange factors. *Nat Rev Mol Cell Biol*. 6:167-80.
- Rottner, K., A. Hall, and J.V. Small. 1999. Interplay between Rac and Rho in the control of substrate contact dynamics. *Curr Biol*. 9:640-8.
- Roy, C., M. Martin, and P. Mangeat. 1997. A dual involvement of the amino-terminal domain of ezrin in F- and G-actin binding. *J Biol Chem*. 272:20088-95.
- Rubenstein, P.A., and D.J. Martin. 1983. NH2-terminal processing of actin in mouse L-cells in vivo. *J Biol Chem*. 258:3961-6.
- Russo, C., Y. Gao, P. Mancini, C. Vanni, M. Porotto, M. Falasca, M. Torrisi, Y. Zheng, and A. Eva. 2001. Modulation of oncogenic DBL activity by phosphoinositol phosphate binding to pleckstrin homology domain. *The Journal of biological chemistry*. 276:19524-19531.
- Safer, D., and V.T. Nachmias. 1994. Beta thymosins as actin binding peptides. *Bioessays*. 16:590.
- Sahai, E., and C. Marshall. 2003. Differing modes of tumour cell invasion have distinct requirements for Rho/ROCK signalling and extracellular proteolysis. *Nature cell biology*. 5:711-719.
- Sahai, E., M. Olson, and C. Marshall. 2001. Cross-talk between Ras and Rho signalling pathways in transformation favours proliferation and increased motility. *The EMBO journal*. 20:755-766.
- Samson, T., C. Will, A. Knoblauch, L. Sharek, K. von der Mark, K. Burridge, and V. Wixler. 2007. Def-6, a guanine nucleotide exchange factor for Rac1, interacts with the skeletal muscle integrin chain alpha7A and influences myoblast differentiation. *J Biol Chem*. 282:15730-42.
- Sander, E., J. Klooster, S. van Delft, R. van der Kammen, and J. Collard. 1999. Rac downregulates Rho activity: reciprocal balance between both GTPases determines cellular morphology and migratory behavior. *The Journal of cell biology*. 147:1009-1022.
- Saraste, M., P. Sibbald, and A. Wittinghofer. 1990. The P-loop--a common motif in ATP- and GTP-binding proteins. *Trends in biochemical sciences*. 15:430-434.
- Sasaki, A., C. Janetopoulos, S. Lee, P. Charest, K. Takeda, L. Sundheimer, R. Meili, P. Devreotes, and R. Firtel. 2007. G protein-independent Ras/PI3K/F-actin circuit regulates basic cell motility. *The Journal of Cell Biology*. 178:185-191.
- Sasaki, A.T., C. Chun, K. Takeda, and R.A. Firtel. 2004. Localized Ras signaling at the leading edge regulates PI3K, cell polarity, and directional cell movement. *J Cell Biol*. 167:505-18.

## References

- Sasaki, T., J. Irie-Sasaki, R.G. Jones, A.J. Oliveira-dos-Santos, W.L. Stanford, B. Bolon, A. Wakeham, A. Itie, D. Bouchard, I. Kozieradzki, N. Joza, T.W. Mak, P.S. Ohashi, A. Suzuki, and J.M. Penninger. 2000. Function of PI3Kgamma in thymocyte development, T cell activation, and neutrophil migration. *Science*. 287:1040-6.
- Scheffzek, K., and M. Ahmadian. 2005. GTPase activating proteins: structural and functional insights 18 years after discovery. *Cellular and molecular life sciences : CMLS*. 62:3014-3038.
- Scheffzek, K., M. Ahmadian, W. Kabsch, L. Wiesmüller, A. Lautwein, F. Schmitz, and A. Wittinghofer. 1997. The Ras-RasGAP complex: structural basis for GTPase activation and its loss in oncogenic Ras mutants. *Science (New York, N.Y.)*. 277:333-338.
- Schlunck, G., H. Damke, W.B. Kiosses, N. Rusk, M.H. Symons, C.M. Waterman-Storer, S.L. Schmid, and M.A. Schwartz. 2004. Modulation of Rac localization and function by dynamin. *Mol Biol Cell*. 15:256-67.
- Serrels, B., A. Serrels, V.G. Brunton, M. Holt, G.W. McLean, C.H. Gray, G.E. Jones, and M.C. Frame. 2007. Focal adhesion kinase controls actin assembly via a FERM-mediated interaction with the Arp2/3 complex. *Nat Cell Biol*. 9:1046-56.
- Servant, G., O.D. Weiner, P. Herzmark, T. Balla, J.W. Sedat, and H.R. Bourne. 2000. Polarization of chemoattractant receptor signaling during neutrophil chemotaxis. *Science*. 287:1037-40.
- Sethi, T., M.H. Ginsberg, J. Downward, and P.E. Hughes. 1999. The small GTP-binding protein R-Ras can influence integrin activation by antagonizing a Ras/Raf-initiated integrin suppression pathway. *Mol Biol Cell*. 10:1799-809.
- She, H., S. Rockow, J. Tang, R. Nishimura, E. Skolnik, M. Chen, B. Margolis, and W. Li. 1997. Wiskott-Aldrich syndrome protein is associated with the adapter protein Grb2 and the epidermal growth factor receptor in living cells. *Molecular biology of the cell*. 8:1709-1721.
- Shepherd, P.R., D.J. Withers, and K. Siddle. 1998. Phosphoinositide 3-kinase: the key switch mechanism in insulin signalling. *Biochem J*. 333 ( Pt 3):471-90.
- Shinohara, M., W.-H. Shang, M. Kubodera, S. Harada, J. Mitsushita, M. Kato, H. Miyazaki, H. Sumimoto, and T. Kamata. 2007. Nox1 Redox Signaling Mediates Oncogenic Ras-induced Disruption of Stress Fibers and Focal Adhesions by Down-regulating Rho. *Journal of Biological Chemistry*. 282:17640-17648.
- Shinohara, M., Y. Terada, A. Iwamatsu, A. Shinohara, N. Mochizuki, M. Higuchi, Y. Gotoh, S. Ihara, S. Nagata, H. Itoh, Y. Fukui, and R. Jessberger. 2002. SWAP-70 is a guanine-nucleotide-exchange factor that mediates signalling of membrane ruffling. *Nature*. 416:759-63.
- Shuster, C., and I. Herman. 1995. Indirect association of ezrin with F-actin: isoform specificity and calcium sensitivity. *The Journal of Cell Biology*. 128:837-848.
- Sivalenka, R.R., and R. Jessberger. 2004. SWAP-70 regulates c-kit-induced mast cell activation, cell-cell adhesion, and migration. *Mol Cell Biol*. 24:10277-88.
- Skene, J.H., and I. Virag. 1989. Posttranslational membrane attachment and dynamic fatty acylation of a neuronal growth cone protein, GAP-43. *J Cell Biol*. 108:613-24.
- Small, J.V. 1995. Getting the actin filaments straight: nucleation-release or treadmilling? *Trends Cell Biol*. 5:52-5.
- Small, J.V., and M. Gimona. 1998. The cytoskeleton of the vertebrate smooth muscle cell. *Acta Physiol Scand*. 164:341-8.
- Small, J.V., and G.P. Resch. 2005. The comings and goings of actin: coupling protrusion and retraction in cell motility. *Curr Opin Cell Biol*. 17:517-23.
- Small, J.V., K. Rottner, I. Kaverina, and K.I. Anderson. 1998. Assembling an actin cytoskeleton for cell attachment and movement. *Biochim Biophys Acta*. 1404:271-81.

## References

- Spaargaren, M., G.A. Martin, F. McCormick, M.J. Fernandez-Sarabia, and J.R. Bischoff. 1994. The Ras-related protein R-ras interacts directly with Raf-1 in a GTP-dependent manner. *Biochem J.* 300 ( Pt 2):303-7.
- Srinivasan, S., F. Wang, S. Glavas, A. Ott, F. Hofmann, K. Aktories, D. Kalman, and H.R. Bourne. 2003. Rac and Cdc42 play distinct roles in regulating PI(3,4,5)P<sub>3</sub> and polarity during neutrophil chemotaxis. *The Journal of cell biology.* 160:375-385.
- Steffen, A., K. Rottner, J. Ehinger, M. Innocenti, G. Scita, J. Wehland, and T.E. Stradal. 2004. Sra-1 and Nap1 link Rac to actin assembly driving lamellipodia formation. *Embo J.* 23:749-59.
- Stephens, L., A. Eguinoa, S. Corey, T. Jackson, and P.T. Hawkins. 1993. Receptor stimulated accumulation of phosphatidylinositol (3,4,5)-trisphosphate by G-protein mediated pathways in human myeloid derived cells. *Embo J.* 12:2265-73.
- Stock, A., M.O. Steinmetz, P.A. Janmey, U. Aebi, G. Gerisch, R.A. Kammerer, I. Weber, and J. Faix. 1999. Domain analysis of cortexillin I: actin-bundling, PIP(2)-binding and the rescue of cytokinesis. *Embo J.* 18:5274-84.
- Stradal, T.E., K. Rottner, A. Disanza, S. Confalonieri, M. Innocenti, and G. Scita. 2004. Regulation of actin dynamics by WASP and WAVE family proteins. *Trends Cell Biol.* 14:303-11.
- Stradal, T.E., and G. Scita. 2006. Protein complexes regulating Arp2/3-mediated actin assembly. *Curr Opin Cell Biol.* 18:4-10.
- Suetsugu, S., S. Kurisu, T. Oikawa, D. Yamazaki, A. Oda, and T. Takenawa. 2006. Optimization of WAVE2 complex-induced actin polymerization by membrane-bound IRSp53, PIP<sub>3</sub>, and Rac. *The Journal of Cell Biology.* 173:571-585.
- Suire, S., P. Hawkins, and L. Stephens. 2002. Activation of phosphoinositide 3-kinase gamma by Ras. *Curr Biol.* 12:1068-75.
- Sumi, T., K. Matsumoto, and T. Nakamura. 2001a. Specific activation of LIM kinase 2 via phosphorylation of threonine 505 by ROCK, a Rho-dependent protein kinase. *J Biol Chem.* 276:670-6.
- Sumi, T., K. Matsumoto, A. Shibuya, and T. Nakamura. 2001b. Activation of LIM kinases by myotonic dystrophy kinase-related Cdc42-binding kinase alpha. *J Biol Chem.* 276:23092-6.
- Sumi, T., K. Matsumoto, Y. Takai, and T. Nakamura. 1999. Cofilin phosphorylation and actin cytoskeletal dynamics regulated by rho- and Cdc42-activated LIM-kinase 2. *The Journal of cell biology.* 147:1519-1532.
- Sun, H.Q., K. Kwiatkowska, and H.L. Yin. 1995. Actin monomer binding proteins. *Curr Opin Cell Biol.* 7:102-10.
- Takai, Y., T. Sasaki, and T. Matozaki. 2001. Small GTP-binding proteins. *Physiological reviews.* 81:153-208.
- Tang, Y., J. Yu, and J. Field. 1999. Signals from the Ras, Rac, and Rho GTPases converge on the Pak protein kinase in Rat-1 fibroblasts. *Molecular and cellular biology.* 19:1881-1891.
- Totsukawa, G., Y. Wu, Y. Sasaki, D.J. Hartshorne, Y. Yamakita, S. Yamashiro, and F. Matsumura. 2004. Distinct roles of MLCK and ROCK in the regulation of membrane protrusions and focal adhesion dynamics during cell migration of fibroblasts. *J Cell Biol.* 164:427-39.
- Tsukita, S., K. Oishi, N. Sato, J. Sagara, and A. Kawai. 1994. ERM family members as molecular linkers between the cell surface glycoprotein CD44 and actin-based cytoskeletons. *J Cell Biol.* 126:391-401.
- Tsukita, S., and S. Yonemura. 1997. ERM proteins: head-to-tail regulation of actin-plasma membrane interaction. *Trends in biochemical sciences.* 22:53-58.
- Tsukita, S., and S. Yonemura. 1999. Cortical actin organization: lessons from ERM (ezrin/radixin/moesin) proteins. *The Journal of biological chemistry.* 274:34507-34510.

## References

- Uberall, F., K. Hellbert, S. Kampfer, K. Maly, A. Villunger, M. Spitaler, J. Mwanjewe, G. Baier-Bitterlich, G. Baier, and H.H. Grunicke. 1999. Evidence that atypical protein kinase C-lambda and atypical protein kinase C-zeta participate in Ras-mediated reorganization of the F-actin cytoskeleton. *The Journal of cell biology*. 144:413-425.
- van den Boom, F., H. Dussmann, K. Uhlenbrock, M. Abouhamed, and M. Bähler. 2007. The Myosin IXb motor activity targets the myosin IXb RhoGAP domain as cargo to sites of actin polymerization. *Mol Biol Cell*. 18:1507-18.
- van der Kaay, J., M. Beck, A. Gray, and C. Downes. 1999. Distinct phosphatidylinositol 3-kinase lipid products accumulate upon oxidative and osmotic stress and lead to different cellular responses. *The Journal of biological chemistry*. 274:35963-35968.
- Van Haastert, P.J., and P.N. Devreotes. 2004. Chemotaxis: signalling the way forward. *Nat Rev Mol Cell Biol*. 5:626-34.
- Vandekerckhove, J., and K. Weber. 1978. At least six different actins are expressed in a higher mammal: an analysis based on the amino acid sequence of the amino-terminal tryptic peptide. *J Mol Biol*. 126:783-802.
- Vandermoere, F., I. El Yazidi-Belkoura, Y. Demont, C. Slomianny, J. Antol, J. Lemoine, and H. Hondermarck. 2007. Proteomics exploration reveals that actin is a signaling target of the kinase Akt. *Mol Cell Proteomics*. 6:114-24.
- Vavvas, D., X. Li, J. Avruch, and X.F. Zhang. 1998. Identification of Nore1 as a potential Ras effector. *J Biol Chem*. 273:5439-42.
- Verkhovskiy, A.B., T.M. Svitkina, and G.G. Borisy. 1999. Self-polarization and directional motility of cytoplasm. *Curr Biol*. 9:11-20.
- Vetter, I.R., and A. Wittinghofer. 2001. The guanine nucleotide-binding switch in three dimensions. *Science*. 294:1299-304.
- Vignjevic, D., S. Kojima, Y. Aratyn, O. Danciu, T. Svitkina, and G.G. Borisy. 2006. Role of fascin in filopodial protrusion. *J Cell Biol*. 174:863-75.
- Vinogradova, O., A. Velyvis, A. Velyviene, B. Hu, T. Haas, E. Plow, and J. Qin. 2002. A structural mechanism of integrin alpha(IIb)beta(3) "inside-out" activation as regulated by its cytoplasmic face. *Cell*. 110:587-97.
- von Wichert, G., B. Haimovich, G.S. Feng, and M.P. Sheetz. 2003. Force-dependent integrin-cytoskeleton linkage formation requires downregulation of focal complex dynamics by Shp2. *Embo J*. 22:5023-35.
- Wakamatsu, I., S. Ihara, and Y. Fukui. 2006. Mutational analysis on the function of the SWAP-70 PH domain. *Mol Cell Biochem*. 293:137-45.
- Wang, F., P. Herzmark, O. Weiner, S. Srinivasan, G. Servant, and H. Bourne. 2002a. Lipid products of PI(3)Ks maintain persistent cell polarity and directed motility in neutrophils. *Nature cell biology*. 4:513-518.
- Wang, F., P. Herzmark, O.D. Weiner, S. Srinivasan, G. Servant, and H.R. Bourne. 2002b. Lipid products of PI(3)Ks maintain persistent cell polarity and directed motility in neutrophils. *Nat Cell Biol*. 4:513-8.
- Wang, H.-R., Y. Zhang, B. Ozdamar, A. Ogunjimi, E. Alexandrova, G. Thomsen, and J. Wrana. 2003. Regulation of cell polarity and protrusion formation by targeting RhoA for degradation. *Science (New York, N.Y.)*. 302:1775-1779.
- Watanabe, N., P. Madaule, T. Reid, T. Ishizaki, G. Watanabe, A. Kakizuka, Y. Saito, K. Nakao, B.M. Jockusch, and S. Narumiya. 1997. p140mDia, a mammalian homolog of Drosophila diaphanous, is a target protein for Rho small GTPase and is a ligand for profilin. *Embo J*. 16:3044-56.
- Watanabe, N., and T.J. Mitchison. 2002. Single-molecule speckle analysis of actin filament turnover in lamellipodia. *Science*. 295:1083-6.

## References

- Wear, M.A., A. Yamashita, K. Kim, Y. Maeda, and J.A. Cooper. 2003. How capping protein binds the barbed end of the actin filament. *Curr Biol.* 13:1531-7.
- Weaver, A.M., A.V. Karginov, A.W. Kinley, S.A. Weed, Y. Li, J.T. Parsons, and J.A. Cooper. 2001. Cortactin promotes and stabilizes Arp2/3-induced actin filament network formation. *Curr Biol.* 11:370-4.
- Weber, A., C.R. Pennise, G.G. Babcock, and V.M. Fowler. 1994. Tropomodulin caps the pointed ends of actin filaments. *J Cell Biol.* 127:1627-35.
- Wegner, A. 1976. Head to tail polymerization of actin. *J Mol Biol.* 108:139-50.
- Weiner, O.D., P.O. Neilsen, G.D. Prestwich, M.W. Kirschner, L.C. Cantley, and H.R. Bourne. 2002. A PtdInsP(3)- and Rho GTPase-mediated positive feedback loop regulates neutrophil polarity. *Nat Cell Biol.* 4:509-13.
- Welch, H., W. Coadwell, C. Ellson, G. Ferguson, S. Andrews, H. Erdjument-Bromage, P. Tempst, P. Hawkins, and L. Stephens. 2002. P-Rex1, a PtdIns(3,4,5)P3- and Gbetagamma-regulated guanine-nucleotide exchange factor for Rac. *Cell.* 108:809-821.
- Welch, M.D., and R.D. Mullins. 2002. Cellular control of actin nucleation. *Annu Rev Cell Dev Biol.* 18:247-88.
- Wellington, A., S. Emmons, B. James, J. Calley, M. Grover, P. Tolia, and L. Manseau. 1999. Spire contains actin binding domains and is related to ascidian posterior end mark-5. *Development.* 126:5267-74.
- Wennerberg, K., and C.J. Der. 2004. Rho-family GTPases: it's not only Rac and Rho (and I like it). *J Cell Sci.* 117:1301-12.
- Wennerberg, K., K.L. Rossman, and C.J. Der. 2005. The Ras superfamily at a glance. *J Cell Sci.* 118:843-6.
- Wessels, D., H. Vawter-Hugart, J. Murray, and D.R. Soll. 1994. Three-dimensional dynamics of pseudopod formation and the regulation of turning during the motility cycle of Dictyostelium. *Cell Motil Cytoskeleton.* 27:1-12.
- Wittinghofer, A., and E. Pai. 1991. The structure of Ras protein: a model for a universal molecular switch. *Trends in biochemical sciences.* 16:382-387.
- Wolfman, A., and I.G. Macara. 1987. Elevated levels of diacylglycerol and decreased phorbol ester sensitivity in ras-transformed fibroblasts. *Nature.* 325:359-61.
- Woolfson, D.N. 2005. The design of coiled-coil structures and assemblies. *Advances in protein chemistry.* 70:79-112.
- Wozniak, M.A., L. Kwong, D. Chodniewicz, R.L. Klemke, and P.J. Keely. 2005. R-Ras controls membrane protrusion and cell migration through the spatial regulation of Rac and Rho. *Mol Biol Cell.* 16:84-96.
- Xu, J., F. Wang, A. Van Keymeulen, P. Herzmark, A. Straight, K. Kelly, Y. Takuwa, N. Sugimoto, T. Mitchison, and H.R. Bourne. 2003. Divergent signals and cytoskeletal assemblies regulate self-organizing polarity in neutrophils. *Cell.* 114:201-14.
- Xu, J., D. Wirtz, and T. Pollard. 1998. Dynamic cross-linking by alpha-actinin determines the mechanical properties of actin filament networks. *The Journal of biological chemistry.* 273:9570-9576.
- Yao, X., L. Cheng, and J.G. Forte. 1996. Biochemical characterization of ezrin-actin interaction. *The Journal of biological chemistry.* 271:7224-7229.
- Yoshii, S., M. Tanaka, Y. Otsuki, D. Wang, R. Guo, Y. Zhu, R. Takeda, H. Hanai, E. Kaneko, and H. Sugimura. 1999. alphaPIX nucleotide exchange factor is activated by interaction with phosphatidylinositol 3-kinase. *Oncogene.* 18:5680-5690.
- Young, P., and M. Gautel. 2000. The interaction of titin and alpha-actinin is controlled by a phospholipid-regulated intramolecular pseudoligand mechanism. *Embo J.* 19:6331-40.
- Zaidel-Bar, R., C. Ballestrem, Z. Kam, and B. Geiger. 2003. Early molecular events in the assembly of matrix adhesions at the leading edge of migrating cells. *Journal of cell science.* 116:4605-4613.



## References

- Zaidel-Bar, R., M. Cohen, L. Addadi, and B. Geiger. 2004. Hierarchical assembly of cell-matrix adhesion complexes. *Biochemical Society transactions*. 32:416-420.
- Zamir, E., and B. Geiger. 2001. Molecular complexity and dynamics of cell-matrix adhesions. *J Cell Sci*. 114:3583-90.
- Zhao, C., G. Du, K. Skowronek, M.A. Frohman, and D. Bar-Sagi. 2007. Phospholipase D2-generated phosphatidic acid couples EGFR stimulation to Ras activation by Sos. *Nat Cell Biol*. 9:706-12.
- Zhao, Z.S., E. Manser, T.H. Loo, and L. Lim. 2000. Coupling of PAK-interacting exchange factor PIX to GIT1 promotes focal complex disassembly. *Mol Cell Biol*. 20:6354-63.
- Zheng, L., G. Sekerkova, K. Vranich, L.G. Tilney, E. Mugnaini, and J.R. Bartles. 2000. The deaf jerker mouse has a mutation in the gene encoding the espin actin-bundling proteins of hair cell stereocilia and lacks espins. *Cell*. 102:377-85.
- Zheng, Y., H. Liu, J. Coughlin, J. Zheng, L. Li, and J.C. Stone. 2005. Phosphorylation of RasGRP3 on threonine 133 provides a mechanistic link between PKC and Ras signaling systems in B cells. *Blood*. 105:3648-54.
- Zicha, D., I.M. Dobbie, M.R. Holt, J. Monypenny, D.Y. Soong, C. Gray, and G.A. Dunn. 2003. Rapid actin transport during cell protrusion. *Science*. 300:142-5.
- Zigmond, S.H., M. Evangelista, C. Boone, C. Yang, A.C. Dar, F. Sicheri, J. Forkey, and M. Pring. 2003. Formin leaky cap allows elongation in the presence of tight capping proteins. *Curr Biol*. 13:1820-3.

## **8. Appendices**

### **8.1 Abbreviations**

°C	degree Celsius
μ.	micro- (10 <sup>-6</sup> )
A	adenin
aa	Amino acid
ad.	Fill up
ADP	Adenosine diphosphate
APS	Ammonium peroxodisulfate
Arf	ADP ribosylation factor
ARS	actin ring structures
AT	Actin targeting
ATP	Adenosine triphosphate
ATPase	Adenosine 5'-triphosphatase
BBS	BES-buffered saline
BCR	B-cell receptor
BES	N,N-bis-(2-hydroxyethyl)-2-aminoethan sulfonic acid
bp	Base pairs
BSA	Bovine serum albumin
C	Cytosine
C1	Protein kinase C homology 1
CaCl <sub>2</sub>	Calciumchloride
CC	Coiled-coil
CCD	Charge-coupled device
Ccd42	Cell division cycle 42
cDNA	complementary DNA
CRIB	Cdc42/Rac1 interactive binding
C-terminus	Carboxyl terminus
Da	Dalton
DEF6	differentially expressed in FDCP-mix 6
DH	Dbl homology
DMSO	Dimethyl sulfoxide
DNA	Deoxyribonucleic acid
dNTP	Deoxynucleotide triphosphate

## Appendices

DTT	1,4-Dithiothreitol
E. coli	Escherichia coli
e.g.	example given
EDTA	Ethylene-diamine-tetraacetic acid
EF-hand	Calcium-binding motif
EGF	epidermal growth factor
EGTA	Ethylene-glycol-tetraacetic acid
<i>et al.</i>	<i>et al/teri</i>
FACS	Fluorescence activated cells sorting
F-actin	Filamentous actin
FcεRI	IgE-receptor
Fig.	Figure
g	Acceleration of gravity
G	Guanine
G-actin	Globular actin
GAP	GTPase activating protein
GBD	GTPase binding domain
GEF	Guanine nucleotide exchange factor
GFP	Green fluorescent protein
GSH	Reduced glutathione
GST	Glutathion-S-transferase
GTPase	Guanin-triphosphatase
h	hour
HCl	Hydrochloric acid
HEPES	N-[2-hydroxyethyl] piperazin-N'-[2-ethan-sulfate]
IBP	IRF-4 binding protein
IgE	immunoglobulin ε
IgG	Immunoglobulin γ
IPTG	Isopropyl β-D-1-thiogalactopyranoside
k-	kilo
kb	kilo base pair
kDa	kilo dalton
l	liter
Laser	Light amplification by stimulated emission of radiation
LB	Luria-Bertani
LFA-1	Lymphocyte function-associated antigen 1
LPS	Lipo-polysaccharides

## Appendices

LSM	confocal laserscanning microscope
m	meter
m-	milli
M	molar
mAK	Monoclonal antibody
MAPK	Mitogen-activated protein kinase
mCherry	Monomeric cherry
MCS	Multiple cloning site
min	Minute
MLC	myosin light chain
MTOC	microtubule organization center
n-	nano-
NGS	Normal goat serum
NPF	Nucleation promoting factor
N-terminus	Amine-terminus
OD	Optical density
PAGE	Polyacrylamide gel-electrophoresis
PAK	p21-activated kinase
PBS	Phosphate buffered saline
PCR	Polymerase chain reaction
PDGF	Platelet derived growth factor
PFA	Paraformaldehyde
pH	negative decadic logarithm of hydrogen-concentration
PH	Pleckstrin homology
Pi	Inorganic phosphate
PKC	Protein kinase C
PM	Palmitoylated
PMA	Phorbol 12-myristate 13-acetate
P-Tyr	Phospho-tyrosine
PVDF	Polyvinylidene fluoride
Rab	Ras-like proteins from brain
Rac	Ras related C3 botulinum toxin substrate
Raf	rapid growing fibrosarcoma
Ran	Ras related nuclear transport
Ras	Rat sarcoma
RasGRP	Ras guanly releasing protein
Rho	Ras-homologue

## Appendices

RNA	Ribonucleic acid
RNAse	Ribonuclease
rPM	Rounds per minute
RT	Room temperature
s	second
SDS	Sodium dodecyl-sulfate
SLAT	SWAP-70 like adaptor of T-cells
SOS	Son of sevenless
SWAP	Switch associated protein
TAE	Tris-acetate EDTA
TBS	Tris buffered saline
TBST	Tris-buffered saline with Tween 20
TCR	T-cell receptor
TEMED	Tetramethylethylenediamine
TIRF	total internal reflection fluorescence
Tirs	Trishydroxymethylaminomethane
TNF	Tumor necrosis factor
TRAF	Tumor necrosis factor associated factors
Tween 20	Polysorbate 20
U	Unit
UV	Ultraviolet
v/v	Volume per volume
w/v	Weight per volume

## 8.2 Supplemental Data

Videos	Description
S1	<p><b>In B16F1 cells expressing very low levels of PM-SWAP-70, the fusion protein predominantly localizes along the cell body, but also in the lamella of the cell.</b></p> <p>24 h after transfection with PM-GFP-SWAP-70, the cells were replated on laminin-coated coverslips and analyzed by live-microscopy. Individual frames were taken each 5 s. Left side: PM-GFP-SWAP-70. Right side. Phase contrast. Bar: 10 <math>\mu</math>m</p>
S2	<p><b>B16F1 cells with a higher expression level of PM-SWAP-70 are non-motile and exhibit strong ruffling activity and microspike formation.</b></p> <p>24 h after transfection with PM-GFP-SWAP-70, the cells were replated on laminin coated coverslips and analyzed by live-microscopy. Individual frames were taken each 5 s. Left side: PM-GFP-SWAP-70. Right side. Phase contrast. Bar: 10 <math>\mu</math>m</p>
S3	<p><b>Cotransfection of dominant active H-Ras (12V) with GFP-SWAP-70 result in association of GFP-SWAP-70 with F-actin arrays behind the leading edge of the cell. These F-actin arrays labeled by SWAP-70 are oriented parallel to the leading edge and move towards the cell center.</b> 16 h after cotransfection with GFP-SWAP-70 and myc-H-Ras (V12), the cells were replated on laminin-coated coverslips and analyzed by live-microscopy after 4 hours. Individual frames were taken each 8 s. Left side: GFP-SWAP-70. Right side. Phase contrast. Cells were considered as cotransfected because of the SWAP-70 localization that was typical for H-Ras (12V) cotransfections. Bar: 10 <math>\mu</math>m</p>
S4	<p><b>Cotransfection of dominant active H-Ras (12V) with GFP-SWAP-70 result in association of GFP-SWAP-70 with F-actin arrays behind the leading edge of the cell. These F-actin arrays labeled by SWAP-70 are oriented parallel to the leading edge and move towards the cell center.</b> 16 h after cotransfection with GFP-SWAP-70 and myc-H-Ras (V12), the cells were replated on laminin-coated coverslips and analyzed by live-microscopy after 4 hours. Individual frames were taken each 8 s. Cells were considered as cotransfected because of the SWAP-70 localization that was typical for cells cotransfected with dominant active Ras. Bar: 10 <math>\mu</math>m</p>
S5	<p><b>Cotransfection of dominant active R-Ras (38V) with GFP-SWAP-70 leads to association of GFP-SWAP-70 with F-actin arrays behind lamellipodia of the cell. These F-actin arrays labeled by SWAP-70 move towards the cell center irrespective of forward-protrusion of the lamellipodia</b></p> <p>16 h after cotransfection with GFP-SWAP-70 and myc-R-Ras (38V), the cells were replated on laminin-coated coverslips and analyzed by live-microscopy after 4 hours. Individual frames were taken each 8 s. Cells were considered as cotransfected because of the SWAP-70 localization that was typical for cells cotransfected with dominant active Ras. Bar: 10 <math>\mu</math>m</p>
S6	<p><b>The association of SWAP-70 with dominant R-Ras induced F-actin arrays is abolished by the PI3 kinase inhibitor LY294002.</b></p> <p>16 h after cotransfection with GFP-SWAP-70 and myc-R-Ras (38V), the cells were replated on laminin-coated coverslips and analyzed by live-microscopy after 4 hours. Individual frames were taken each 8 s. In frame 30, LY294002 was added to an end-concentration of 50 <math>\mu</math>M. Living cells were judged to express R-Ras (38V) based on the characteristic morphology and the GFP-SWAP-70 distribution. Left side: GFP-SWAP-70. Right side. Phase contrast. Bar: 10 <math>\mu</math>m</p>
S7	<p><b>GFP-RasGRP1 associates with tubular vesicles and endomembranes in R-Ras (38V) cotransfected B16F1 cells plated on laminin.</b> 16 h after cotransfection with GFP-SWAP-70 and</p>

## Appendices

	myc-R-Ras (38V), the cells were replated on laminin-coated coverslips and analyzed 4 h later by live-cell-microscopy. Individual frames were taken each 8 s. Living cells were judged to express R-Ras (38V) based on the characteristic morphology. Left side: GFP-SWAP-70. Right side. Phase contrast. Bar: 10 $\mu$ m
S8	<b>GFP-RasGRP1 associates with tubular vesicles and probably the endoplasmatic reticulum in R-Ras (38V) cotransfected B16F1 cells plated on laminin.</b> 16 h after cotransfection with GFP-SWAP-70 and myc-R-Ras (38V), the cells were replated on laminin coated coverslips and analyzed 4 h later by live-cell-microscopy. Individual frames were taken each 8 s. Living cells were judged to express R-Ras (38V) based on the characteristic morphology. Left side: GFP-SWAP-70. Right side. Phase contrast. Bar: 10 $\mu$ m
S9	<b>Higher magnification of the lamella and lamellipodium of the video S8</b>
S10	<b>GFP-RasGRP1 localizes in numerous spots in the lamella of a transfected B16F1 cell behind a ruffling lamellipodium and follows the ruffling activity.</b> 16 h after transfection with GFP-RasGRP1, B16F1 cells were replated on glass coverslips and analyzed by live-microscopy on the next day. Individual frames were taken each 5 s. Bar: 10 $\mu$ m
S11	<b>Higher magnification of video S11</b> 16 h after transfection with GFP-RasGRP1, B16F1 cells were replated on glass coverslips and analyzed by live-microscopy on the next day. Individual frames were taken each 5 s. Bar: 10 $\mu$ m
S12	<b>mCherry SWAP-70 partly colocalizes with GFP-RasGRP1 in the lamella of a cotransfected B16F1 cell plated on glass.</b> 16 h after cotransfection with mCherry-SWAP-70 and GFP-RasGRP1, B16F1 cells were replated on glass coverslips and analyzed by live-microscopy on the next day. Individual frames were taken each 5 s. Bar: 10 $\mu$ m
S13	<b>Higher magnification of video S12</b>
S14	<b>GFP-RasGRP1 localizes in the lamella of a B16F1 cell even when mCherry-SWAP-70 can not be detected.</b> 16 h after cotransfection with mCherry-SWAP-70 and GFP-RasGRP1, B16F1 cells were replated on glass coverslips and analyzed by live-microscopy on the next day. Individual frames were taken each 5 s. Bar: 10 $\mu$ m
S15	<b>GFP-SWAP-70 colocalizes with mCherry-RasGRP1 on macropinosomes in NIH/3T3 cells.</b> Cells were cotransfected with GFP-SWAP-70 and mCherry-RasGRP1 and replated on glass coverslips 16 h after transfection. Cells were analyzed by live-video microscopy after additional 24 hours. Macropinocytosis was induced with 10 nM PMA. Video analysis begins ~5 min after PMA addition. Top left: GFP-SWAP-70, top right: mCherry-RasGRP1, bottom left: phase contrast. Bar: 10 $\mu$ m
S16	<b>mCherry-SWAP-70 localizes to circular constricting structures in the lamella that give rise to macropinosome-formation.</b> B16F1 cells were cotransfected with mCherry-SWAP-70 and GFP-Tensin and replated on fibronectin coated coverslips 16 h after transfection. Cells were analyzed after additional 5 hours by live-cell-video-microscopy. Frames were taken each 5 s. Upper left: mCherry-SWAP-70, upper right: GFP-Tensin, lower left: phase contrast. Note the membranous reorganization in the lamella of the cell visible in the phase contrast. Bar: 10 $\mu$ m
S17	<b>GFP-SWAP-70 localizes to loose filamentous structures in the lamella of motile B16F1 cells.</b>
S18	<b>High expression levels of PM-SWAP-70 leads to the formation of numerous microspikes and an elongated cell-morphology.</b>
S19	<b>PM-SWAP-70 (1-525) labels macropinosomes in a NIH/3T3 cell expressing low levels of the construct.</b> Cells were transfected with the indicated construct and analyzed by live-video microscopy on the next day. Bar: 10 $\mu$ m

## Appendices

S20	<p><b>SWAP-70 and RasGRP1 colocalize in a protrusion of a B16F1 cell plated on laminin</b></p> <p>B16F1 cells were cotransfected with mCherry-SWAP-70 and GFP-RasGRP1 and replated on laminin coated coverslips 16 h after transfection. Cells were analyzed after additional 5 hours by live-cell-video-microscopy. Frames were taken each 8 s. Upper left: mCherry-SWAP-70, upper right: GFP-RasGRP1, lower left: merge (SWAP-70: red, RasGRP1: green).</p>
S21	<p><b>GFP-RasGRP1 localizes on endomembranes in a NIH/3T3 cell 20 min after addition of 10 pM PMA.</b> Cells were transfected with GFP-RasGRP1 and analyzed by live-video microscopy on the next day. Individual frames were taken each 8 s. Bar: 10 <math>\mu\text{m}</math></p>
S22	<p><b>GFP-RasGRP1 localizes on ruffles and vesicles in a NIH/3T3 cell 10 min after addition of 10 pM PMA.</b> Cells were transfected with GFP-RasGRP1 and analyzed by live-video microscopy on the next day. Individual frames were taken each 8 s. Bar: 10 <math>\mu\text{m}</math></p>
S23	<p><b>Intermediate expression level of PM-SWAP-70 induce elongated cell morphology and bulge-like swelling in a B16F1 cell plated on laminin.</b></p> <p>Animation of a Z-series through a confocal stack of a PM-GFP-SWAP-70 transfected B16F1 cell plated on laminin. Left: GFP-SWAP-70 Right: Vinculin staining. Bar: <math>\mu\text{m}</math> 10</p>





### 8.4 Danksagung

Zum Gelingen dieser Arbeit haben viele Menschen beigetragen, denen ich für ihre Unterstützung dankbar bin.

Für die ausgezeichnete wissenschaftliche Betreuung möchte ich mich bei Martin Bähler herzlich bedanken, der stetes Interesse an dem SWAP-70-Projekt hatte und immer Zeit für meine Fragen und Ideen fand. Diese Arbeit und meine Einsicht in die Welt der Forschung sind durch die vielen konstruktiven Diskussionen und Anregungen gewachsen.

Herrn Prof. Dr. Gerke danke ich sehr für die freundliche Übernahme des Zweitgutachtens meiner Arbeit.

Herrn Prof. Dr. Klämbt danke ich herzlich für seine Bereitschaft, mich als Drittprüfer zu prüfen.

Michael Kessels und Britta Qualmann sowie Jon Dang danke ich für die freundliche Bereitstellung verschiedener SWAP-70 Konstrukte.

Ich möchte meinen ehemaligen „Mitreiterinnen“ Sandra und Kati für die vielen guten Gespräche und die lustigen Stunden danken, die wir innerhalb und außerhalb des Institutes zusammen hatten. Pia Oberbanscheidt danke ich sehr herzlich für die Einarbeitung in das „SWAP-Projekt“ und Frank van den Boom für die Tipps und Kniffe hinsichtlich der Tücken der Mikroskopie. Besonderer Dank gilt Margrit und Birgit, die beide mit ihrer großen Hilfsbereitschaft Stützen dieser Arbeit waren. Petra und Marita bin ich zu großem Dank für die Pflege der Mäuse verpflichtet; ohne ihre aufopferungsvolle Arbeit würden viele Dinge im Institut stillstehen. Kay Grobe danke ich für zahlreiche Diskussionen über das Wesen der Welt und der Wissenschaft sowie sein Händchen für das Mixen guter Caipirinhas. Ullrike Honnert danke ich für immer hilfreiche Tips in Sachen Laborleben und Klonierungen; Srinivas Pallerla für die Einführung in indische Mythologie und Götterkunde. Gäbe es nicht den vielseitig begabten Uwe Pieper, stünden wir wahrscheinlich schon länger ohne funktionstüchtige Zentrifugen und Computer da. Vielen Dank auch an Friederike Rosenfeld, die im Sekretariat immer ein Rettungsring in den Fluten der Bürokratie war. Vermissen werde ich auch die Teilnehmerinnen der morgendlichen Diskussionsrunde, ohne die das Leben am Institut nur schwer vorzustellen wäre, sowie die „wilden Diplomanden“ des Sommers 2006, die ambitionierten Bacheloretten Maïke, Steffi und Ruth und „meine“ Bachelors Jan, Markus und Christian. Euch allen viel Glück! Fehlen werden mir auch „die Neuen“... Tabea, weil sie weiß, wie man nach der Arbeit Borbarads Turm erstürmt. Balaji, der durch seinen kreativen Humor das Labor zu einem besseren Platz macht und jederzeit für eine wissenschaftliche Diskussion zu haben ist. Und natürlich Marouan, der mit seiner (noch zu beweisenden) „das Leben ist eine Gurke“- Hypothese an den Fundamenten der Philosophie rüttelt. Yan und Wan-Quin danke ich für fernöstliche kulinarische Genüsse und wünsche ihnen zusammen mit Fereshteh viel Erfolg. Vermissen werde ich auch den Charme von „Elf“ Elfrink, die gerne paddelt und nebenher gerne angeln geht... eine gute Überleitung zur erweiterten Instituts-Familie. Der „Kuschelgruppe“ Linke verdanke ich viele Lachfalten und die Bekanntschaft einiger sehr wichtiger Menschen. Christine danke ich für viele schöne Erinnerungen, Christian Andresen für seine wertvolle Freundschaft und Sepp, Patrick, Judith, Annika und Martina für viele nette Worte, gute Antikörper, gute Kaffees, audiophile Hörspielereignisse und zahllose Pointen. Das gleiche gilt für Sven, Hendrikje, Daniela und all die anderen netten Mitarbeiter der AG-Püschel. Ich werde Euch alle nicht vergessen.

In ganz besonderem Maße möchte ich meiner Familie danken. Frauke, Arno, Jens... vielen vielen Dank für Eure immerwährende Unterstützung in jeglicher Lebenslage! Dito für Takeshi und Shuji, die mir in schwierigen Stunden immer mit gutem Rat zur Seite standen.